



UNIVERSITY OF TRENTO

International PhD Program in Biomolecular Sciences

XXVI Cycle

“Antisense-mediated splicing correction approaches for retinal dystrophies and dysfunctions”

Tutor

Prof. Michela A. Denti

CIBIO - University of Trento

Neuroscience Institute – National Research Council (CNR), Padova

Advisor

Prof. Simona Casarosa

CIBIO - University of Trento

Neuroscience Institute – National Research Council (CNR), Pisa

Ph.D. Thesis of

Niccolò Bacchi

CIBIO – University of Trento

Academic Year 2013-2014

Declaration

I confirm that this is my own work and the use of all material from other sources has been properly and fully acknowledged.

A handwritten signature in cursive script, appearing to read "Medo Pahi", written in black ink.

Candidate Signature

“The real voyage of discovery consists not in seeking new landscapes, but in having new eyes.”

Marcel Proust, *In Search of Lost Time*

1 Index

1	Index	7
2	Abstract	9
3	Introduction¹	11
3.1	The mRNA splicing process	12
3.2	The retina and photoreceptor cells	13
3.3	Retinal dystrophies	15
3.4	Mutations leading to retinal diseases	16
3.5	Antisense oligonucleotides	19
3.6	Chimeric and adapted snRNAs	23
3.7	<i>Trans</i> -splicing	25
3.8	RNA interference	27
3.9	Retinal cone dystrophy and the alpha2delta subunits of voltage gated calcium channels	29
3.9.1	Voltage gated calcium channels and phototransduction	29
3.9.2	Alpha2-delta subunits	31
3.9.3	CACNA2D4	33
3.10	The patch clamp technique	34
3.11	Retinitis pigmentosa and RPGR	37
3.12	Usher syndrome and USH2A	39
4	Aims of the PhD project	41
5	Results	43
5.1	Identification of candidate genes for splicing-correction approaches	43
5.2	CACNA2D4	45
5.2.1	Computational analysis of Cacna2d4 splicing	45
5.2.2	In vivo characterization of E25 splicing	51
5.2.3	A splicing-reporter minigene for Cacna2d4	53
5.2.4	In vitro characterization of exon 25 splicing	55
5.2.5	Analysis of $\alpha_2\delta_4\Delta E16$ splicing isoform expression in the central nervous system (CNS) and neuroendocrine system	57
5.2.6	Functional characterization of different $\alpha_2\delta_4$ variants	58
5.3	RPGR	66

5.3.1	Computational analysis of RPGR exon 9a splicing-relevant sequences	66
5.3.2	Design of U1snRNAs and reporter minigenes for exon 9a skipping.....	68
5.3.3	Testing different chimeric U1snRNAs for exon 9a skipping.....	70
5.4	USH2A.....	72
6	Discussion.....	75
6.1	CACNA2D4.....	76
6.2	RPGR.....	81
6.3	USH2A.....	83
7	Materials and Methods.....	85
7.1	Computational analysis of Cacna2d4 E25 splicing.....	85
7.2	Computational analysis of RPGR exon 9a splicing	85
7.3	Animals	86
7.4	Cloning of different constructs.....	86
7.6	RNA extraction and cDNA synthesis.....	89
7.7	Cell culture and transfection conditions.....	89
7.8	Luciferase activity assay.....	90
7.9	RT-PCR and densitometric analysis	90
7.10	RT-qPCR.....	90
7.11	Protein extraction and Western blot.....	91
7.13	Electrophysiological recordings	92
7.14	Statistics	93
9	Contributions to this work.....	94
10	Bibliography.....	95
11	Attachments.....	109
11.1	Papers	109
12.2	List of supplementary tables and figures attached to the work.....	165
13	Acknowledgments.....	169

2 Abstract

Retinal dystrophies are a large and extremely variegated group of diseases causing visual impairments and eventually blindness. As of today, no cures are available for such conditions, and the most advanced clinical approaches are based on classical gene transfer techniques. The recent development of genetic tools designed to manipulate splicing offers a unique opportunity to target several of these diseases, potentially reaching a highly specific and controlled effect in contrast to the more investigated gene supplementation therapies. These molecular tools are mainly part of two classes: antisense oligonucleotides (AONs) and chimeric or adapted small nuclear RNAs (snRNAs). They function by altering how the splicing machinery recognizes a target sequence, usually an exon, allowing to increase its presence (exon inclusion) or decrease it (exon skipping) in mature mRNA.

The first aim of this work has been the identification of genes causing retinal dystrophies having mutations potentially targetable by splicing-correction approaches. Following screening of mutation databases we identified three genes, each of them having mutations with characteristics interesting for a possible application of such approaches: *CACNA2D4*, *RPGR*, and *USH2A*.

The *CACNA2D4* gene encodes for an accessory subunit of high-voltage-activated (HVA) calcium channels and, when mutated, causes retinal cone dystrophy 4 (RCD4). It was selected because of the presence of a mouse model of retinal dystrophy (Wycisk et al., 2006a), allowing an *in vivo* test of the designed strategy. Since the approach consisted in inducing skipping of the exon hosting the mutation, we analysed the splicing pattern of the target exon *in vivo* and *in vitro*; the functionality of the rescued protein resulting from therapeutic exon skipping. The analysis revealed on one side that the rescued protein was not functional, therefore showing how the approach was not feasible for *CACNA2D4*. Interestingly, we found evidence of two newly identified splicing isoforms of the gene, one of which mimics the effect of the mutation.

A mutation in *RPGR* intron 9 has been shown to cause retinitis pigmentosa by increasing the inclusion in mature mRNA of an alternatively spliced exon (E9a) (Neidhardt et al., 2007). Using splicing reporter minigene assays, we were able to

design efficient chimeric U1snRNAs able to mediate E9a skipping thus correcting the genetic defect. In the *USH2A* gene we instead identified an interesting region hosting 5% of known mutation which could be approachable with exon skipping. The implementation of assays able to assess functionality of *USH2A* and *RPGR* will be fundamental for the development of new splicing-correction approaches for these genes.

3 Introduction¹

Retinal dystrophies are an extremely diversified group of genetic diseases all characterized by visual dysfunctions that, in the worst cases, can lead to blindness. Today there are more than 200 genes responsible for syndromic and nonsyndromic retinal dystrophies (Daiger et al., 1998), each of them carrying several types of mutations leading to very different clinical phenotypes. The development of different gene therapy approaches has given a hope for the implementation of therapies for these otherwise incurable conditions. Messenger RNA (mRNA) splicing is a fundamental and extremely complex cellular process that has been so far barely considered as a therapeutic target (Bonnal et al., 2012; Havens et al., 2013), even if it can be considered as highly appealing given its importance in the cell. The ability to modulate splicing can in fact offer several advantages over other conventional gene replacement approaches, especially in the context of retinal dystrophies. By definition, antisense-based therapeutic approaches act following base-pairing with their mRNA target, thus giving the possibility of obtaining a great specificity of action. Since they act at the mRNA level, the endogenous transcriptional regulation of the target gene is always maintained. This means that the therapeutic effect is obtained only where and when the target pre-mRNA is present. In a highly specialized and organized tissue like the retina it is particularly important to maintain endogenous gene regulation. Therapeutic interventions for delicate processes like the phototransduction cascade would require the preservation of this control for desirable outcomes (Smith et al., 2012). Splicing-correction approaches allow also a fine-tuning over the relative abundance of splicing isoforms because, by acting at a pre-mRNA level, it is relatively easy to modulate their ratio. The availability of several different molecular tools that can be used to manipulate splicing renders these approaches a versatile and promising strategy for the multitude of retinal dystrophies known today. Moreover, the retina has some characteristics that make it a perfect target tissue for those therapies. First of all it is an easy tissue to

¹ It has been included in the introduction part of the PhD candidate's review "Splicing-Correcting Therapeutic Approaches for Retinal Dystrophies: Where Endogenous Gene Regulation and Specificity Matter" (Invest Oph- thalmol Vis Sci. 2014;55:3285–3294. DOI:10.1167/iovs.14-14544), with the authorisation of the copyright holder ARVO.

access, and different drug delivery routes are in use today (Gomes Dos Santos et al., 2005; Martin et al., 2002). Being that the eye is relatively small, enclosed and separated from the rest of the body by the blood-brain barrier, it minimizes both the required dose and the unwanted systemic dissemination of the therapeutic agent, thus avoiding possible complications due to widespread side effects of the therapy (Surace and Auricchio, 2008). The eye is also an immune-privileged organ, limiting the potential immune response to the delivered agent (Stein-Streilein, 2008). The retina is composed by nondividing cells, it is thus easier to induce prolonged effects or transgene expression, without the need of using integrating vectors. Regarding gene delivery, the presence of different adeno-associated viral (AAV) vector serotypes able to efficiently and stably transduce all retinal layers (Vandenberghe and Auricchio, 2012) is a great advantage for splicing-modulating genetic tools.

3.1 The mRNA splicing process

Once transcription of a gene begins in the nucleus, the transcript undergoes a complex series of co-transcriptional processes all devoted to the production of a mature mRNA, collectively dubbed "mRNA processing". One of these events, called mRNA splicing, consists in the removal of intervening sequences (introns) and the joining of the coding portions of the transcript (exons). Messenger RNA splicing is a major way by which the cell can induce transcriptional diversity, mainly through alternative splicing, and apply a fine control on this diversity. The proper recognition of introns and exons is mediated by *cis*-acting sequences and *trans*-acting factors. The principal *cis*-acting elements that spatially organize the splicing reaction consist in the splice donor (DS) site (or 5' splice site), the polypyrimidine tract (Py), the branch-site (BS) and the splice acceptor (AS) site (or 3' splice site). There are also other *cis*-acting sequences that are fundamental for mRNA splicing (Lam and Hertel, 2002): exonic splicing enhancers (ESE) or silencers (ESS), that enhance or inhibit recognition of the exon in which they lay; intronic splicing enhancers (ISE) or silencers (ISS), intronic sequences that promote or suppress recognition of the nearby exons. *Trans*-acting factors are

instead several proteins and ribonucleoproteins able to recognize the different *cis*-elements. Small nuclear RNA (snRNA) are constitutive components of the small nuclear ribonucleoproteins (snRNP) U1, U2, U4, U5, U6, and allow them to base-pair with the *cis*-acting sequences that mediate the cascade of events leading to the splicing reaction. For example the U1 snRNP recognizes the DS site, whereas U2 binds to the branch site. The other two groups of *trans*-acting splicing factors are represented by heterogeneous nuclear ribonucleoproteins (hnRNPs), that mainly have a repressive function, and by serine- and arginine-rich (SR) proteins, that play an important role in splicing regulations mainly by binding to ESE and ISE, thus promoting splicing (Busch and Hertel; Jean-Philippe et al., 2013; Kafasla et al., 2012; Pozzoli and Sironi, 2005; Zhou and Fu, 2013). All these factors assemble together in a precise temporal sequence in a complex called spliceosome, the cellular machinery devoted to the splicing process. For a more exhaustive description of the splicing process we refer the reader to more detailed reviews (De Conti et al., 2013; Hoskins and Moore, 2012; Kornblihtt et al., 2013).

3.2 The retina and photoreceptor cells

The retina is a highly structured neural tissue that covers the inner part of the eye cup. It is organized in different layers, which carry specific functions. The retina is delimited by the retinal pigmented epithelium (RPE), a pigmented non-neuronal tissue dedicated to two important functions. The RPE layer absorbs the photons not captured by photoreceptor cells, thus improving the quality of vision. It also undertakes several metabolic and trafficking functions in support of photoreceptor cells, such as performing many biochemical steps of the visual cycle and phagocytizing photoreceptor outer membranes. Photoreceptors are the sensory cells of the retina. Phototransduction starts in their outer segment, a modified and specialized cilium in close proximity to RPE cells, that contains a multitude of tightly-packed membrane disks where the different light-sensitive proteins (opsins) are located and where the phototransduction

cascade occurs. The connective cilium joins the outer segment of photoreceptors with their inner segment, where the nucleus and other organelles are located. Photoreceptors are classified into rods and cones. While cones are fundamental for color vision, rods are more sensitive to light and are important in dark/dim light conditions. The outer nuclear layer (ONL) of the retina consists of the nuclei of rods and cones.

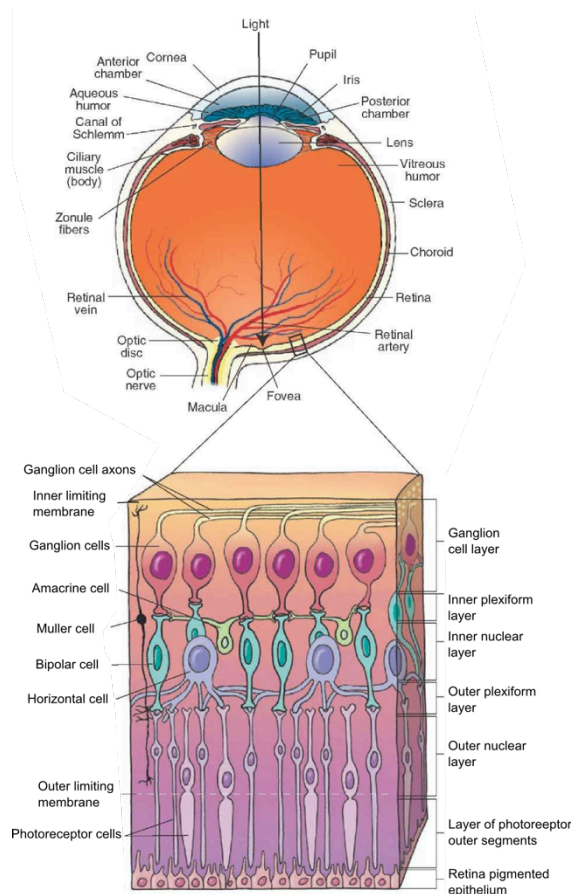


FIGURE 1. Eye and retina structure

Photoreceptors make synapses with other photoreceptors and second-order neurons in the outer plexiform layer (OPL). There are three types of second-order neurons in the retina: horizontal cells, which are interconnecting neurons that integrate the visual input horizontally; bipolar cells, which are responsible for transferring the visual input vertically to third-order neurons; and amacrine cells. Cell bodies of bipolar, horizontal and amacrine cells constitute the inner nuclear layer (INL) of the retina. Amacrine cells are another class of interneurons that integrate the signal laterally, like horizontal cells, making synapses with bipolar cells and the third-order neurons, the retinal ganglion cells. Synapses between bipolar

cells, amacrine cells and retinal ganglion cells are organized spatially in the inner plexiform layer (IPL) of the retina. Retinal ganglion cell axons form the optic nerve and reach the visual cortex. Spanning across all retinal layer, Muller glia cells have a supportive function for the different retinal neurons. Their connection with photoreceptor cell inner segments form the outer limiting membrane (OLM), while their more internal protrusions constitute the inner limiting membrane of the retina (ILM), where the retina enters in contact with the vitreous humour.

3.3 Retinal dystrophies

Degeneration of photoreceptor or of RPE cells is the initial sign of most retinal dystrophies, which are genetic diseases that affect the eye. Degenerations can start in one of the two types of photoreceptors (rods or cones) and later diffuse also the other type, or can start in both types from the beginning. Symptoms can be highly variable, and generally depend on which region of the retina is the first to be affected and which type of photoreceptor starts degenerating first. They can comprise decrease in central or peripheral vision, decrease in visual acuity, problems in photopic (during dark) or scotopic (during light) vision, and can lead to blindness in advanced stages. The current classification takes into account several aspects: if the disease affects primarily rods (rod dominated), cones (cone dominated) or both (generalized degeneration), if the degeneration is stationary or progressive, and if it involves only the retina (non syndromic) or also other districts of the body (syndromic). Additionally, the different dystrophies can be classified following the pattern of inheritance which can be autosomal dominant, autosomal recessive, X-linked or mitochondrial. The genetic diversity of retinal dystrophies is astonishing, with many different genes accounting for different proportion of cases of the same disease, and other situations where one gene can be responsible for different diseases. They affect around 2 million people worldwide (Berger et al., 2010), and in many patients the genetic cause is still unknown. The first gene therapy strategy to enter the clinic aiming to cure a retinal dystrophy was designed for Leber congenital amaurosis (LCA), a severe non-syndromic generalized photoreceptor diseases caused by mutations in RPE65 and other genes. The therapy was based on an AAV serotype 2 (rAAV2) encoding for human RPE65 (Maguire et al., 2008). Success in safety and efficacy parameters of the conducted trials for LCA (Jacobson et al., 2012; Maguire et al., 2009; Simonelli et al., 2010) makes gene therapy the most promising and advanced approach for the cure of retinal dystrophies, and we will hopefully see other clinical studies starting in the close future.

3.4 Mutations leading to retinal diseases

Retinal dystrophies are caused by mutations in many different genes, leading to a multitude of disease conditions (Berger et al., 2010; Daiger et al., 1998) (Tab. 1). Today

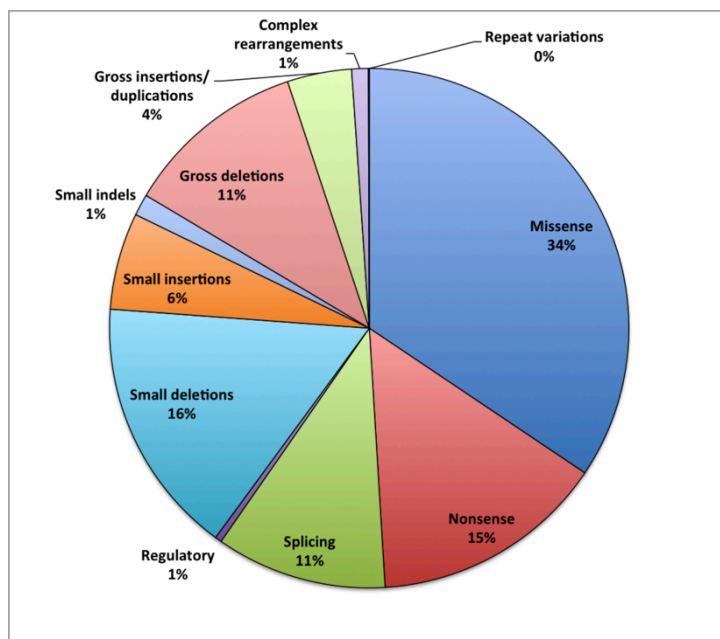


FIGURE 2. Mutation pattern of genes causing retinal diseases.

there are 219 genes identified as causative of retinal diseases, and the number is still growing (Daiger et al., 1998). The total number of known mutations for 208 of these genes, annotated in the Human Gene Mutation Database (provided in the public domain by HGMD professional,

<http://www.hgmd.cf.ac.uk/ac>

[/index.php](http://www.hgmd.cf.ac.uk/ac/index.php)), is 13.668 (Stenson et al., 2003). The large majority of these are represented by missense mutations, accounting for 34% of the total (Fig. 2). Small deletions follow as the second most abundant type of genetic defect (16%). Bona fide splicing mutations represent 11% of the total. Generally, mutations residing in introns are categorized as splicing mutations because the amino acid sequence of the protein is not altered, thus the problem most likely concerns proper splicing. These mutations can be located in any of the *cis*-acting elements present in introns. Splicing mutations can also be found in exons, altering or not the coding sequence. In this case their identification as splicing mutations is much more difficult, as it requires analysis of the splicing pattern. Today it is believed that more than 25% of mutations, normally categorized as missense, nonsense, or silent, actually act by altering the splicing pattern (Lim et al., 2011a; López-Bigas et al., 2005; Sterne-Weiler et al., 2011). Their effect can be the disruption of a *cis*-acting sequence, or the formation of a new one, resulting in exon skipping, intron retention or use of alternative DS and AS sites. Correct identification of these mutations is of pivotal importance for the development of therapeutic approaches. Aside from splicing mutations, antisense-mediated splicing-correction approaches can potentially be utilized for the correction of missense and nonsense mutations, as well as

for small insertions and deletions. In all cases where a mutation causes the introduction of a stop codon or frameshift leading to a premature termination of the transcript, the possibility to interfere with the proper recognition, by the splicing machinery, of the exon carrying the mutation (therapeutic exon skipping) can be the right strategy to follow. The result of this approach is a shorter mature mRNA, missing the portion encoded by the skipped exon, but resulting in a restored ORF. It is then necessary to assess the functionality of the rescued smaller protein. This strategy is more easily applicable to cases in which the mutated exon encodes for a repetitive structural element whose loss in the final protein product is less likely to cause structural and functional defects of the protein itself, whereas it is a riskier approach in other cases, where proper function of the skipped protein is less predictable.

Disease Category	Involved Genes
Cone or cone-rod dystrophy/dysfunctions	ABCA4 ADAM9 AIPL1 BBS12 C2orf71 C8orf37 CA4 CABP4 CACNA1F CACNA2D4 CDHR1 CERKL CNGA3 CNGB3 CNNM4 CRB1 CRX GNAT2 GUCA1A GUCY2D KCNV2 MERK MKS1 NR2E3 NRL OPN1LW OPN1MW PDE6C PDE6H PITPNM3 PROM1 PRPH2 RAB28 RAX2 RDH12 RIMS1 RLBP1 RPE65 RPGRIP1 TULP1 UNC119
Retinitis pigmentosa	ABCA4 ARL2BP ARL6 BBS1 BEST1 C2orf71 C8orf37 CA4 CEP290 CERKL CLRN1 CNGA1 CNGB1 CRB1 CRX CYP4V2 DHDDS EMC1 EYS FAM161A FSCN2 GPR125 GRK1 GUCA1A GUCA1B GUCY2D IDH3B IMPDH1 IMPG2 KIAA1549 KLHL7 LCA5 LRAT MAK MERK MFRP MYO7A NR2E3 NRL OFD1 PDE6A PDE6B PDE6G PRCD PROM1 PRPF3 PRPF31 PRPF6 PRPF8 PRPH2 RBP3 RDH12 RGR RHO RLBP1 RP1 RP1L1 RP2 RP9 RPE65 RPGR RPGRIP1 SAG SEMA4A SNRNP200 SPATA7 TOPORS TULP1 USH2A VCAN ZNF513
Leber congenital amaurosis	AIPL1 BBS4 BEST1 CABP4 CEP290 CNGA3 CRB1 CRX DTHD1 GUCY2D IMPDH1 IQCB1 KCNJ13 LCA5 LRAT MERK MYO7A NMNAT1 NRL RD3 RDH12 RPE65 RPGRIP1 RPGRIP1L SPATA7 TULP1
Macular dystrophy/degeneration	ABCA4 ABCC6 BEST1 CNGB3 CRX EFEMP1 ELOVL4 GUCY2D PAX2 PROM1 PRPH2 RP1L1 TIMP3
Stargardt disease	ABCA4 ELOVL4 PRPH2 CFH HMCN1
Age-related macular degeneration	ABCA4 ARMS2 BEST1 C3 CFH ELOVL4 ERCC6 FBLN5 HMCN1 HTRA1 RAX2 SLC24A1
Stationary night blindness	CACNA1F CABP4 GNAT1 GPR179 GRK1 GRM6 LRIT3 NYX PDE6B RHO SAG SLC24A1 TRPM1
Color blindness	CNGA3 CNGB3 GNAT2 OPN1LW OPN1MW OPN1SW PDE6C PDE6H
Usher syndrome	ABHD12 CACNA1F CDH23 CIB2 CLRN1 DFNB31 GPR98 GUCY2D HARS LRAT MYO7A PCDH15 PDZD7 TRIM32 USH1C USH1G USH2A
Chorioretinal atrophy/degeneration	ABCA4 CRB1 TEAD1
Retinal dystrophies/dysfunctions/degeneration	ABCC6 ABCA4 ADAMTS18 AIPL1 BEST1 C1QTNF5 CAPN5 CDHR1 CERKL CHM CRB1 CYP4V2 FZD4 GUCA1B KCNV2 LRAT LRP5 MERK NDP NR2E3 NRL OTX2 PANK2 PLA2G5 PROM1 PRPH2 RD3 RDH12 RDH5 RGS9 RGS9BP RLBP1 RPE65 SLC24A1 TSPAN12
Retinopathy of prematurity	LRP5 NDP FZD4
Optic atrophy/aplasia	MFN2 OPA1 OPA3 OTX2 SLC24A1 TMEM126A WFS1
Wagner syndrome	VCAN COL2A1
Bardet-Biedl syndrome	ARL6 BBS1 BBS10 BBS12 BBS2 BBS4 BBS5 BBS7BBS9 CEP290 LZTFL1 MKKS MKS1 RPGRIP1L SDCCAG8 TRIM32 TTC8 WDPCP
Other systemic/syndromic diseases involving the retina	ABCC6 ABHD12 ADAMTS18 AH11 ALMS1 ATXN7 CC2D2A CDH3 CEP290 CISD2 CLN3 COL11A1 COL2A1 COL9A1 ERCC6 FLVCR1 GNPTG IFT140 INPP5E IQCB1 ITM2B JAG1 KIF11 LRP5 NPHP1 NPHP4 OFD1 OPA3 OTX2 PANK2 PAX2 PEX1 PEX2 PEX7 PHYH RBP4 RPGRIP1L SDCCAG8 TIMM8A TMEM237 TREX1 TTPA TTPA USH1C WFS1

TABLE 1. List of genes causing retinal diseases. All RetNet identified genes have been searched and allocated to disease categories according to HGMD professional entries at December 2013.

3.5 Antisense oligonucleotides

A versatile tool to target splicing is represented by antisense oligonucleotides (AONs). These are chemically synthesized molecules, generally around 20 nucleotides long, able to mimic the RNA structure and bind by reverse complementarity to specific cellular RNA targets. Even if they are normally used to block mRNA translation or to degrade mRNA by RNase H-mediated cleavage, these effects are unwanted when the goal is to interfere with splicing. By the use of several different chemistries (Järver et al., 2013; Saleh et al., 2012) available today for their design, it is in fact possible to direct AONs toward splicing relevant sequences on the pre mRNA, masking them, and to avoid RNase H activity after binding. The first splice-switch oligonucleotides used a phosphothioate linkage to join nucleosides (DNA-PS) (De Clercq et al., 1969). However, these AONs were retaining undesired RNase H activity (Saleh et al., 2012). A second generation of oligonucleotides was created from the DNA-PS structure. Inclusion at the 2' oxygen of a methyl (2'OMe) or a methoxyethyl (2'MOE) protecting group to increase oligonucleotides resistance to degradation and block RNase H activity originates 2'OMe-PS (Sproat et al., 1989) and 2'MOE-PS (Martin P., 1995) ribonucleosides, respectively. The third generation comprised locked nucleic acids (LNA), peptide nucleic acids (PNA) and phosphorodiamidate morpholino oligonucleotides (PMO). Locked nucleic acids derive from the addition of a methylene bridge between the 2' oxygen and the 5' carbon on a DNA-PS backbone (Koshkin et al., 1998; Obika et al., 1998). They have an increased affinity to target RNA and do not activate RNase H. In PNAs the DNA backbone is instead substituted by a peptide-like mimicry (Nielsen et al., 1991). Peptide nucleic acids do not cause RNase H degradation of their target and show strong affinity to it. Since they are neutrally charged, addition of a Lysine residue is commonly used to increase their water solubility and cell-uptake. Phosphorodiamidate morpholino oligonucleotides derive from the substitution of the ribose rings with morpholine ones, and their joining by phosphorodiamidate groups (Summerton and Weller, 1997). PMOs are neutrally charged oligonucleotides that do not activate RNase H and are lowly susceptible to degradation. For a comprehensive understanding of these chemistries we refer the reader to more specific reviews (Järver et al., 2013; Kole et al., 2012; Kurreck, 2003; Saleh et al., 2012).

In order to be able to regulate splicing, AONs must gain access to the cell nucleus. There are different splicing regulatory sequences that have been so far targeted with AONs on pre-mRNA to achieve splicing modulation (Fig. 3).

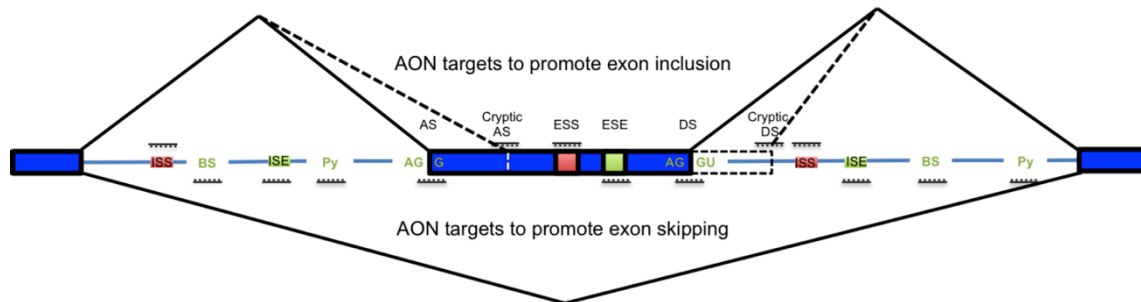


FIGURE 3. Possible AONs targets to induce splicing modulation. Schematic representation of *cis*-acting sequences that are possible target of AONs. *Cis*-acting sequences that promote exon recognition are reported in green, whereas sequences that suppress it are highlighted in red. AONs designed to induce exon skipping are shown in the bottom part. AONs designed to promote proper exon inclusion are shown in the upper part.

For example, by targeting splicing enhancers or silencers it is possible to induce respectively exon skipping or exon retention by blocking access of splicing factors to their target sites. Another common target of AONs are splice sites that, when bound by an AON, are no longer free to take part in the splicing reaction, thus obliging the spliceosome to use alternative “downstream“ sites, again inducing exon skipping. In few cases, AONs have also been engineered to carry an additional tail containing *cis*-acting sequences that can be bound by splicing factors able to enhance (Baughan et al., 2006, 2009; Osman et al., 2012; Owen et al., 2011; Skordis et al., 2003) or silence (Brosseau et al., 2013; Dickson et al., 2008; Gendron et al., 2006; Villemaire et al., 2003) splicing of specific exons. In this way, apart from their antisense activity toward a splicing-relevant sequence, these bifunctional AONs can induce additional effects depending on the sequence they carry on the tail. Since AONs act by base-pairing, they are generally believed to allow a high specificity of action for their desired target. No undesired mis-spliced products of the target gene or of chosen unrelated genes were in fact detected when investigated after therapeutic application of AONs (van Deutekom et al., 2007; Kalbfuss et al., 2001). Even if these findings are not generalizable and proper design of the antisense molecule should always be considered, they underline the potentiality of AONs in the context of target selectivity. Splicing modulation finds its more advanced application in the cure of Duchenne muscular dystrophy (DMD). Duchenne muscular dystrophy is an X-linked recessive disease caused by mutations in

the dystrophin gene. Dystrophin is an important cellular protein whose main role in muscle fibers is the connection of the cellular cytoskeleton with the extracellular matrix. Different mutations in the 79 exons of the gene cause protein truncation due to the loss of the open reading frame. The majority of these mutations can be addressed by exon skipping (Aartsma-Rus et al., 2009). The commonly mutated exon 51 has been the first target for exon skipping. In the clinical trials completed so far for exon 51 skipping, the different chemistries applied (2'OMe-PS, PMOs) showed overall efficacy and absence of serious adverse effects (Cirak et al., 2011; van Deutekom et al., 2007; Goemans et al., 2011; Kinali et al., 2009).

A phase I clinical trial using a 2'MOE-PS oligonucleotide for splicing modulation has also been recently completed for spinal muscular atrophy (SMA), and a phase II trial has recently started (Zanetta et al., 2014). Mutations in the survival motor neuron 1 (*SMN1*) gene are causative of the disease. In humans, *SMN1* has a paralogue, named *SMN2*. The two genes are identical, apart from a silent mutation in exon 7 of *SMN2*. This mutation, however, causes exon 7 of *SMN2* to be less recognized by the splicing machinery. If exon 7 is not included, the protein is truncated. So a therapeutic strategy is to mask exon 7 ESS using AONs, thus promoting exon 7 inclusion, which results in the production of a functional full length SMN protein from *SMN2*, that can compensate for mutations on *SMN1*.

Antisense oligonucleotides are known to be able to target all retinal layers following intravitreal, subretinal or topical administration (Bhisitkul et al., 2005; Cloutier et al., 2012; Dvorchik and Marquis, 2000; Shen and Rakoczy, 2001; Shen et al., 1999; Thaler et al., 2006). They have long been used to elicit RNase H degradation or to block transcription in the eye for several different diseases, having been applied for example against cytomegalovirus (CMV), herpes simplex virus (HSV), vascular endothelial growth factor (VEGF), transforming growth factor- β (TGF-G), fibroblast growth factor (FGF) (Fattal and Bochot, 2006; Gomes Dos Santos et al., 2005).

An example of the use of splice-switch oligonucleotides in the eye is that of vascular endothelial growth factor receptor 2 (KDR). The *KDR* gene has two distinct products: membrane-bound KDR (mbKDR), that is prohemangiogenic, and soluble KDR (sKDR), antilymphangiogenic. sKDR needs the recognition of an alternative polyadenylation site

on *KDR* intron 13 to be translated. By intravitreal administration of PMO directed against murine *Kdr* exon 13 DS site, it was possible to increase the sKDR/mbKDR ratio at mRNA and protein level in the retina and vitreous, interfering with the spliceosome ability of mediating intron 13 splicing (Uehara et al., 2013) (Fig. 4). This resulted in a block of hemangiogenesis and lymphangiogenesis in a model of choroidal neovascularization and corneal injury (Uehara et al., 2013). Another recent example of the use of AONs as splicing regulators to treat a retinal dystrophy is that of the gene

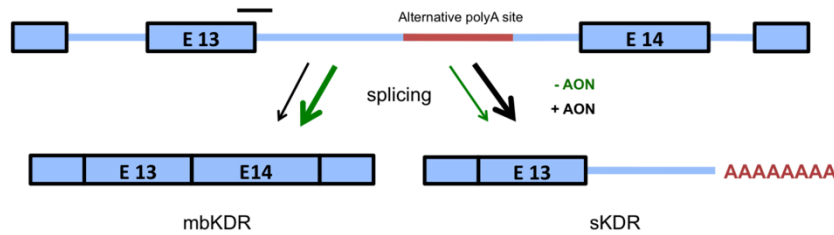


FIGURE 4. AONs approach for *KDR*. Scheme of action of AON against *KDR* exon 13 DS site: normally mbKDR, originating from intron 13 splicing, is more abundant than sKDR, that is instead generated by the use of an alternative polyadenylation site in the retained intron 13. By interfering with the E13 DS site it was possible to increase the sKDR form, and decrease the mbKDR one.

centrosomal protein 290kDa, (*CEP290*). *CEP290* mutations are responsible for ~15% (den Hollander et al., 2008; Perrault et al., 2007) of Leber congenital amaurosis cases, as well as for

other genetic diseases such as Joubert syndrome, Senior-Løken syndrome, Meckel-Gruber syndrome and Bardet-Biedl syndrome. A transition on intron 26 (c.2991+1655A>G) is among the most common mutations of *CEP290* (den Hollander et al., 2006). The mutation introduces a new DS site on intron 26, causing an aberrant exon to be included in the mature messenger RNA between exon 26 and 27. This aberrant exon carries a stop codon, resulting in a premature truncation of the protein. By

the design of 2'OMe-PS directed towards predicted ESE sequences at the 3' of the aberrant exon it was possible to demonstrate, on patient fibroblasts, its skipping from the mature mRNA, so to efficiently restore proper splicing between exon 26 and

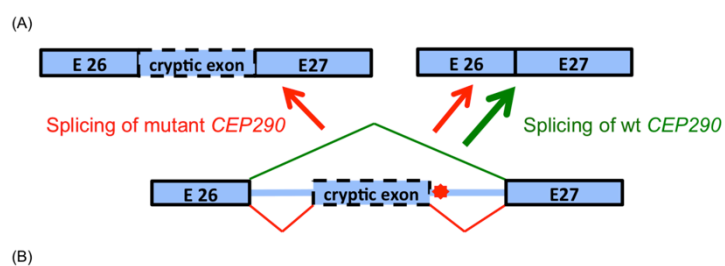


FIGURE 5. AONs approach for *CEP290*. (A): Proper joint of *CEP290* exon 26 and 27 (green lines and arrow) is impaired by a mutation in intron 26 (red star). The mutation causes the aberrant inclusion of a cryptic exon in a portion of the mature mRNA (red arrows). (B) Using different AONs (black lines) it was possible to augment the fraction of correctly spliced mRNA (black arrows).

27 (Collin et al., 2012) (Fig. 5). Another study by Gerard and colleagues, by using 2'OMe-PS targeting a different predicted ESE sequence, came to similar result.

Moreover, they were able to show an increase of full-length protein levels in patient fibroblasts following AON administration, as well as a faster ciliation (Gerard et al., 2012).

3.6 Chimeric and adapted snRNAs

The use of AONs as a therapeutic approach for genetic diseases poses one major problem. Their effect is time-limited, so to have a durable effect, repeated administration is required. In this view the use of engineered snRNAs offer a major advantage, as they can be delivered in expression cassettes in the same way as it is done in conventional gene replacement therapies. By using viral or nonviral delivery systems it is in fact possible to transduce or transfect target cells, and then produce the snRNA exploiting endogenous transcription. As for AONs, one of the advantages of this class of RNA molecules is their specificity of action, as undesired activity of snRNAs has not been reported so far when investigated (Pinotti et al., 2008; Schmid et al., 2013). Today there are two classes of snRNAs that have been successfully modified to be able to modulate splicing: U1 and U7. The first step of spliceosome assembly is mediated by U1 recognition of the DS site (Patel and Bellini, 2008). U7 snRNA is instead not involved in splicing, but in the processing of the 3' end of histone mRNA (Dominski and Marzluff, 2007). They both can be used to manipulate splicing exactly as AONs. Antisense U1 and U7 snRNA have been applied for masking *cis*-acting sequences, thus inducing therapeutic exon skipping, for Duchenne muscular dystrophy (Denti et al., 2006, 2008; Goyenvalle et al., 2012). Bifunctional U7 snRNA, acting in a similar way as bifunctional AONs, have also been designed for DMD (Goyenvalle et al., 2009) and SMA (Marquis et al., 2007; Voigt et al., 2010). snRNAs can also be applied to a specific set of mutations not targetable by AONs. When a mutation disrupts a DS site, it

leads to complete or partial loss of the ability of the the splicing machinery to recognize it. The design of mutation-adapted U1 snRNA able to interact by base pairing with the mutated splice site can re-establish spliceosome recognition (Pinotti et al., 2008; Susani et al., 2004). This is possible by exploiting U1 natural function in splicing.

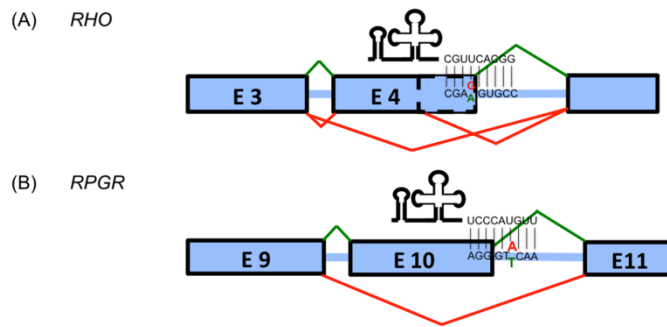


FIGURE 6. Mutation-adapted U1 snRNA for *RHO* and *RPGR* DS site mutations. The altered splicing pattern caused by the different mutations is reported in red. The correct splicing pattern is reported in green. The antisense sequence of the best U1 snRNA used to correct the effect of each mutation is reported. (A) Mutation at the last base of exon 4 of *RHO* causes skipping of the exon or mis-splicing due to the use of an alternative DS site. (B) An intronic mutation affecting the DS site of exon 10 of *RPGR* leads to exon 10 skipping.

Unfortunately the same strategy so far is not applicable in a similar way to mutations of the AS site. The only strategy that has been applied to mutations in the polypyrimidine tract of the AS site relies on the use of exon-specific U1 snRNAs (ExSpeU1) engineered to recognize not the mutation but unconserved intronic sequences close to the DS site, in a mutation-independent way (Alanis et al., 2012). The ExSpeU1s have

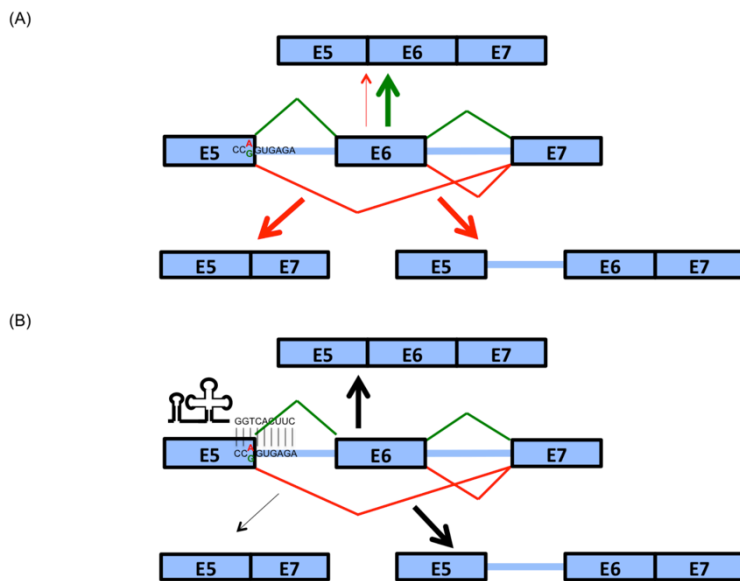


FIGURE 7. Mutation-adapted U1 snRNA for *BBS1* DS site mutations. (A) Normal splicing of *BBS1* (green) is altered (red) by a mutation at the end of exon 5. The mutation causes exon 6 skipping (bottom, left) or intron 5 retention (bottom, right). Arrows dimension represent the amount of the different splicing products. (B) Black arrows represents the correcting effect of the best mutation-adapted U1 snRNA, able to partially restore proper splicing.

been also shown to correct DS site and exonic mutations (Alanis et al., 2012). It is also possible to engineer any viral vector even with a combination of different snRNAs, by taking advantage of their limited size (Goyenvalle et al., 2012). Tanner and colleagues applied mutation-adapted U1 snRNAs to rhodopsin (*RHO*), one of the genes responsible for autosomal

dominant retinitis pigmentosa. An exonic point mutation interfering with the DS site was found responsible for exon 4 mis-splicing. By using minigenes as reporter systems

in COS 7 cells they were able to show rescue of exon 4 proper recognition with an average efficiency of 90% after treatment with mutation-adapted U1 snRNAs (Tanner et al., 2009) (Fig. 6). The same strategy was used for a splice donor mutation of RPGR inducing exon 10 skipping. Proper inclusion of exon 10 was achieved in patient fibroblasts using mutation-adapted U1snRNAs (Glaus et al., 2011) (Fig. 6). Mutations in BBS1 result in more than 20 % of Bardet–Biedl syndrome (BBS) cases. BBS is a ciliopathy characterized by retinal dystrophy, cognitive impairment, obesity, polydactyly, hypogonadism and renal disease (Mockel et al., 2011). BBS1 is a member of a protein complex called BBSome, involved in trafficking of vesicles to the cilia (Nachury et al., 2010). Schmidt and collaborators identified in a family affected by BBS a splice donor mutation on exon 5 of BBS1 causing mis-splicing (Schmid et al., 2011). They were able to show, after administration of mutation-adapted U1 snRNAs, restoration of proper splicing in COS-7 cells, using minigenes as splicing reporter. Similar results were obtained in patient-derived fibroblast transduced with lentiviral vectors encoding for the modified U1-snRNAs (Fig. 7). A recent innovative approach has been developed for the treatment of mutations occurring at position +5 of DS sites (Schmid et al., 2013). The synergic use of both mutation-adapted U1 and U6 snRNAs was sufficient to achieve efficient correction of aberrant splicing caused by BBS1 mutations, whereas the only use of mutation-adapted U1 snRNAs resulted in low levels of splicing correction.

3.7 *Trans-splicing*

Another correction approach that acts at the splicing level is spliceosome-mediated RNA *trans*-splicing (SMaRT). This technology is based on a cellular process called *trans*-splicing. Initially discovered in trypanosome (Murphy et al., 1986; Sutton and Boothroyd, 1986), *trans*-splicing has also been described in mammals (Caudevilla et al., 1998; Flouriot et al., 2002). It consists in the ability of two different pre-mRNAs to originate a chimeric mature mRNA following a recombination event during splicing. *Trans*-splicing can be exploited to correct aberrant mRNA by using an artificial RNA sequence, called pre *trans*-splicing molecules (PTM). The PTM consists of a correct portion of the cDNA of the gene of interest, flanked by a region containing all important

elements for splicing and the binding domain (BD), important for specific binding of the PTM to the target endogenous pre mRNA, mainly on an intronic sequence. There are three types of PTMs that can be exploited to achieve 5' *trans*-splicing, 3' *trans*-splicing or internal exon replacement, correcting respectively the 5', the 3', or a central region of a transcript (Fig. 8). PTMs are delivered in expressing vectors as in a normal gene transfer approach. They have been administered *in vivo* using different viral vectors (Avale et al., 2013; Chao et al., 2003a; Tahara et al., 2004), or non-viral delivery systems (Coady and Lorson, 2010; Coady et al., 2008; Shababi et al., 2011).

The peculiarity of this technique, compared to other splicing-correction approaches, is the fact that it is mutation-independent, thus

the same PTM can be used to treat different mutations located in the same region of the transcript.

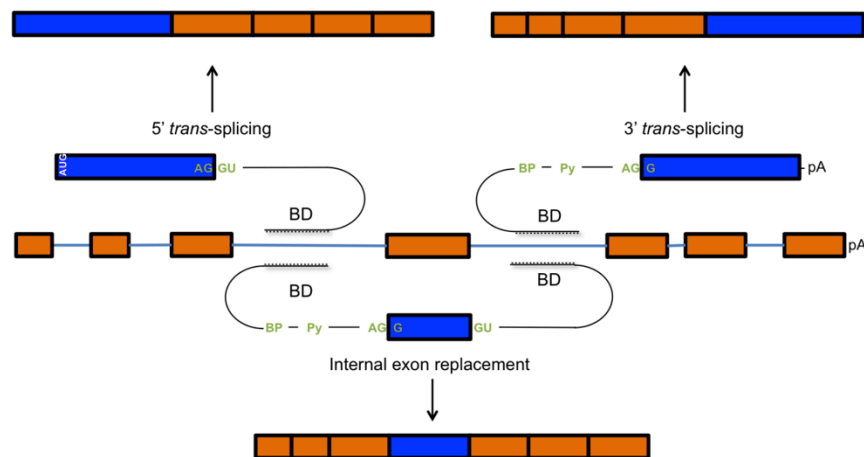


FIGURE 8. *Trans*-splicing approaches: Schematic representation of the three possible *trans*-splicing approaches. The different PTMs are constituted by a region harbouring: splicing *cis*-acting sequences, shown in green; the coding sequence in blue; and the binding domain (BD). The mature mRNA resulting from the three *trans*-splicing approaches is shown, with in orange the endogenous sequence, and in blue the sequence introduced by the PTMs.

Even if SMaRT has never been applied so far for the correction of a genetic disease of the retina, it has been successfully tested in several *in vivo* models for spinal muscular atrophy (Coady and Lorson, 2010), haemophilia A (Chao et al., 2003b), hyper-IgM X-linked immunodeficiency (Tahara et al., 2004) and tauopathy (Avale et al., 2013). As there are already exhaustive reviews (Mansfield et al., 2004; Wally et al., 2012) about the first three *in vivo* approaches, to give an example of a possible application of SMaRT, we will spend a few words on the last and more novel one regarding tauopathy caused by mutations in *MAPT*, the gene encoding tau protein. Tau, a protein important for microtubule stabilization in the CNS, is subject to active alternative splicing as six different isoforms are present in humans (Niblock and Gallo, 2012). Tau exon 10 encodes for a tandem repeat and by alternative splicing originates

two sets of different tau isoforms: with 4 (4R; +E10) or 3 (3R; -E10) tandem repeats. Splicing mutations that lead to a change in the levels of E10 containing transcripts cause an imbalance in the 4R/3R isoform ratio, and leads to frontotemporal dementia with parkinsonism linked to chromosome 17 (FTDP-17). Avale and colleagues designed a PTM for 3' *trans*-splicing with the BD binding to intron 9, and carrying the cDNA of the last 3 exons of tau (E10-E11-E12) (Avale et al., 2013). They applied the PTMs to Htau mice, that express only human *MAPT*, resulting in equal amounts of 4R and 3R (Andorfer et al., 2003). Since normal adult mice express only the 4R isoform, the model recapitulates the effect of a splicing mutation abolishing E10 inclusion. Following delivery of the PTM in the prefrontal cortex of Htau mice by stereotaxic injection using lentiviral vectors, they were able to show effective *trans*-splicing at RNA and protein level.

3.8 RNA interference

RNA interference (RNAi) is a regulatory mechanism used by the cell to silence specific transcripts at the post-transcriptional level. The endogenous effectors of this mechanism are micro RNAs (miRNAs). They are transcribed into primary precursors (pri-miRNA) that are then cleaved first by Drosha into a ~70 bp precursor hairpin (pre-miRNA), and then by Dicer into a ~22 bp RNA/RNA duplex (Krol et al., 2010). One of the two strands (the guide strand) is then loaded into the RNA-induced silencing complex (RISC) as a mature miRNA, where it can recognize complementary mRNAs. Silencing by RISC is caused by translational repression if the complementarity between the miRNA and its target mRNA is not perfect. When the miRNA perfectly matches its target, silencing is instead mediated by cleavage and subsequent degradation of the mRNA. Small interfering RNAs (siRNAs) are double stranded RNA-molecules that result from processing by Dicer of exogenous double strand RNAs. Alternatively they can be chemically synthesized and delivered as such for therapeutic purposes. siRNAs are directly loaded onto RISC. Another class of interfering RNA is composed by short hairpin RNAs (shRNAs), stem-loop structures that enter the miRNA processing pathway as substrates for Dicer. shRNAs are often obtained from the transcription of a delivered DNA transgene hereby guaranteeing stable expression. On the contrary the

effect of siRNAs is transient, even if different chemistries are today available to improve their stability. siRNA have been used to treat retinal diseases since already a few years. The first RNAi therapeutic applications to enter the clinical phase have in fact been two naked siRNAs developed for the treatment of age-related macular degeneration (AMD): Bevasiranib, directed against vascular endothelial growth factor (VEGF); and AGN211745, targeting VEGF receptor (VEGFR1). Clinical development of these two drugs has been discontinued during the last years, mainly because of their failure in meeting efficacy endpoints (Vaishnav et al., 2010). Even if other clinical trials are in progress for other naked siRNA (Kanasty et al., 2013), the lessons that we can learn from the two described trials is that it is a challenge to deliver naked siRNA into cells, even in an easy system such as the eye, and that their efficacy is not mediated by RNAi, but via an off-target sequence independent effect on cell surface Toll-like receptor-3 (TLR3) (Cho et al., 2009; Kleinman et al., 2008). New chemistries seem to overcome these limitations (Byrne et al., 2013), and the availability of different types of formulations (polymer or lipid coated nanoparticles, oligonucleotide nanoparticles and conjugates delivery systems (Kanasty et al., 2013)) can potentially help in improving cellular uptake in the retina. However the current trend for *in vivo* applications is to utilize viral vectors to deliver shRNAs to different retinal layers (Askou et al., 2012; Chadderton et al., 2009; Hu et al., 2013; Jiang et al., 2013; Yuan et al., 2010; Zhu et al., 2013).

By exploiting the mechanism of RNAi-mediated gene silencing it is possible to solve different situations in which correct splicing is compromised. Mutations that cause impairment in the splicing process can lead to mis-spliced products that in some cases can show a dominant negative or gain of function effect. If this is the case, the simple decrease of the mis-spliced mRNA, without affecting the correctly spliced counterpart, can revert the pathological condition. This is possible using RNAi (Seyhan, 2011). A recent example of the application of this strategy in the retina has been shown for retinitis pigmentosa (Hernan et al., 2011). Mutations in rhodopsin (*RHO*) are the most prevalent cause of autosomal dominant retinitis pigmentosa (adRP), accounting for 25% of the cases (Fingert et al., 2008). Two mutations causing adRP (c.531-2A>G and c.937-1G>T) generate mis-splicing products. They abolish the proper recognition of the DS site of exon 3 and 5 respectively. Mutation c.531-2A>G originates two mis-spliced mRNAs with a partial intron 2 retention or a partial deletion of exon 3. Mutation c.937-

1G>T results in a partial deletion of exon 5. Using RNAi against the mis-spliced mRNA their level was successfully reduced without affecting the properly spliced isoform, with the exception of the second product of c.531-2A>G mutation, where the RNAi was not able to distinguish between the wild type and the aberrant mRNA (Fig. 9).

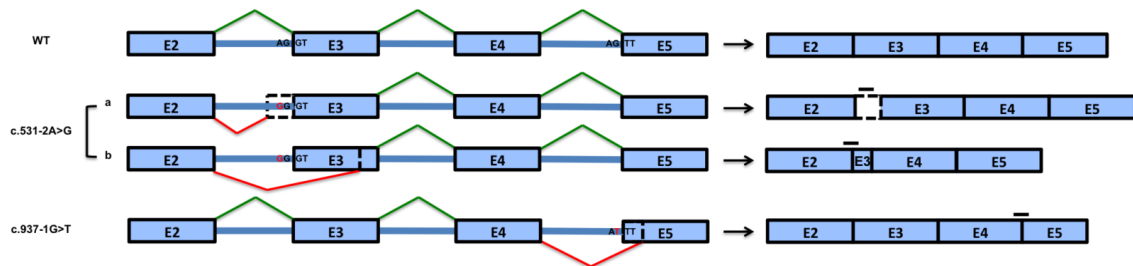


FIGURE 9. RNAi for adRP splicing mutations. Left: the effect on splicing of the two *RHO* mutations c.531-2A>G and c.937-1G>T is shown. Mutation c.531-2A>G originates two mis-spliced products (a-b). Right: The different mis-spliced products can be selectively recognized by siRNA (black lines) targeting sequences or exon-exon junctions absent in the wt transcript. siRNA directed towards mis-spliced product b of c.531-2A>G mutation was not able to discriminate between the wt mature mRNA and the aberrant one. Adapted from Hernan et al., IOVS, 2011.

3.9 Retinal cone dystrophy and the alpha2delta subunits of voltage gated calcium channels

3.9.1 Voltage gated calcium channels and phototransduction

Voltage gated calcium (Ca^{2+}) channels are a large family of channels found in many excitable and non-excitable cells where they are fundamental for different cellular processes. They activate upon membrane depolarization and allow calcium influx in the cell, which in turn regulates several processes such as neurotransmitter or hormone release, cell contraction, gene expression, enzyme activity and many other. Based on their biophysical properties, they can be divided in two major subgroups: high voltage-activated (HVA) and low-voltage activated (LVA) (Fig. 10). Low voltage-activated calcium channels show smaller conductance and open in response to a milder depolarization of the cell membrane when compared to HVA. Another important

difference between the two groups is their need for auxiliary subunits. While HVA calcium channels are heteromultimeric protein complexes constituted of $\alpha 1$, β , $\alpha 2\delta$ and sometime γ subunits, there are today no evidences that this is true also for LVA calcium channels (Huc et al., 2009). In HVA channels, the $\alpha 1$ subunit forms the pore, whereas β , $\alpha 2\delta$ and γ subunits conduct ancillary functions related to trafficking and modulation of the biophysical properties of the α subunit. Regarding inactivation properties, the major subgroup of HVA calcium channels is represented by long lasting calcium channels (L-type), which show a slow voltage-dependent inactivation. In contrast, LVA calcium channels are also called T-type, because they show a faster inactivation resulting in transient currents.

At the latest step of the phototransduction cascade, L-type calcium channels are responsible for the release of the neurotransmitter glutamate at retinal ribbon synapses. During light exposure, photoreceptors are hyperpolarized and L-type calcium channels are closed. When the light stimulus ends, thus in the dark, photoreceptors depolarize and L-type calcium channels open. The influx of calcium stimulates the presynaptic release of glutamate, which transfers the signal to bipolar cells. Among the different L-type calcium channels expressed in the retina there are several lines of evidence

GENE	PROTEIN	CHANNEL TYPE	TISSUE	CHANNELOPATHIES	
CACNA1S	Cav1.1	L	Skeletal muscle	<ul style="list-style-type: none"> Hypokalemic Periodic Paralysis -1 Malignant Hyperthermia -5 	<ul style="list-style-type: none"> HypoPP1 MHS5
CACNA1C	Cav1.2				
CACNA1D	Cav1.3		Cardiac nodal tissues Cochlear cells	Sinoatrial node dysfunction & deafness	SANDD
CACNA1F	Cav1.4		Retina, Mast cells	<ul style="list-style-type: none"> Congenital Stationary Night Blindness-2 X-linked cone-rod dystrophy -3 	<ul style="list-style-type: none"> CSNB2 CORDX3
HVA					
CACNA1A	Cav2.1	P/Q	Cerebellum, neurons Presynaptic terminals	<ul style="list-style-type: none"> Spinocerebellar Ataxia -6 Episodic Ataxia-2 Familial Hemiplegic Migraine -1 	<ul style="list-style-type: none"> SCA6 EA2 FHM1
CACNA1B	Cav2.2	N	Neurons, Presynaptic terminals		
CACNA1E	Cav2.3	R	Neurons		
LVA					
CACNA1G	Cav3.1	T	Neurons, Cardiac nodal tissues	Juvenile Myoclonic Epilepsy	JME
CACNA1H	Cav3.2		Neurons	<ul style="list-style-type: none"> Childhood Absence Epilepsy Autism Spectrum Disorder 	<ul style="list-style-type: none"> CAE ASD
CACNA1I	Cav3.3		Neurons		

FIGURE 10. Voltage gated calcium channels. The classification of the different known voltage-gated calcium channels is presented, together with tissue distribution and related diseases (Bidaud and Lory, 2011).

suggesting that Cav1.4 $\alpha 1$ subunit is the one responsible for neurotransmitter release in photoreceptors. This channel is expressed mainly in the retina, where it locates to the retinal ribbon

synapse (Knoflach et al., 2013; McRory et al., 2004; Morgans et al., 2005). Mutations in this gene result in an X-linked form of night blindness, incomplete stationary night

blindness type 2 (CSNB2) (Striessnig et al., 2010). This disease is characterized by an abnormal electroretinogram (ERG) showing a normal a-wave and a reduced b-wave, suggesting a defect in connectivity between photoreceptors and secondary neurons like bipolar cells. Patients show a normal fundus, and the following symptoms, which may not all occur together: problems in visual acuity, night blindness, nystagmus, defects in colour vision, and myopia (Striessnig et al., 2010; Zeitz et al., 2014).

3.9.2 *Alpha2-delta subunits*

HVA calcium channels show highly diversified characteristics in different tissues and cell types. This property is made possible by the presence of different genes coding for the different subunits of the channel, which together form a repertoire of building blocks that can be exchanged in order to modulate channel properties. Apart from the previously discussed heterogeneity of the α_1 subunit, we know today 4 genes encoding for β subunits (CACNB1-4), 4 encoding for $\alpha_2\delta$ subunits (CACNA2D1-4) and 8 encoding for γ subunits (CACNG1-8). Regarding $\alpha_2\delta$ subunits, the vast majority of our current knowledge refers to studies conducted on $\alpha_2\delta_1$, encoded by CACNA2D1. However, since the four orthologous genes share high similarity, we will refer generally to $\alpha_2\delta$ while describing general characteristics of the family. The $\alpha_2\delta$ subunits are

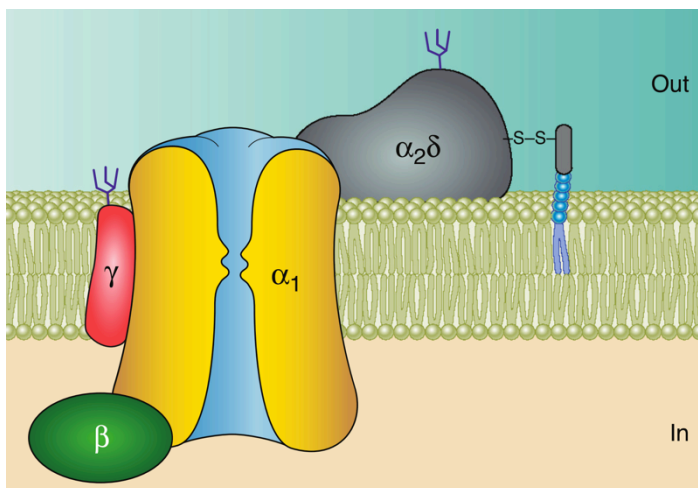


FIGURE 11 Subunit organization of HVA calcium channels. (Buraei and Yang, 2010)

extracellular glycosyl-phosphatidylinositol (GPI)-anchored proteins (Davies et al., 2010). They are translated as a single peptide which is then cleaved generating a N terminal (α_2) and a C terminal (δ) fragment. The two peptides are then joined together by a disulfide bond and are subject to glycosylation (Sandoval et al., 2004) (Fig. 11). The δ peptide is

responsible for membrane anchoring, while the α_2 peptide directly interacts with the α_1

subunit (Gurnett et al., 1997). The α_2 peptide hosts different structural domains: a Von Willebrand Factor A (VWF-A) (Springer, 2006; Whittaker and Hynes, 2002) domain and two Cache domains (Vivek and Aravind, 2000). The VWF-A domain is a common domain for extracellular proteins, and is important for protein-protein interactions. The Cache domain is found in bacterial chemotaxis receptors and, apart from $\alpha_2\delta$, is not present in other eukaryotic proteins. The exact role of these domains in $\alpha_2\delta$ subunits have not been elucidated so far.

The principal known function of $\alpha_2\delta$ subunits is to increase the number of functional channels on the plasma membrane. The result of this activity is an increase of 2-9 fold in current densities originated from HVA calcium channels when a functional $\alpha_2\delta$ subunit is co-expressed (Dolphin, 2013). The mechanism by which $\alpha_2\delta$ subunits are able to mediate such an effect is probably a combination of trafficking facilitation and reduced turnover of $\alpha_1\beta$ complexes (Bernstein and Jones, 2007; Cantí et al., 2005; Hoppa et al., 2012). Another observed characteristics of $\alpha_2\delta$ subunits is their ability to change the voltage-dependency of activation and inactivation of HVA calcium channels in some experimental settings. However, the evidence obtained so far does not allow the drawing of a precise picture of their effect on such biophysical properties because results differ greatly, probably as a consequence of the different combination of α_1 and β subunit used, and/or of the chosen expression systems (Dolphin, 2013). The $\alpha_2\delta$ subunits are also known to increase the inactivation rate of HVA calcium channels in several settings (Felix et al., 1997; Hobom et al., 2000; Shirokov et al., 1998; Sipos et al., 2000). Of the different known splice variants of $\alpha_2\delta$ subunits, all those characterized were able to modulate in a similar way HVA calcium channels (Klugbauer et al., 2000; Lana et al., 2014).

3.9.3 *CACNA2D4*

The last gene of the $\alpha_2\delta$ family to have been identified is *CACNA2D4*, encoding for $\alpha_2\delta_4$. First cloned from human brain, $\alpha_2\delta_4$ was initially identified at protein level in the small intestines, liver, adrenal, pituitary gland, and brain (Qin et al., 2002). *Cacna2d4* was subsequently found mutated in a spontaneous strain of mice showing an autosomal-recessive cone-rod dystrophy. The mice presented an ERG with a reduced b-wave and a thinner OPL in the retina. Both characteristics point to a problem in connectivity between photoreceptor and second-order neurons (Wycisk et al., 2006a). The mutation consists in a single nucleotide insertion on *Cacna2d4* exon 25 (E25) and truncates the open reading frame (ORF) after the first Cache domain, causing loss of the second Cache domain and of the whole δ peptide (Fig. 12).

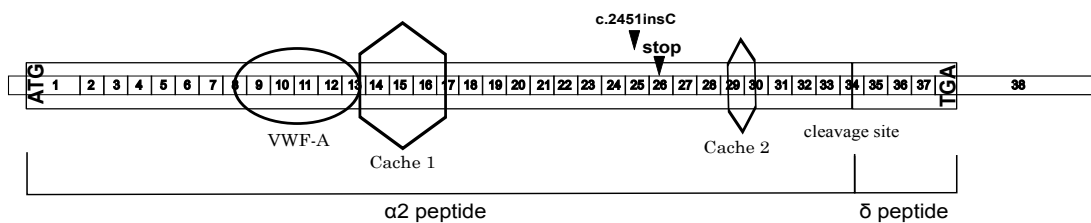


FIGURE 12. Scheme of *Cacna2d4* transcript. Schematic representation of *Cacna2d4* transcript (not in scale). The various exons are numbered. Positions of the von Willebrand factor A (VWF-A) domain and of the two Cache domains of the protein are shown. The murine c.2451insC¹ mutation site and the resulting nonsense codon are indicated by black arrowheads.

Animals homozygous for the mutation were showing reduced levels of *Cacna2d4* mRNA in the retina compared to wild types. In humans, *CACNA2D4* was found mutated in a family affected by autosomal recessive cone dystrophy (RCD4) (Wycisk et al., 2006b). Symptoms included a decrease in visual acuity, photophobia and defects in colour vision. As in the mouse strain, ERG had a reduced b-wave, a sign of incomplete stationary night blindness. Nevertheless the patients were not accusing night blindness, and the disease was progressive and not stationary. The causative mutation was found to be a substitution in E25 of *CACNA2D4* resulting in termination of the ORF, similarly to

¹ We have changed the annotation of the mutation from c.2367insC to c.2451insC since the transcription start site of *Cacna2d4* has been recently moved to an upstream position on the NCBI database.

what was observed in the mouse strain. Different studies have then characterized expression of $\alpha_2\delta_4$ in the retina, where it is found mainly associated with photoreceptors terminals, Müller glia cells, bipolar cells, and displaced ganglion cells (Mercer et al., 2011; De Sevilla Müller et al., 2013). There are today four known splicing isoform of CACNA2D4, consisting in two alternative N- and two alternative C-terminals (Qin et al., 2002). CACNA2D4 effects on calcium currents have been so far barely investigated, and assessed only on one of the identified splicing isoforms. Human $\alpha_2\delta_4$ has been found to increase Cav1.2 α_1/β_3 calcium influx in HEK293 cells (Qin et al., 2002). More recently, human $\alpha_2\delta_4$ has been proven to interact with Cav1.4 α_1 and β_2 subunits at photoreceptor ribbon synapses (Lee et al., 2014). In comparison to $\alpha_2\delta_1$, $\alpha_2\delta_4$ was found to shift the voltage dependence of activation of Cav1.4 to more positive potentials and to evoke smaller current densities when co-expressed with Cav1.4 α_1 and β_2 (Lee et al., 2014).

3.10 The patch clamp technique

Patch clamp is a developed of voltage-clamp, first introduced in 1952 by Hodgkin and Huxley (Hodgkin and Huxley, 1952) to describe the action potential in axons. Voltage-clamp is performed inserting two microelectrodes inside the cell, one for applying a certain potential to the cell membrane (clamping), the other for recording currents evoked by changes in the membrane potential. A problem of this technique was related to the control of the membrane potential at the recording site since the clamping and recording sites were not spatially overlapping. Originally invented in 1976 for single-channel measurements by Neher and Sakmann (Hamill et al., 1981), patch-clamp solved this problem and has revealed to be a very powerful tool in the investigation of cell excitability and ionic channel function. The word patch-clamp define the voltage-clamp of a membrane patch. In other words, it means to set a define voltage on a piece of membrane with the goal of measuring the current passing through it. Even if clamping can also be referred to the set of a defined current trough the membrane patch, with the goal of measuring changes in voltage (current-clamp), we will not consider this application further as it is not relevant to the purpose of this work.

The basic components needed in a patch-clamp experiments are an amplifier, a reference electrode, a measuring electrode, an experimental chamber, and a bath solution (Fig. 13). The reference electrode, immersed in the bath solution, is grounded and keeps the potential outside the cell membrane at 0 mV. The measuring electrode, connected with the amplifier, is inserted into a glass capillary (pipette) filled with a solution able to conduct currents (internal solution). In order to patch-clamp a cell, the pipette is first heated and pulled several times to obtain a sharp and very small aperture (0.5-2 μm). Once the pipette enters the bath solution, the circuit is closed. After having moved the pipette in contact with the cell, it is possible to control the electrical potential across the cell membrane with the patch-clamp amplifier. The membrane patch is formed by the portion of the cell membrane closing the end of the capillary. Only the patch is then voltage-clamped through the capillary, remaining almost completely isolated from the rest of the cell membrane.

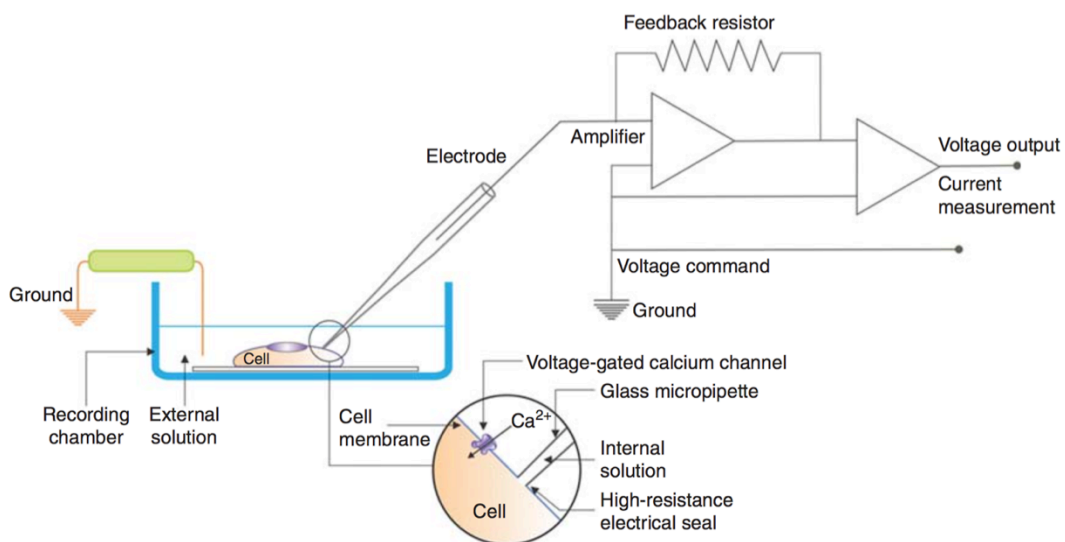


FIGURE 13. Schematic representation of the basic components of a patch-clamp setup (Gandini et al., 2014).

An early improvement of this technique has been the introduction of the cell-attached mode. By applying suction into the capillary it is in fact possible to obtain a giga-seal, a very high resistance between the capillary edge and the plasma membrane. The cell-attached configuration allows single-channel recordings, and is the starting point to obtain all other measurement configurations: whole cell, perforated patch, inside-out

and outside-out (Fig. 14). In the whole-cell mode an additional suction is applied, resulting in the rupture of the membrane patch closing the end of the capillary. Now the solution contained in the capillary (pipette solution) is in contact with the cytoplasm. The low resistance between the pipet and the cytoplasm (access resistance) and the retention of the giga-seal between the pipet and the membrane allow the clamping of the whole cell membrane. This results in the ability of recording currents occurring along the whole plasma membrane. The fact that the cytoplasm is now in contact with the pipette solution can represent a problem in experiment where the intracellular conditions need to be maintained. The perforated-patch configuration permits to overcome this issue by adding a pore-forming antibiotic (amphotericin-B or nystatin) to the pipette solution (Horn and Korn, 1992). When the cell-attached configuration is reached, the antibiotic forms channels in the plasma membrane, providing electrical continuity from the pipette to the cytoplasm without breaking the membrane. Additional variants of the patch-clamp technique allow the easy exposure to different solutions of the interior or exterior of the plasma membrane, as well as a fine control of the membrane potential. These single-channel configurations are called inside-out and outside-out. If the pipette is withdrawn from the cell after reaching the cell-attached configuration, the membrane patch can be detached from the cell obtaining the outside-out configuration. The inside surface of the plasma membrane is in fact now in contact with the bath solution, while the outside faces the pipette solution. The opposite situation, or outside-out, is obtained from the whole-cell configuration by slowly withdrawing the pipette.

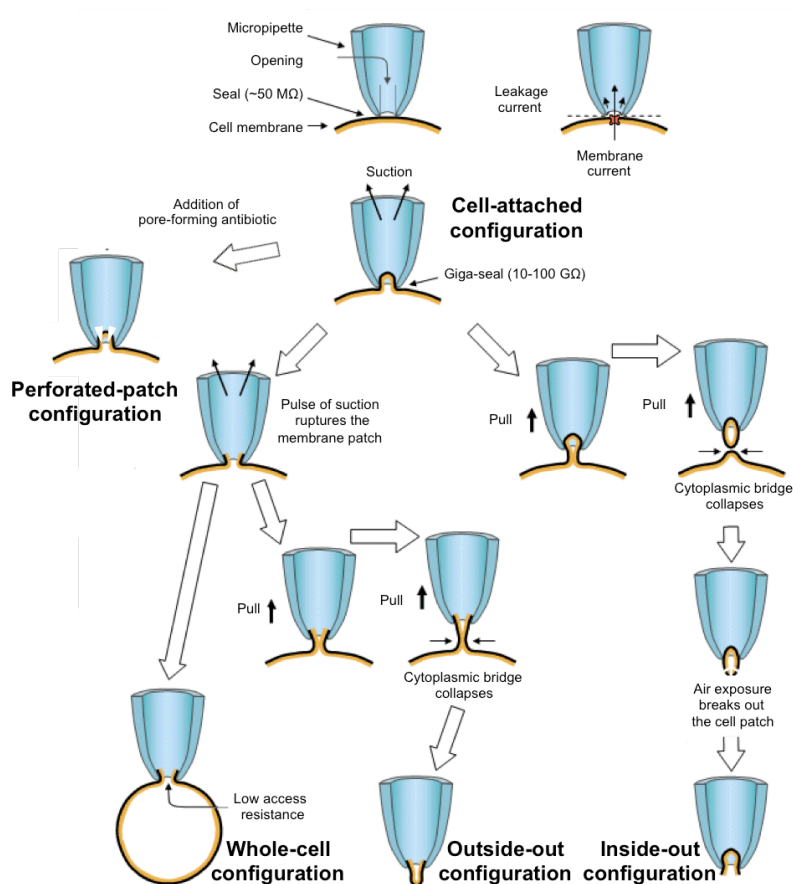


FIGURE 14. Different patch-clamp configurations. (Adapted from Malmivuo and Plonsey, 1995)

3.11 Retinitis pigmentosa and RPGR

Among different types of retinal degenerations, retinitis pigmentosa (RP) is the most common form, affecting one in 4000 individuals (Hartong et al., 2006). The disease commonly manifests during adolescence, and patients experience progressive visual impairments. Night blindness and loss of peripheral vision are usually the first symptoms, and eventually the disease can evolve into complete blindness due to the progressive loss of photoreceptor cells. Generally rods are first affected, and subsequently also cones start to degenerate. A typical sign of the disease is the appearance in the fundus of a bone-spicule pigmentation caused by migration of RPE cells. Although clinical symptoms of RP are similar among RP patients, the pattern of inheritance is complex, as mutations in 56 different genes can cause the disease (Daiger

et al., 2013). Autosomal recessive RP accounts for 50-60% of the cases, whereas autosomal dominant RP for 30-40%, and X-linked RP for 5–20% (Berger et al., 2010). Mutations in the retinitis pigmentosa GTPase regulator gene (*RPGR*) are responsible for 70% of X-linked RP cases, the most severe form of RP (Petrs-Silva and Linden, 2014). *RPGR* encodes for a protein of still not well-elucidated function. It is known to be expressed in several tissues, where it is found associated with the primary cilia (Hong, 2003; Khanna et al., 2005; Shu et al., 2005). In photoreceptor cells it is localized to the transition zone of the connective cilium (Hong and Li, 2002; Mavlyutov et al., 2002), where it is known to interact with the RPGR interacting protein 1 (RPGRIP1) (Boylan and Wright, 2000; Roepman et al., 2000; Zhao et al., 2003). The constitutive isoform of *RPGR* is encoded by 19 exons and is present in different tissues (Kirschner et al., 2001; Meindl et al., 1996; Roepman et al., 1996; Yan et al., 1998). This isoform consist of an N-terminal portion, which contain a Regulator of Chromosome Condensation 1 homologus (RCC1h) protein domain encoded by exon 1 to 11, and a less structured C-terminal portion (Meindl et al., 1996). The RCC1h domain is important for RPGR binding to RPGRIP1 (Roepman et al., 2000). In the retina instead a large subset of transcripts contains exon ORF15, that corresponds to the constitutive exon 15 plus a portion of intron 15. ORF15 encodes for a purine- rich C terminal, terminates the reading frame of the protein and is an hotspot for mutations (Vervoort et al., 2000).

A recently discovered splicing isoform of *RPGR* contains a new exon, exon 9a (E9a), downstream of exon 9 (Neidhardt et al., 2007). Exon 9a inclusion in the mature mRNA terminates the reading frame of the gene, deleting a portion of the RCC1h domain. This deletion modifies how RPGR interact with RPGRIP1, as it has been shown that E9a+ protein interacts with different variants of RPGRIP1 (Neidhardt et al., 2007). Moreover this isoform has a peculiar expression pattern. It is in fact mainly found in cones rather than in rods in human retina, and localizes in the inner segment of cones, whereas normally RPGR is present in the connective cilium (Neidhardt et al., 2007). In an RP patient a substitution was found 55 bp upstream of exon 9a. This mutation affects exon 9a recognition by the splicing machinery, increasing the levels of transcripts containing the exon (Neidhardt et al., 2007). The elucidation of a splicing-modulating therapy to restore the levels of exon 9a can potentially be beneficial for carriers of this mutation.

3.12 Usher syndrome and USH2A

Usher syndrome (USH) is a disease characterized by deafness and RP, and is classified in three clinical types: USH1, USH2 and USH3 (Reiners et al., 2006). The three types can be distinguished by disease onset and severity. Patients affected by USH1 are congenitally deaf and show sign of RP in childhood. USH2 patients show hearing defects from birth, and RP can start during puberty. The most rare form, USH3, is also the less severe, and shows progressive hearing impairments, RP, and vestibular dysfunctions. Mutations in different genes have been found for each condition. The majority of mutations in USH2 patients are located on USH2A gene, encoding for usherin (Weston et al., 2000). There are today two known splicing isoforms of usherin: a 5Kb transcript that is translated in a 170 kDa protein predicted to be completely extracellular (Bhattacharya et al., 2002), and a 15 Kb long transcript, translated in a 600 kDa protein predicted to be mainly extracellular, but still spanning across the plasma membrane (van Wijk et al., 2004). The predictions are based on the presence of several domains shared with other extracellular proteins, which are involved in protein-matrix and protein-protein interactions. The longer isoform adds several additional domains to the C-terminal of the shorter one, and results in having, from N to C terminal: 1 laminin G-like domain (LamGL), 1 laminin N-terminal domain (Lam NT), 10 laminin-like EGF-like domains (EGF-Lam), 4 fibronectin type 3 domains (FN3), 2 laminin G domains (LamG), 28 FN3 domains, 1 transmembrane region and 1 PDZ-1 binding domain (Fig. 15). USH2A is expressed in different tissues, but plays a key role mainly in the retina and cochlea. In the retina, it was found expressed in Bruch's membrane, as well as at photoreceptor terminals and associated with the connective cilium (Bhattacharya et al., 2002; Reiners et al., 2006). A recent study has found that the

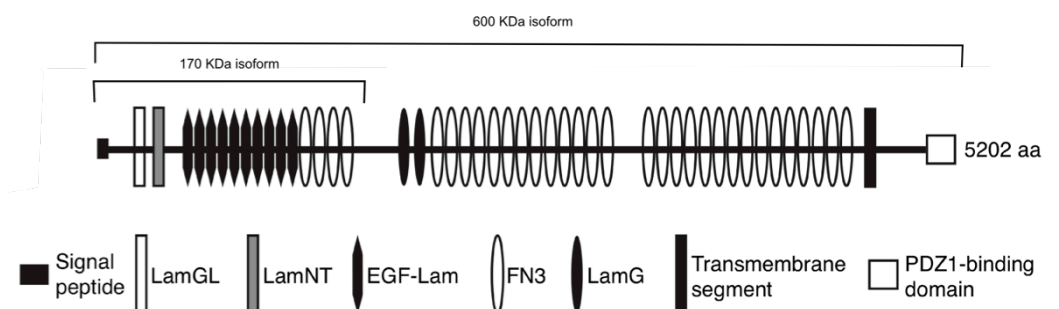


FIGURE 15. Domain organization of USH2A 600kDa and 170KDa isoforms.

prevalent form of usherin in the retina is the longer isoform, which is only present associated to the membrane just around the connective cilium, which is actually wrapped by usherin (Liu et al., 2007). Similar to dystrophin in muscle, USH2A can be considered a promising target for exon-skipping strategies due to its modular structure of repetitive domains.

4 Aims of the PhD project

Antisense-mediated splicing-correction approaches have just begun to be applied to correct retinal dystrophies. Implementation of new therapeutic strategies in general, and for retinal dystrophies more specifically, is however slowed by the difficulty in having reliable animal models where to assess the efficacy and safety of the therapeutic approach. Such models should in fact not only resemble the human disease phenotype, but also its genotype. In particular, the mRNA of the target gene needs to be present in the model, and the splicing pattern of the gene, as well as the introduced mutations, need to be similar. Moreover not all genes and not all mutations can be effectively targeted by splicing-modulating approaches, and a careful evaluation of the type of mutation and of the host gene needs to be achieved. A third difficulty in developing such therapies is the lack of characterization of disease genes. The function of the majority of genes causing retinal dystrophies is in fact not understood or poorly characterized.

The aims of this project were first of all to analyse existing databases in order to identify the most promising genes having mutations targetable with antisense-mediated splicing-correction approaches. After identification, the second goal was to design and apply such approaches to restore the functionality of the altered proteins.

In order to identify new interesting targets for splicing-correction approaches, we first undertook a survey of available databases of disease genes and mutations, as well as recent literature. We focused our research on disease genes of known function for which was available an animal model fitting the previously mentioned characteristics, and we identified one potential target for exon-skipping (CACNA2D4). Characterization of this model revealed how the protein resulting from exon skipping is no more functional, showing the unfeasibility of our therapeutic approach. However we identified for the first time two splicing isoform of the gene which do not show the same properties as the canonical one. We finally reported an additional effect on splicing of the studied mutation.

We thus extended the initial search to other genes not having an animal model, identifying other two promising targets for antisense-mediated splicing-correction approaches (RPGR and USH2A), and successfully achieving splicing correction in one of them (RPGR).

5 Results

5.1 Identification of candidate genes for splicing-correction approaches

We started our work with the aim of identifying new candidate genes in which the application of antisense splicing-correction approaches would be feasible and potentially beneficial for patients affected by retinal dystrophies. We focused our attention on genes and mutations that would benefit from strategies aiming at reducing or abolishing presence of exons, rather than increasing their recognition. Our choice was based on the fact that the design of antisense molecules for such strategies is considered easier since more is known about sequences that are fundamental for an exon to be recognized as such (SD, SA, ESE, ESS, BS, Py) compared to those inhibiting exon recognition (ESS, ISS). Furthermore the correction of splice site mutations affecting exon recognition, the most abundant form of identified splicing mutations at the moment, is particularly difficult and only mutations in some positions have been effectively rescued. We also decided to prioritize our search to genes for which animal models exist, with mutations similar to those encountered in human patients.

With this goal we started listing all genes present in the RetNet database, a database of genes and loci causing retinal diseases (Daiger et al. 1998). Having excluded from this list the unidentified genes, we obtained a list of 222 genes out of 269 total entries. We then excluded genes present on the mitochondrial genome, which do not undergo splicing (7 genes). Of the remaining 215 genes, we selected those causing autosomal recessive or X-linked diseases, in order to exclude dominant and multifactorial diseases. Even if antisense splicing-correcting approaches can in theory be applied also to dominant genetic diseases, the implementation of a therapeutic strategy for those genes is considered more risky. In fact in a dominant disease one should be able to selectively target the mutant allele and not the correct one, aspect which is rarely feasible with splicing-correcting approaches. Moreover, a recessive condition in which the normal gene product is absent can benefit more of even a partial restoration of the functional protein levels, whereas in a dominant disease, especially in the case of gain of function mutations, only a significant reduction of the aberrant gene product can result in a beneficial correction of the phenotype. Following this line we thus reduced the

candidate genes to 133. A further reduction was obtained by eliminating genes for which even a preliminary characterization or an hypothesized function in the retina was completely absent. The remaining 100 genes were searched on the Human Genetic Mutation Database (HGMD) professional (Stenson et al. 2009) in order to identify all known mutations linked to each of them. A list of all identified genes (Tab. S1) as well as of all mutations found in all RetNet genes (Tab. S2) is present in the attachments. We then started searching the literature for animal models presenting mutations similar to any of those listed in the HGMD database. We focused our attention on animal models having mutations similar to those observed in human patients, falling in one of the following situations: having mutations interrupting the reading frame of an exon which is affected also in humans by the same type of mutation; having deep intronic mutations in the same intron as the human counterpart; having synonym exonic mutations in the same exon as in humans. We were able to identify only one animal model with such characteristics. This animal model is a mouse bearing a spontaneous insertion on *Cacna2d4* exon 25 (K. A. Wycisk et al. 2006) leading to frameshift in a similar way to the nonsense mutation on the same exon of *CACNA2D4* found in a family affected by retinal dystrophy (K. A. Wycisk et al. 2006).

We then decided to expand our search also to genes lacking an animal model, but having a modular structure similar to that of the dystrophin gene. This because in such genes an exon-skipping approach can be more feasible since the removal of one domain in a protein where such domain is repeated in a series is less likely to severely impact protein functionality. We were able to identify a gene with such characteristics, *USH2A*, where many known mutations fall into exons coding for the repeated EGF-Lam and FN3 domains.

We finally searched for genes having newly identified mutations in deep intronic regions far from the consensus for SD and SA splice sites which increase exon inclusion as a pathological mechanism. By this final search we were able to identify a mutation in *RPGR* (Neidhardt et al. 2007).

5.2 CACNA2D4

5.2.1 Computational analysis of *Cacna2d4* splicing

To correct the genetic defects caused by CACNA2D4 mutations on E25 we decided to base our strategy on exon-skipping chimeric U1 snRNAs masking sites important for splicing. The skipping of E25 alone is not applicable, since the joining of exons 24 and 26 results in frameshift both in humans and mice. To solve this problem, the minimal region that needs to be skipped comprises exons 23-24-25-26 both in humans and mice. In mice, also removal of only exons 23-24-25 is enough to restore the reading frame. Skipping of these exons would result in a rescued protein that is no more truncated after the first Cache domain, since it is retaining all structural domains encoded by the exons downstream of the mutation: the second Cache domain and the δ peptide (Fig. 16). For the design of a multiexon-skipping approach, U1snRNAs need to be directed against splicing-relevant sequences present on all exons that need to be skipped. Alignment of both human and mouse coding sequences revealed an overall 85% homology, percentage maintained between exons 23-24-25-26 (Fig. S1) and in the alignment of the corresponding protein sequences (Fig. S2). The multiexon-skipping strategy has been considered for Duchenne muscular dystrophy, in order to expand the pool of patients which can be addressed by a single mix of AONs (Aartsma-Rus et al. 2004). In alternative to that, a relatively simpler approach consist in targeting only the first and last exon. Their targeting by chimeric U1 snRNA can in fact induce the generation of splicing events which skip all the four or only three exons.

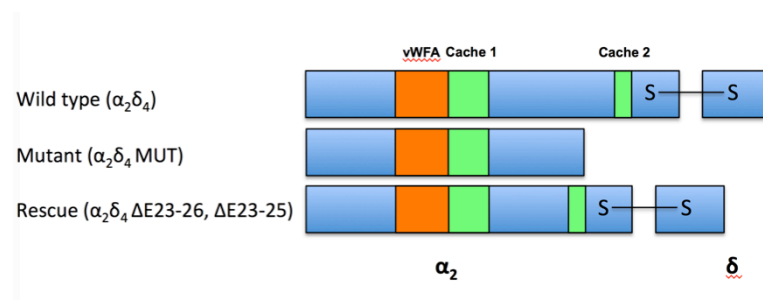


FIGURE 16. Schematic representation of the effect of the exon-skipping approach on CACNA2D4. The effect of the mutation is to truncate the ORF of CACNA2D4 after the first Cache domain ($\alpha_2\delta_4$ MUT). The rescued transcripts, resulting from skipping of exons 23 to 26 or 23 to 25, would encode for a shorter protein, missing the part encoded by the skipped exons, but retaining the domains located downstream of the mutation ($\alpha_2\delta_4 \Delta E23-26, \alpha_2\delta_4 \Delta E23-25$)

Even if all CACNA2D4 targeted exons are believed to be constitutive exons of *Cacna2d4*, the multiexon-skipping approach is complex, and can potentially generate different mis-spliced products. Therefore the design of an exon-skipping strategy must envision, at the best approximation possible, how splicing normally occurs among this exons in presence and absence of the mutation. In this regard, and focusing first on the mouse model, we started applying a bioinformatics strategy aiming at retrieving all existing data on *Cacna2d4* splicing, with a particular emphasis on the region surrounding E25.

From a first analysis of deposited sequences, we realized that an incorrectly annotated NCBI entry for *Cacna2d4* full-length was actually a potential new splicing isoform, missing exon 16 (BC 141091.1). Since nothing is known about murine *Cacna2d4* and its splicing isoforms, and since there is no indication on which is the functional isoform able to increase expression of functional L-type calcium channels in the murine retina, we decided to consider also this isoform as relevant to our investigation.

We then started searching the Gene Expression Omnibus (GEO) database for next generation sequencing (NGS) RNA datasets of wild type mouse eye or retina. We found 4 RNA-seq datasets of mouse eye and one dataset of mouse retina (dataset ID GSE38359: sample IDs GSM945628, GSM945631 and GSM945634; dataset ID GSE29752: samples GSM737548 and GSM737550). Alignment of the reads contained in each dataset to the genomic sequence of *Cacna2d4* revealed the splicing pattern of *Cacna2d4*. Interestingly, when focusing on the region delimited by exons 23 and 26, we noticed a significant number of reads covering a portion of intron 25 proximal to the 3' end of exon 25 (Fig. 17). Moreover, some of these reads were partially overlapping with exon 24 and with exon 26, but not with the canonical E25. Thus the identified region in intron 25 can possibly be a new alternatively spliced exon, mutually exclusive with exon 25. We named this putative new exon (205bp long) as exon 25b (E25b). Analysing the relative coverage levels between E25 and E25b it is possible to predict that transcripts containing E25b are less represented than those including E25 (Fig. 17). Inclusion of E25b between exon 24 and 26 creates an new stretch of 53 amino acids followed by a stop codon, resulting in the termination of the *Cacna2d4* reading frame between the two Cache domains and thus in a transcript not encoding for the second Cache domain and for the whole δ peptide. It is curious to note how the c.2451insC

mutation on E25 truncates the reading frame in the same position. We tried to confirm if also in humans E25 was alternatively spliced, but recovered human RNA-seq data presented low coverage of the region of interest and it was thus not possible to analyse the splicing pattern.

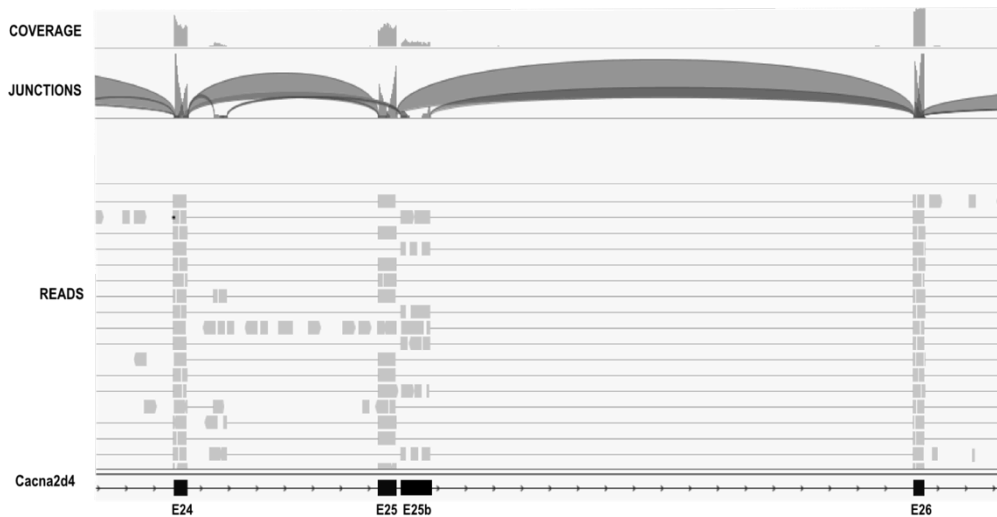


FIGURE 17. Integrative Genomic Viewer (IGV) visualization of the RNA-seq eye sample GSM737548 aligned to *Cacna2d4* genomic sequence. Position of E25b has been included. Junctions represent reads spanning over two exons: alternative splicing of E25 and E25b can be observed.

We also analysed the position of exon 16, to assess the presence of mature transcripts skipping this exon in the retina. Even if in a few reads skipping of exon 16 was present, this isoform does not seem to be the main one present in the eye (Fig. 18).

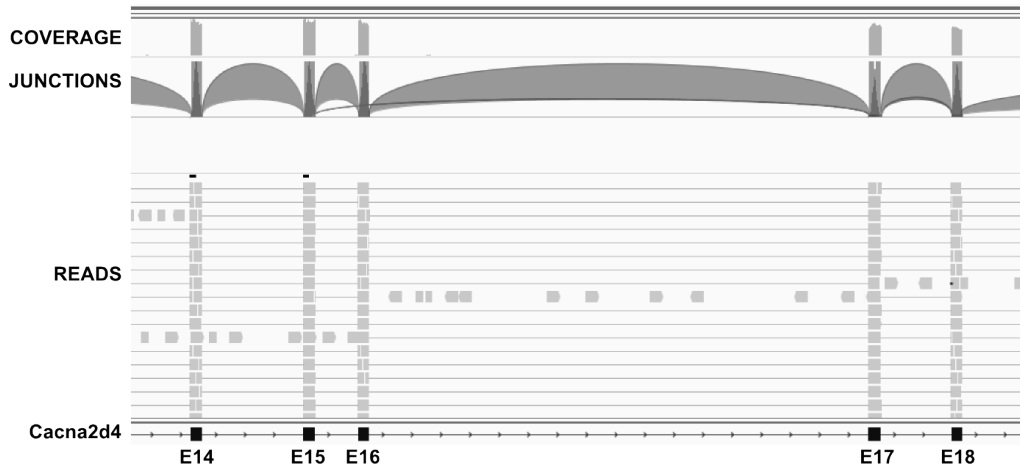


FIGURE 18. IGV visualization of the RNA-seq eye sample GSM737548 aligned to *Cacna2d4* genomic sequence. It is possible to notice the few reads skipping exon 16.

To acquire more evidence in support of E25b presence as a putative alternatively spliced exon, we performed an analysis of the splice sites of all the exons between exon 22 and 27 using the splice-site predictor NNSPLICE 0.9 (Reese et al. 1997). The results show E25b having stronger 3' and 5' splice sites compared to the canonical E25 (Tab. 2). In particular the 3' splice site of E25 is very weak, while the 3' splice site of E25b is relatively strong. This strengthens the hypothesis that E25 is alternatively spliced with E25b in the retina.

	Score	Sequence 5' > 3'
E22 5'splice site	0.52	ctggagt g tgagttc
E23 3'splice site	0.92	ttcctgtgactttaccctc ag gtgacgaggaactggtgcgg
E23 5'splice site	0.85	tctctga g tacgtac
E24 3'splice site	0.93	tgttgttgctttgcctcgc ag agagtcagagcctggcgtgg
E24 5'splice site	0.99	ctgacag g tgagccc
E25 3'splice site	0.43	acatcaatcctactctc acag gaagttcctgaccctgaag
E25 5'splice site	0.92	ggaccag g tAACGga
E25b 3'splice site	0.93	cctctctgtgctcttcccc ag agtggaaaaaggagatgtg
E25b 5'splice site	0.99	tccaag g tgagatc
E26 3'splice site	0.98	caataattctcattttcc ag atagcccaggcaagccagtg
E26 5'splice site	1.00	gcagcag g tAAGagc
E27 3'splice site	0.98	cctcctcctgtttcctgc ag ctgtgggatccagatgcaa

TABLE 2. Splice site scores of *Cacna2d4* exon 22 to 27. The higher is the score, the stronger is the splice site. A perfect match to the splice site consensus sequence is indicated with 1.

The presence of the putative E25b can give a different light to the effect of the mutation found in the murine model. It is in fact possible that the mutation not only truncates the reading frame of the protein, but also alters the way E25 is recognized by

the splicing machinery. We therefore investigated the possible role of this mutation on splicing using the webserver spliceAid (Piva et al. 2009). SpliceAid is a regularly updated and manually curated tool which predicts *cis*-acting sequences that enhance or inhibit exon recognition, giving positive scores for the first and negative for the second. The higher is the absolute value of the score, the better is the prediction presented. The analysis of E25 sequence in presence and absence of the mutation (Fig. 19) revealed how the mutation is predicted to introduce a new ESS, which may impair recognition of the mutated exon 25. Specifically, the mutation creates a sequence of 8 cytosines which is predicted to be recognized with high scores by 8 different splicing factors inhibiting exon recognition. Only one *trans*-acting splicing factor improving exon recognition was predicted with a low score (Tab. 3).

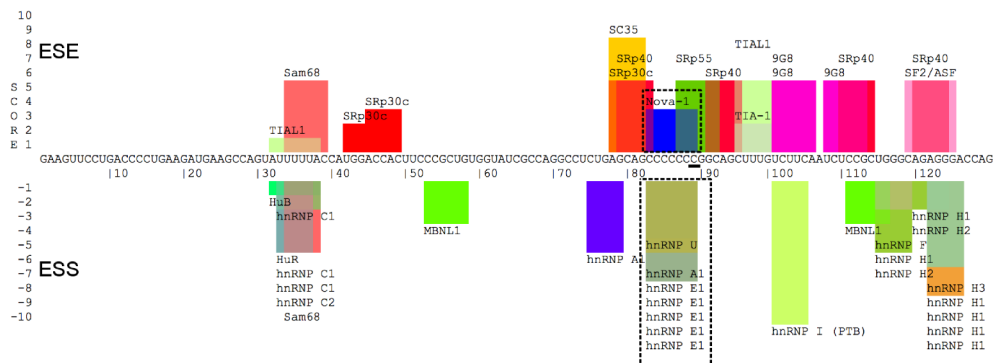


FIGURE 19. Prediction for ESE and ESS in Cacna2d4 E25. New predictions generated by the c.2451insC mutation are reported. The site of the mutation is underlined in black.

Protein Name	Position in E25 mut	Recognized Sequence	Score	Function
hnRNP E1	83-89	CCCCCCC	-7	ESS
hnRNP E2	83-89	CCCCCCC	-7	ESS
hnRNP K	83-89	CCCCCCC	-7	ESS
HuR	83-89	CCCCCCC	-7	ESS
hnRNP I (PTB)	83-89	CCCCCCC	-7	ESS
hnRNP A1	83-89	CCCCCCC	-5	ESS
RBM5	83-89	CCCCCCC	-5	ESS
hnRNP U	83-89	CCCCCCC	-4	ESS
Nova-1	83-89	CCCCCCC	3	ESE

TABLE 3. Complete list of predicted *trans*-acting splicing factors binding to mutant E25 only. The higher is the absolute value of the score, the better is the binding prediction. The sign of the prediction reveals if the protein is believed to impair exon recognition (negative scores, ESS), or promote it (positive scores, ESE).

Performing the same analysis on human E25, it is possible to predict a similar effect. The CACNA2D4 mutation c.2406C→A in fact abolishes an ESE and replaces it with an ESS (Fig. 20). If E25 is alternatively spliced also in humans, the mutation could therefore change the ratio between the two exons in mature mRNA.

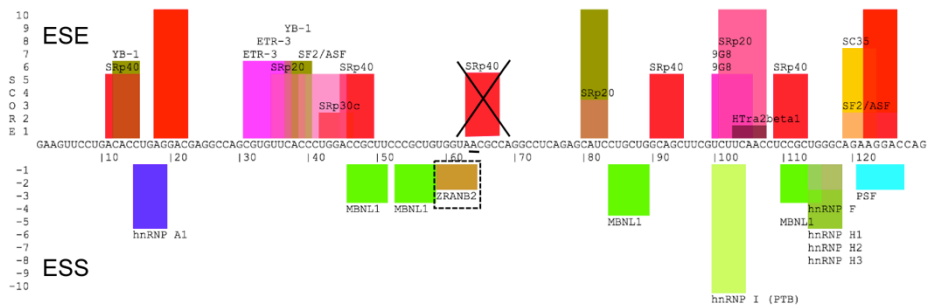


FIGURE 20. Prediction for ESE and ESS in CACNA2D4 E25. The figure underlines changes induced by the human mutation in E25. The position of the nucleotide substitution is underlined in black. Abolished ESE are crossed, new ESS are boxed.

5.2.2 *In vivo* characterization of E25 splicing

Following our bioinformatics analysis, we decided to confirm the presence of E25b *in vivo* in mouse retinae and investigate a possible role for the c.2451insC mutation on splicing. RT-PCR was conducted on retinae of wild type and mutant animals using primers on exon 24 and on exon 26. Discrimination between E25 and E25b containing transcripts was possible thanks to the different size of the two alternatively-spliced exons (E25: 128bp; E25b: 205bp). By this analysis, we were able to confirm the presence of *Cacna2d4* E25b alongside the canonical one in the retina of wild type and mutant mice (Fig. 21 A). The effect of the mutation was to decrease levels of E25 containing transcripts, as observed by densitometric analysis of the obtained bands (Fig. 21 B). Levels of E25b were instead similar in presence or absence of the mutation. For a better understanding of how the mutation impacts on the level of the two splicing isoforms in the retina, we performed RT-qPCR analysis using specific primers for the two splicing isoforms. Our results showed a marked three-fold decrease in the levels of E25 in the mutant compared to wild type retinae (Fig. 22 A), in line with what observed with densitometric analysis. The reduction in E25 containing transcripts follows the general reduction observed in *Cacna2d4* mRNA using primers on the 3' untranslated region (UTR) and previously observed with RT-qPCR performed on the last exon of the gene (K. A. Wycisk et al. 2006). This reduction could be ascribed, apart from the effect of the mutation on splicing, to nonsense mediate decay acting on the mutant transcripts. Exon 25b levels are instead much less affected in the mutant (Fig. 22 A). We then compared the relative levels of E25 versus E25b in presence and absence of the mutation. In normal conditions E25 is three times more abundant in final transcripts than E25b. In presence of the mutation in E25, the situation changes dramatically, and both exons are present almost at the same levels (Fig. 22 B).

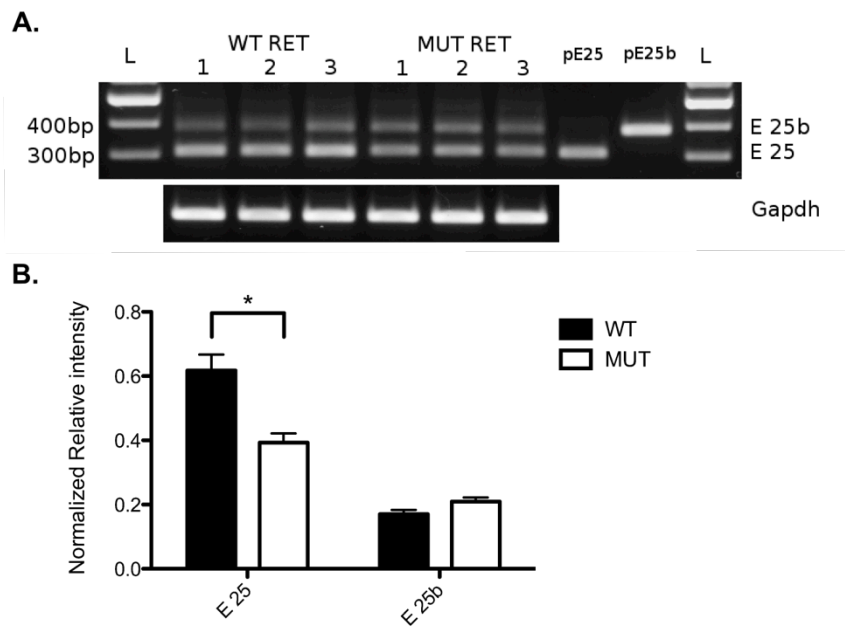


FIGURE 21. RT-PCR of wild type and mutant mouse retinae. (A) Numbers represent different pools of wild type and mutant retinae. Plasmids containing *Cacna2d4* sequence with E25 (pE25) or with E25b (pE25b) were used as controls. Presence of both E25 and E25b can be observed. (B) Densitometric analysis of the RT-PCR on wild type and mutant mouse retinae reveals a reduction of E25 containing plasmid ($P < 0.05$).

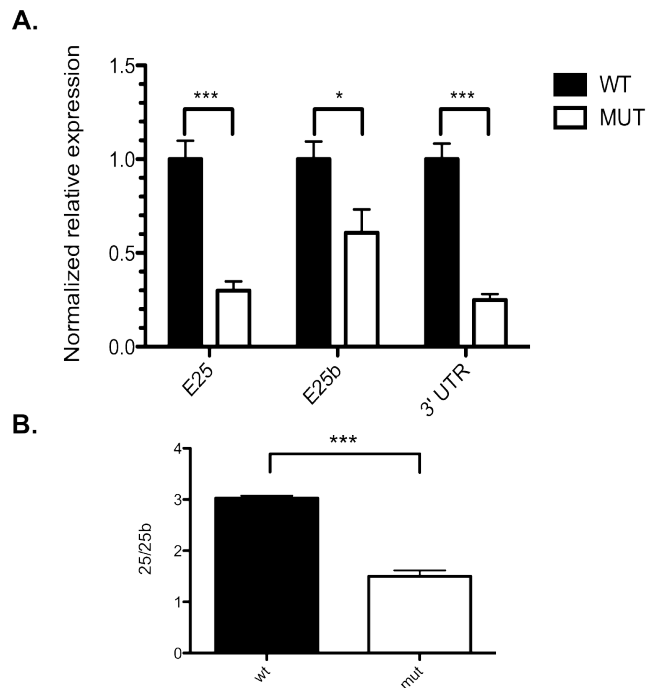


FIGURE 22. RT-qPCR of wild type and mutant mouse retinas. (A) Quantification of *Cacna2d4* E25, E25b and 3' UTR using RT-qPCR on three different pools of mouse retinas. A more pronounced reduction of E25 ($p < 0.001$) compared to E25b ($p < 0.05$) containing transcripts was observed. (B) Relative abundance of E25 over E25b containing transcripts in mouse retinas. The mutation favours E25b presence ($p < 0.001$).

5.2.3 A splicing-reporter minigene for *Cacna2d4*

Splicing-reporter minigenes are potent instruments for the investigation of the effect that mutations have on splicing, and for the validation of different antisense molecular tools designed to modulate splicing. In our specific case, a minigene able to recapitulate all splicing events between exons 22 and 27 would offer a unique opportunity to better understand the effect of the 2451insC mutation on splicing of E25, and to effectively screen different chimeric U1snRNAs able to mediate skipping of exons 23 to 25, or 23 to 26. Since the genomic region spanning from *Cacna2d4* exon 22 to exon 27 is too large to be cloned in a plasmid (36 Kb), we decided to partially remove introns larger than 1.5 Kb, with the precaution of leaving 500 bp of intronic sequence around each splice site and the sequence of E25b. A start codon was added at the beginning of exon 22 and a luciferase reporter was cloned after exon 27 (Fig. 23 A). Proper splicing between exon 22 – 23 – 24 – 25 and 27 would permit the ORF between exon 22 and the Luc2 reporter to be maintained, resulting in luciferase expression. We also mutagenized

the minigene to add the insertion on E25. In the mutant minigene luciferase expression would be abolished by presence of the mutant exon, and only rescued by effective skipping of exons 23 to 26 or 23 to 25. Since the presence of all spliced exons before the luciferase reporter encodes for additional 187 residues, this could result in loss of enzymatic activity of the reporter. We thus performed a luciferase assay testing wild type and mutant minigenes transfected in HEK293T cells (Fig. 23 B). The wild type minigene showed poor luciferase activity, at a comparable level with the mutant minigene. This indicates that in fact luciferase can not be the optimal reporter to assess splicing with our minigene, and therefore RT-PCR represents a better choice. A possible explanation for not having observed luciferase activity from the wild-type minigene is that the peptide encoded by *Cacna2d4* exons 22 to 27 blocks the enzymatic activity of the Luciferase.

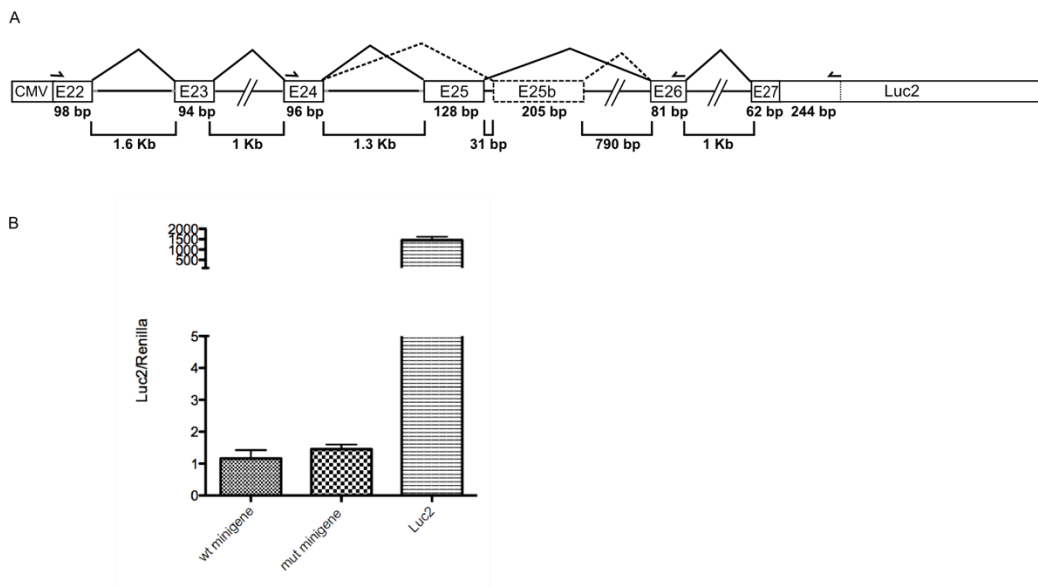


FIGURE 23. *Cacna2d4* splicing-reporter minigene. (A) Schematic representation of *Cacna2d4* splicing-reporter minigene. The length of the different exons (boxes) and introns (straight lines) is shown. Arrows represent the position of the different sets of primers used for the different RT-PCR. The position of the luciferase reporter (Luc2) is shown. (B) Luciferase assay of HEK293T cells transfected with wild type minigene, mutant minigene, or with vector expressing Luc2 (positive control).

5.2.4 *In vitro* characterization of exon 25 splicing

The obtained Cacna2d4 minigenes can be used to better understand the effect of the 2451insC mutation on splicing of exon 25 and 25b in a different system. We therefore transfected HEK293T cells with wild type and mutant minigenes and assessed splicing across all exons present on the minigenes by RT-PCR and RT-qPCR. Using primers on exon 22 and 27 it was possible to observe how the minigene is able to properly recapitulate all splicing events between the different exons, as two bands at around 800 bp were present in both wild type and mutant minigenes. The lower band should represent transcripts including exon 25, the upper one those containing the larger exon 25b (Fig. 24 A, first line). It is interesting to note how, with this first PCR, in the mutant the upper band is more intense than the lower, whereas using the wild type minigene both bands appear to have the same intensity. This finding suggests a role for the mutation on splicing of exon 25b also in HEK293T cells, in which it favours exon 25b presence. To confirm this data we first performed an additional RT-PCR using primers on exon 24 and 26. Two distinct bands were observable: the upper containing exon 25b, the lower containing exon 25 (Fig. 24 A, second line). Also with this PCR the mutation causes an increase in exon 25b containing transcripts, as shown by the densitometric analysis (Fig. 24 B). We finally confirmed this data by RT-qPCR with specific primers for the two splicing isoforms (Fig. 25 A). By direct comparison of the relative abundance of the two splicing isoforms it is possible to observe how the mutation affects the ratio between exon 25 and 25b, showing a trend that favours exon 25b presence (Fig. 25 B). Contrarily to what observed *in vivo*, where the mutation primarily affects exon 25 levels, in transfected cells it does not significantly impact on exon 25 recognition. The effect is instead to favour exon 25b presence.

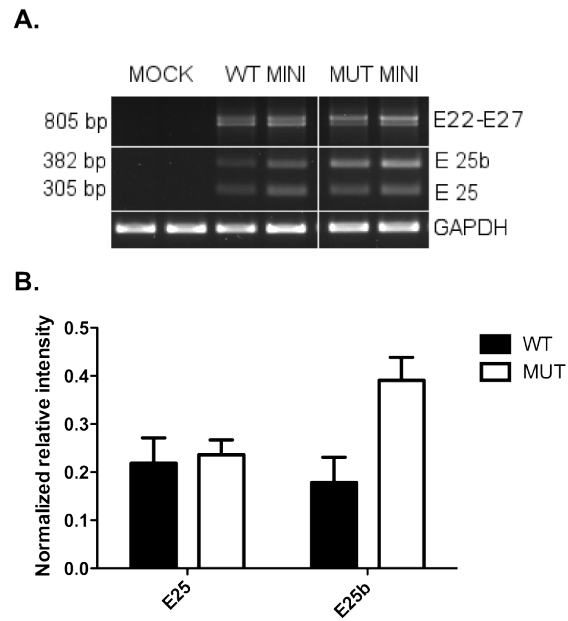


FIGURE 24. RT-PCR on wild type and mutant *Cacna2d4* minigenes in HEK293T cells. (A) The first line shows the occurrence of proper splicing between all exons included in the minigene. Two bands, close to 850 bp, are distinguishable. The lower is caused by E25 inclusion (805bp), the upper by E25b (882bp). The second line confirms the presence of E25b-containing transcripts alongside E25-containing ones. Wild type minigene (wt mini); mutant minigene (mut mini). (B) Densitometric analysis of the RT-PCR on wild type and mutant minigenes. The mutation acts on splicing by favouring E25b inclusion.

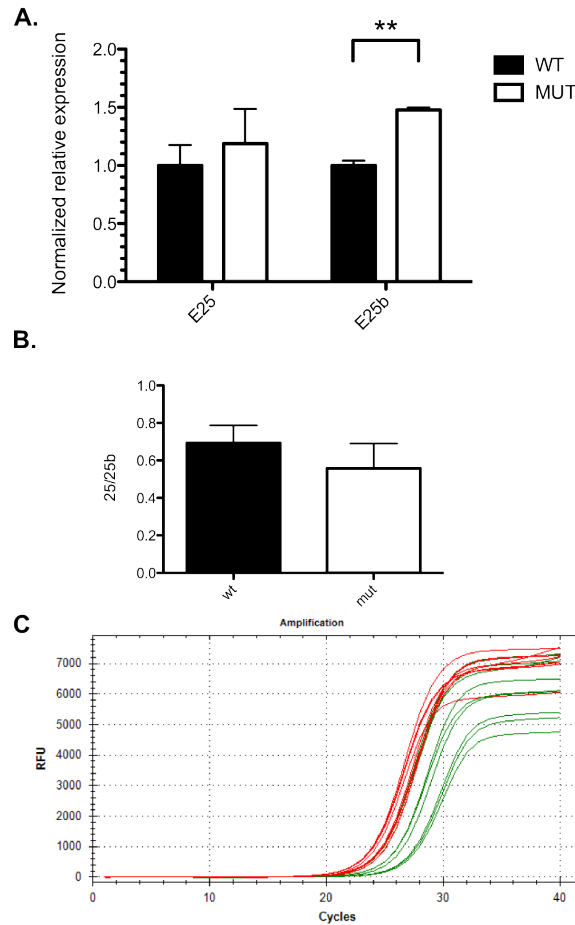


FIGURE 25. RT-qPCR of the two splicing isoforms from HEK293T cells transfected with the different minigenes. (A) The mutation causes an increase in the levels of the splicing isoform including E25b ($p < 0.01$). (B) Relative abundance of E25 over E25b containing transcripts in HEK293T cells transfected with minigene splicing reporter systems. The mutation favours E25b presence. (C) Amplification curves of E25b in presence (red, mutant minigene) or absence (green, wild-type minigene) of the mutation.

5.2.5 Analysis of $\alpha_2\delta_4\Delta E16$ splicing isoform expression in the central nervous system (CNS) and neuroendocrine system.

From our bioinformatics analysis we noticed the presence of an uncharacterized splicing isoform of *Cacna2d4* missing exon 16 ($\alpha_2\delta_4\Delta E16$) coming from a whole brain cDNA library. Skipping of exon 16 causes the removal of a consistent portion of the first Cache domain of *Cacna2d4*, and thus this isoform can show different properties compared to the full-length one. Aiming at understanding the relevance of this isoform in the mouse retina and possibly in other districts, we performed an RT-PCR analysis using primers on exon 15 and 17. In line with the analysed RNA-seq data, $\alpha_2\delta_4\Delta E16$

was not detectable in wild type or mutant mouse retinae, where exon 16 is constitutively present (Fig. 26 A, B). The same splicing pattern is present in the pituitary gland. Interestingly, in the cerebellum (CB), somatosensory cortex (SSC), occipital cortex (OC) and hippocampus the only detected isoform is $\alpha_2\delta_4 \Delta E16$, which is present at very low levels. The hypothalamus (HPT) is instead the only analysed region where both splicing isoform are present.

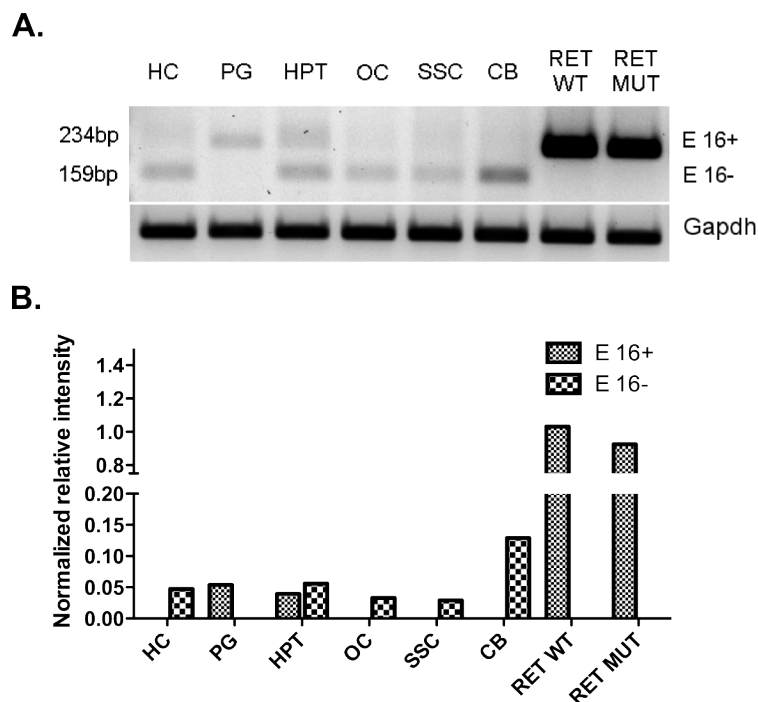


FIGURE 26 Analysis of $\alpha_2\delta_4 \Delta E16$ splicing isoform presence in the CNS and neuroendocrine system. (A) RT-PCR with primers flanking E16 on mouse hippocampus (HC), pituitary gland (PG), hypothalamus (HPT), occipital cortex (OC), somatosensory cortex (SSC), cerebellum (CB), WT (RET WT) and mutant (RET MUT) retina. (B) Densitometric analysis of RT-PCR.

5.2.6 Functional characterization of different $\alpha_2\delta_4$ variants

In order to assess the feasibility of the envisioned exon-skipping approach, the functionality of the $\alpha_2\delta_4$ proteins resulting from the removal of exons 23 to 26 ($\alpha_2\delta_4 \Delta E23-26$) or of exons 23 to 25 ($\alpha_2\delta_4 \Delta E23-25$) needs to be assessed. To achieve this goal, the characterization of full length $\alpha_2\delta_4$ is first needed. Moreover we decided to characterize the two newly identified splicing variants $\alpha_2\delta_4 \Delta E16$ and $\alpha_2\delta_4 E25b$.

The $\alpha_2\delta$ subunit of HVA calcium channels is known to increase the number of functional channel complexes on the plasma membrane, therefore increasing current densities of stimulated cells in which the different components of the channel are expressed. Another characteristic shared by different members of this protein family is to speed up the rate at which HVA calcium channels inactivate after stimulation (Dolphin, 2013). To investigate these aspects we exploited the potentiality of whole-cell patch clamp applied to an heterologous expression system: tsA-201 cells. We therefore cloned in expression vectors the different subunits of the mouse Cav1.4 calcium channel, believed to be those interacting in mouse photoreceptors: Cav1.4 α_1 , β_2 , and $\alpha_2\delta_4$. We also obtained the different $\alpha_2\delta_4$ variants, all cloned in pIRES2-EGFP vectors for being able to select transfected cells during recordings. A summary of all obtained constructs is presented (Fig.27).

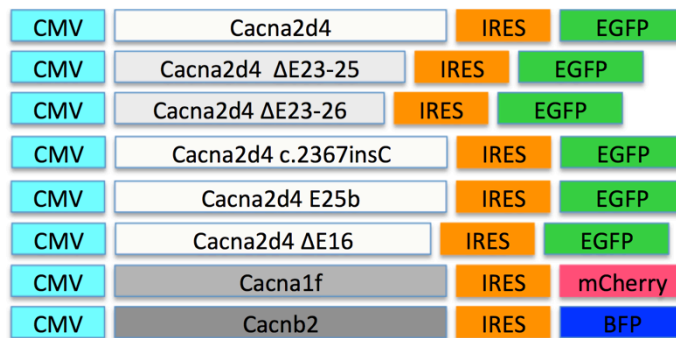


FIGURE 27. Scheme of the different constructs for electrophysiological analysis cloned in pIRES vectors.

Following transfection of tsA-201 cells with mouse Cav1.4 α_1 , β_2 and $\alpha_2\delta_4$ we never succeeded in obtaining conditions in which transfected cells were recordable. We tried different transfection conditions, different amounts of DNA transfected, and we also tried to use culture conditions with low calcium. Cells were always very difficult to patch, unstable, and those recordable were showing no inducible currents. We therefore tried substituting mouse Cav1.4 α_1 and β_2 with human Cav1.4 α_1 (Sinnegger-brauns et al. 2009) and rat β_3 (Castellano et al. 1993). With this conditions we succeeded in having recordable cells, thus we used them in all shown experiments.

Since the alteration of the $\alpha_2\delta_4$ open reading frame due to protein truncation (for $\alpha_2\delta_4$ MUT and $\alpha_2\delta_4$ E25b) or a partial deletion (for $\alpha_2\delta_4$ Δ E23-25, $\alpha_2\delta_4$ Δ E23-26 and $\alpha_2\delta_4$

$\alpha_2\delta_4 \Delta E16$) could potentially result in protein instability, we confirmed by Western blot the presence of the different $\alpha_2\delta_4$ variants in tsA-201 cells after transfection. As shown in figure 4, $\alpha_2\delta_4$ is present in all condition tested (lines 2-7) and absent in tsA-201 (line 1). The $\alpha_2\delta_4$ MUT and $\alpha_2\delta_4$ E25b show the smallest dimension, since the protein is truncated in both cases after exon 25. The $\alpha_2\delta_4 \Delta E16$ is instead very close to the wild type ($\alpha_2\delta_4$) size, missing only exon 16. The two constructs $\alpha_2\delta_4 \Delta E23-25$, $\alpha_2\delta_4 \Delta E23-26$ show an intermediate size, since they lack three or four exons compared to the wild-type, but retain the portion of the protein downstream of them, which is instead not present in $\alpha_2\delta_4$ MUT and $\alpha_2\delta_4$ E25b.

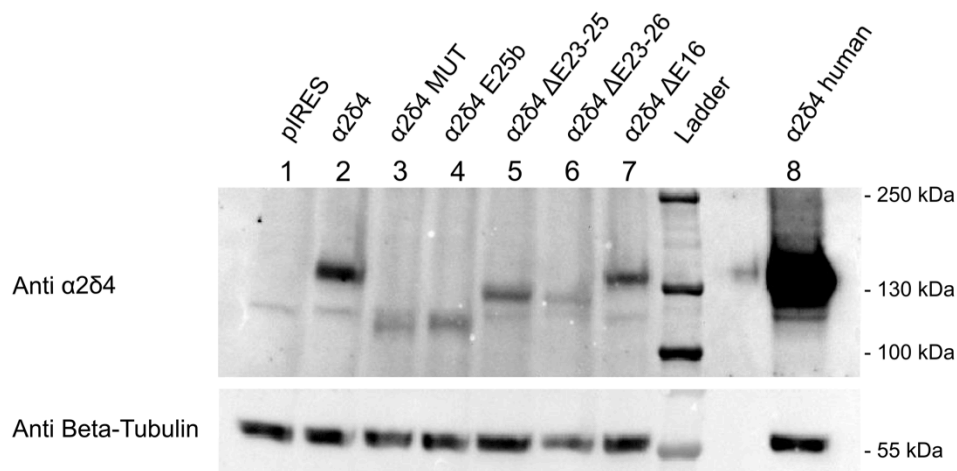


FIGURE 28. Expression of the different $\alpha_2\delta_4$ variants in tsA-201 cells after transfection. A specific band for $\alpha_2\delta_4$ is visible following tsA-201 transfection with Cav1.4 α_1 , β_3 , and constructs encoding all the different $\alpha_2\delta_4$ variants utilized (lanes 2-7). The $\alpha_2\delta_4$ band changes in size accordingly to the relative length of the expressed variant. In the negative control (lane 1) $\alpha_2\delta_4$ is not detectable, proving the absence of endogenous $\alpha_2\delta_4$ in tsA-201 cells. A condition where human $\alpha_2\delta_4$ was transfected ($\alpha_2\delta_4$ human) has been added as an additional positive control (lane 8).

We began by analysing current densities evoked by an activation protocol in presence of 15mM Ca^{2+} as charge carrier. The protocol consisted in 50 ms pulses at different potentials, ranging from -79 to 52 mV (Fig. 26 A). We first compared full length $\alpha_2\delta_4$ with the more investigated $\alpha_2\delta_1$ (Koschak et al., 2003) and noticed how $\alpha_2\delta_4$ expression is able to mediate an increase in current densities at the different tested potentials even if to a lower degree than $\alpha_2\delta_1$, in a similar way to what has been recently shown with human $\alpha_2\delta_4$ by Lee and collaborators (Lee et al. 2014) (Fig. 29 A-B). We then tested the two different splicing isoforms $\alpha_2\delta_4 \Delta E16$ and $\alpha_2\delta_4$ E25b, and showed how they are not able to mediate an increase in current densities, as their effects are similar to that of mutant $\alpha_2\delta_4$ ($\alpha_2\delta_4$ MUT) or of the empty vector (pIRES) (Fig. 29 A-B-C). We statistically compared the different tested conditions considering the maximal

current densities obtained for each recorded cell. Of the different $\alpha_2\delta_4$ splice variants, only full length $\alpha_2\delta_4$ was able to mediate a significant increase of about three-folds in current densities (Fig. 29 C, Tab. 4). For the condition from which we were able to obtain an activation curve, we compared the obtained parameters for the voltage of half-maximum activation ($V_{0.5, act}$) and the slope of the curve (K_{act}). No differences were observable in relation to Cav1.4 $\alpha_1 + \beta_3$ alone, indicating that none of the tested $\alpha_2\delta_4$ constructs is able to affect the activation of Cav1.4 calcium channels (Fig. 31 A, Tab 4).

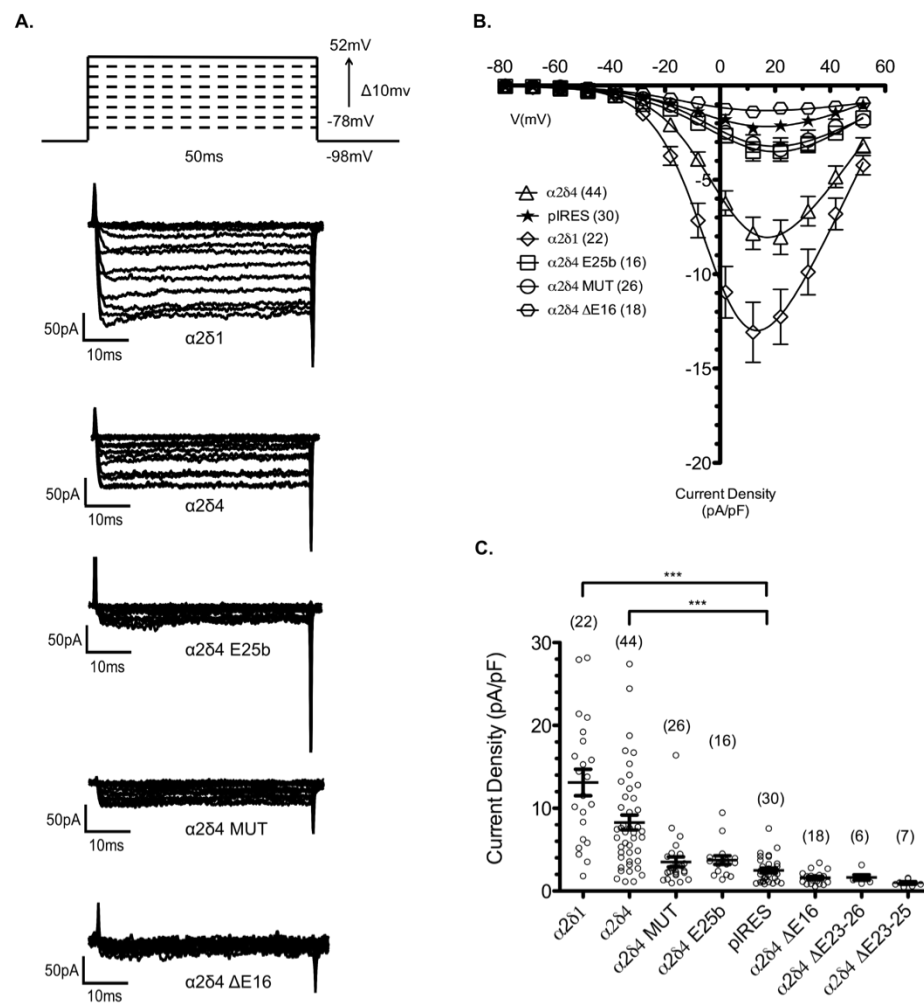


FIGURE 29. Effect of different $\alpha_2\delta_4$ variants on Cav1.4 mediated current density. (A) Scheme of the recording protocol and representative sample traces for some of the different tested conditions. (B) Representation of the changes in current density at the different voltages tested for $\alpha_2\delta_1$, $\alpha_2\delta_4$, $\alpha_2\delta_4$ E25b, $\alpha_2\delta_4$ MUT (c.2451insC), $\alpha_2\delta_4$ Δ E16, pIRES (empty vector). Mean values, SEM, and the best fits of the current voltage relation are shown. The total number of cells considered for each curve is reported in parentheses. (C) Voltage-dependent activation curve of $\alpha_2\delta_1$, $\alpha_2\delta_4$, $\alpha_2\delta_4$ E25b, $\alpha_2\delta_4$ MUT (c.2451insC), $\alpha_2\delta_4$ Δ E16, pIRES (empty vector). (D) Maximal current densities of cells measured in the presence of different $\alpha_2\delta_4$ subunits in comparison to $\alpha_2\delta_1$ and pIRES. For each condition mean and SEM are shown. Selected pairs of conditions were compared using Kruskal-Wallis test followed by Dunn's multiple comparison post-test ($p < 0.001 = ***$).

Since the purpose of our exon-skipping approach is to resolve the functional problem caused by mutations on CACNA2D4 exon 25 which lead to truncation of the gene ORF, we tested if the rescued protein $\alpha_2\delta_4 \Delta E23-26$ and $\alpha_2\delta_4 \Delta E23-26$ were able to stimulate current densities through Cav1.4 calcium channels more effectively than $\alpha_2\delta_4$ MUT. As evident from the comparison of observed maximal current densities, this was not the case (Fig. 29 C). This result strongly indicates that the designed therapeutic approach is actually unfeasible because the protein region that is deleted as a consequence of exon skipping is fundamental for the functionality of the protein. Such a conclusion was unpredictable as no characterization of the protein region was available before hand.

Aiming at better investigating a possible regulatory function of the two splicing isoforms $\alpha_2\delta_4 \Delta E16$ and $\alpha_2\delta_4 E25b$ on Cav1.4 calcium channels, we tested if they showed a dominant-negative effect on the activity of functional channels. Being that in both isoforms the normal architecture of $\alpha_2\delta$ subunits is not preserved, these isoforms can actually act by negatively counteracting the effect of a functional $\alpha_2\delta_4$. To test this hypothesis we transfected tsA-201 cells with constructs encoding for Cav1.4 α_1 , β_3 and $\alpha_2\delta_4$. In addition to the full length $\alpha_2\delta_4$, we added in the transfection mix the same amounts of constructs encoding for $\alpha_2\delta_4 \Delta E16$ or $\alpha_2\delta_4 E25b$, and measured current densities obtained from transfected cells stimulated with the same protocol described before. None of the isoforms tested showed an ability to significantly impair $\alpha_2\delta_4$ activity of stimulating current density levels through Cav1.4 calcium channels (Fig. 30 A,B). Therefore a possible dominant-negative effect of the different isoforms on $\alpha_2\delta_4$ was excluded.

To complete the characterization of $\alpha_2\delta_4$, we finally tested its effect on inactivation of Cav1.4. At first we analysed voltage-dependent inactivation of Cav1.4 in presence of $\alpha_2\delta_4$ and compared it to that observed with $\alpha_2\delta_1$. For this purpose we utilized an inactivation protocol consisting in a 50ms test-pulse before and after 5s pulses at different potentials (from -98 to 22 mV). The calculated parameters of the inactivation slope were comparable between $\alpha_2\delta_4$ and $\alpha_2\delta_1$, showing that $\alpha_2\delta_4$ and $\alpha_2\delta_1$ have similar effects on voltage-dependent inactivation of Cav1.4 (Fig. 31 B, Tab 4). We also looked at a possible effect of $\alpha_2\delta_4$ on calcium-dependent inactivation. We therefore applied 300ms pulses at different potentials in presence of Ca^{2+} and Ba^{2+} . Expression of $\alpha_2\delta_4$ did

not induce an increased inactivation rate of Cav1.4 over 250 ms (r_{250}) in presence of Ca^{2+} compared to Ba^{2+} over a voltage range from -40 to +40 mV, and results were comparable to those obtained with $\alpha_2\delta_1$ by Burtscher and collaborators using the same settings (Burtscher et al. 2014) (Fig. 31 D). The percentage of remaining current during 250 ms test pulse to 2 and 12 mV (which was the voltage of the maximum current with Ba^{2+} and Ca^{2+}) was 90% for Ba^{2+} and 91% for Ca^{2+} , with no significant difference observed ($P = 0.56$). Comparable results were recently reported using human $\alpha_2\delta_4$ subunit (Lee et al. 2014).

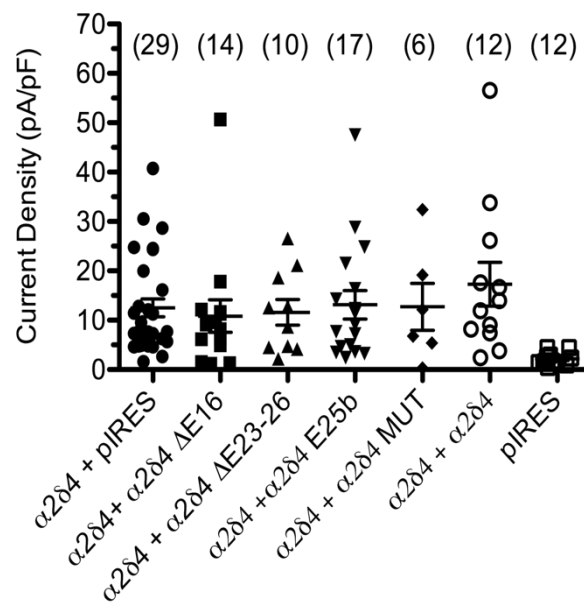


FIGURE 30. Effect of the coexpression of full length $\alpha_2\delta_4$ with other $\alpha_2\delta_4$ variants. The full length $\alpha_2\delta_4$ construct was cotransfected with equal amounts of other $\alpha_2\delta_4$ variants. No significant differences on maximal current density were observed in any of the tested conditions as compared with $\alpha_2\delta_4 + \alpha_2\delta_4$, or with $\alpha_2\delta_4 + \text{pIRES}$. As a result no dominant negative effect of the different variants on $\alpha_2\delta_4$ activity was observable in the employed experimental conditions.

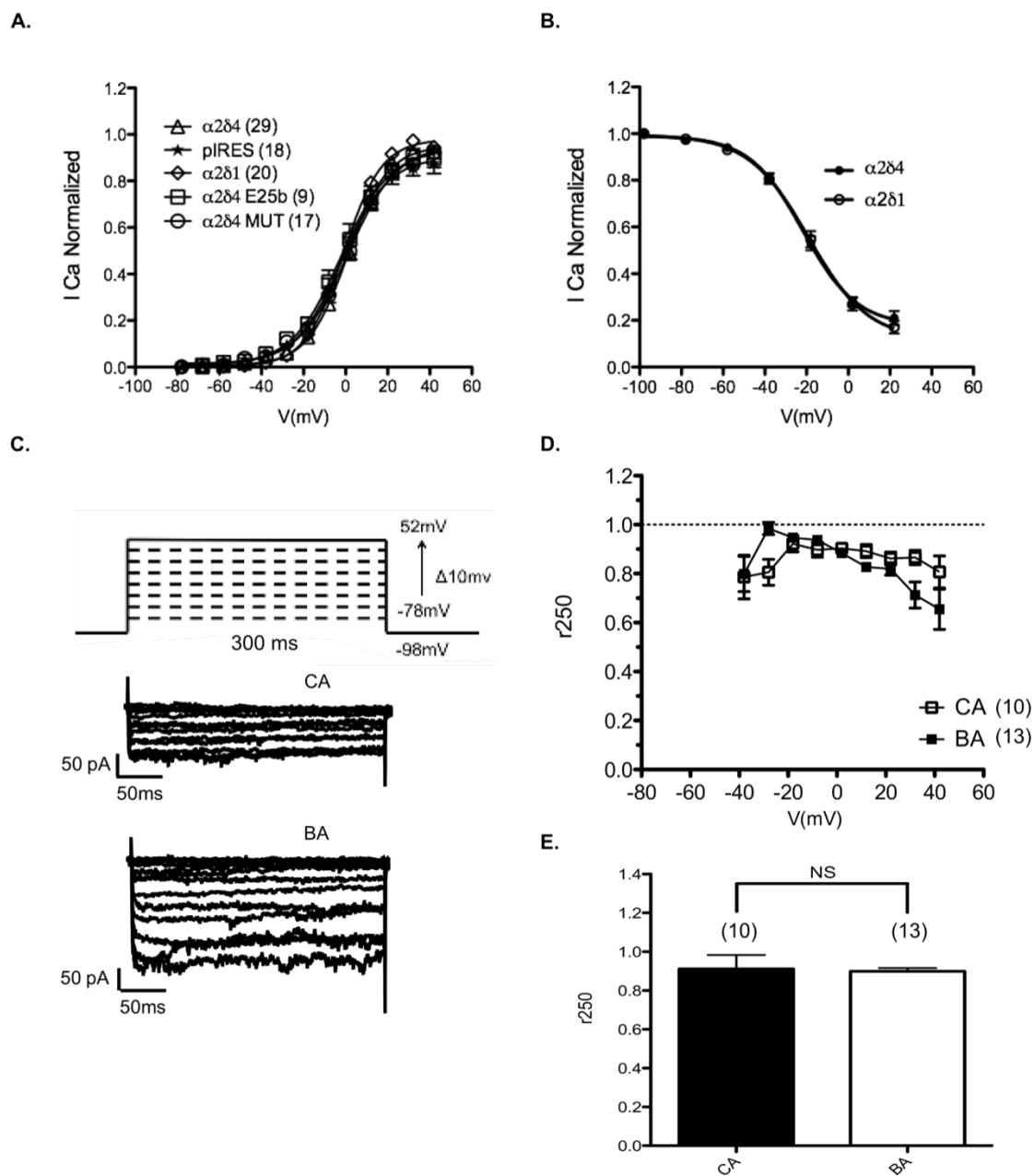


FIGURE 31. Characterization of $\alpha_2\delta_4$ activity on Cav1.4 mediated currents. (A) Voltage-dependent activation curve of $\alpha_2\delta_1$, $\alpha_2\delta_4$, $\alpha_2\delta_4$ E25b, $\alpha_2\delta_4$ MUT (c.2451insC), $\alpha_2\delta_4$ Δ E16, piRES (empty vector). (B) Voltage-dependent inactivation curve of $\alpha_2\delta_1$ and $\alpha_2\delta_4$. Mean values, SEM, and the best fits of the current voltage relation are shown. (C) Protocol used for the analysis of calcium-dependent inactivation and sample traces for $\alpha_2\delta_4$ in presence of 15mM Ca^{2+} (CA) or Ba^{2+} (BA). (D) Representation of the change in current at the beginning and at the end of 250ms depolarization (r_{250}) at different potentials using Ca^{2+} (CA) or Ba^{2+} (BA). (E) Comparison of the r_{250} values obtained for $\alpha_2\delta_4$ at the maximal current with Ca^{2+} (CA) and Ba^{2+} (BA).

	CD	$V_{0.5, \text{act}}$	K_{act}	$V_{0.5, \text{inact}}$	K_{inact}
$\alpha 2\delta 4$	$8.28 \pm 0.90^{***}$ N = 44	1.64 ± 0.55 N = 29	9.87 ± 0.30 N = 29	-20.24 ± 2.29 N = 15	-13.00 ± 0.97 N = 15
$\alpha 2\delta 4$ E25b	3.74 ± 0.52 N = 16	-0.98 ± 2.61 N = 9	11.37 ± 1.13 N = 9	ND	ND
$\alpha 2\delta 4$ mut	3.51 ± 0.61 N = 26	1.03 ± 1.76 N = 17	10.99 ± 0.57 N = 17	ND	ND
$\alpha 2\delta 1$	$13.12 \pm 1.60^{***}$ N = 22	-1.05 ± 0.44 N = 20	9.11 ± 0.17 N = 20	-17.81 ± 2.27 N = 29	-14.39 ± 1.28 N = 29
pIRES	2.49 ± 0.29 N = 30	0.52 ± 2.38 N = 18	10.80 ± 0.69 N = 18	ND	ND
A2 δ 4 Δ E16	1.59 ± 0.19 N = 18	ND	ND	ND	ND
A2 δ 4 Δ E23-26	1.64 ± 0.33 N = 6	ND	ND	ND	ND
A2 δ 4 Δ E23-25	0.97 ± 0.16 N = 7	ND	ND	ND	ND

TABLE 4. Calculated biophysical parameters of Cav1.4 calcium channels in the different experiments conducted. Experiments were performed in tsA-201 cells using 15mM Ca^{2+} as charge carrier. Data are given as mean \pm SEM. CD_{max} = maximum current density, $V_{0.5, \text{act}}$ = half-maximum activation voltage, K_{act} = slope parameter of the activation curve, $V_{0.5, \text{inact}}$ = half-maximum inactivation voltage, K_{inact} = slope parameter of the inactivation curve, N= sample size, ND= not determined. Statistically significant differences are indicated by asterisks ($P < 0.001 = ***$). For multiple comparisons (CD_{max} ; $V_{0.5, \text{act}}$; K_{act}), significance is given in relation to Cav1.4 $\alpha 1 + \beta_3 + \text{pIRES}$. For single comparison ($V_{0.5, \text{inact}}$; K_{inact}) significance is given in relation to Cav1.4 $\alpha 1 + \beta_3 + \alpha 2\delta 1$. Data for $\alpha 2\delta 1$ $V_{0.5, \text{inact}}$ and K_{inact} were taken from Burtscher et al (Burtscher et al. 2014) to allow comparison.

5.3 RPGR

5.3.1 Computational analysis of RPGR exon 9a splicing-relevant sequences

The intronic mutation g.26652G>A of RPGR increases the levels of the alternative exon 9a. The mutation is located 55 bp upstream of exon 9a 3' splice site. Aiming at the design of an exon-skipping approach which could decrease the levels of exon 9a in presence of the mutation, we undertook a bioinformatics analysis of relevant sequences important for recognition of the alternative exon. At the same time we tried to understand the effect of the mutation on such sequences. We first analysed exon 9a splice sites with NNSPLICE 0.9. The results show how exon 9a has a weak consensus for its 3' splice site, whereas its 5' splice is more similar to the consensus sequence (Tab. 5).

	Score	Sequence 5' > 3'
E9 3'splice site	0.97	ttcattatTTTTGCATTT AG atcggccttatgtatact
E9 5'splice site	0.99	caatagag GT aaattc
E9a 3'splice site	0.00	ataaacaagcgTTTTGGC AG ggcacgggtggctcactcctg
E9a 5'splice site	0.93	tagccag GT atgatg
E10 3'splice site	0.83	ttctgtggatttatgctgc AG gttgcttgggtggatgtoa
E10 5'splice site	0.19	agagagg GT acaatt

TABLE 5 Splice site scores of *Cacna2d4* exon 22 to 27. The higher is the score, the stronger is the splice site. A perfect match to the splice site consensus sequence is indicated with 1.

Recognition of a defined ESE sequence on exon 9a can constitute a target site for the design of chimeric U1snRNAs able to mediate exon 9a skipping. SpliceAid predictions for exon 9a did not show presence of a clear and defined ESE along its sequence, since ESEs and ESSs seem to be present in the same regions (Fig. 32). Moreover, SpliceAid analysis of the site of the wild type and mutant sequence did not reveal a change in *cis*-acting sequences important for splicing (data not shown). We therefore applied another prediction tools, ESEFinder. ESEFinder uses an experimentally-generated matrix to weight consensus motif for a set of SR proteins, which mainly act by enhancing exon recognition (Smith et al. 2006; Cartegni et al. 2003). This tool predicts a binding site for an SR protein, SRSF2 (SC35), to be suppressed by the mutation (Fig. 33). Even if this result seems to be inconsistent with the effect of the mutation, which actually increases

exon 9a presence, it is known that in some condition SRSF2 can act as a splicing silencer, particularly when binding to introns, therefore the removal of its binding site can result in augmented exon recognition (Raponi et al. 2011; Erkelenz et al. 2013; Dembowski et al. 2012). If the prediction is correct, the mutation site cannot represent a target for chimeric U1snRNAs designed to impair exon recognition, since there are no indications that the mutation is creating a new ISE. Another possible effect of the mutation could be the creation of a new branch site with a stronger consensus. We investigated this possibility using the branch point sequence analysis tool of Human Splicing Finder (Desmet et al. 2009). The performed prediction does not show a change in the branch sites pattern of intron 9 (data not shown).

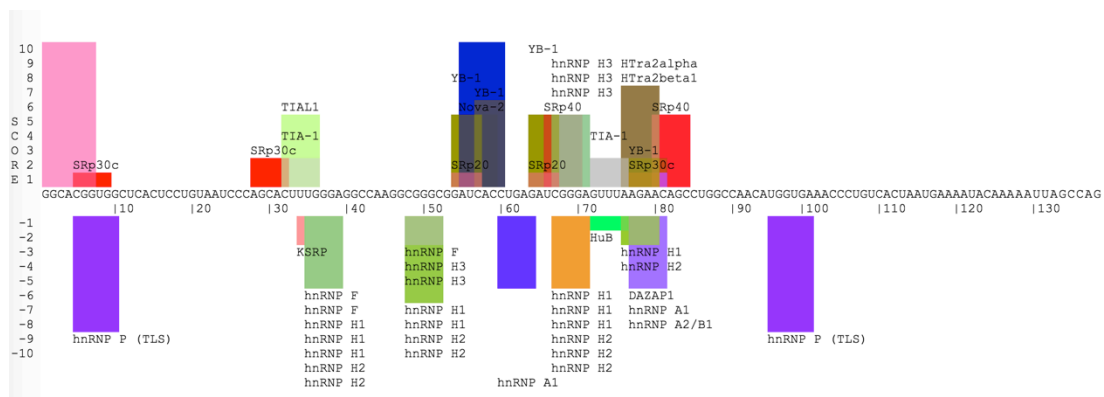


FIGURE 32. Prediction for ESE and ESS in RPGR E9a using SpliceAid. All predicted ESE are overlapping with predicted ESS, thus a clear ESE is not defined.

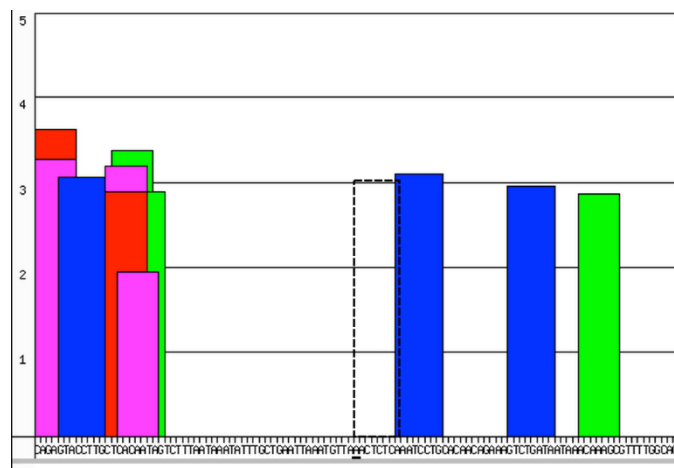


FIGURE 33. ESEFinder prediction of the effect of the intronic g.26652G>A mutation. The last portion of intron 9a before exon 9a is shown. The site of the mutation is underlined. The mutation is predicted to abolish an ISE (boxed).

5.3.2 Design of U1snRNAs and reporter minigenes for exon 9a skipping

The results of our bioinformatics prediction suggests that exon 9a does not have evident ESEs, and that the mutation site can not represent a valid target for inducing exon skipping. Therefore we decided to target exon 9a splice sites. Masking these sites should in fact result in skipping of exon 9a as a consequence of the failure of the splicing machinery to recognize these important *cis*-acting sequences. In particular we generated three chimeric U1snRNAs targeting the 3' splice site (U1_3'), the 5'(U1_5') splice site, and both sites (U1_3'5'). To test the effect of this U1snRNA on exon 9a splicing we designed a minigene reporter system cloning the RPGR genomic region around exon 9a in an expression vector. The minigene was designed to contain exon 9, the whole intron 9, exon 9a and exon 10 (Fig. 34 C). This construct was subsequently mutated to introduce the intronic mutation g.26652G>A. Following transfection of the wild type and mutant minigenes in HEK293T cells it is possible to observe how in this cell line the effect of the mutation is similar to what observed in human patients, were it has been shown to increase the levels of exon 9a (Fig. 34 A, B). The mutation in fact is able to significantly increase exon 9a levels of about one fold in the minigene (Fig. 34 D, E). Similar results were obtained in 661w cells (Al-Ubaidi et al., 1992), a photoreceptor-derived cell line (Fig. 34 F, G).

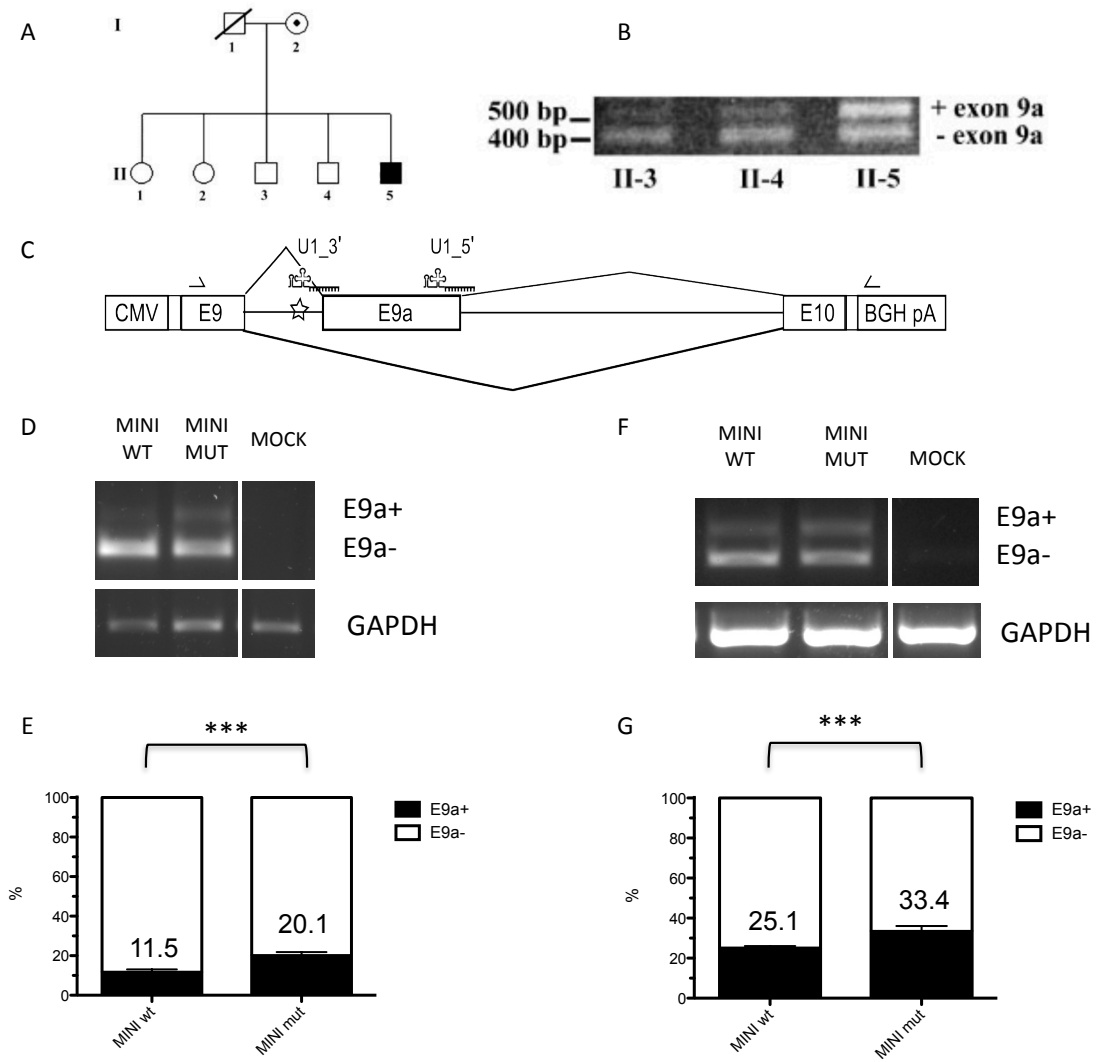


FIGURE 34. The intronic mutation g.26652G>A and RPGR minigene. (A) Pedigree of the family of the affected patient (from Neidhardt et al., 2007). (B) RT-PCR amplification of transcripts either lacking or including exon 9a of RPGR using total RNA from blood. The transcripts including exon 9a are increased in patient II-5, compared to his nonaffected brothers (patients II-3 and II-4) (from Neidhardt et al., 2007). (C) Schematic representation (not to scale) of the minigene. Position of the mutation is indicated by a star. The binding sites of U1_3' and U1_5' are reported. Position of the primers used for the analysis of E9a presence are indicated by arrows. (D) RT-PCR of HEK293T cells transfected with wild type or mutant RPGR minigene. (E) Densitometric analysis of the bands (N=3) reveals how the mutation increases E9a presence (p<0.001). The mean % of E9a+ is given. (F) RT-PCR of 661w cells transfected with wild type or mutant RPGR minigene. (G) Densitometric analysis of the bands (N=3) reveals how the mutation increases E9a presence (p<0.001). The mean % of E9a+ is given.

5.3.3 Testing different chimeric U1snRNAs for exon 9a skipping

We then applied the different chimeric U1snRNAs to HEK293T cells transfected with the mutant minigene. From densitometric analysis of the RT-PCR performed in the different conditions, using U1_3' and U1_3'5' we were able to observe a reduction of exon 9a+ mRNAs of about 50% compared to transfection of the minigene alone. Interestingly, the U1_5' is able to stimulate exon 9a recognition, doubling the levels of exon 9a presence in mature mRNA. Instead, when both construct were used together, the results did not match those observed using U1_3'5'. In fact, presence of both U1_3' and of U1_5' still promotes exon 9a splicing, even though at a lower degree than U1_5' alone. This suggests that the effect of U1_5' expression is more pronounced of that of U1_3' and that U1_5' is in fact not masking the splice site, but actually improving its recognition in the same way as the normal U1 snRNA does (Fig. 35). Even if chimeric U1snRNAs are normally used to increase exon recognition impaired by different mutations, in our case the U1_5' was designed to have a very long (24 bp) complementarity with the 5' splice site with the objective of impeding its detachment thus masking the splice site.

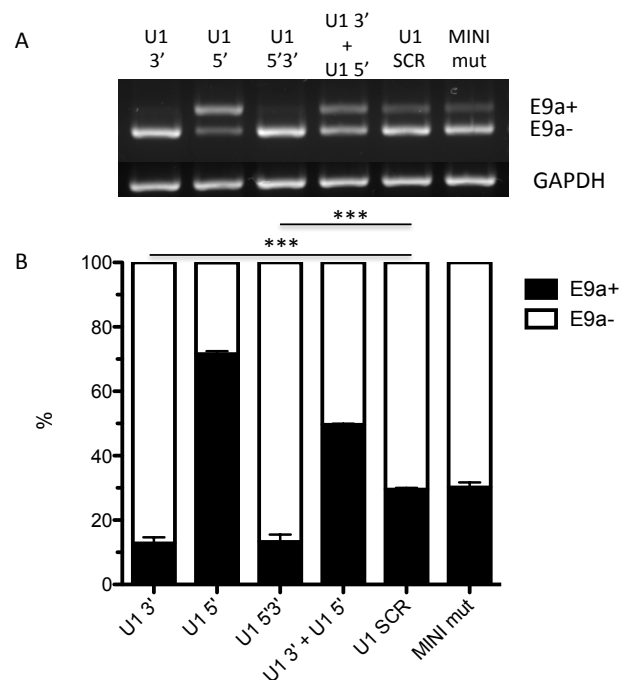


FIGURE 35. Effect of different chimeric U1 snRNAs on exon 9a splicing. (A) RT-PCR of HEK293T cells transfected with RPGR mutant minigene plus the different U1. U1_SCR: scramble U1. Mini mut: mutant minigene alone. (B) Densitometric analysis of the bands (N=3). Statistically significance for exon 9a reduction using U1_3' or U1_5' is reported ($p < 0.001$) compared to U1 SCR.

We then selected our best-performing chimeric U1 snRNA (U1_3') and tested it at different concentrations in HEK293T cells to assess the dose-dependency of its effect in comparison to the scramble U1 (U1_SCR). As expected, while the U1_SCR does not affect exon 9a levels at the different tested doses, U1_3' does, showing a visible decrease in exon 9a skipping ability at lower doses (Fig. 36).

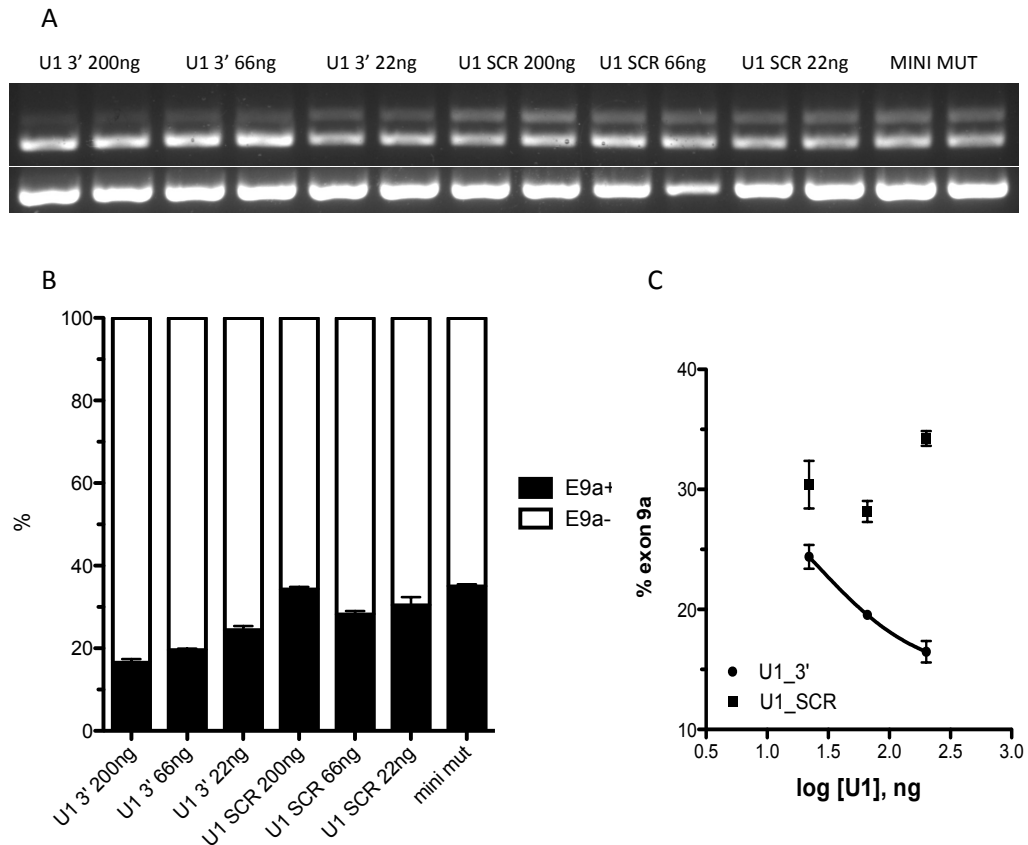


FIGURE 36. Dose-dependent skipping effect of U1_3'. (A) RT-PCR of HEK293T cells transfected with the *RPGR* mutant minigene plus different doses of U1 3' and U1 SCR. (B) Densitometric analysis of the bands (N=2). (C) Fit of the dose-response curve for U1_3' and U1_SCR dilutions. Only datas of U1_3' dilutions were able to fit a dose-response curve.

5.4 USH2A

The USH2A gene encodes for usherin, a modular protein found associated with the photoreceptor connective cilium. Presence of repetitive domains renders a protein an interesting target for exon-skipping therapeutic applications, as is the case of dystrophin, one of the first successful targets for splicing-modulating interventions (Matsuo, 1996). This is due to the fact that removal of exons coding for one of the repetitive domains is unlikely to completely impair protein functionality, as long as an ORF is maintained. We therefore started to analyse the known mutations of USH2A to find those falling in exons which could be easily targeted by antisense approaches. The candidate exon must be located in a region of usherin where repetitive domains are present, must be relatively small (less than 300 bp), and must be symmetrical. A symmetrical exon has a length in base pairs which is a multiple of 3, and thus its removal does not impact the reading frame of the protein. Apart from deep intronic mutations, which are an obvious target for splicing-correcting approaches, the candidate mutation is a small insertion or deletion which leads to frameshift, or a nonsense mutation. We identified in USH2A a region encoding for repetitive FN3 domains where different exons have the desired characteristics (Fig. 37). In particular, of the 72 USH2A exons, exons number 29, 30, 32, 38, 43, 45, 50, 53, 56, 59, 62 are all approachable and have different mutations causing Usher syndrome type 2 (Tab. S3).

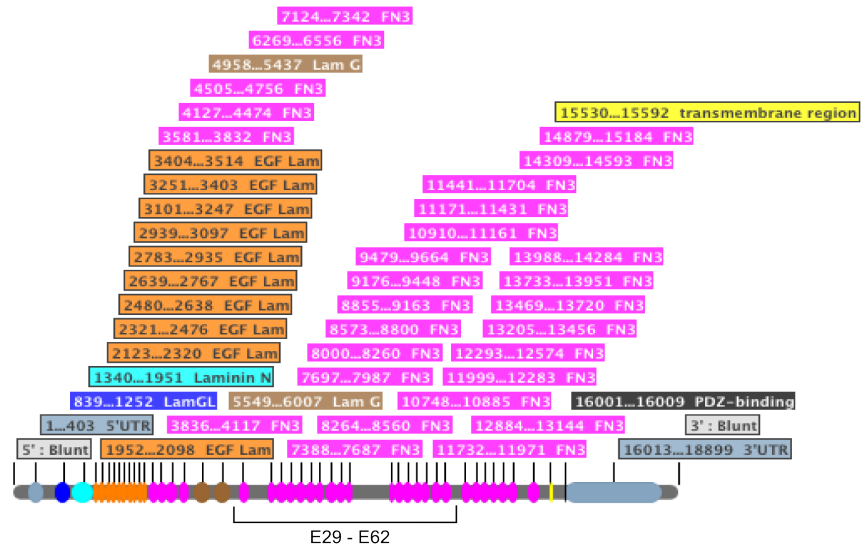


FIGURE 37. USH2A exons approachable by exon-skipping. All domains of USH2A are represented in scale. The region of repeated FN3 domains encoded by exons 29 to 62 is marked.

6 Discussion

The application of antisense-based splicing-correcting therapeutic approaches to retinal dystrophies offers great opportunities and challenges. The technique allows a highly specific and controlled effect, thanks to the fact that its function relies on base-pairing, and that it acts only where and when the endogenous target pre-mRNA is transcribed. This specificity however comes at a cost, which is that the technique is mainly patient-specific and therefore difficult to develop to a clinical setting for a broad range of diseases. The successful example of exon-skipping applications for Duchenne muscular dystrophy (Douglas and Wood, 2013) teaches us much on the importance of selecting a good candidate gene for the implementation of such approaches. Effective development of new treatments requires the presence of different factors: a tissue in which it is easy to deliver the therapeutic agent, availability of formulations and/or vectors able to reach the relevant cell type, selection of genes having mutations which would benefit from such approaches, and presence of animal models in which the approach can be tested, therefore speeding up the development process. We realized that the retina, as tissue, offers many of the requirements needed for a successful application of new antisense-based splicing-correcting therapeutic approaches. However, among the genes causing retinal dystrophies, the presence of a candidate which would have all characteristics important for an optimal application of these approaches was not evident. We therefore started a survey of all genes causing retinal dystrophies to understand which were those more promising, merging all available information from databases as well as from the literature. Thanks to this analysis, we focused our attention on three genes, each one having some characteristics which rendered it an interesting target for splicing-correcting approaches in the retina: *CACNA2D4*, *RPGR* and *USH2A*.

6.1 CACNA2D4

In this work we have studied the applicability of an exon-skipping therapeutic approach for *CACNA2D4* mutations causing recessive cone dystrophy. This gene was selected for two main reasons. First, because of the presence of a spontaneous mouse model (Wycisk et al., 2006a) having an insertion on the same exon hosting a nonsense mutation in humans (E25). Presence of this model offered a great chance to assess the feasibility of an exon skipping approach *in vivo* in the eye for the first time. Second, because the gene encoded a protein of known predicted function, being it part of a family of accessory subunits of voltage-gated calcium channels. Even if the murine subunit was not characterized, the human counterpart was known to induce calcium influx from HVA calcium channels (Qin et al., 2002), a property shared with all others known $\alpha_2\delta$ subunits. This property can be measured electrophysiologically, therefore allowing a precise analysis of the functionality of the rescued protein resulting from exon skipping. We therefore started designing the possible approach and evaluating its applicability to the target gene.

During our investigation we realized that E25 was not a constitutive exon in mice. In fact we confirmed the presence of an alternatively spliced exon (E25b), which is mutually exclusive with E25. This exon is of particular importance for the study of the role of *Cacna2d4* function, since its incorporation terminates the reading frame of the protein after the first Cache domain, in a similar way as the c.2451insC mutation. Another important finding that we made is that this mutation on exon 25 has a second effect to that of prematurely terminating the reading frame. In fact it acts on splicing as well. The mutation is predicted to create a new exonic splicing silencer (ESS) in E25, which is recognized by several *trans*-acting splicing factors mediating inhibition of exon recognition. In mouse retinae the mutation mainly affects E25 levels, reducing its levels in mature mRNA. This resulted in a dramatic change of the relative ratio between E25 and E25b splicing isoforms, changing them from 3:1 in favour of E25, to almost 1:1. When the effect of the mutation was tested *in vitro*, it instead mainly increased E25b levels in mature mRNA, without affecting E25. Even if the result of the mutation is to favour the relative presence of E25b over E25 both *in vivo* and *in vitro*, there is a difference in how this effect is mediated in the two systems. This difference can be

ascribed to two players: *trans*-acting splicing factors and nonsense-mediated decay. Presence of a different subset of *trans*-acting splicing factors in the mouse retina and in HEK293T cells can in fact explain the different mechanism of action of the mutation. For example, the family of RNA-binding proteins Fox-1 is exclusively expressed in brain, skeletal muscle and heart (Jin et al., 2003; Shibata et al., 2000; Underwood et al., 2005). Fox-1 is known to recognize a specific intronic RNA sequence (UGCAUG) and to promote alternative splicing (Jin et al., 2003). Where Fox-1 is expressed it is possible to observe, in different genes, alternative splicing of exons surrounded by the sequence recognized by Fox-1 (Kuroyanagi, 2009). Nonsense-mediated decay (NMD), a mechanism that targets and degrades mRNAs with a premature stop codon, can constitute another important element to consider, especially *in vivo* where we have shown a general reduction of *Cacna2d4* transcripts in the mutant. There is an increasing amount of evidence that links alternative splicing and NMD as a system used by cells to regulate gene expression (Lareau et al., 2007; Lejeune and Maquat, 2005; Sibley, 2014). In particular, alternative spliced exons can be included or excluded to generate premature termination codons which will trigger the NMD machinery, resulting in a decrease of transcript levels. In the fumarylacetoacetate hydrolase (*fah*) gene, for example, skipping of exon 8 generates a splicing isoform with a premature termination codon. This isoform is subject to NMD, but a protein product is still present (Dreumont et al., 2005). To clarify the role of different splicing factors in the recognition of E25 and E25b, a possible future approach can consist in the analysis of minigene splicing in cells after silencing of relevant factors predicted to bind only in presence of the mutation. At the same time, block of NMD *in vivo* by pharmacological treatment (Keeling et al. 2013) can help to assess the contribution of this mechanism on the relative abundance of E25 and E25b in the retina of *Cacna2d4* mutant mice.

The effect that mutations in the coding region of genes have on splicing is normally underestimated: evidences pinpoint a role in splicing for more than a quarter of these mutations (López-Bigas et al. 2005; Sterne-Weiler et al. 2011; Lim et al. 2011). The early understanding of how splicing patterns change in response to a mutation is highly significant for the successful development of strategies aiming at correcting such defects. In this effort, splicing-reporter minigene assays are a fantastic tool which can be

of assistance (Cooper, 2005). We have successfully used for the first time a minigene system able to properly recall all splicing events across 6.5 Kb and six different exons. Following implementation of more efficient gene synthesis services the design and application of functional minigenes could become easier and more powerful.

By analysis of the electrophysiological properties of Cav1.4 calcium channels in the presence of murine $\alpha_2\delta_4$, we were able to confirm its predicted function of accessory subunit. In fact, $\alpha_2\delta_4$ is able to increase Cav1.4-mediated currents in an heterologous expression system. In the presence of $\alpha_2\delta_4$, current densities were augmented of three-folds, in line with what described observing calcium influx in cells expressing human $\alpha_2\delta_4$ (Qin et al. 2002). Moreover, we noticed how $\alpha_2\delta_4$ is less able than $\alpha_2\delta_1$ to mediate such increase, as recently observed in another work (Lee et al. 2014). Regarding activation, we noticed no significant effect on Cav1.4 calcium channels in presence or absence of $\alpha_2\delta_4$. In a recent work (Lee et al. 2014) human $\alpha_2\delta_4$ has been described to shift the voltage-dependence of activation to more positive potentials when compared to $\alpha_2\delta_1$. Even if in our analysis the $V_{0.5, act}$ in presence of $\alpha_2\delta_4$ was more positive than that observed with $\alpha_2\delta_1$, the difference was not significant. We finally showed how presence of $\alpha_2\delta_4$, in a similar way to what has been found for $\alpha_2\delta_1$ (Burtscher et al. 2014), does not facilitate calcium-dependent inactivation of Cav1.4. Since $\alpha_2\delta_4$ is highly expressed in the retina together with Cav1.4, and both localize to photoreceptor terminals, (De Sevilla Müller et al. 2013; Knoflach et al. 2013; Busquet et al. 2010; Specht et al. 2009) we can therefore suggest that this is the subunit helping trafficking of Cav1.4 α_1 subunit to the plasma membrane of photoreceptors, as it is able to mediate the same effect on the channel in an heterologous system.

Regarding *Cacna2d4* c.2451insC mutation, we confirmed its pathophysiological role in abolishing $\alpha_2\delta_4$ ability to mediate an increase in functional Cav1.4 channels at the plasma membrane. In fact, no activity of the mutant protein was observed in stimulating current density through Cav1.4 channels. This can definitely result in an impairment in connectivity between photoreceptors and second-order neurons in the retina. Interestingly, similarly to mutant $\alpha_2\delta_4$, also the newly identified $\alpha_2\delta_4$ E25b splicing isoform shares the same characteristics. In both cases, the protein ORF is interrupted between the two Cache domains, and as a result both proteins lack the δ peptide, important for membrane anchoring (Davies et al. 2010; Kadurin et al. 2012). Alpha2-

delta subunits lacking the membrane anchor have been shown to still be able to enhance calcium currents, but they lose this property when the whole δ peptide is deleted (Kadurin et al. 2012; Gurnett, De Waard, and Campbell 1996). It is therefore peculiar the presence in the retina of a *Cacna2d4* splicing isoform which is mimicking the effect of a disease-causing mutation. The role of this isoform remains therefore elusive, even because, by missing the membrane anchor, the protein would probably be secreted. An additional important element to assess would be the presence of a similar isoform in humans. Existence or absence of a splicing isoform of *CACNA2D4* that resembles the effect of murine E25b incorporation would be interesting to better understand the role of both murine and human mutations in exon 25. In fact, if an alternatively spliced exon which truncates *CACNA2D4* ORF between the two Cache domains also exists in the human retina, in this case as well the c.2406C→A mutation could potentially favour this inclusion. Moreover presence of this isoform also in humans would help understanding the role of $\alpha_2\delta_4$ E25b isoform. We hypothesize that the mutation, by mimicking the effect of E25b inclusion, offers a specific advantage in heterozygosity (overdominance) in a district where $\alpha_2\delta_4$ is normally expressed. Specifically, since a truncated version of $\alpha_2\delta_4$ normally exists, its overexpression caused by an allele coding only for this isoform (the mutant allele) in a defined moment or tissue can potentially exert a positive function, which in heterozygosity is not undermined by the detrimental effects on vision of loss of full-length $\alpha_2\delta_4$. This would allow the conservation of different mutations in the same position sharing the same mimicking effect.

We have identified an additional splicing isoform of *Cacna2d4* which arises from skipping of exon 16. The $\alpha_2\delta_4$ Δ E16 transcript is not present in the retina, but we found it in different regions of the brain, where it is the only or the more abundant form present. However, *Cacna2d4* expression in the brain regions analysed is very low compared to what observed in the retina, in line with what found in previous work (Schlick, Flucher, and Obermair 2012). Additionally, in a recent study, a smaller (~165kDa instead of ~170kDa) $\alpha_2\delta_4$ was detected by Western blots in mouse brain, which could possibly correspond to $\alpha_2\delta_4$ Δ E16 (De Sevilla Müller et al. 2013). It is actually possible that this isoform is expressed by specific cell populations in the brain. Even in this case, the role of this isoform remains elusive, since we have shown it does not alter current properties of Cav1.4 channels. Skipping of exon 16 results in a large

deletion of the first Cache domain sequence. The corresponding region in $\alpha 2\delta 1$ is known to be subject to alternative splicing in a similar way (Angelotti and Hofmann, 1996). having two regions, A and B, part of the first Cache domain, which can be present in different arrangements in the mature mRNA: A+B, $\Delta A+\Delta B$, $\Delta A+B$. Even if the $\Delta A+B$ isoform is able to mediate an increase of current densities through HVA calcium channels, the functional characterization of the $\Delta A+\Delta B$ isoform is still missing (Lana et al., 2014). It would be therefore interesting to test if this isoform shares with $\alpha 2\delta 4 \Delta E16$ the same inability in inducing an increase in HVA calcium channels current densities. Analysis of localization, interacting partners, and possible function of this isoform would therefore shine a light on the importance of Cache domains for $\alpha 2\delta$ subunits.

We have discovered in this work the first two splicing isoforms of an $\alpha 2\delta$ subunit ($\alpha 2\delta 4$ E25b and $\alpha 2\delta 4 \Delta E16$) which are proven to not mediate an increase in HVA calcium channels current densities. These results strengthen the current view (Dolphin 2012) that $\alpha 2\delta$ subunits may be involved, in the retina and CNS, in different roles not directly related to the enhancement of trafficking of functional calcium channels on the plasma membrane. Present literature suggest that they can be involved in synaptic formation and organization independently from their role in HVA calcium channel trafficking (Kurshan et al., 2009). Work conducted in *Drosophila* showed that $\alpha 2\delta 3$ null flies were not able to properly form the synaptic bouton of motor neurons, which is instead correctly formed in $\alpha 1$ -null animals. Moreover, the presence of an allele coding for $\alpha 2$ but not for the δ peptide was able to revert the phenotype. This suggests that $\alpha 2\delta 4$ E25b, which lacks the δ peptide as well, may be fundamental for similar functions. In this perspective, we can speculate a role for $\alpha 2\delta$ subunits as secreted and membrane-associated signalling molecules like semaphorins, a class of proteins important for axonal guidance. Since $\alpha 2\delta$ are not exclusive of neural tissues, additional functions are also highly possible. Further analysis of the role of this subunits should therefore be undertaken, first of all identifying the cell types in which they are expressed and their subcellular localization. It is also possible that they play an important role during development, when the organization of neural circuits takes place, and therefore their expression should be followed over time in relevant model organisms.

Aiming at validating a possible exon-skipping therapeutic approach for *CACNA2D4*, we found out that the region encoded by exons 23 to 26 is of fundamental importance for the function of $\alpha_2\delta_4$. The removal of this portion is indeed enough to impair $\alpha_2\delta_4$ activity of promoting calcium currents mediated by Cav1.4 α_1 subunits. The same is true for the deletion of exons 23, 24 and 25 only. The region encoded by these exons is located between the two Cache domains and it is not known to be part of any domain of the protein. Moreover, in an $\alpha_2\delta_1$ paralogue, insertion of an HA tag in the corresponding region did not cause any defect in the protein ability to mediate an increase in currents (Kadurin et al. 2012). This region may be important for hosting glycosylation sites necessary for functionality of the accessory subunit (Gurnett, De Waard, and Campbell 1996). These findings render inapplicable our therapeutic strategy aimed at correcting the retinopathy caused by c.2451insC mutation. This strategy was relying on the therapeutic skipping of exon 23 to 26 or 23 to 25 from pre-mRNA in order to eliminate the frameshift mutation on E25 and restore the downstream ORF.

6.2 RPGR

Intronic mutations affecting splicing and not altering the consensus sequence of splice sites are an optimal target for splicing-modulating approaches. These mutations mainly act by: creating or deleting ISS and/or ISE, creating new cryptic splice sites or changing the strength of the consensus sequence of the branch point (Cooper et al., 2009; Lewandowska, 2013; Tazi et al., 2009). The advantages of targeting these mutations instead of mutations leading to frameshifts are two. First, since they act on splicing, achieving correction of the splicing pattern is enough to have a therapeutic benefit: since constitutive exons are not skipped, there is no need for testing the functionality of the rescued proteins which results from exon-skipping approaches directed towards mutations terminating the proteins ORF. Second, when the mutations effect is to create new cis-acting sequences, the disease can be easily addressed by masking those sequences with antisense approaches. For these reasons we selected the

intronic mutation g.26652G>A of *RPGR* (Neidhardt et al., 2007) as a potential target for splicing-correcting approaches in the retina. Even if the effect of this mutation is to increase levels of the alternatively spliced exon 9a (Neidhardt et al., 2007), from our bioinformatics analysis it is not clear if it acts by creating or deleting cis-acting sequences. We therefore decided to design chimeric U1snRNAs directed towards both splice sites of exon 9a, aiming at reducing its recognition in presence of the mutation.

Using an U1 snRNA directed towards the 3' splice site in HEK293T cells transfected with splicing-reporter minigenes we were able to show a significant decrease of exon 9a levels. On the contrary, the U1 snRNA directed towards the 5' unexpectedly caused a significant increase in exon 9a levels. U1 snRNA normally recognize the 5' splice site during splicing by binding with its 5' end to the -3/+6 exon/intron consensus sequence. This binding needs to be reversible, since U1 snRNA is required to detach from the 5' splice site for the splicing reaction to take place. It follows from this observation that rendering the U1 unable to easily detach from the 5' splice site by increasing the length of the region it recognises (24 base pair for our U1_5') is a strategy that can be used to achieve exon skipping (De Angelis et al., 2002). In our case instead the chimeric U1 snRNA increased exon 9a recognition by binding to the 5' splice site, probably acting in a similar way as adapted U1s, which are normally designed with shorter complementarity (around 10 bp) (Glaus et al., 2011; Sánchez-Alcudia et al., 2011). This effect was not present when the bifunctional U1_5'3' was used, since U1_5'3' caused exon 9a skipping, at a comparable level of that induced by U1_3'. Contrary to the effect of U1_5'3', the use of both U1_3' and U1_5' induced exon 9a levels which lay in between those observable by using U1_3' or U1_5' alone, a sign of competition of the two snRNA to skip (U1_3') or include (U1_5') exon 9a. Given the current knowledge on bifunctional U1 snRNAs it is difficult to predict the reason for this difference in action. The results suggest that in the bifunctional U1_5'3', the region which is complementary to the 5' splice site of exon 9a is not able to exert its function of helping exon 9a recognition. This can be caused by its position at the 5' end of the chimeric U1, when instead the antisense region for the 3' splice site lays between the U1 stem-loop structure and the antisense region for the 5' splice site. In this direction it could be of interest to test the effect of a U1_5'3' where position of the antisense sequence for the 5' splice site is exchanged with that for the 3' splice site, and observe if in this case the

U1_5'3' behaves like the U1_5' alone and no more like the U1_3' alone.

Assessment of the effect of the different engineered U1s in 661w cells, investigation of exon 9a presence and consequent application of the best U1snRNAs (U1_3' and U1_5'3') in patient-derived fibroblasts would allow additional validation of the designed therapeutic approach. The use of patient-derived fibroblasts would also allow other important analysis. Since RPGR isoforms containing exon 9a have been shown to interact with a different subset of isoforms of its interacting partner RPGRIP1 (Neidhardt et al. 2007), correction of this effect can be potentially checked in patients fibroblasts. Moreover, investigation of restored RPGR localization along the primary cilium of patient fibroblasts can be analysed as a surrogate model of the photoreceptor connective cilium, in a similar way to what has been recently done for other RPGR isoforms (Da Costa et al. 2015).

6.3 USH2A

We identified the *USH2A* gene as a particularly interesting target for splicing-modulating therapeutic interventions. Its modular domain architecture is in fact a peculiar property of this gene, and can represent a great advantage for exon-skipping approaches aiming at preventing the inclusion in the mature mRNA of exons hosting mutations leading to truncation of the protein ORF. In line with what has been observed with dystrophin (Matsuo, 1996), it is possible that the removal of selected exons encoding for some of the repetitive domains of the protein does not significantly impair protein functionality, thus permitting the application of such therapies. We have identified, in the second region of the protein encoding for FN3 domains, eleven exons which can constitute a starting point for the application of exon skipping in the cure of Usher syndrome type 2. Overall, 5% of all *USH2A* mutations known today are approachable by skipping of these exons. Currently, the development of assays able to investigate the functionality of the different rescued proteins originating from exon

skipping is the main challenge for further development of such therapies. These assays should investigate protein localization and protein-protein interactions during and after ciliogenesis, using for example patient fibroblasts as a model.

7 Materials and Methods

7.1 Computational analysis of *Cacna2d4* E25 splicing

Mouse eye RNA-seq samples were downloaded from the Gene Expression Omnibus (Edgar et al., 2002) (dataset ID GSE38359: sample IDs GSM945628, GSM945631 and GSM945634; dataset ID GSE29752: samples GSM737548 and GSM737550). Reads were trimmed at the 3' end by removing nucleotides having Q score < 30 by means of Trimmomatic (Bolger et al., 2014), and then mapped to the mouse genome (mm10 assembly) by means of TopHat2 (Kim et al., 2013). The resulting alignment and the observed exon-exon junctions were eventually visualized with Integrative Genomic Viewer (IGV) (Thorvaldsdóttir et al., 2013).

The genomic sequence from *Cacna2d4* E22 to E27 was analysed using NNSPLICE 0.9. (Reese et al., 1997) Resulting scores for the different splice sites were reported.

Cacna2d4 E25 sequence was analysed using SpliceAid (Piva et al., 2009) in presence and absence of c.2451insC mutation. Differentially predicted splicing regulatory elements were showed.

7.2 Computational analysis of *RPGR* exon 9a splicing

The genomic sequence from *RPGR* exon 9 to exon 10 was analysed using NNSPLICE 0.9. (Reese et al., 1997) Resulting scores for the different splice sites were reported. *RPGR* intron 9 and exon 9a were analysed using SpliceAid and ESEFinder in presence and absence of the g.26652G>A mutation.

Cacna2d4 E25 sequence was analysed using SpliceAid (Piva et al., 2009) in presence and absence of c.2451insC mutation. Differentially predicted splicing regulatory elements were showed. The sequence of intron 9 preceding exon 9a was analysed using the branch point sequence analysis tool of Human Splicing Finder.

7.3 Animals

Experiments were conducted in conformity with the European Community Directive 2010/63/EU and the ARVO Statement for the Use of Animals in Ophthalmic and Vision Research and were approved by the Italian Ministry of Health. *Cacna2d4* mutant and wild-type mice of C57BL/10 background (Wycisk et al., 2006a) were used for extraction of retina tissue. C57BL/6 mice were used for analysis of *Cacna2d4* Δ E16 expression in the CNS.

7.4 Cloning of different constructs

Cacna2d4 Δ E16 clone (GenBank: BC141091.1; IMAGE ID 9055703) was ordered from Source Bioscience, amplified by PCR using primers For: 5'-GACTGCTAGCCACTTGCATGC and Rev: 5'-CTTGTCGACGTCAGATGGGAT, and cloned into pIRES2-EGFP (Clontech, Mountain View, CA) using *NheI* and *Sall* restriction sites. Exon 16 was subsequently amplified from murine genomic DNA using primers For: 5'-AGCTGGCACCCCGATATAAGCTTGGGGTGCATGGC and Rev: 5'-AGCTTCTTGCCTTCTCTGTACAAAGGTCGGAGGTCAG. The resulting PCR fragment was used as megaprimer (Wang and El-Deiry, 2010) for site-directed mutagenesis (Quickchange II site-directed mutagenesis kit, Agilent, Santa Clara, CA) and added to *Cacna2d4* Δ E16 to generate *Cacna2d4* full-length (*Cacna2d4*). The c.2451insC mutation on E25 was introduced by site directed mutagenesis of *Cacna2d4* using primers For: 5'-GAGCAGCCCCCGGCAGCTTTGTCTTC and Rev: 5'-GAAGACAAAGCTGCCGGGGGGCTGCTC. The obtained construct was named "Cacna2d4 MUT". E25b was amplified from murine retina cDNA using primers For: 5'-AGAGTCAGAGCCTGGCGTGG and Rev: 5'-CTGCTGCAATGGCCGTCTTCC. The PCR product was extracted from gel to avoid E25-containing transcript and purified. The product was then used as megaprimer for site-directed mutagenesis to obtain E25b inclusion in place of E25 (*Cacna2d4* E25b). The *Cacna2d4* full-length construct had been subsequently utilised as template for the generation of *Cacna2d4* Δ E23-25. For this intent a PCR using primers For: 5'-atagcccaggcaagccagt and Rev: 5'-actccaggtctggatccac was performed, followed by ligation of the PCR product. The

Cacna2D4 Δ E23-26 cDNA construct was obtained from overlapping PCR on Cacna2d4 template. For this purpose two different primer pairs were used to originate the two overlapping fragments: For: 5'-CTACGTGACTGCTAGCCACTTGCATGCCCAGGA, and Rev: 5'-ATCTGGATGCCACAGACTCCAGGTCTGGATCC for first reaction; For: 5'-GATCCAGACCTGGAGTCTGTGGGCATCCAGATG and Rev: 5'-CTACGACTCTTGGATCCGTCAGATGGGATGGAGTC for the second reaction. The two generated fragments were then purified and used together with the primer pair For: 5'-GACTGCTAGCCACTTGCATGC and Rev: 5'-CTTGTCGACGTCAGATGGGAT in a different PCR reaction to generate Cacna2D4 Δ E23-26.

The Cacna2d4 minigene construct was assembled from four fragments amplified from murine genomic DNA and digested with specific restriction enzymes. The first fragment was amplified using primers For: 5'-CTAAAGCTTATGATCTACTGTATCACAGA and Rev: 5'-GTCGCTAGCAGTAATGTCACCTCGG and digested with HindIII + NheI; the second with primers For: 5'-CGCACTAGTGTTTGGAAAGGAGTGATGGT and Rev: 5'-TATGCGGCCGCAGTCTGGTTTTTCCTC and with SpeI + NotI; the third with primers For: 5'-CTAGCGGCCGCACAGTCTTGATTGTTA and Rev: 5'-CAGACTAGTTCTTACATGAGACTTTGGAT and with NotI + SpeI; the fourth using primers For: 5'-GTAGCTAGCGCGTGTGAACATGGACTGG and Rev: 5'-CGTCTCGAGTCTGCTGCATGGCTGCC and NheI + Xho. The resulting digested and purified fragments were ligated together with a pCDNA3-Luc2 vector digested with HindIII + XhoI. The c.2451insC mutation was inserted on the minigene by site-directed mutagenesis using the same primer pair utilized for Cacna2d4 MUT.

Cacna1f clone (encoding for murine Cav1.4 α_1) was ordered from Source Bioscience (GenBank: BC156573.1), amplified using primers For CCACCATGTTCGGAATCTGAAG, and Rev CCATGAGGCCTTAGAGGGC, and cloned into pIRES2-mCherry vector using SmaI restriction enzyme. Cacnb2 clone (encoding for murine β_2 subunit) was ordered from Source Bioscience (GenBank: BC115871), amplified using primers For GCTAGATCTTTTTGCCGATGGTCC and Rev GACGGATCCTGCAGCTGTACTAG, and cloned into pIRES2-BFP vector using BamHI and BglII restriction enzymes.

RPGR minigene was obtained by amplification of human genomic DNA with primer For CTAGGTACCCACAGAGACCATAGAGAGTG and Rev CTACTCGAGAAGTTTGTAGCACTCAACTCTAA and cloned into a pCDNA plasmid using KpnI and XhoI restriction enzymes. The g.26652G>A mutation was added by insertional mutagenesis using primers For GCTGAATTAAATGTAAACTCTCAAATCCTGCACAACAG and Rev CTGTTGTGCAGGATTTGAGAGTTTAACATTTAATTCAGC.

The four chimeric U1 constructs for *RPGR* were obtained by ligation of two different inverse polymerase chain reaction (PCR) products, the first containing the U1 promoter, and the second containing the U1 sequence plus the chimeric sequence. to generate the U1_5', U1_3' and U1_SCR constructs, a first PCR was performed on the human U1 snRNA gene using as forward primer U1cas-up: 5'-CTAGCTAGCGGTAAGGACCAGCTTCTTTG and three different reverse primer: (U1_5'rpgr-1: 5'-caaaaattagccaggtatgatggcatgagatcttgggcctctgc, U1_3'rpgr-1: cgtttggcagggcacggtggatgagatcttgggcctctgc, U1_SCRrpgr-1: tcaattattccgcgagacgcagcatgagatcttgggcctctgc was performed. Each of the three obtained PCR fragment was then ligated with the product of a PCR on the human U1 snRNA gene performed using primers U1-univ For: 5'-GGCAGGGGAGATACCATGATC and U1cas-down Rev: 5'-CTAGCTAGCGGTTAGCGTACAGTCTAC. For the generation of the U1_5'3' constructs a first PCR product obtained using primers U1cas-up and U1_5'rpgr-1 was ligated with a second PCR product obtained using primer U1_3'rpgr-2 For: 5'-ccaccgtgcctgcaaaaacgggcagggagataccatgac and U1cas-down. All the ligation product were subsequently amplified by PCR using primer U1cas-up and U1cas-down and cloned into pAAV2.1-CMV-EGFP plasmid at the NheI restriction site upstream of the CMV promoter.

All obtained clones have been fully checked by sequencing.

7.6 RNA extraction and cDNA synthesis

Adult mice tissues were dissected and homogenized using a plastic pestle. Total RNA was extracted from each tissue from a pool of three different animals using Trizol (Trizol Reagent, Life Technologies, Carlsbad, CA) according to manufacturer's instructions, treated with DNase (Roche,) and purified using columns (NucleoSpin RNA, Macherey-Nagel, Düren, Germany). cDNA synthesis was performed using random primers (SuperScript VILO cDNA Synthesis Kit, Life Technologies, Carlsbad, CA), according to manufacturer's instructions. RNA extraction of transfected cells was performed two days after transfection with Trizol and RNA was treated with DNase (TURBO DNA-free Kit, Life Technologies, Carlsbad, CA). cDNA synthesis was performed using oligo(dT)₁₈ (RevertAid First Strand cDNA Synthesis Kit, Thermo Scientific, Waltham, MA).

7.7 Cell culture and transfection conditions

Hek293T, tsA-201, and 661W cells were maintained in DMEM supplemented with 10% FBS, 2mM Glutamine, 100 U/ml Pen/Strep, and grown at 37°C, 10% CO₂.

For transfection with minigenes and chimeric U1 snRNAs, Lipofectamine 2000 (Life-Technologies, Carlsbad, CA) was used, according to manufacturer's instructions, on 24 well plates. For Cacna2d4 minigenes, 600 ng of each construct were used. Regarding RPGR, 400 ng of minigene, plus 200 ng of each different chimeric U1 snRNAs were used, unless specifically mentioned.

For electrophysiological recordings tsA-201 cells were split into 6cm dishes one day before transfections. Transfection was performed using Turbofect transfection reagent (Thermo Scientific, Waltham, MA) with 0.5 µg of Cav1.4 α_1 (Sinnegger-Brauns et al., 2009), 0.5 µg of β_3 (Castellano et al., 1993), and 0.5 µg of different $\alpha_2\delta$ constructs in pIRES2-EGFP expressing vectors and 1 µg pUC. Data $\alpha_2\delta_1$ for were taken from (Ellis et al., 1988). One day after transfection cells were seeded at low confluence on 3 cm dishes coated with poly-D-lysine and stored over night at 30°C, 5% CO₂. Recordings were performed the following day. In experiments where different $\alpha_2\delta$ constructs were

present in the same transfection, the following amount were used: 0.5 μg of Cav1.4 α_1 (Sinnegger-Brauns et al., 2009), 0.5 μg of β_3 (Castellano et al., 1993), 0.5 μg of each different $\alpha_2\delta$ subunit, and 0.5 μg pUC.

7.8 Luciferase activity assay

For the luciferase assay, 600 ng of the Cacna2d4 minigene encoding for Luc2 were transfected together with 100 ng of pRL-SV40 encoding for Renilla. As positive control, 600 ng of pGL3 vector were used. Two days after transfection, luciferase activity was measured using the Dual-Glo Luciferase Assay System (Promega) in a Tecan infinite 200 PRO microplate reader.

7.9 RT-PCR and densitometric analysis

For all amplifications we used a protocol consisting in: a 1 min denaturing step at 94°C, 35 amplification cycles (30 sec at 94°C, 30 sec at 58°C, and 1min at 72°C), and a final 7 min step at 72°C. For utilised primer pairs see Tab. S4. Densitometric analysis of obtained bands was conducted using software Imagelab 2.0 (Biorad, Hercules, CA). Bands intensities, corrected for background, were normalized to the corresponding Gapdh values.

7.10 RT-qPCR

RT-qPCR was performed in a C1000 thermal cycler with a CFX384 real-time detection system (Biorad, Hercules, CA), using the KAPA SYBR FAST master mix (Kapa Biosystems, Cape Town, South Africa). Glyceraldehyde 3-phosphate dehydrogenase (GAPDH/Gapdh) was used as a reference gene for normalization, using the ΔCt method. All used primer pairs are reported in Table S4. Data were analysed using the CFX Manager 2.1 software (BioRad, Hercules, CA). For direct comparison of E25 and E25b transcripts levels, amplification efficiency and y-intercept with the two

primer pairs was compared using serial dilutions of plasmid containing E25 or E25b. Equivalence of the obtained slopes and y-intercept was assessed with extra sum-of-square F test (Fig. S1). Data are shown as $2^{(-\Delta Ct(E25))} / 2^{(-\Delta Ct(E25b))}$.

7.11 Protein extraction and Western blot

tsA-201 cells transfected with all the constructs used for electrophysiological analysis as described above were detached from 6 cm dishes using PBS, centrifuged briefly to remove PBS, and lysed with 100 μ l of lysis buffer (50 mM Tris-HCl pH 8, 150 mM NaCl, NP40 1%, Na-deoxycholate 0,25 %, 1mM EDTA, 2mM PMSF, 2mM sodium orthovanadate 0,1M protease inhibitors cocktail (Sigma Aldrich, St. Louis, MO)). Protein concentration was assessed using Pierce BCA protein assay kit (Thermo Scientific, Waltham, MA). 100 μ g of proteins (50 μ g in the case of transfections with human $\alpha_2\delta_4$) were run on a precast 3-8% Tris-Acetate gel (Life Technologies, Carlsbad, CA). Proteins were transferred to a Hybond ECL nitrocellulose membrane (Sigma Aldrich, St. Louis, MO) using a transfer buffer (25 mM Tris-HCl, 192 mM glycine, 20% methanol, 0.1% SDS). The membrane was blocked for 1 h at room temperature by exposure to 5% non-fat dry milk in 20mM Tris-HCl pH 8, 0.5M NaCl, 0.1% Tween-20 (Sigma Aldrich, St. Louis, MO). The membrane was then incubated overnight at 4 °C with rabbit polyclonal anti human CACNA2D4 antibody, 1:400, (Sigma Aldrich, St. Louis, MO) or for 1 h at RT with mouse monoclonal anti rat β -Tubulin antibody, 1:10000 (Santa Cruz, Dallas, TX). As secondary antibody a goat anti rabbit IgG-HRP or a goat anti-mouse IgG-HRP, 1:10000 (Santa Cruz, Dallas, TX) were used for 1h at room temperature. A chemiluminescence-based kit (Amersham ECL Select Western Blotting Detection Reagent, GE Healthcare, Little Chalfont, UK) was used for detection.

7.13 Electrophysiological recordings

Whole-cell patch-clamp experiments were performed using an Axopatch 700B amplifier (Molecular Devices, Sunnyvale, CA). Borosilicate glass pipets (external diameter 1.5 mm; wall thickness 0.32 mm; Science Products, Frankfurt/Main, Germany) were pulled using a micropipette puller (P97, Sutter Instruments, Novato, CA) to obtain electrodes with a resistance of 1.5-3 M Ω . pClamp10.2 (Molecular Devices, Sunnyvale, CA) and Prism 5 (Graphpad, La Jolla, CA) softwares were used for data-analysis. For recordings were used: a pipet internal solution at pH 7.4 containing 135 mM CsCl, 10 mM HEPES, 10 mM EGTA, 1 mM MgCl₂, and a bath solution adjusted to pH 7.4 (with CsOH) containing 15 mM CaCl₂ or BaCl₂, 10 mM HEPES, 150 mM Choline-Cl, 1 mM MgCl₂. Recording were performed at room temperature (19-22 °C). All voltages were corrected for a liquid junction potential of -8mV. In all protocol used a holding potential of -98mV was applied. Current-voltage (IV) relationship was analysed by applying 50 ms pulses at different potentials from -78mV to 52 mV using 15mM Ca²⁺ as charge carrier. To determine current densities (CD), peak current amplitudes were normalized to the membrane capacitance (C_m). For each analysed cell, the maximum observed current density (CD_{max}) was reported. The following equation was used for fitting the IV curves for CD:

$$CD = G_{\max}(V-V_{\text{rev}})/(1+\exp((V_{0.5, \text{act}}-V)/k_{\text{act}})),$$

where G_{\max} is the maximum slope conductance V is the applied potential, V_{rev} is the reverse potential, $V_{0.5, \text{act}}$ is the half-maximum activation voltage, and k_{act} is the slope parameter of the curve. To study the voltage-dependence of activation, peak current amplitudes were normalized to the maximum current (I_{\max}). The derived I_{norm} values were fitted using the previous formula to calculate G_{\max} and V_{rev} parameters. Those parameter were used to convert the I_{norm} values into points of an activation curve using the formula:

$$\text{Act}(\%) = I_{\text{norm}}/(G_{\max} \times (V-V_{\text{rev}}))$$

The obtained values of the activation curve were fitted using the Boltzmann equation:

$$\text{Act}(\%) = \text{ISS} + (1 - \text{ISS})/(1 + \exp((V_{0.5, \text{act}} - V)/k_{\text{act}}))$$

to obtain $V_{0.5, \text{act}}$ and k_{act} parameters. ISS is the non activating fraction. To analyse the voltage-dependence of inactivation, 50ms test pulses were applied before (initial pulse) and after (final pulse) a 5s pulse at potentials from -98 to 22 mV. Final peak currents were normalized to the initial ones and reported as % of inactivation (Inact(%)). Obtained data were fitted using the Boltzmann equation to extrapolate the half-maximum inactivation voltage ($V_{0.5, \text{inact}}$) and the slope parameter of the curve (k_{inact}). Calcium-dependent inactivation (CDI) was investigated using the same protocol applied for the IV curve, but with 300 ms pulses instead of 50 ms. Experiments were conducted using 15mM Ca^{2+} or 15mM Ba^{2+} as charge carriers. Inactivation was measured as the ratio between the current after 250 ms from the peak current and the peak current itself at the different voltage applied (r250).

7.14 Statistics

Statistical analysis was performed with Prism 5 and statistical significance set at $P < 0.05$ for all conducted tests. RT-PCR densitometric analysis, RT-qPCR, and r250 data are represented as means \pm SD, and compared using unpaired two-tailed student-t test. Electrophysiological data are represented as mean \pm SEM, and analysed by Kruskal–Wallis test followed by Dunn’s post-hoc test for multiple comparisons. Mann–Whitney U-test was used for single comparisons. The fit of the dose-response curve ($Y = \text{Bottom} + (\text{Top} - \text{Bottom}) / (1 + 10^{((X - \text{LogIC50}))})$) for U1_3’ and U1_SCR was performed using Prism 5 with the least square method and no constrains.

8 Contributions to this work

We would like to thank Erik Dassi for his precious contribution in processing the RNA-seq data, Andrea Messina for fruitful discussions about RT-qPCR, Western blotting, and for having provided the retina RNA of *Cacna2d4* wild type and mutant mouse, Giovanni Provenzano and Giusy Covello for having provided respectively the RNA samples from mouse brain and the U1_SCR clone. Finally, the assistance of Verena Burtscher has been fundamental in learning how to perform whole-cell patch clamp and how to analyse the electrophysiological data.

9 Bibliography

- Aartsma-Rus, A., Fokkema, I., Verschuuren, J., Ginjaar, I., van Deutekom, J., van Ommen, G.-J., and den Dunnen, J.T. (2009). Theoretic applicability of antisense-mediated exon skipping for Duchenne muscular dystrophy mutations. *Hum. Mutat.* *30*, 293–299.
- Al-Ubaidi, M.R., Font, R.L., Quiambao, A.B., Keener, M.J., Liou, G.I., Overbeek, P.A., and Baehr, W. (1992). Bilateral retinal and brain tumors in transgenic mice expressing simian virus 40 large T antigen under control of the human interphotoreceptor retinoid-binding protein promoter. *J. Cell Biol.* *119*, 1681–1687.
- Alanis, E.F., Pinotti, M., Mas, A.D., Balestra, D., Cavallari, N., Rogalska, M.E., Bernardi, F., and Pagani, F. (2012). An exon-specific U1 small nuclear RNA (snRNA) strategy to correct splicing defects. *Hum. Mol. Genet.* *21*, 2389–2398.
- Andorfer, C., Kress, Y., Espinoza, M., De Silva, R., Tucker, K.L., Barde, Y.-A., Duff, K., and Davies, P. (2003). Hyperphosphorylation and aggregation of tau in mice expressing normal human tau isoforms. *J. Neurochem.* *86*, 582–590.
- De Angelis, F.G., Sthandier, O., Berarducci, B., Toso, S., Galluzzi, G., Ricci, E., Cossu, G., and Bozzoni, I. (2002). Chimeric snRNA molecules carrying antisense sequences against the splice junctions of exon 51 of the dystrophin pre-mRNA induce exon skipping and restoration of a dystrophin synthesis in Delta 48-50 DMD cells. *Proc. Natl. Acad. Sci. U. S. A.* *99*, 9456–9461.
- Angelotti, T., and Hofmann, F. (1996). Tissue-specific expression of splice variants of the mouse voltage-gated calcium channel alpha2/delta subunit. *FEBS Lett.* *397*, 331–337.
- Askou, A.L., Pournaras, J.C., Pihlmann, M., Svalgaard, J.D., Dagnæs-hansen, F., Mikkelsen, J.G., Jensen, T.G., and Corydon, T.J. (2012). Reduction of choroidal neovascularization in mice endothelial growth factor short hairpin RNA. *J Gene Med* 632–641.
- Avale, M.E., Rodríguez-Martín, T., and Gallo, J.-M. (2013). Trans-splicing correction of tau isoform imbalance in a mouse model of tau mis-splicing. *Hum. Mol. Genet.* *22*, 2603–2611.
- Bacchi, N., Casarosa, S., and Denti, M.A. (2014). Splicing-correcting therapeutic approaches for retinal dystrophies: Where endogenous gene regulation and specificity matter. *Investig. Ophthalmol. Vis. Sci.* *55*, 3285–3294.
- Ball, S.L., Powers, P. a, Shin, H.-S., Morgans, C.W., Peachey, N.S., and Gregg, R.G. (2002). Role of the beta(2) subunit of voltage-dependent calcium channels in the retinal outer plexiform layer. *Invest. Ophthalmol. Vis. Sci.* *43*, 1595–1603.
- Baughan, T., Shababi, M., Coady, T.H., Dickson, A.M., Tullis, G.E., and Lorson, C.L. (2006). Stimulating full-length SMN2 expression by delivering bifunctional RNAs via a viral vector. *Mol. Ther.* *14*, 54–62.
- Baughan, T.D., Dickson, A., Osman, E.Y., and Lorson, C.L. (2009). Delivery of bifunctional RNAs that target an intronic repressor and increase SMN levels in an animal model of spinal muscular atrophy. *Hum. Mol. Genet.* *18*, 1600–1611.
- Berger, W., Kloeckener-Gruissem, B., and Neidhardt, J. (2010). The molecular basis of human retinal and vitreoretinal diseases. *Prog. Retin. Eye Res.* *29*, 335–375.

- Bernstein, G.M., and Jones, O.T. (2007). Kinetics of internalization and degradation of N-type voltage-gated calcium channels: Role of the $\alpha 2/\delta$ subunit. *Cell Calcium* 41, 27–40.
- Bhattacharya, G., Miller, C., Kimberling, W.J., Jablonski, M.M., and Cosgrove, D. (2002). Localization and expression of usherin: A novel basement membrane protein defective in people with Usher's syndrome type IIa. *Hear. Res.* 163, 1–11.
- Bhisitkul, R.B., Robinson, G.S., Moulton, R.S., Claffey, K.P., Gragoudas, E.S., and Miller, J.W. (2005). An antisense oligodeoxynucleotide against vascular endothelial growth factor in a nonhuman primate model of iris neovascularization. *Arch. Ophthalmol.* 123, 214–219.
- Bidaud, I., and Lory, P. (2011). Hallmarks of the channelopathies associated with L-type calcium channels: a focus on the Timothy mutations in Ca(v)1.2 channels. *Biochimie* 93, 2080–2086.
- Bolger, A.M., Lohse, M., and Usadel, B. (2014). Trimmomatic: A flexible trimmer for Illumina sequence data. *Bioinformatics* 30, 2114–2120.
- Bonnal, S., Vigevani, L., and Valcárcel, J. (2012). The spliceosome as a target of novel antitumour drugs. *Nat. Rev. Drug Discov.* 11, 847–859.
- Boylan, J.P., and Wright, A.F. (2000). Identification of a novel protein interacting with RPGR. 9, 2085–2093.
- Brosseau, J.-P., Lucier, J.-F., Lamarche, A.-A., Shkreta, L., Gendron, D., Lapointe, E., Thibault, P., Paquet, E., Perreault, J.-P., Abou Elela, S., et al. (2013). Redirecting splicing with bifunctional oligonucleotides. *Nucleic Acids Res.* 6868, 1–14.
- Buraei, Z., and Yang, J. (2010). The Beta Subunit of Voltage-Gated Calcium Channels. *Physiol. Rev.* 90, 1461–1506.
- Burtscher, V., Schicker, K., Novikova, E., Pöhn, B., Stockner, T., Kugler, C., Singh, A., Zeitz, C., Lancelot, M.-E., Audo, I., et al. (2014). Spectrum of Cav1.4 dysfunction in congenital stationary night blindness type 2. *Biochim. Biophys. Acta* 1838, 2053–2065.
- Busch, A., and Hertel, K.J. Evolution of SR protein and hnRNP splicing regulatory factors. *Wiley Interdiscip. Rev. RNA* 3, 1–12.
- Busquet, P., Nguyen, N.K., Schmid, E., Tanimoto, N., Seeliger, M.W., Ben-Yosef, T., Mizuno, F., Akopian, A., Striessnig, J., and Singewald, N. (2010). Cav1.3 L-type Ca²⁺ channels modulate depression-like behaviour in mice independent of deaf phenotype. *Int. J. Neuropsychopharmacol.* 13, 499–513.
- Byrne, M., Tzekov, R., Wang, Y., Rodgers, A., Cardia, J., Ford, G., Holton, K., Pandarinathan, L., Lapierre, J., Stanney, W., et al. (2013). Novel hydrophobically modified asymmetric RNAi compounds (sd-rxRNA) demonstrate robust efficacy in the eye. *J. Ocul. Pharmacol. Ther.* 29, 855–864.
- Cantí, C., Nieto-Rostro, M., Foucault, I., Hebllich, F., Wratten, J., Richards, M.W., Hendrich, J., Douglas, L., Page, K.M., Davies, A., et al. (2005). The metal-ion-dependent adhesion site in the Von Willebrand factor-A domain of alpha2delta subunits is key to trafficking voltage-gated Ca²⁺ channels. *Proc. Natl. Acad. Sci. U. S. A.* 102, 11230–11235.
- Castellano, A., Wei, X., Birnbaumer, L., and Perez-Reyes, E. (1993). Cloning and expression of a third calcium channel beta subunit. *J. Biol. Chem.* 268, 3450–3455.

- Caudevilla, C., Serra, D., Miliar, A., Codony, C., Asins, G., Bach, M., and Hegardt, F.G. (1998). Natural trans-splicing in carnitine octanoyltransferase pre-mRNAs in rat liver. *Proc. Natl. Acad. Sci. U. S. A.* *95*, 12185–12190.
- Chadderton, N., Millington-Ward, S., Palfi, A., O'Reilly, M., Tuohy, G., Humphries, M.M., Li, T., Humphries, P., Kenna, P.F., and Farrar, G.J. (2009). Improved retinal function in a mouse model of dominant retinitis pigmentosa following AAV-delivered gene therapy. *Mol. Ther.* *17*, 593–599.
- Chao, H., Mansfield, S.G., Bartel, R.C., Hiriyanna, S., Mitchell, L.G., Garcia-Blanco, M.A., and Walsh, C.E. (2003a). Phenotype correction of hemophilia A mice by spliceosome-mediated RNA trans-splicing. *Nat. Med.* *9*, 1015–1019.
- Chao, H., Mansfield, S.G., Bartel, R.C., Hiriyanna, S., Mitchell, L.G., Garcia-Blanco, M.A., and Walsh, C.E. (2003b). Phenotype correction of hemophilia A mice by spliceosome-mediated RNA trans-splicing. *Nat. Med.* *9*, 1015–1019.
- Cho, W.G., Albuquerque, R.J.C., Kleinman, M.E., Tarallo, V., Greco, A., Nozaki, M., Green, M.G., Baffi, J.Z., Ambati, B.K., De Falco, M., et al. (2009). Small interfering RNA-induced TLR3 activation inhibits blood and lymphatic vessel growth. *Proc. Natl. Acad. Sci. U. S. A.* *106*, 7137–7142.
- Cirak, S., Arechavala-Gomez, V., Guglieri, M., Feng, L., Torelli, S., Anthony, K., Abbs, S., Garralda, M.E., Bourke, J., Wells, D.J., et al. (2011). Exon skipping and dystrophin restoration in patients with Duchenne muscular dystrophy after systemic phosphorodiamidate morpholino oligomer treatment: an open-label, phase 2, dose-escalation study. *Lancet* *378*, 595–605.
- De Clercq, E., Eckstein, E., and Merigan, T.C. (1969). Interferon induction increased through chemical modification of a synthetic polyribonucleotide. *Science* *165*, 1137–1139.
- Cloutier, F., Lawrence, M., Goody, R., Lamoureux, S., Al-Mahmood, S., Colin, S., Ferry, A., Conduzorgues, J.-P., Hadri, A., Cursiefen, C., et al. (2012). Antiangiogenic activity of aganirsin in nonhuman primate and rodent models of retinal neovascular disease after topical administration. *Invest. Ophthalmol. Vis. Sci.* *53*, 1195–1203.
- Coady, T.H., and Lorson, C.L. (2010). Trans-splicing-mediated improvement in a severe mouse model of spinal muscular atrophy. *J. Neurosci.* *30*, 126–130.
- Coady, T.H., Baughan, T.D., Shababi, M., Passini, M. a, and Lorson, C.L. (2008). Development of a single vector system that enhances trans-splicing of SMN2 transcripts. *PLoS One* *3*, e3468.
- Collin, R.W., den Hollander, A.I., van der Velde-Visser, S.D., Bennicelli, J., Bennett, J., and Cremers, F.P. (2012). Antisense Oligonucleotide (AON)-based Therapy for Leber Congenital Amaurosis Caused by a Frequent Mutation in CEP290. *Mol. Ther. Nucleic Acids* *1*, e14.
- De Conti, L., Baralle, M., and Buratti, E. (2013). Exon and intron definition in pre-mRNA splicing. *Wiley Interdiscip. Rev. RNA* *4*, 49–60.
- Cooper, T.A. (2005). Use of minigene systems to dissect alternative splicing elements. *Methods* *37*, 331–340.
- Cooper, T.A., Wan, L., and Dreyfuss, G. (2009). RNA and Disease. *Cell* *136*, 777–793.
- Daiger, S., Rossiter, B., Greenberg, J., Christoffels, A., and Hide, W. (1998). Data services and software for identifying genes and mutations causing retinal degeneration. *Invest. Ophthalmol. Vis. Sci.* *39*, S295.
- Daiger, S.P., Sullivan, L.S., and Bowne, S.J. (2013). Genes and mutations causing retinitis pigmentosa. *Clin. Genet.* *84*, 132–141.

- Davies, A., Kadurin, I., Alvarez-Laviada, A., Douglas, L., Nieto-Rostro, M., Bauer, C.S., Pratt, W.S., and Dolphin, A.C. (2010). The $\alpha 2\delta$ subunits of voltage-gated calcium channels form GPI-anchored proteins, a posttranslational modification essential for function. *Proc. Natl. Acad. Sci. U. S. A.* *107*, 1654–1659.
- Denti, M.A., Rosa, A., D'Antona, G., Sthandier, O., De Angelis, F.G., Nicoletti, C., Allocca, M., Pansarasa, O., Parente, V., Musarò, A., et al. (2006). Body-wide gene therapy of Duchenne muscular dystrophy in the mdx mouse model. *Proc. Natl. Acad. Sci. U. S. A.* *103*, 3758–3763.
- Denti, M.A., Incitti, T., Sthandier, O., Nicoletti, C., De Angelis, F.G., Rizzuto, E., Auricchio, A., Musarò, A., and Bozzoni, I. (2008). Long-term benefit of adeno-associated virus/antisense-mediated exon skipping in dystrophic mice. *Hum. Gene Ther.* *19*, 601–608.
- Van Deutekom, J.C., Janson, A. a, Ginjaar, I.B., Frankhuizen, W.S., Aartsma-Rus, A., Bremmer-Bout, M., den Dunnen, J.T., Koop, K., van der Kooi, A.J., Goemans, N.M., et al. (2007). Local dystrophin restoration with antisense oligonucleotide PRO051. *N. Engl. J. Med.* *357*, 2677–2686.
- Dickson, A., Osman, E., and Lorson, C.L. (2008). A Negatively Acting Bifunctional RNA Increases Survival Motor Neuron Both In Vitro and In Vivo. *Hum. Gene Ther.* *19*, 1307–1315.
- Dolphin, A.C. (2012). Calcium channel auxiliary $\alpha 2\delta$ and β subunits: trafficking and one step beyond. *Nat. Rev. Neurosci.* *13*, 542–555.
- Dolphin, A.C. (2013). The $\alpha 2\delta$ subunits of voltage-gated calcium channels. *Biochim. Biophys. Acta - Biomembr.* *1828*, 1541–1549.
- Dolphin, A.C., Wyatt, C.N., Richards, J., Beattie, R.E., Craig, P., Lee, J., Cribbs, L.L., and Volsen, S.G. (1999). The effect of $\alpha 2\delta$ and other accessory subunits on expression and properties of the calcium channel $\alpha 1G$. *519.1*, 35–45.
- Dominski, Z., and Marzluff, W.F. (2007). Formation of the 3' end of histone mRNA: getting closer to the end. *Gene* *396*, 373–390.
- Douglas, A.G.L., and Wood, M.J.A. (2013). Splicing therapy for neuromuscular disease. *Mol. Cell. Neurosci.* *56*, 169–185.
- Dreumont, N., Maresca, A., Boisclair-Lachance, J.-F., Bergeron, A., and Tanguay, R.M. (2005). A minor alternative transcript of the fumarylacetoacetate hydrolase gene produces a protein despite being likely subjected to nonsense-mediated mRNA decay. *BMC Mol. Biol.* *6*, 1.
- Dvorchik, B.H., and Marquis, J.K. (2000). Disposition and toxicity of a mixed backbone antisense oligonucleotide, targeted against human cytomegalovirus, after intravitreal injection of escalating single doses in the rabbit. *Drug Metab. Dispos.* *28*, 1255–1261.
- Edgar, R., Domrachev, M., and Lash, A.E. (2002). Gene Expression Omnibus: NCBI gene expression and hybridization array data repository. *Nucleic Acids Res.* *30*, 207–210.
- Ellis, S.B., Williams, M.E., Ways, N.R., Brenner, R., Sharp, a H., Leung, a T., Campbell, K.P., McKenna, E., Koch, W.J., and Hui, a (1988). Sequence and expression of mRNAs encoding the alpha 1 and alpha 2 subunits of a DHP-sensitive calcium channel. *Science* *241*, 1661–1664.
- Fattal, E., and Bochot, A. (2006). Ocular delivery of nucleic acids: antisense oligonucleotides, aptamers and siRNA. *Adv. Drug Deliv. Rev.* *58*, 1203–1223.
- Felix, R., Gurnett, C.A., Waard, M. De, Campbell, K.P., and Roche, I.J. (1997). Dissection of Functional Domains of the Voltage-Dependent Ca^{2+} Channel $\alpha 2\delta$ Subunit. *J. Neurosci.* *17*, 6884–6891.

- Fingert, J.H., Oh, K., Chung, M., Scheetz, T.E., Andorf, J.L., Johnson, R.M., Sheffield, V.C., and Stone, E.M. (2008). Association of a novel mutation in the retinol dehydrogenase 12 (RDH12) gene with autosomal dominant retinitis pigmentosa. *Arch. Ophthalmol.* *126*, 1301–1307.
- Flouriort, G., Brand, H., Seraphin, B., and Gannon, F. (2002). Natural trans-spliced mRNAs are generated from the human estrogen receptor- α (hER α) gene. *J. Biol. Chem.* *277*, 26244–26251.
- Gandini, M. a., Sandoval, a., and Felix, R. (2014). Patch-Clamp Recording of Voltage-Sensitive Ca²⁺ Channels. *Cold Spring Harb. Protoc.* *2014*, pdb.top066092 – pdb.top066092.
- Gendron, D., Carriero, S., Garneau, D., Villemaire, J., Klinck, R., Elela, S.A., Damha, M.J., and Chabot, B. (2006). Modulation of 5' splice site selection using tailed oligonucleotides carrying splicing signals. *BMC Biotechnol.* *6*, 5.
- Gerard, X., Perrault, I., Hanein, S., Silva, E., Bigot, K., Defoort-Delhemmes, S., Rio, M., Munnich, A., Scherman, D., Kaplan, J., et al. (2012). AON-mediated Exon Skipping Restores Ciliation in Fibroblasts Harboring the Common Leber Congenital Amaurosis CEP290 Mutation. *Mol. Ther. Nucleic Acids* *1*, e29.
- Glaus, E., Schmid, F., Da Costa, R., Berger, W., and Neidhardt, J. (2011). Gene therapeutic approach using mutation-adapted U1 snRNA to correct a RPGR splice defect in patient-derived cells. *Mol. Ther.* *19*, 936–941.
- Goemans, N.M., Tulinius, M., van den Akker, J.T., Burm, B.E., Ekhart, P.F., Heuvelmans, N., Holling, T., Janson, A.A., Platenburg, G.J., Sipkens, J.A., et al. (2011). Systemic administration of PRO051 in Duchenne's muscular dystrophy. *N. Engl. J. Med.* *364*, 1513–1522.
- Gomes Dos Santos, a L., Bochot, A., and Fattal, E. (2005). Intraocular delivery of oligonucleotides. *Curr. Pharm. Biotechnol.* *6*, 7–15.
- Goyenville, A., Babbs, A., van Ommen, G.-J.B., Garcia, L., and Davies, K.E. (2009). Enhanced exon-skipping induced by U7 snRNA carrying a splicing silencer sequence: Promising tool for DMD therapy. *Mol. Ther.* *17*, 1234–1240.
- Goyenville, A., Wright, J., Babbs, A., Wilkins, V., Garcia, L., and Davies, K.E. (2012). Engineering multiple U7snRNA constructs to induce single and multiexon-skipping for Duchenne muscular dystrophy. *Mol. Ther.* *20*, 1212–1221.
- Gurnett, C. a, De Waard, M., and Campbell, K.P. (1996). Dual function of the voltage-dependent Ca²⁺ channel α 2 delta subunit in current stimulation and subunit interaction. *Neuron* *16*, 431–440.
- Gurnett, C.A., Felix, R., and Campbell, K.P. (1997). Extracellular interaction of the voltage-dependent Ca²⁺ channel α 2delta and α 1 subunits. *J. Biol. Chem.* *272*, 18508–18512.
- Hamill, O.P., Marty, A., Neher, E., Sakmann, B., and Sigworth, F.J. (1981). Improved patch-clamp techniques for high-resolution current recording from cells and cell-free membrane patches. *Pflügers Arch. Eur. J. Physiol.* *391*, 85–100.
- Hartong, D.T., Berson, E.L., and Dryja, T.P. (2006). Retinitis pigmentosa. *Lancet* *368*, 1795–1809.
- Havens, M. a, Duelli, D.M., and Hastings, M.L. (2013). Targeting RNA splicing for disease therapy. *Wiley Interdiscip. Rev. RNA* *4*, 247–266.
- Hernan, I., Gamundi, M.J., Planas, E., Borràs, E., Maseras, M., and Carballo, M. (2011). Cellular expression and siRNA-mediated interference of rhodopsin cis-acting splicing mutants associated with autosomal dominant retinitis pigmentosa. *Invest. Ophthalmol. Vis. Sci.* *52*, 3723–3729.

- Hobom, M., Dai, S., Marais, E., Lacinova, L., Hofmann, F., Klugbauer, N., and Str, B. (2000). Neuronal distribution and functional characterization of the calcium channel $\alpha_2\text{-2}$ subunit. *Eur. J. Neurosci.* *12*, 1217–1226.
- Hodgkin, A.L., and Huxley, A.F. (1952). A quantitative description of membrane current and its applications to conduction and excitation in nerve. *J. Physiol.* *117*, 500–544.
- Den Hollander, A.I., Koenekoop, R.K., Yzer, S., Lopez, I., Arends, M.L., Voeselek, K.E.J., Zonneveld, M.N., Strom, T.M., Meitinger, T., Brunner, H.G., et al. (2006). Mutations in the CEP290 (NPHP6) gene are a frequent cause of Leber congenital amaurosis. *Am. J. Hum. Genet.* *79*, 556–561.
- Den Hollander, A.I., Roepman, R., Koenekoop, R.K., and Cremers, F.P.M. (2008). Leber congenital amaurosis: genes, proteins and disease mechanisms. *Prog. Retin. Eye Res.* *27*, 391–419.
- Hong, D.-H. (2003). RPGR Isoforms in Photoreceptor Connecting Cilia and the Transitional Zone of Motile Cilia. *Invest. Ophthalmol. Vis. Sci.* *44*, 2413–2421.
- Hong, D.-H., and Li, T. (2002). Complex expression pattern of RPGR reveals a role for purine-rich exonic splicing enhancers. *Invest. Ophthalmol. Vis. Sci.* *43*, 3373–3382.
- Hoppa, M., Lana, B., Margas, W., Dolphin, A., and Ryan, T. (2012). Alpha 2 Delta Expression Sets Presynaptic Calcium Channel Abundance and Release Probability. *Nature* *486*, 122–125.
- Horn, R., and Korn, S.J. (1992). Prevention of rundown in electrophysiological recording. *Methods Enzymol.* *207*, 149–155.
- Hoskins, A. a, and Moore, M.J. (2012). The spliceosome: a flexible, reversible macromolecular machine. *Trends Biochem. Sci.* *37*, 179–188.
- Hu, J., Wu, Q., Li, T., Chen, Y., and Wang, S. (2013). Inhibition of high glucose-induced VEGF release in retinal ganglion cells by RNA interference targeting G protein-coupled receptor 91. *Exp. Eye Res.* *109*, 31–39.
- Huc, S., Monteil, A., Bidaud, I., Barbara, G., Chemin, J., and Lory, P. (2009). Regulation of T-type calcium channels: signalling pathways and functional implications. *Biochim. Biophys. Acta* *1793*, 947–952.
- Jacobson, S.G., Cideciyan, A. V., Ratnakaram, R., Heon, E., Schwartz, S.B., Roman, A.J., Peden, M.C., Aleman, T.S., Boye, S.L., Sumaroka, A., et al. (2012). Gene Therapy for Leber Congenital Amaurosis Caused by RPE65 Mutations: Safety and Efficacy in 15 Children and Adults Followed Up to 3 Years. *Arch. Ophthalmol.* *130*, 9–24.
- Järver, P., O’Donovan, L., and Gait, M.J. (2013). A Chemical View of Oligonucleotides for Exon Skipping and Related Drug Applications. *Nucleic Acid Ther.* *24*.
- Jean-Philippe, J., Paz, S., and Caputi, M. (2013). hnRNP A1: the Swiss army knife of gene expression. *Int. J. Mol. Sci.* *14*, 18999–19024.
- Jiang, L., Li, T.Z., Boye, S.E., Hauswirth, W.W., Frederick, J.M., and Baehr, W. (2013). RNAi-mediated gene suppression in a GCAP1(L151F) cone-rod dystrophy mouse model. *PLoS One* *8*, e57676.
- Jin, Y., Suzuki, H., Maegawa, S., Endo, H., Sugano, S., Hashimoto, K., Yasuda, K., and Inoue, K. (2003). A vertebrate RNA-binding protein Fox-1 regulates tissue-specific splicing via the pentanucleotide GCAUG. *EMBO J.* *22*, 905–912.

- Jones, L.P., Wei, S., and Yue, D.T. (1998). Mechanism of Auxiliary Subunit Modulation of Neuronal $\alpha 1E$ Calcium Channels. *J. Gen. Physiol.* *112*.
- Kadurin, I., Alvarez-Laviada, A., Ng, S.F.J., Walker-Gray, R., D'Arco, M., Fadel, M.G., Pratt, W.S., and Dolphin, A.C. (2012). Calcium currents are enhanced by $\alpha 2\delta$ -1 lacking its membrane anchor. *J. Biol. Chem.* *287*, 33554–33566.
- Kafasla, P., Mickleburgh, I., Llorian, M., Coelho, M., Gooding, C., Cherny, D., Joshi, A., Kotik-Kogan, O., Curry, S., Eperon, I.C., et al. (2012). Defining the roles and interactions of PTB. *Biochem. Soc. Trans.* *40*, 815–820.
- Kalbfuss, B., Mabon, S. a, and Misteli, T. (2001). Correction of alternative splicing of tau in frontotemporal dementia and parkinsonism linked to chromosome 17. *J. Biol. Chem.* *276*, 42986–42993.
- Kanasty, R., Dorkin, J.R., Vegas, A., and Anderson, D. (2013). Delivery materials for siRNA therapeutics. *Nat. Mater.* *12*, 967–977.
- Khanna, H., Hurd, T.W., Lillo, C., Shu, X., Parapuram, S.K., He, S., Akimoto, M., Wright, A.F., Margolis, B., Williams, D.S., et al. (2005). RPGR-ORF15, which is mutated in retinitis pigmentosa, associates with SMC1, SMC3, and microtubule transport proteins. *J. Biol. Chem.* *280*, 33580–33587.
- Kim, D., Pertea, G., Trapnell, C., Pimentel, H., Kelley, R., and Salzberg, S.L. (2013). TopHat2: accurate alignment of transcriptomes in the presence of insertions, deletions and gene fusions. *Genome Biol.* *14*, R36.
- Kinali, M., Arechavala-Gomez, V., Feng, L., Cirak, S., Hunt, D., Adkin, C., Guglieri, M., Ashton, E., Abbs, S., Nihoyannopoulos, P., et al. (2009). Local restoration of dystrophin expression with the morpholino oligomer AVI-4658 in Duchenne muscular dystrophy: a single-blind, placebo-controlled, dose-escalation, proof-of-concept study. *Lancet Neurol.* *8*, 918–928.
- Kirschner, R., Erturk, D., Zeitz, C., Sahin, S., Ramser, J., Cremers, F.P., Ropers, H.H., and Berger, W. (2001). DNA sequence comparison of human and mouse retinitis pigmentosa GTPase regulator (RPGR) identifies tissue-specific exons and putative regulatory elements. *Hum. Genet.* *109*, 271–278.
- Kleinman, M.E., Yamada, K., Takeda, A., Chandrasekaran, V., Nozaki, M., Baffi, J.Z., Albuquerque, R.J.C., Yamasaki, S., Itaya, M., Pan, Y., et al. (2008). Sequence- and target-independent angiogenesis suppression by siRNA via TLR3. *Nature* *452*, 591–597.
- Klugbauer, N., Lacinova, L., Hobom, M., and Hofmann, F. (2000). Molecular Diversity of the Calcium Channel $\alpha 2\delta$ Subunit. *J. Neurosci.* *19*, 684–691.
- Knoflach, D., Kerov, V., Sartori, S.B., Obermair, G.J., Schmuckermair, C., Liu, X., Sothilingam, V., Garrido, M.G., Baker, S.A., Glösmann, M., et al. (2013). Cav1.4 IT mouse as model for vision impairment in human congenital stationary night blindness type 2. *Channels* *7*.
- Kole, R., Krainer, A.R., and Altman, S. (2012). RNA therapeutics: beyond RNA interference and antisense oligonucleotides. *Nat. Rev. Drug Discov.* *11*, 125–140.
- Kornbliht, A.R., Schor, I.E., Alló, M., Dujardin, G., Petrillo, E., and Muñoz, M.J. (2013). Alternative splicing: a pivotal step between eukaryotic transcription and translation. *Nat. Rev. Mol. Cell Biol.* *14*, 153–165.
- Koschak, A., Reimer, D., Walter, D., Hoda, J.-C., Heinzle, T., Grabner, M., and Striessnig, J. (2003). Cav1.4 α 1 subunits can form slowly inactivating dihydropyridine-sensitive L-type Ca²⁺ channels lacking Ca²⁺-dependent inactivation. *J. Neurosci.* *23*, 6041–6049.

- Koshkin, A.A., Singh, S.K., Nielsen, P., Rajwanshi, V.K., Kumar, R., Meldgaard, M., Olsen, C.E., and Wengel, J. (1998). LNA (Locked Nucleic Acids): Synthesis of the adenine, cytosine, guanine, 5-methylcytosine, thymine and uracil bicyclonucleoside monomers, oligomerisation, and unprecedented nucleic acid recognition. *Tetrahedron* *54*, 3607–3630.
- Krol, J., Loedige, I., and Filipowicz, W. (2010). The widespread regulation of microRNA biogenesis, function and decay. *Nat. Rev. Genet.* *11*, 597–610.
- Kuroyanagi, H. (2009). Fox-1 family of RNA-binding proteins. *Cell. Mol. Life Sci.* *66*, 3895–3907.
- Kurreck, J. (2003). Antisense technologies. Improvement through novel chemical modifications. *Eur. J. Biochem.* *270*, 1628–1644.
- Kurshan, P.T., Oztan, A., and Schwarz, T.L. (2009). Presynaptic $\alpha 2\delta$ -3 is required for synaptic morphogenesis independent of its Ca^{2+} -channel functions. *Nat. Neurosci.* *12*, 1415–1423.
- Lam, B.J., and Hertel, K.J. (2002). A general role for splicing enhancers in exon definition. *RNA* *8*, 1233–1241.
- Lana, B., Schlick, B., Martin, S., Pratt, W.S., Page, K.M., Goncalves, L., Rahman, W., Dickenson, A.H., Bauer, C.S., and Dolphin, A.C. (2014). Differential upregulation in DRG neurons of an $\alpha 2\delta$ -1 splice variant with a lower affinity for gabapentin after peripheral sensory nerve injury. *Pain* *155*, 522–533.
- Lareau, L.F., Brooks, A.N., Soergel, D.A.W., Meng, Q., and Brenner, S.E. (2007). The coupling of alternative splicing and nonsense-mediated mRNA decay. *Adv. Exp. Med. Biol.* *623*, 190–211.
- Lee, A., Wang, S., Williams, B., Hagen, J., Scheetz, T.E., and Haeseleer, F. (2014). Characterization of Cav1.4 Complexes ($\alpha 1.4$, $\beta 2$, $\alpha 2\delta 4$) in HEK293T cells and in the Retina. *J. Biol. Chem.*
- Lejeune, F., and Maquat, L.E. (2005). Mechanistic links between nonsense-mediated mRNA decay and pre-mRNA splicing in mammalian cells. *Curr. Opin. Cell Biol.* *17*, 309–315.
- Lewandowska, M.A. (2013). The missing puzzle piece: Splicing mutations. *Int. J. Clin. Exp. Pathol.* *6*, 2675–2682.
- Lim, K.H., Ferraris, L., Filloux, M.E., Raphael, B.J., and Fairbrother, W.G. (2011a). Using positional distribution to identify splicing elements and predict pre-mRNA processing defects in human genes. *Proc. Natl. Acad. Sci. U. S. A.* *108*, 11093–11098.
- Lim, K.H., Ferraris, L., Filloux, M.E., Raphael, B.J., and Fairbrother, W.G. (2011b). Using positional distribution to identify splicing elements and predict pre-mRNA processing defects in human genes. *Proc. Natl. Acad. Sci. U. S. A.* *108*, 11093–11098.
- Liu, X., Bulgakov, O. V., Darrow, K.N., Pawlyk, B., Adamian, M., Liberman, M.C., and Li, T. (2007). Usherin is required for maintenance of retinal photoreceptors and normal development of cochlear hair cells. *Proc. Natl. Acad. Sci. U. S. A.* *104*, 4413–4418.
- López-Bigas, N., Audit, B., Ouzounis, C., Parra, G., and Guigó, R. (2005). Are splicing mutations the most frequent cause of hereditary disease? *FEBS Lett.* *579*, 1900–1903.
- Maguire, A.M., Simonelli, F., Pierce, E.A., Pugh, E.N., Mingozzi, F., Bennicelli, J., Banfi, S., Marshall, K.A., Testa, F., Surace, E.M., et al. (2008). Safety and efficacy of gene transfer for Leber's congenital amaurosis.

- Maguire, A.M., High, K. a., Auricchio, A., Wright, J.F., Pierce, E. a., Testa, F., Mingozzi, F., Bencicelli, J.L., Ying, G.S., Rossi, S., et al. (2009). Age-dependent effects of RPE65 gene therapy for Leber's congenital amaurosis: a phase 1 dose-escalation trial. *Lancet* *374*, 1597–1605.
- Malmivuo, J., and Plonsey, R. (1995). *Bioelectromagnetism: Principles and Applications of Bioelectric and Biomagnetic Fields*.
- Mansfield, S.G., Chao, H., and Walsh, C.E. (2004). RNA repair using spliceosome-mediated RNA trans-splicing. *Trends Mol. Med.* *10*, 263–268.
- Marquis, J., Meyer, K., Angehrn, L., Kämpfer, S.S., Rothen-Rutishauser, B., and Schümperli, D. (2007). Spinal muscular atrophy: SMN2 pre-mRNA splicing corrected by a U7 snRNA derivative carrying a splicing enhancer sequence. *Mol. Ther.* *15*, 1479–1486.
- Martin, K.R.G., Klein, R.L., and Quigley, H. a (2002). Gene delivery to the eye using adeno-associated viral vectors. *Methods* *28*, 267–275.
- Martin P. (1995). New access to 2-O-alkylated ribonucleosides and properties of 2-O-alkylated oligoribonucleotides. *Helv. Chim. Acta* *486*⁵⁰⁴.
- Matsuo, M. (1996). Duchenne/Becker muscular dystrophy: from molecular diagnosis to gene therapy. *Brain Dev.* *7604*, 167–172.
- Mavlyutov, T.A., Zhao, H., and Ferreira, P.A. (2002). Species-specific subcellular localization of RPGR and RPGRIP isoforms : implications for the phenotypic variability of congenital retinopathies among species. *11*, 1899–1907.
- McRory, J.E., Hamid, J., Doering, C.J., Garcia, E., Parker, R., Hamming, K., Chen, L., Hildebrand, M., Beedle, A.M., Feldcamp, L., et al. (2004). The CACNA1F gene encodes an L-type calcium channel with unique biophysical properties and tissue distribution. *J. Neurosci.* *24*, 1707–1718.
- Meindl, A., Dry, K., Herrmann, K., Manson, F., Ciccodicola, A., Edgar, A., Carvalho, M.R., Achatz, H., Hellebrand, H., Lennon, A., et al. (1996). A gene (RPGR) with homology to the RCC1 guanine nucleotide exchange factor is mutated in X-linked retinitis pigmentosa (RP3). *Nat. Genet.* *13*, 35–42.
- Mercer, A.J., Chen, M., and Thoreson, W.B. (2011). Lateral mobility of presynaptic L-type calcium channels at photoreceptor ribbon synapses. *J. Neurosci.* *31*, 4397–4406.
- Mockel, a, Perdomo, Y., Stutzmann, F., Letsch, J., Marion, V., and Dollfus, H. (2011). Retinal dystrophy in Bardet-Biedl syndrome and related syndromic ciliopathies. *Prog. Retin. Eye Res.* *30*, 258–274.
- Morgans, C.W., Bayley, P.R., Oesch, N.W., Ren, G., Akileswaran, L., and Taylor, W.R. (2005). Photoreceptor calcium channels: insight from night blindness. *Vis. Neurosci.* *22*, 561–568.
- Murphy, W.J., Watkins, K.P., and Agabian, N. (1986). Identification of a novel Y branch structure as an intermediate in trypanosome mRNA processing: evidence for trans splicing. *Cell* *47*, 517–525.
- Nachury, M. V, Seeley, E.S., and Jin, H. (2010). Trafficking to the ciliary membrane: how to get across the periciliary diffusion barrier? *Annu. Rev. Cell Dev. Biol.* *26*, 59–87.
- Neidhardt, J., Glaus, A.E., Barthelmes, D., Zeitz, C., Fleischhauer, J., and Berger, W. (2007). Identification and Characterization of a Novel RPGR Isoform in Human Retina. *28*, 797–807.
- Niblock, M., and Gallo, J.-M. (2012). Tau alternative splicing in familial and sporadic tauopathies. *Biochem. Soc. Trans.* *40*, 677–680.

- Nicholson, P., Yepiskoposyan, H., Metze, S., Zamudio Orozco, R., Kleinschmidt, N., and Mühlemann, O. (2010). Nonsense-mediated mRNA decay in human cells: mechanistic insights, functions beyond quality control and the double-life of NMD factors. *Cell. Mol. Life Sci.* *67*, 677–700.
- Nielsen, P.E., Egholm, M., Berg, R.H., and Buchardt, O. (1991). Sequence-selective recognition of DNA by strand displacement with a thymine-substituted polyamide. *Science* *254*, 1497–1500.
- Obika, S., Nanbu, D., Hari, Y., Andoh, J., Morio, K., Doi, T., and Imanishi, T. (1998). Stability and structural features of the duplexes containing nucleoside analogues with a fixed N-type conformation, 2'-O,4'-C-methyleneribonucleosides. *Tetrahedron Lett.* *39*, 5401–5404.
- Osman, E.Y., Yen, P.-F., and Lorson, C.L. (2012). Bifunctional RNAs targeting the intronic splicing silencer N1 increase SMN levels and reduce disease severity in an animal model of spinal muscular atrophy. *Mol. Ther.* *20*, 119–126.
- Owen, N., Zhou, H., Malygin, A. a, Sangha, J., Smith, L.D., Muntoni, F., and Eperon, I.C. (2011). Design principles for bifunctional targeted oligonucleotide enhancers of splicing. *Nucleic Acids Res.* *39*, 7194–7208.
- Patel, S.B., and Bellini, M. (2008). The assembly of a spliceosomal small nuclear ribonucleoprotein particle. *Nucleic Acids Res.* *36*, 6482–6493.
- Perrault, I., Delphin, N., Hanein, S., Gerber, S., Dufier, J.-L., Roche, O., Defoort-Dhellemmes, S., Dollfus, H., Fazzi, E., Munnich, A., et al. (2007). Spectrum of NPHP6/CEP290 mutations in Leber congenital amaurosis and delineation of the associated phenotype. *Hum. Mutat.* *28*, 416.
- Pets-Silva, H., and Linden, R. (2014). Advances in gene therapy technologies to treat retinitis pigmentosa. *Clin. Ophthalmol.* *8*, 127–136.
- Pinotti, M., Rizzotto, L., Balestra, D., Lewandowska, M.A., Cavallari, N., Marchetti, G., Bernardi, F., and Pagani, F. (2008). U1-snRNA-mediated rescue of mRNA processing in severe factor VII deficiency. *Blood* *111*, 2681–2684.
- Piva, F., Giulietti, M., Nocchi, L., and Principato, G. (2009). SpliceAid: A database of experimental RNA target motifs bound by splicing proteins in humans. *Bioinformatics* *25*, 1211–1213.
- Pozzoli, U., and Sironi, M. (2005). Silencers regulate both constitutive and alternative splicing events in mammals. *Cell. Mol. Life Sci.* *62*, 1579–1604.
- Qin, N., Yagel, S., Momplaisir, M., Codd, E.E., and Andrea, M.R.D. (2002). Molecular Cloning and Characterization of the Human Voltage-Gated Calcium Channel $\alpha 2\delta 4$ Subunit. *Mol. Pharmacol.* *62*, 485–496.
- Reese, M.G., Eeckman, F.H., Kulp, D., and Haussler, D. (1997). Improved splice site detection in Genie. *J. Comput. Biol.* *4*, 311–323.
- Reiners, J., Nagel-Wolfrum, K., Jürgens, K., Märker, T., and Wolfrum, U. (2006). Molecular basis of human Usher syndrome: Deciphering the meshes of the Usher protein network provides insights into the pathomechanisms of the Usher disease. *Exp. Eye Res.* *83*, 97–119.
- Roepman, R., Van Duijnhoven, G., Rosenberg, T., Pinckers, A.J.L.G., Bleeker-Wagemakers, L.M., Bergen, A.A.B., Post, J., Beck, A., Reinhardt, R., Ropers, H.H., et al. (1996). Positional cloning of the gene for X-linked retinitis pigmentosa 3: Homology with the guanine-nucleotide-exchange factor RCC1. *Hum. Mol. Genet.* *5*, 1035–1041.

- Roepman, R., Bernoud-hubac, N., Schick, D.E., Mauerer, A., Berger, W., Ropers, H., Cremers, F.P.M., and Ferreira, P.A. (2000). The retinitis pigmentosa GTPase regulator (RPGR) interacts with novel transport-like proteins in the outer segments of rod photoreceptors. *9*, 2095–2106.
- Saleh, A.F., Arzumanov, A.A., and Gait, M.J. (2012). Overview of alternative oligonucleotide chemistries for exon skipping. *Methods Mol. Biol.* *867*, 365–378.
- Sánchez-Alcudia, R., Pérez, B., Pérez-Cerdá, C., Ugarte, M., and Desviat, L.R. (2011). Overexpression of adapted U1snRNA in patients' cells to correct a 5' splice site mutation in propionic acidemia. *Mol. Genet. Metab.* *102*, 134–138.
- Sandoval, A., Oviedo, N., Andrade, A., and Felix, R. (2004). Glycosylation of asparagines 136 and 184 is necessary for the $\alpha_2\delta_1$ subunit-mediated regulation of voltage-gated Ca²⁺ channels. *FEBS Lett.* *576*, 21–26.
- Schlick, B., Flucher, B.E., and Obermair, G.J. (2012). VOLTAGE-ACTIVATED CALCIUM CHANNEL EXPRESSION PROFILES IN MOUSE BRAIN AND CULTURED HIPPOCAMPAL NEURONS. *Neuroscience* *167*, 786–798.
- Schmid, F., Glaus, E., Barthelmes, D., Fliegau, M., Gaspar, H., Nürnberg, G., Nürnberg, P., Omran, H., Berger, W., and Neidhardt, J. (2011). U1 snRNA-mediated gene therapeutic correction of splice defects caused by an exceptionally mild BBS mutation. *Hum. Mutat.* *32*, 815–824.
- Schmid, F., Hiller, T., Korner, G., Glaus, E., Berger, W., and Neidhardt, J. (2013). A gene therapeutic approach to correct splice defects with modified U1 and U6 snRNPs. *Hum. Gene Ther.* *24*, 97–104.
- De Sevilla Müller, L.P., Liu, J., Solomon, A., Rodriguez, A., and Brecha, N.C. (2013). Expression of voltage-gated calcium channel $\alpha(2)\delta(4)$ subunits in the mouse and rat retina. *J. Comp. Neurol.* *521*, 2486–2501.
- Seyhan, A. a (2011). RNAi: a potential new class of therapeutic for human genetic disease. *Hum. Genet.* *130*, 583–605.
- Shababi, M., Glascock, J., and Lorson, C.L. (2011). Combination of SMN trans-splicing and a neurotrophic factor increases the life span and body mass in a severe model of spinal muscular atrophy. *Hum. Gene Ther.* *22*, 135–144.
- Shen, W.Y., and Rakoczy, P.E. (2001). Uptake dynamics and retinal tolerance of phosphorothioate oligonucleotide and its direct delivery into the site of choroidal neovascularization through subretinal administration in the rat. *Antisense Nucleic Acid Drug Dev.* *11*, 257–264.
- Shen, W.Y., Garrett, K.L., da Cruz, L., Constable, I.J., and Rakoczy, P.E. (1999). Dynamics of phosphorothioate oligonucleotides in normal and laser photocoagulated retina. *Br. J. Ophthalmol.* *83*, 852–861.
- Shibata, H., Huynh, D.P., and Pulst, S.M. (2000). A novel protein with RNA-binding motifs interacts with ataxin-2. *Hum. Mol. Genet.* *9*, 1303–1313.
- Shirokov, R., Ferreira, G., Yi, J., and Ríos, E. (1998). Inactivation of Gating Currents of L-Type Calcium Channels Specific Role of the $\alpha_2\delta$ Subunit. *111*.
- Shu, X., Fry, a M., Tulloch, B., Manson, F.D.C., Crabb, J.W., Khanna, H., Faragher, a J., Lennon, a, He, S., Trojan, P., et al. (2005). RPGR ORF15 isoform co-localizes with RPGRIP1 at centrioles and basal bodies and interacts with nucleophosmin. *Hum. Mol. Genet.* *14*, 1183–1197.

- Sibley, C.R. (2014). Regulation of gene expression through production of unstable mRNA isoforms. *Biochem. Soc. Trans.* *42*, 1196–1205.
- Simonelli, F., Maguire, A.M., Testa, F., Pierce, E.A., Mingozzi, F., Bencicelli, J.L., Rossi, S., Marshall, K., Banfi, S., Surace, E.M., et al. (2010). Gene therapy for Leber's congenital amaurosis is safe and effective through 1.5 years after vector administration.
- Sinnegger-Brauns, M.J., Huber, I.G., Koschak, A., Wild, C., Obermair, G.J., Einzinger, U., Hoda, J.-C., Sartori, S.B., and Striessnig, J. (2009). Expression and 1,4-dihydropyridine-binding properties of brain L-type calcium channel isoforms. *Mol. Pharmacol.* *75*, 407–414.
- Sipos, I., Pika-Hartlaub, U., Hofmann, F., Flucher, B.E., and Melzer, W. (2000). Effects of the dihydropyridine receptor subunits gamma and alpha2delta on the kinetics of heterologously expressed L-type Ca²⁺ channels. *Pflugers Arch. Eur. J. Physiol.* *439*, 691–699.
- Skordis, L. a, Dunckley, M.G., Yue, B., Eperon, I.C., and Muntoni, F. (2003). Bifunctional antisense oligonucleotides provide a trans-acting splicing enhancer that stimulates SMN2 gene expression in patient fibroblasts. *Proc. Natl. Acad. Sci. U. S. A.* *100*, 4114–4119.
- Smith, a J., Bainbridge, J.W.B., and Ali, R.R. (2012). Gene supplementation therapy for recessive forms of inherited retinal dystrophies. *Gene Ther.* *19*, 154–161.
- Specht, D., Wu, S.-B., Turner, P., Dearden, P., Koentgen, F., Wolfrum, U., Maw, M., Brandstätter, J.H., and tom Dieck, S. (2009). Effects of presynaptic mutations on a postsynaptic Cacna1s calcium channel colocalized with mGluR6 at mouse photoreceptor ribbon synapses. *Invest. Ophthalmol. Vis. Sci.* *50*, 505–515.
- Springer, T.A. (2006). Complement and the Multifaceted Functions of VWA and Integrin I Domains. *Structure* *14*, 1611–1616.
- Sproat, B.S., Lamond, A.I., Beijer, B., Neuner, P., and Ryder, U. (1989). Highly efficient chemical synthesis of 2'-O-methyloligoribonucleotides and tetrabiotinylated derivatives; novel probes that are resistant to degradation by RNA or DNA specific nucleases. *Nucleic Acids Res.* *17*, 3373–3386.
- Stein-Streilein, J. (2008). Immune regulation and the eye. *Trends Immunol.* *29*, 548–554.
- Stenson, P.D., Ball, E. V, Mort, M., Phillips, A.D., Shiel, J. a, Thomas, N.S.T., Abeyasinghe, S., Krawczak, M., and Cooper, D.N. (2003). Human Gene Mutation Database (HGMD): 2003 update. *Hum. Mutat.* *21*, 577–581.
- Sterne-Weiler, T., Howard, J., Mort, M., Cooper, D.N., and Sanford, J.R. (2011). Loss of exon identity is a common mechanism of human inherited disease. *Genome Res.* *21*, 1563–1571.
- Striessnig, J., Bolz, H.J., and Koschak, A. (2010). Channelopathies in Cav1.1, Cav1.3, and Cav1.4 voltage-gated L-type Ca²⁺ channels. *Pflugers Arch.* *460*, 361–374.
- Summerton, J., and Weller, D. (1997). Morpholino antisense oligomers: design, preparation, and properties. *Antisense Nucleic Acid Drug Dev.* *7*, 187–195.
- Surace, E.M., and Auricchio, A. (2008). Versatility of AAV vectors for retinal gene transfer. *Vision Res.* *48*, 353–359.
- Susani, L., Pangrazio, A., Sobacchi, C., Taranta, A., Mortier, G., Savarirayan, R., Villa, A., Orchard, P., Vezzoni, P., Albertini, A., et al. (2004). TCIRG1-dependent recessive osteopetrosis: mutation analysis, functional identification of the splicing defects, and in vitro rescue by U1 snRNA. *Hum. Mutat.* *24*, 225–235.

- Sutton, R.E., and Boothroyd, J.C. (1986). Evidence for trans splicing in trypanosomes. *Cell* 47, 527–535.
- Tahara, M., Pergolizzi, R.G., Kobayashi, H., Krause, A., Luettich, K., Lesser, M.L., and Crystal, R.G. (2004). Trans-splicing repair of CD40 ligand deficiency results in naturally regulated correction of a mouse model of hyper-IgM X-linked immunodeficiency. *Nat. Med.* 10, 835–841.
- Tanner, G., Glaus, E., Barthelmes, D., Ader, M., Fleischhauer, J., Pagani, F., Berger, W., and Neidhardt, J. (2009). Therapeutic strategy to rescue mutation-induced exon skipping in rhodopsin by adaptation of U1 snRNA. *Hum. Mutat.* 30, 255–263.
- Tazi, J., Bakkour, N., and Stamm, S. (2009). Alternative splicing and disease. *Biochim. Biophys. Acta* 1792, 14–26.
- Thaler, S., Rejdak, R., Dietrich, K., Ladewig, T., Okuno, E., Kocki, T., Turski, W.A., Junemann, A., Zrenner, E., and Schuettauf, F. (2006). A selective method for transfection of retinal ganglion cells by retrograde transfer of antisense oligonucleotides against kynurenine aminotransferase II. *Mol. Vis.* 12, 100–107.
- Thorvaldsdóttir, H., Robinson, J.T., and Mesirov, J.P. (2013). Integrative Genomics Viewer (IGV): High-performance genomics data visualization and exploration. *Brief. Bioinform.* 14, 178–192.
- Uehara, H., Cho, Y., Simonis, J., Cahoon, J., Archer, B., Luo, L., Das, S.K., Singh, N., Ambati, J., and Ambati, B.K. (2013). Dual suppression of hemangiogenesis and lymphangiogenesis by splice-shifting morpholinos targeting vascular endothelial growth factor receptor 2 (KDR). *FASEB J.* 27, 76–85.
- Underwood, J.G., Boutz, P.L., Dougherty, J.D., Stoilov, P., and Black, D.L. (2005). Homologues of the *Caenorhabditis elegans* Fox-1 protein are neuronal splicing regulators in mammals. *Mol. Cell. Biol.* 25, 10005–10016.
- Vaishnav, A.K., Gollob, J., Gamba-vitalo, C., Hutabarat, R., Sah, D., Meyers, R., De, T., and Maraganore, J. (2010). A status report on RNAi therapeutics Review. *Silence* 1–13.
- Vandenbergh, L.H., and Auricchio, A. (2012). Novel adeno-associated viral vectors for retinal gene therapy. *Gene Ther.* 19, 162–168.
- Vervoort, R., Lennon, A., Bird, A.C., Tulloch, B., Axton, R., Miano, M.G., Meindl, A., Meitinger, T., Ciccodicola, A., and Wright, A.F. (2000). Mutational hot spot within a new RPGR exon in X-linked retinitis pigmentosa. *Nat. Genet.* 25, 462–466.
- Villemaire, J., Dion, I., Elela, S.A., and Chabot, B. (2003). Reprogramming alternative pre-messenger RNA splicing through the use of protein-binding antisense oligonucleotides. *J. Biol. Chem.* 278, 50031–50039.
- Vivek, A., and Aravind, L. (2000). Cache – a signaling domain common to channel subunits and a class of prokaryotic chemotaxis receptors. *Trends Biochem. Sci.* 25, 535–537.
- Voigt, T., Meyer, K., Baum, O., and Schümperli, D. (2010). Ultrastructural changes in diaphragm neuromuscular junctions in a severe mouse model for Spinal Muscular Atrophy and their prevention by bifunctional U7 snRNA correcting SMN2 splicing. *Neuromuscul. Disord.* 20, 744–752.
- Wally, V., Murauer, E.M., and Bauer, J.W. (2012). Spliceosome-mediated trans-splicing: the therapeutic cut and paste. *J. Invest. Dermatol.* 132, 1959–1966.
- Wang, W., and El-Deiry, W. (2010). Large Insertions : Two Simple Steps Using QuikChange II Site-Directed Mutagenesis Kits. *Agil. Technol. Appl. Note* 4, 1–4.

- Weston, M.D., Eudy, J.D., Fujita, S., Yao, S., Usami, S., Cremers, C., Greenberg, J., Ramesar, R., Martini, a, Moller, C., et al. (2000). Genomic structure and identification of novel mutations in usherin, the gene responsible for Usher syndrome type IIa. *Am. J. Hum. Genet.* *66*, 1199–1210.
- Whittaker, C.A., and Hynes, R.O. (2002). Distribution and Evolution of von Willebrand / Integrin A Domains: Widely Dispersed Domains with Roles in Cell Adhesion and Elsewhere. *Mol. Biol. Cell* *13*, 3369–3387.
- Van Wijk, E., Pennings, R.J.E., te Brinke, H., Claassen, A., Yntema, H.G., Hoefsloot, L.H., Cremers, F.P.M., Cremers, C.W.R.J., and Kremer, H. (2004). Identification of 51 novel exons of the Usher syndrome type 2A (USH2A) gene that encode multiple conserved functional domains and that are mutated in patients with Usher syndrome type II. *Am. J. Hum. Genet.* *74*, 738–744.
- Wycisk, K.A., Budde, B., Feil, S., Skosyrski, S., Buzzi, F., Neidhardt, J., Glaus, E., Nürnberg, P., Ruether, K., and Berger, W. (2006a). Structural and functional abnormalities of retinal ribbon synapses due to Cacna2d4 mutation. *Invest. Ophthalmol. Vis. Sci.* *47*, 3523–3530.
- Wycisk, K.A., Zeitz, C., Feil, S., Wittmer, M., Forster, U., Neidhardt, J., Wissinger, B., Zrenner, E., Wilke, R., Kohl, S., et al. (2006b). Mutation in the auxiliary calcium-channel subunit CACNA2D4 causes autosomal recessive cone dystrophy. *Am. J. Hum. Genet.* *79*, 973–977.
- Yan, D., Swain, P.K., Breuer, D., Tucker, R.M., Wu, W., Fujita, R., Rehemtulla, A., Burke, D., and Swaroop, A. (1998). Biochemical characterization and subcellular localization of the mouse retinitis pigmentosa GTPase regulator (mRpgr). *J. Biol. Chem.* *273*, 19656–19663.
- Yuan, M.-K., Tao, Y., Yu, W.-Z., Kai, W., and Jiang, Y.-R. (2010). Lentivirus-mediated RNA interference of vascular endothelial growth factor in monkey eyes with iris neovascularization. *Mol. Vis.* *16*, 1743–1753.
- Zanetta, C., Nizzardo, M., Simone, C., Monguzzi, E., Bresolin, N., Comi, G.P., and Corti, S. (2014). Molecular therapeutic strategies for spinal muscular atrophies: current and future clinical trials. *Clin. Ther.* *36*, 128–140.
- Zeitz, C., Robson, A.G., and Audo, I. (2014). Congenital stationary night blindness: An analysis and update of genotype-phenotype correlations and pathogenic mechanisms. *Prog. Retin. Eye Res.*
- Zhao, Y., Hong, D., Pawlyk, B., Yue, G., Adamian, M., Grynberg, M., Godzik, A., and Li, T. (2003). The retinitis pigmentosa GTPase regulator (RPGR) - interacting protein : Subserving RPGR function and participating in disk morphogenesis. *100*.
- Zhou, Z., and Fu, X.-D. (2013). Regulation of splicing by SR proteins and SR protein-specific kinases. *Chromosoma* *122*, 191–207.
- Zhu, H., Qian, J., Wang, W., Yan, Q., Xu, Y., Jiang, Y., Zhang, L., Lu, F., Hu, W., Zhang, X., et al. (2013). RNA interference of GADD153 protects photoreceptors from endoplasmic reticulum stress-mediated apoptosis after retinal detachment. *PLoS One* *8*, e59339.

10 Attachments

10.1 Papers

- Niccolò Bacchi, Andrea Messina, Verena Burtscher, Erik Dassi, Giovanni Provenzano, Yuri Bozzi, Gian Carlo Demontis, Alexandra Koschak, Michela A. Denti and Simona Casarosa. **A new splicing isoform of *Cacna2d4* mimicking the effects of c.2451insC mutation in the retina. Novel molecular and electrophysiological insights.** (Submitted to Invest Ophthalmol Vis Sci)
- Niccolò Bacchi, Simona Casarosa, Michela A. Denti. **Splicing-Correcting Therapeutic Approaches for Retinal Dystrophies: Where Endogenous Gene Regulation and Specificity Matter.** Review, Invest Ophthalmol Vis Sci. 2014;55:3285–3294. DOI:10.1167/iovs.14-14544

TITLE

A new splicing isoform of *Cacna2d4* mimicking the effects of c.2451insC mutation in the retina. Novel molecular and electrophysiological insights.

AUTHORS

Niccolò Bacchi¹, Andrea Messina¹, Verena Burtscher², Erik Dassi¹, Giovanni Provenzano¹, Yuri Bozzi^{1,3}, Gian Carlo Demontis⁴, Alexandra Koschak^{2,*}, Michela A. Denti^{1,5,*} and Simona Casarosa^{1,3,*}

¹Centre for Integrative Biology (CIBIO), University of Trento, Via Sommarive 9, 38123, Trento, Italy

²Medical University of Vienna, Center for Physiology and Pharmacology, Department of

Neurophysiology and –pharmacology, Schwarzspanierstrasse 17, 1090, Vienna, Austria

³Neuroscience Institute – National Research Council (CNR), Via Moruzzi 1, 56124, Pisa, Italy

⁴Department of Pharmacy, University of Pisa, Via Bonanno Pisano 6, 56126, Pisa, Italy

⁵Neuroscience Institute – National Research Council (CNR), Via Giuseppe Colombo 3, 35121, Padova, Italy

*Corresponding authors

Grant information: Italian Ministry of Health Project GR-2008-1136933 to M.A.D. and Austrian Science Funds FWF-P26881-B23 to A.K.

Running Title: Activity of $\alpha_2\delta_4$ splicing isoforms.

Precis: We describe a novel splicing isoform of *Cacna2d4* found in mouse retina. This isoform lacks activity on L-type calcium channels and truncates the gene open reading frame in the same position as the c.2451insC mutation does.

ABSTRACT

Purpose. Mutations in *CACNA2D4* exon 25 cause photoreceptor dysfunction in humans (c.2406C→A mutation) and mice (c.2451insC mutation). We investigated the feasibility of an exon-skipping therapeutic approach by evaluating the splicing patterns and functional role of targeted exons.

Methods. Splicing of the targeted $\alpha_2\delta_4$ (*CACNA2D4*) exons in presence and absence of the mutation was assessed by RT-PCR *in vivo* on mouse retinae and *in vitro* in HEK293T cells using splicing-reporter minigenes. Whole-cell patch-clamp recordings were performed to evaluate the impact of different *Cacna2d4* variants on the biophysical properties of Cav1.4 L-type calcium channels (CACNA1F).

Results. Splicing analysis revealed the presence of a previously unknown splicing isoform of $\alpha_2\delta_4$ in the retina which truncates the gene open reading frame (ORF) in a similar way as the c.2451insC mutation. This isoform originates from alternative splicing of exon 25 (E25) with a new exon (E25b). Moreover, the c.2451insC mutation has an effect on splicing and increases the proportion of transcripts including E25b. Our electrophysiological analyses showed that only full-length $\alpha_2\delta_4$ was able to increase Cav1.4/ β_3 mediated currents while all other $\alpha_2\delta_4$ variants did not mediate such effect.

Conclusions. The designed exon-skipping strategy is not applicable because the resulting skipped $\alpha_2\delta_4$ are non-functional. $\alpha_2\delta_4$ E25b splicing variant is normally present in mouse retina and mimics the effect of c.2451insC mutation. Since this variant does not promote significant Cav1.4 mediated calcium current, it could possibly mediate a different function, unrelated to modulation of calcium channel properties at the photoreceptor terminals.

INTRODUCTION

Exon skipping therapeutic approaches offer a unique opportunity for intervention in patients affected by retinal dystrophies, as different types of mutations can be potentially treated in a patient-specific way.(Bacchi et al., 2014) Among the potential applications, it is possible to use different antisense molecular tools to induce intronization of selected exons. This strategy can be beneficial where the targeted exons are carrying nonsense mutations or insertions/deletions leading to frameshift. However the precise splicing pattern of the mutated target exon(s) and the functionality of the skipped protein need to be carefully evaluated. We selected the *CACNA2D4* gene as a potential therapeutic target in the retina: this gene encodes for $\alpha_2\delta_4$, a member of $\alpha_2\delta$ accessory subunits of high voltage activated (HVA) calcium channels.(Qin et al., 2002) HVA calcium channels are multiprotein complexes composed of an α_1 subunit, which constitutes the channel pore, and different accessory subunits ($\alpha_2\delta$, β , and in some cases γ). $\alpha_2\delta$ subunits are known to regulate HVA calcium channels mainly by increasing channel presence on the cell membrane, and by modulating channel gating properties.(Dolphin, 2013) They are translated as a single protein but then cleaved into α_2 and δ peptides, which are subsequently joined together by a disulphide bond. The α_2 peptide is extracellular, while the δ mediates membrane anchoring.(Davies et al., 2010) In the retina $\alpha_2\delta_4$ is the main accessory subunit(Knoflach et al., 2013; Wycisk et al., 2006a, 2006b) where it is suggested to form a complex with Cav1.4 α_1 and β_2 subunits,(Lee et al., 2014) since mutations in all these genes are linked to retinal dystrophies.(Ball et al., 2002; Burtscher et al., 2014; Knoflach et al., 2013; Wycisk et al., 2006a) So far, two mutations in *Cacna2d4* exon 25 were reported to cause cone and cone-rod dystrophies in humans and mice respectively.(Wycisk et al., 2006a, 2006b) Both mutations are expected to result into a truncated protein, likely to be non-functional due to the loss of the δ peptide and other functional domains downstream of the mutation (Fig. 1A). Since the skipping of the sole mutation-carrying exon 25 in $\alpha_2\delta_4$ would result in frameshift, skipping of exon 23-24-25-26 ($\alpha_2\delta_4$ Δ E23-26) or of exons 23-24-25 ($\alpha_2\delta_4$ Δ E23-25) is needed to restore the reading frame downstream of the skipped exons. We hypothesized that this strategy would result in a rescued protein missing the skipped exons, but retaining the δ peptide and other structural elements.

Moreover the targeted exons do not contain any known domain important for $\alpha_2\delta$ function. The presence of a mouse model and ability to test the functionality of the skipped protein by electrophysiology offer a clear advantage in assessing the feasibility of this exon-skipping approach. We thus generated constructs lacking these exons and tested their functionality by electrophysiology in cells in which the whole channel complex had been reconstituted.

METHODS

Computational analysis of *Cacna2d4* E25 splicing

Mouse eye RNA-seq samples were downloaded from the Gene Expression Omnibus (Edgar et al., 2002) (dataset ID GSE38359: sample IDs GSM945628, GSM945631 and GSM945634; dataset ID GSE29752: samples GSM737548 and GSM737550). Reads were trimmed at the 3' end by removing nucleotides having Q score < 30 with Trimmomatic (Bolger et al., 2014), and then mapped to the mouse genome (mm10 assembly) with TopHat2 (Kim et al., 2013). The resulting alignment and the observed exon-exon junctions were eventually visualized with Integrative Genomics Viewer (IGV) (Thorvaldsdóttir et al., 2013).

The genomic sequence of *Cacna2d4* between E22 and E27 was analysed using NNSPLICE 0.9 (Reese et al., 1997) and scores for the different splice sites were reported.

Cacna2d4 and *CACNA2D4* E25 sequences were analysed using SpliceAid (Piva et al., 2009) in presence and absence of the c.2451insC mutation obtaining predictions of differentially binding splicing regulatory elements.

Animals

Cacna2d4 mutant and wild type (WT) mice with C57BL/10 background (Wycisk et al., 2006a) (2 months old) were used for retinal tissue extraction. C57BL/6 mice (3-5 months old) were used for analysis of *Cacna2d4* Δ E16 expression in the CNS. Experiments were approved by the Italian Ministry of Health and conducted in conformity with the European Community Directive 2010/63/EU and the ARVO Statement for the Use of Animals in Ophthalmic and Vision Research.

Cloning

Cacna2d4 ΔE16 clone (GenBank: BC141091.1; IMAGE ID 9055703) was ordered from Source Bioscience, amplified by PCR using primers For: 5'-GACTGCTAGCCACTTGCATGC and Rev: 5'-CTTGTCGACGTCAGATGGGAT, and cloned into pIRES2-EGFP (Clontech, Mountain View, CA) using NheI and Sall restriction sites. Exon 16 was subsequently amplified from murine genomic DNA using primers For: 5'-AGCTGGCACCCCGATATAAGCTTGGGGTGCATGGC and Rev: 5'-AGCTTCTTGCCTTCTCTGTACAAAGGTCGGAGGTCAG. The resulting PCR fragment was used as megaprimer (Wang and El-Deiry, 2010) for site-directed mutagenesis (Quickchange II site-directed mutagenesis kit, Agilent, Santa Clara, CA) and added to *Cacna2d4* ΔE16 to generate *Cacna2d4* full-length ($\alpha_2\delta_4$). The c.2451insC mutation on E25 was introduced by site directed mutagenesis of *Cacna2d4* using primers For: 5'-GAGCAGCCCCCGGCAGCTTTGTCTTC and Rev: 5'-GAAGACAAAGCTGCCGGGGGGGCTGCTC. The obtained construct was named " $\alpha_2\delta_4$ MUT". E25b was amplified from mouse retina cDNA using primers For: 5'-AGAGTCAGAGCCTGGCGTGG and Rev: 5'-CTGCTGCAATGGCCGTCTTCC. The PCR product was extracted from gel to avoid E25-containing transcript and purified. The product was then used as megaprimer for site-directed mutagenesis to obtain E25b inclusion in place of E25 ($\alpha_2\delta_4$ E25b). The $\alpha_2\delta_4$ full-length construct has been subsequently utilised as template for the generation of $\alpha_2\delta_4$ ΔE23-25. For this intent a PCR using primers For: 5'-atagcccaggcaagccagt and Rev: 5'-actccaggtctggatccac was performed, followed by ligation of the PCR product. The $\alpha_2\delta_4$ ΔE23-26 cDNA construct was obtained from overlapping PCR on *Cacna2d4* template. For this purpose two different primer pairs were used to originate the two overlapping fragments: For: 5'-CTACGTGACTGCTAGCCACTTGCATGCCAGGA, and Rev: 5'-ATCTGGATGCCACAGACTCCAGGTCTGGATCC for first reaction; For: 5'-GATCCAGACCTGGAGTCTGTGGGCATCCAGATG and Rev: 5'-CTACGACTCTTGGATCCGTCAGATGGGATGGAGTC for the second reaction. The two generated fragments were then purified and used together with the primer pair For: 5'-GACTGCTAGCCACTTGCATGC and Rev: 5'-CTTGTCGACGTCAGATGGGAT in a different PCR reaction to generate $\alpha_2\delta_4$ ΔE23-26. The *Cacna2d4* minigene construct was assembled from four fragments amplified from mouse genomic DNA and digested with specific restriction enzymes. For a detailed list of utilized primers and restriction enzymes see Table S1. The resulting digested and purified fragments were ligated

together with a pCDNA3-Luc2 vector digested with HindIII and XhoI. The introduction of c.2451insC mutation into the minigene was performed by site-directed mutagenesis using the same primer pair utilized for $\alpha_2\delta_4$ MUT. All obtained clones were checked by sequencing.

RNA extraction and cDNA synthesis

Tissues from adult mice (n=3) were dissected and total RNA was extracted using Trizol Reagent (Life Technologies, Carlsbad, CA), treated with DNase (Roche, Basel, Switzerland) and purified using NucleoSpin RNA columns (Macherey-Nagel, Düren, Germany). cDNA synthesis was performed using random examers (SuperScript VILO cDNA Synthesis Kit, Life Technologies, Carlsbad, CA). RNA extraction of transfected HEK293T cells was performed two days after transfection as described above.

Cell culture and transfection conditions

HEK293T or tsA-201 cells were maintained in DMEM supplemented with 10% FBS, 2mM glutamine, 100 U/ml Pen/Strep, and grown at 37°C, 10% CO₂. For transfection with minigenes, Lipofectamine 2000 (Life-Technologies, Carlsbad, CA) was used. For electrophysiological recordings tsA-201 cells were split into 6 cm dishes one day before transfections. Transfection was performed using Turbofect transfection reagent (Thermo Scientific, Waltham, MA) with 0.5 µg of Cav1.4 α_1 (Sinnegger-Brauns et al., 2009), 0.5 µg of β_3 (Castellano et al., 1993), and 0.5 µg of different $\alpha_2\delta$ constructs in pIRES2-EGFP expressing vectors and 1 µg pUC. The $\alpha_2\delta_1$ sequence utilized was described previously. (Ellis et al., 1988) For $\alpha_2\delta_1$ (Ellis et al., 1988) transfections, 0.05 µg of a GFP expressing plasmid were cotransfected. One day after transfection cells were seeded at low confluence on 3 cm dishes coated with poly-D-lysine and stored over night at 30°C, 5% CO₂. Recordings were performed the following day. In experiments where different $\alpha_2\delta$ constructs were present in the same transfection, the following amounts were used: 0.5µg of Cav1.4 α_1 (Sinnegger-Brauns et al., 2009), 0.5µg of β_3 (Castellano et al., 1993), 0.5µg of each different $\alpha_2\delta$ subunit, and 0.5 µg pUC.

RT-PCR and densitometric analysis

PCR protocol consisted in denaturation (94°C; 1 min), 35 amplification cycles (94°C, 30 sec; 58°C, 30 sec; 72°C, 1 min) and final extension (72°C, 7 min); primers are reported in Table S2. Densitometric analysis was conducted using Imagelab 2.0 software (Biorad, Hercules, CA). Band intensities, corrected for background, were normalized to the corresponding Glyceraldehyde 3-phosphate dehydrogenase (*Gapdh*) values.

RT-qPCR

RT-qPCR was performed in a C1000 thermal cycler with a CFX384 real-time detection system (Biorad, Hercules, CA), using the KAPA SYBR FAST master mix (Kapa Biosystems, Cape Town, South Africa). *Gapdh* was used as a reference gene for normalization, using the ΔCt method. Primers are reported in Table S2. Data were analysed using the CFX Manager 2.1 software (BioRad, Hercules, CA). For direct comparison of E25 and E25b transcripts levels, amplification efficiency and y-intercept with the two primer pairs was compared using serial dilutions of plasmid containing E25 or E25b. Equivalence of the obtained slopes and y-intercept was assessed with extra sum-of-square F test. Data are shown as $2^{(-\Delta\text{Ct}(\text{E25}))} / 2^{(-\Delta\text{Ct}(\text{E25b}))}$.

Electrophysiological recordings

Whole-cell patch-clamp experiments were performed using an Axopatch 700B amplifier (Molecular Devices, Sunnyvale, CA). Borosilicate glass pipets (external diameter 1.5 mm; wall thickness 0.32 mm; Science Products, Frankfurt/Main, Germany) were pulled using a micropipette puller (P97, Sutter Instruments, Novato, CA) to obtain electrodes with a resistance of 1.5-3 M Ω . pClamp10.2 (Molecular Devices, Sunnyvale, CA) and Prism 5 (Graphpad, La Jolla, CA) softwares were used for data-analysis. Recordings were executed at pH 7.4 (with CsOH). In [mM], the internal solution contained 135 CsCl, 10 HEPES, 10 EGTA, 1 MgCl₂, and the bath

solution 15 CaCl₂ or BaCl₂, 10 HEPES, 150 Choline-Cl, 1 MgCl₂. Recording were performed at room temperature (19-22 °C). All voltages were corrected for a liquid junction potential of -8mV. In all protocols used a holding potential of -98mV was applied. To determine current densities (CD), peak current amplitudes were normalized to the membrane capacitance. For each analysed cell, the maximum observed current density (CD_{max}) was reported. Protocols for the voltage-dependence of activation and inactivation, as well as calcium-dependent inactivation were used as described in Burtscher and colleagues (Burtscher et al., 2014)

Statistics

Statistical analysis was performed with Prism 5 and significance set at P<0.05 for all tests. PCR data are represented as mean ± SD, and compared using unpaired two-tailed student-t test. Electrophysiological data are represented as mean ± SEM, and analysed by Kruskal–Wallis test followed by Dunn's post-hoc test for multiple comparisons. Mann–Whitney U-test was used for single comparisons.

RESULTS

Computational analysis of *Cacna2d4* exon 25 splicing

We first investigated the feasibility of an exon-skipping approach for the c.2451insC mutation (previously annotated as c.2367insC) in exon 25 of *Cacna2d4* (Wycisk et al., 2006a) (registered sequence (NM_001033382.2)). We first analysed the splicing pattern of this and surrounding exons by an *in-silico* approach using RNA-seq data from four eyes and one retina of C57BL/6 mice. Datasets showed that the canonical exon 25 (128 bp) was not always included in the final transcript. In these cases it was substituted by a new exon included between exon 24 and 26 (Fig. 1B). This putative exon of 205 bp, named E25b, is located in intron 25 in close proximity to exon 25. If E25b is included instead of E25, it terminates the open reading frame of *Cacna2d4* in a way similar to the known mutation c.2451insC, as it carries a stop codon. E25b was present in less reads compared to E25, suggesting that it may be included in a smaller fraction of *Cacna2d4* transcripts. To further corroborate the existence of this new exon we undertook a bioinformatics analysis of the 5' and 3' splice sites of E25b (Table 1) and discovered that the putative E25b showed higher prediction scores with respect to the canonical E25. In particular, the 3' splice site of E25 is very weak, while the 3' splice site of E25b is relatively strong. This strengthens the idea that E25b may be included in place of E25, thereby generating an alternatively spliced variant of *Cacna2d4*. Moreover, it suggests that nucleotide variations in E25 sequence may significantly affect its inclusion levels in mature transcripts, favouring E25b containing transcripts. We hypothesized that the c.2451insC insertion could have such an effect, and computationally tested whether it might increase E25b inclusion using the SpliceAid webserver (Piva et al., 2009). The output of the comparisons between WT and mutant E25 revealed how the insertion in E25 mainly establishes new exonic splicing silencers (ESS) (Fig. 1C). In fact, the prediction showed 7 new ESS with scores between -4 and -7 in the mutant and only one new exonic splicing enhancer (ESE) with a score of 4 (Table S3), all absent in the wt sequence. We thus predict a change in the ratio of E25 and E25b containing transcripts between WT and mutant alleles, with the c.2451insC insertion favouring E25b inclusion. These results were supported by analysing the effect

of human c.2406C→A mutation in E25, where a predicted ESE is abolished and substituted with an ESS (Fig. S1).

In vivo and *in vitro* characterization of exon 25 splicing

We then verified our above hypothesis by analysing E25 splicing in retinæ of *Cacna2d4* WT and mutant mice. (Wycisk et al., 2006a) We performed an RT-PCR using primers on exon 24 and 26 to confirm the presence of E25b along with E25 thanks to a clear difference in size (Fig. 2A). Densitometric analysis of PCR products revealed that E25b is less abundant than E25 in mature transcripts found in WT retinæ. A significant decrease in E25 containing transcripts was instead observed in the mutant retina (Fig. 2B), while E25b levels remained constant. RT-qPCR performed with specific primers for exon 25 and exon 25b confirmed that E25-containing transcripts were significantly diminished in mutant mice compared to WT; E25b-containing mRNAs were also reduced, although to a much lower extent (Fig. 2C). Quantification of E25 and E25b containing transcripts revealed that the ratio between the two isoforms changed in favour of E25b in mutant animals (Fig. 2D).

We next assessed the effect of the mutation using a minigene reporter system, generated by cloning the exons surrounding E25 (exons 22 to 27) together with portions of intronic sequences (introns 22 to 26) in an expression cassette (Fig. 2E). Following minigene transfection in HEK293T cells, proper splicing between the different exons was observed by RT-PCR using primers on E22 and on the plasmid downstream of E27 (Fig. 2F). Minigene analysis also showed alternative splicing between E25 and E25b, as previously described *in vivo*. Interestingly, in HEK293T cells the effect of the mutation was to increase E25b inclusion without affecting E25 levels, as observed by densitometric analysis of the RT-PCR (Fig 2G) and confirmed by RT-qPCR (Fig. 2H) for the two isoforms. The ratio of E25 over E25b levels revealed that the ratio between the two isoforms tended to change in favour of E25b in mutant animals (Fig. 2I).

Analysis of $\alpha_2\delta_4$ $\Delta E16$ splicing isoform expression in the CNS and neuroendocrine system.

By databases analyses, we found the presence of another putative splicing isoform of *Cacna2d4*, obtained from the sequencing of a whole brain cDNA library. This isoform is characterized by the absence of exon 16 ($\alpha_2\delta_4$ $\Delta E16$, GenBank: BC141091.1), an exon that encodes for a portion of the first Cache domain of $\alpha_2\delta_4$, which is conserved in all known $\alpha_2\delta$ subunits.(Davies et al., 2010) We thus investigated the presence of this isoform in retina, CNS, and neuroendocrine system by RT-PCR (Fig. 3A). The $\Delta E16$ isoform was absent in the retina and in the pituitary gland, where all *Cacna2d4* transcripts contained E16. Instead, $\Delta E16$ mRNA was the predominant isoform expressed in cerebellum, hippocampus, occipital cortex and somatosensory cortex; both variants were present in hypothalamus. Densitometric analysis showed that *Cacna2d4* is highly expressed in the retina, while lower levels were detected in other areas of the CNS (Fig. 3B).

Functional characterization of different $\alpha_2\delta_4$ variants

The $\alpha_2\delta$ accessory subunits have different effects on HVA calcium channels: they primarily increase calcium influx by increasing the number of channels on the plasma membrane; (Dolphin et al., 1999; Hobom et al., 2000; Jones et al., 1998; Klugbauer et al., 2000) in addition, they fasten the inactivation kinetic of some HVA calcium channels.(Felix et al., 1997; Hobom et al., 2000; Sipos et al., 2000) To identify how $\alpha_2\delta_4$ subunit modulate Cav1.4 L-type calcium currents, we undertook whole-cell patch-clamp recordings in tsA-201 cells transfected together with β_3 subunits and compared its biophysical properties with the more investigated $\alpha_2\delta_1$ (Burtscher et al., 2014; Koschak et al., 2003) Co-expression of full-length $\alpha_2\delta_4$ resulted in a three-fold increase in current density, similarly to $\alpha_2\delta_1$ (Fig. 4A, 4B, 4D). In addition, $\alpha_2\delta_4$ and $\alpha_2\delta_1$ displayed comparable voltage-dependent activation and inactivation properties (Fig. 4C and Table 2). We finally tested the effect of $\alpha_2\delta_4$ on calcium-dependent inactivation of Cav1.4, and identified no differences in the inactivation kinetic between Ba^{2+} and Ca^{2+} driven

currents. The percentage of remaining current during 250 ms test pulse to 2 and 12 mV (which was the voltage of the maximum current with Ba^{2+} and Ca^{2+}) was 90% for Ba^{2+} and 91% for Ca^{2+} , with no significant difference observed ($P = 0.56$). No difference was found over a voltage range from -40 to +40 mV, as also previously noted with $\alpha_2\delta_1$ using the same experimental settings.(Burtscher et al., 2014) Similar results were fairly recently reported also for human $\alpha_2\delta_4$ subunits.(Lee et al., 2014)

Since our primary aim was to test the feasibility of exon skipping as a potential therapeutic approach for $\alpha_2\delta_4$ mutant subunits, we assessed the functionality of proteins missing either three (E23-24-25) or four (E23-24-25-26) exons. Neither construct increased current densities and were comparable to our negative control (Cav1.4, β_3 and pIRES vector) (Fig 4D and Table 2). We also characterized the electrophysiological properties of the E25b isoform, which we expected to mimic the c.2451insC mutant, and the ΔE16 variant: none of these variants evoked a change in current density levels (Fig. 4A, 4B, 4D, Table 2), and activation gating properties of Cav1.4 were not altered with any of the variants for which we were able to obtain an activation curve (Fig 4C, Table 2). We finally tested whether we could exert a possible dominant negative effect of the different splicing isoforms or the mutant by expressing them together with full length $\alpha_2\delta_4$ in a 1:1 ratio. We ruled out a possible dominant negative effect of the different splicing isoforms as no changes in current densities were appreciated if compared to $\alpha_2\delta_4$ alone (Fig. 5).

DISCUSSION

We discovered that the previously described c.2451insC mutation,(Wycisk et al., 2006a) causing retinopathy in mice, apart from truncating the ORF of the gene after the first Cache domain, also affects splicing. The mutation favours inclusion of a newly identified alternatively spliced exon, E25b, which also terminates the ORF. The mutation created new ESSs on E25, and promoted E25b inclusion in place of E25. *In vivo*, the mutation mainly affected E25, impairing its incorporation in mature mRNA. When using a minigene reporter system in HEK293T cells, its effect is instead to favour E25b inclusion, without significantly affecting E25 levels. The observed difference of action could be due to the presence of different *trans*-acting splicing factors in the two analysed systems: HEK293T cell line and mouse retinae. Differences in the impact of nonsense mediated decay on the overall levels of transcripts(Nicholson et al., 2010) might also be involved, especially *in vivo* where we see a general reduction of *Cacna2d4* mRNA.

Our findings are also pathophysiologically relevant, since we confirmed the predicted role of murine $\alpha_2\delta_4$ as an accessory subunit of Cav1.4 by characterizing its biophysical properties. This subunit is able to increase current densities by three-fold in an heterologous expression system, in accordance with the changes in calcium influx previously described using human $\alpha_2\delta_4$.(Qin et al., 2002) Moreover $\alpha_2\delta_4$ has no effect on the activation properties of Cav1.4 and is comparable to $\alpha_2\delta_1$ when inactivation is investigated. We therefore suggest that, since $\alpha_2\delta_4$ is highly expressed in the retina together with Cav1.4, where both localize to photoreceptor terminals,(Busquet et al., 2010; Knoflach et al., 2013; De Sevilla Müller et al., 2013; Specht et al., 2009) this is likely the subunit helping trafficking of Cav1.4 to the plasma membrane of photoreceptors, as it is able to mediate the same effect on the channel in an heterologous system.

The $\alpha_2\delta_4$ isoform resulting from E25b inclusion completely lacks the δ peptide, important for membrane anchoring.(Davies et al., 2010; Kadurin et al., 2012) Even if $\alpha_2\delta$ subunits lacking the membrane anchor site are still able to enhance calcium currents, they lose this ability when the whole δ peptide is deleted.(Gurnett et al., 1996;

Kadurin et al., 2012) Indeed, $\alpha_2\delta_4$ c.2451insC and $\alpha_2\delta_4$ E25b did not increase current densities. Therefore, the role of the $\alpha_2\delta_4$ E25b splicing isoform in the retina remains elusive, as the protein would be secreted. Elucidation of the presence of a splicing event in human *CACNA2D4*, that resembles the effect of murine E25b incorporation, would be important. Specifically, if an alternatively spliced exon truncating *CACNA2D4* ORF between the two Cache domains exists also in the human gene, also in this case the c.2406C→A mutation could favour this inclusion.

We show that the region encoded by exons 23 to 26 is of fundamental importance for the functionality of $\alpha_2\delta_4$. The removal of this portion indeed impairs $\alpha_2\delta_4$ ability to promote calcium currents mediated by Cav1.4 α_1 subunits. The region encoded by these exons spans between the two Cache domains and it is not part of any known domain of the protein. Moreover, in an $\alpha_2\delta_1$ paralogue, insertion of an HA tag in the corresponding region did not affect the protein ability to mediate an increase in currents.(Kadurin et al., 2012) This region may host glycosylation sites important for its functionality.(Gurnett et al., 1996) This impairs our therapeutic strategy aiming at correcting the retinopathy caused by c.2451insC mutation, since this strategy was relying on the therapeutic skipping of exon 23 to 26 or 23 to 25 from transcripts in order to eliminate the frameshift mutation on E25 and restore the ORF downstream of it.

We described the presence of two newly identified splicing isoform (*Cacna2d4* E25b and *Cacna2d4* Δ E16) that were unable to influence Cav1.4 currents. In keeping with previous studies, (Schlick et al., 2012) *Cacna2d4* Δ E16 is present at low levels in the analysed CNS areas. Moreover, in a recent study, a smaller (~165kDa instead of ~170kDa) $\alpha_2\delta_4$ was detected by Western blots in mouse brain, possibly being $\alpha_2\delta_4$ Δ E16.(De Sevilla Müller et al., 2013) These results strengthen the current hypothesis(Dolphin, 2012) that $\alpha_2\delta$ subunits may fulfill, in the retina and CNS, different functions not directly related to trafficking of calcium channels on the plasma membrane. The reason for occurrence of two different frameshift-causing mutations both on E25 in humans and mice and the presence of a splicing isoform that recapitulates the effect of the mutation in mice remains elusive. It is likely that the mutation, by mimicking the effect of E25b inclusion, offers a specific advantage in heterozygosity (overdominance) in the eye or in other districts where $\alpha_2\delta_4$ is normally expressed. This would allow the conservation of different mutations sharing the same

mimicking effect.

The effect that mutations in the coding region of genes have on splicing is generally underestimated: it is today believed that more than a quarter of these mutations interfere with proper splicing. (Lim et al., 2011b; López-Bigas et al., 2005; Sterne-Weiler et al., 2011) As we showed in this work, early investigation of how splicing patterns change in response to a mutation is of pivotal importance for the implementation of therapies involving antisense-mediated splicing-correcting approaches. To this end, splicing-reporter minigene assays can constitute a precious ally in this effort: we described here for the first time the design and use of a minigene system able to properly recall all splicing events across 6.5 Kb and six different exons. With the implementation of more efficient gene synthesis services this powerful approach could become relatively easy to use.

ACKNOWLEDGMENTS

The authors thank Klaus Schicker, Dagmar Knoflach, Margherita Grasso and Valerio del Vescovo for valuable experimental support. This work was funded by the Italian Ministry of Health Project GR-2008-1136933 to M.A.D. and Austrian Science Funds FWF-P26881-B23 to A.K.

REFERENCES

- Aartsma-Rus, A., Fokkema, I., Verschuuren, J., Ginjaar, I., van Deutekom, J., van Ommen, G.-J., and den Dunnen, J.T. (2009). Theoretic applicability of antisense-mediated exon skipping for Duchenne muscular dystrophy mutations. *Hum. Mutat.* *30*, 293–299.
- Al-Ubaidi, M.R., Font, R.L., Quiambao, A.B., Keener, M.J., Liou, G.I., Overbeek, P.A., and Baehr, W. (1992). Bilateral retinal and brain tumors in transgenic mice expressing simian virus 40 large T antigen under control of the human interphotoreceptor retinoid-binding protein promoter. *J. Cell Biol.* *119*, 1681–1687.
- Alanis, E.F., Pinotti, M., Mas, A.D., Balestra, D., Cavallari, N., Rogalska, M.E., Bernardi, F., and Pagani, F. (2012). An exon-specific U1 small nuclear RNA (snRNA) strategy to correct splicing defects. *Hum. Mol. Genet.* *21*, 2389–2398.
- Andorfer, C., Kress, Y., Espinoza, M., De Silva, R., Tucker, K.L., Barde, Y.-A., Duff, K., and Davies, P. (2003). Hyperphosphorylation and aggregation of tau in mice expressing normal human tau isoforms. *J. Neurochem.* *86*, 582–590.
- De Angelis, F.G., Sthandier, O., Berarducci, B., Toso, S., Galluzzi, G., Ricci, E., Cossu, G., and Bozzoni, I. (2002). Chimeric snRNA molecules carrying antisense sequences against the splice junctions of exon 51 of the dystrophin pre-mRNA induce exon skipping and restoration of a dystrophin synthesis in Delta 48-50 DMD cells. *Proc. Natl. Acad. Sci. U. S. A.* *99*, 9456–9461.
- Angelotti, T., and Hofmann, F. (1996). Tissue-specific expression of splice variants of the mouse voltage-gated calcium channel $\alpha 2/\delta$ subunit. *FEBS Lett.* *397*, 331–337.
- Askou, A.L., Pournaras, J.C., Pihlmann, M., Svalgaard, J.D., Dagnæs-hansen, F., Mikkelsen, J.G., Jensen, T.G., and Corydon, T.J. (2012). Reduction of choroidal neovascularization in mice endothelial growth factor short hairpin RNA. *J Gene Med* 632–641.
- Avale, M.E., Rodríguez-Martín, T., and Gallo, J.-M. (2013). Trans-splicing correction of tau isoform imbalance in a mouse model of tau mis-splicing. *Hum. Mol. Genet.* *22*, 2603–2611.
- Bacchi, N., Casarosa, S., and Denti, M.A. (2014). Splicing-correcting therapeutic approaches for retinal dystrophies: Where endogenous gene regulation and specificity matter. *Investig. Ophthalmol. Vis. Sci.* *55*, 3285–3294.
- Ball, S.L., Powers, P. a, Shin, H.-S., Morgans, C.W., Peachey, N.S., and Gregg, R.G. (2002). Role of the beta(2) subunit of voltage-dependent calcium channels in the retinal outer plexiform layer. *Invest. Ophthalmol. Vis. Sci.* *43*, 1595–1603.
- Baughan, T., Shababi, M., Coady, T.H., Dickson, A.M., Tullis, G.E., and Lorson, C.L. (2006). Stimulating full-length SMN2 expression by delivering bifunctional RNAs via a viral vector. *Mol. Ther.* *14*, 54–62.
- Baughan, T.D., Dickson, A., Osman, E.Y., and Lorson, C.L. (2009). Delivery of bifunctional RNAs that target an intronic repressor and increase SMN levels in an animal model of spinal muscular atrophy. *Hum. Mol. Genet.* *18*, 1600–1611.
- Berger, W., Kloeckener-Gruissem, B., and Neidhardt, J. (2010). The molecular basis of human retinal and vitreoretinal diseases. *Prog. Retin. Eye Res.* *29*, 335–375.
- Bernstein, G.M., and Jones, O.T. (2007). Kinetics of internalization and degradation of N-type voltage-gated calcium channels: Role of the $\alpha 2/\delta$ subunit. *Cell Calcium* *41*, 27–40.

- Bhattacharya, G., Miller, C., Kimberling, W.J., Jablonski, M.M., and Cosgrove, D. (2002). Localization and expression of usherin: A novel basement membrane protein defective in people with Usher's syndrome type IIa. *Hear. Res.* *163*, 1–11.
- Bhisitkul, R.B., Robinson, G.S., Moulton, R.S., Claffey, K.P., Gragoudas, E.S., and Miller, J.W. (2005). An antisense oligodeoxynucleotide against vascular endothelial growth factor in a nonhuman primate model of iris neovascularization. *Arch. Ophthalmol.* *123*, 214–219.
- Bidaud, I., and Lory, P. (2011). Hallmarks of the channelopathies associated with L-type calcium channels: a focus on the Timothy mutations in Ca(v)1.2 channels. *Biochimie* *93*, 2080–2086.
- Bolger, A.M., Lohse, M., and Usadel, B. (2014). Trimmomatic: A flexible trimmer for Illumina sequence data. *Bioinformatics* *30*, 2114–2120.
- Bonnal, S., Vigevani, L., and Valcárcel, J. (2012). The spliceosome as a target of novel antitumour drugs. *Nat. Rev. Drug Discov.* *11*, 847–859.
- Boylan, J.P., and Wright, A.F. (2000). Identification of a novel protein interacting with RPGR. *9*, 2085–2093.
- Brosseau, J.-P., Lucier, J.-F., Lamarche, A.-A., Shkreta, L., Gendron, D., Lapointe, E., Thibault, P., Paquet, E., Perreault, J.-P., Abou Elela, S., et al. (2013). Redirecting splicing with bifunctional oligonucleotides. *Nucleic Acids Res.* *6868*, 1–14.
- Buraei, Z., and Yang, J. (2010). The Beta Subunit of Voltage-Gated Calcium Channels. *Physiol. Rev.* *90*, 1461–1506.
- Burtscher, V., Schicker, K., Novikova, E., Pöhn, B., Stockner, T., Kugler, C., Singh, A., Zeitz, C., Lancelot, M.-E., Audo, I., et al. (2014). Spectrum of Cav1.4 dysfunction in congenital stationary night blindness type 2. *Biochim. Biophys. Acta* *1838*, 2053–2065.
- Busch, A., and Hertel, K.J. Evolution of SR protein and hnRNP splicing regulatory factors. *Wiley Interdiscip. Rev. RNA* *3*, 1–12.
- Busquet, P., Nguyen, N.K., Schmid, E., Tanimoto, N., Seeliger, M.W., Ben-Yosef, T., Mizuno, F., Akopian, A., Striessnig, J., and Singewald, N. (2010). CaV1.3 L-type Ca²⁺ channels modulate depression-like behaviour in mice independent of deaf phenotype. *Int. J. Neuropsychopharmacol.* *13*, 499–513.
- Byrne, M., Tzekov, R., Wang, Y., Rodgers, A., Cardia, J., Ford, G., Holton, K., Pandarinathan, L., Lapierre, J., Stanney, W., et al. (2013). Novel hydrophobically modified asymmetric RNAi compounds (sd-rxRNA) demonstrate robust efficacy in the eye. *J. Ocul. Pharmacol. Ther.* *29*, 855–864.
- Cantí, C., Nieto-Rostro, M., Foucault, I., Heblich, F., Wratten, J., Richards, M.W., Hendrich, J., Douglas, L., Page, K.M., Davies, A., et al. (2005). The metal-ion-dependent adhesion site in the Von Willebrand factor-A domain of alpha2delta subunits is key to trafficking voltage-gated Ca²⁺ channels. *Proc. Natl. Acad. Sci. U. S. A.* *102*, 11230–11235.
- Castellano, A., Wei, X., Birnbaumer, L., and Perez-Reyes, E. (1993). Cloning and expression of a third calcium channel beta subunit. *J. Biol. Chem.* *268*, 3450–3455.
- Caudevilla, C., Serra, D., Miliar, A., Codony, C., Asins, G., Bach, M., and Hegardt, F.G. (1998). Natural trans-splicing in carnitine octanoyltransferase pre-mRNAs in rat liver. *Proc. Natl. Acad. Sci. U. S. A.* *95*, 12185–12190.

- Chadderton, N., Millington-Ward, S., Palfi, A., O'Reilly, M., Tuohy, G., Humphries, M.M., Li, T., Humphries, P., Kenna, P.F., and Farrar, G.J. (2009). Improved retinal function in a mouse model of dominant retinitis pigmentosa following AAV-delivered gene therapy. *Mol. Ther.* *17*, 593–599.
- Chao, H., Mansfield, S.G., Bartel, R.C., Hiriyanna, S., Mitchell, L.G., Garcia-Blanco, M.A., and Walsh, C.E. (2003a). Phenotype correction of hemophilia A mice by spliceosome-mediated RNA trans-splicing. *Nat. Med.* *9*, 1015–1019.
- Chao, H., Mansfield, S.G., Bartel, R.C., Hiriyanna, S., Mitchell, L.G., Garcia-Blanco, M.A., and Walsh, C.E. (2003b). Phenotype correction of hemophilia A mice by spliceosome-mediated RNA trans-splicing. *Nat. Med.* *9*, 1015–1019.
- Cho, W.G., Albuquerque, R.J.C., Kleinman, M.E., Tarallo, V., Greco, A., Nozaki, M., Green, M.G., Baffi, J.Z., Ambati, B.K., De Falco, M., et al. (2009). Small interfering RNA-induced TLR3 activation inhibits blood and lymphatic vessel growth. *Proc. Natl. Acad. Sci. U. S. A.* *106*, 7137–7142.
- Cirak, S., Arechavala-Gomez, V., Guglieri, M., Feng, L., Torelli, S., Anthony, K., Abbs, S., Garralda, M.E., Bourke, J., Wells, D.J., et al. (2011). Exon skipping and dystrophin restoration in patients with Duchenne muscular dystrophy after systemic phosphorodiamidate morpholino oligomer treatment: an open-label, phase 2, dose-escalation study. *Lancet* *378*, 595–605.
- De Clercq, E., Eckstein, E., and Merigan, T.C. (1969). Interferon induction increased through chemical modification of a synthetic polyribonucleotide. *Science* *165*, 1137–1139.
- Cloutier, F., Lawrence, M., Goody, R., Lamoureux, S., Al-Mahmood, S., Colin, S., Ferry, A., Conduzorgues, J.-P., Hadri, A., Cursiefen, C., et al. (2012). Antiangiogenic activity of aganirsen in nonhuman primate and rodent models of retinal neovascular disease after topical administration. *Invest. Ophthalmol. Vis. Sci.* *53*, 1195–1203.
- Coady, T.H., and Lorson, C.L. (2010). Trans-splicing-mediated improvement in a severe mouse model of spinal muscular atrophy. *J. Neurosci.* *30*, 126–130.
- Coady, T.H., Baughan, T.D., Shababi, M., Passini, M. a, and Lorson, C.L. (2008). Development of a single vector system that enhances trans-splicing of SMN2 transcripts. *PLoS One* *3*, e3468.
- Collin, R.W., den Hollander, A.I., van der Velde-Visser, S.D., Bennicelli, J., Bennett, J., and Cremers, F.P. (2012). Antisense Oligonucleotide (AON)-based Therapy for Leber Congenital Amaurosis Caused by a Frequent Mutation in CEP290. *Mol. Ther. Nucleic Acids* *1*, e14.
- De Conti, L., Baralle, M., and Buratti, E. (2013). Exon and intron definition in pre-mRNA splicing. *Wiley Interdiscip. Rev. RNA* *4*, 49–60.
- Cooper, T.A. (2005). Use of minigene systems to dissect alternative splicing elements. *Methods* *37*, 331–340.
- Cooper, T.A., Wan, L., and Dreyfuss, G. (2009). RNA and Disease. *Cell* *136*, 777–793.
- Daiger, S., Rossiter, B., Greenberg, J., Christoffels, A., and Hide, W. (1998). Data services and software for identifying genes and mutations causing retinal degeneration. *Invest. Ophthalmol. Vis. Sci.* *39*, S295.
- Daiger, S.P., Sullivan, L.S., and Bowne, S.J. (2013). Genes and mutations causing retinitis pigmentosa. *Clin. Genet.* *84*, 132–141.
- Davies, A., Kadurin, I., Alvarez-Laviada, A., Douglas, L., Nieto-Rostro, M., Bauer, C.S., Pratt, W.S., and Dolphin, A.C. (2010). The alpha2delta subunits of voltage-gated calcium channels form GPI-anchored

- proteins, a posttranslational modification essential for function. *Proc. Natl. Acad. Sci. U. S. A.* *107*, 1654–1659.
- Denti, M.A., Rosa, A., D'Antona, G., Sthandier, O., De Angelis, F.G., Nicoletti, C., Allocca, M., Pansarasa, O., Parente, V., Musarò, A., et al. (2006). Body-wide gene therapy of Duchenne muscular dystrophy in the mdx mouse model. *Proc. Natl. Acad. Sci. U. S. A.* *103*, 3758–3763.
- Denti, M.A., Incitti, T., Sthandier, O., Nicoletti, C., De Angelis, F.G., Rizzuto, E., Auricchio, A., Musarò, A., and Bozzoni, I. (2008). Long-term benefit of adeno-associated virus/antisense-mediated exon skipping in dystrophic mice. *Hum. Gene Ther.* *19*, 601–608.
- Van Deutekom, J.C., Janson, A. a, Ginjaar, I.B., Frankhuizen, W.S., Aartsma-Rus, A., Bremmer-Bout, M., den Dunnen, J.T., Koop, K., van der Kooi, A.J., Goemans, N.M., et al. (2007). Local dystrophin restoration with antisense oligonucleotide PRO051. *N. Engl. J. Med.* *357*, 2677–2686.
- Dickson, A., Osman, E., and Lorson, C.L. (2008). A Negatively Acting Bifunctional RNA Increases Survival Motor Neuron Both In Vitro and In Vivo. *Hum. Gene Ther.* *19*, 1307–1315.
- Dolphin, A.C. (2012). Calcium channel auxiliary $\alpha 2\delta$ and β subunits: trafficking and one step beyond. *Nat. Rev. Neurosci.* *13*, 542–555.
- Dolphin, A.C. (2013). The $\alpha 2\delta$ subunits of voltage-gated calcium channels. *Biochim. Biophys. Acta - Biomembr.* *1828*, 1541–1549.
- Dolphin, A.C., Wyatt, C.N., Richards, J., Beattie, R.E., Craig, P., Lee, J., Cribbs, L.L., and Volsen, S.G. (1999). The effect of $\alpha 2\delta$ and other accessory subunits on expression and properties of the calcium channel $\alpha 1G$. *519.1*, 35–45.
- Dominski, Z., and Marzluff, W.F. (2007). Formation of the 3' end of histone mRNA: getting closer to the end. *Gene* *396*, 373–390.
- Douglas, A.G.L., and Wood, M.J.A. (2013). Splicing therapy for neuromuscular disease. *Mol. Cell. Neurosci.* *56*, 169–185.
- Dreumont, N., Maresca, A., Boisclair-Lachance, J.-F., Bergeron, A., and Tanguay, R.M. (2005). A minor alternative transcript of the fumarylacetoacetate hydrolase gene produces a protein despite being likely subjected to nonsense-mediated mRNA decay. *BMC Mol. Biol.* *6*, 1.
- Dvorchik, B.H., and Marquis, J.K. (2000). Disposition and toxicity of a mixed backbone antisense oligonucleotide, targeted against human cytomegalovirus, after intravitreal injection of escalating single doses in the rabbit. *Drug Metab. Dispos.* *28*, 1255–1261.
- Edgar, R., Domrachev, M., and Lash, A.E. (2002). Gene Expression Omnibus: NCBI gene expression and hybridization array data repository. *Nucleic Acids Res.* *30*, 207–210.
- Ellis, S.B., Williams, M.E., Ways, N.R., Brenner, R., Sharp, a H., Leung, a T., Campbell, K.P., McKenna, E., Koch, W.J., and Hui, a (1988). Sequence and expression of mRNAs encoding the alpha 1 and alpha 2 subunits of a DHP-sensitive calcium channel. *Science* *241*, 1661–1664.
- Fattal, E., and Bochot, A. (2006). Ocular delivery of nucleic acids: antisense oligonucleotides, aptamers and siRNA. *Adv. Drug Deliv. Rev.* *58*, 1203–1223.
- Felix, R., Gurnett, C.A., Waard, M. De, Campbell, K.P., and Roche, I.J. (1997). Dissection of Functional Domains of the Voltage-Dependent Ca²⁺ Channel $\alpha 2\delta$ Subunit. *J. Neurosci.* *17*, 6884–6891.

- Fingert, J.H., Oh, K., Chung, M., Scheetz, T.E., Andorf, J.L., Johnson, R.M., Sheffield, V.C., and Stone, E.M. (2008). Association of a novel mutation in the retinol dehydrogenase 12 (RDH12) gene with autosomal dominant retinitis pigmentosa. *Arch. Ophthalmol.* *126*, 1301–1307.
- Flouriort, G., Brand, H., Seraphin, B., and Gannon, F. (2002). Natural trans-spliced mRNAs are generated from the human estrogen receptor-alpha (hER alpha) gene. *J. Biol. Chem.* *277*, 26244–26251.
- Gandini, M. a., Sandoval, a., and Felix, R. (2014). Patch-Clamp Recording of Voltage-Sensitive Ca²⁺ Channels. *Cold Spring Harb. Protoc.* *2014*, pdb.top066092 – pdb.top066092.
- Gendron, D., Carriero, S., Garneau, D., Villemaire, J., Klinck, R., Elela, S.A., Damha, M.J., and Chabot, B. (2006). Modulation of 5' splice site selection using tailed oligonucleotides carrying splicing signals. *BMC Biotechnol.* *6*, 5.
- Gerard, X., Perrault, I., Hanein, S., Silva, E., Bigot, K., Defoort-Delhemmes, S., Rio, M., Munnich, A., Scherman, D., Kaplan, J., et al. (2012). AON-mediated Exon Skipping Restores Ciliation in Fibroblasts Harboring the Common Leber Congenital Amaurosis CEP290 Mutation. *Mol. Ther. Nucleic Acids* *1*, e29.
- Glaus, E., Schmid, F., Da Costa, R., Berger, W., and Neidhardt, J. (2011). Gene therapeutic approach using mutation-adapted U1 snRNA to correct a RPGR splice defect in patient-derived cells. *Mol. Ther.* *19*, 936–941.
- Goemans, N.M., Tulinius, M., van den Akker, J.T., Burm, B.E., Ekhart, P.F., Heuvelmans, N., Holling, T., Janson, A.A., Platenburg, G.J., Sipkens, J.A., et al. (2011). Systemic administration of PRO051 in Duchenne's muscular dystrophy. *N. Engl. J. Med.* *364*, 1513–1522.
- Gomes Dos Santos, a L., Bochot, A., and Fattal, E. (2005). Intraocular delivery of oligonucleotides. *Curr. Pharm. Biotechnol.* *6*, 7–15.
- Goyenvalle, A., Babbs, A., van Ommen, G.-J.B., Garcia, L., and Davies, K.E. (2009). Enhanced exon-skipping induced by U7 snRNA carrying a splicing silencer sequence: Promising tool for DMD therapy. *Mol. Ther.* *17*, 1234–1240.
- Goyenvalle, A., Wright, J., Babbs, A., Wilkins, V., Garcia, L., and Davies, K.E. (2012). Engineering multiple U7snRNA constructs to induce single and multiexon-skipping for Duchenne muscular dystrophy. *Mol. Ther.* *20*, 1212–1221.
- Gurnett, C. a, De Waard, M., and Campbell, K.P. (1996). Dual function of the voltage-dependent Ca²⁺ channel alpha 2 delta subunit in current stimulation and subunit interaction. *Neuron* *16*, 431–440.
- Gurnett, C.A., Felix, R., and Campbell, K.P. (1997). Extracellular interaction of the voltage-dependent Ca²⁺ channel alpha2delta and alpha1 subunits. *J. Biol. Chem.* *272*, 18508–18512.
- Hamill, O.P., Marty, A., Neher, E., Sakmann, B., and Sigworth, F.J. (1981). Improved patch-clamp techniques for high-resolution current recording from cells and cell-free membrane patches. *Pflügers Arch. Eur. J. Physiol.* *391*, 85–100.
- Hartong, D.T., Berson, E.L., and Dryja, T.P. (2006). Retinitis pigmentosa. *Lancet* *368*, 1795–1809.
- Havens, M. a, Duelli, D.M., and Hastings, M.L. (2013). Targeting RNA splicing for disease therapy. *Wiley Interdiscip. Rev. RNA* *4*, 247–266.
- Hernan, I., Gamundi, M.J., Planas, E., Borràs, E., Maseras, M., and Carballo, M. (2011). Cellular expression and siRNA-mediated interference of rhodopsin cis-acting splicing mutants associated with autosomal dominant retinitis pigmentosa. *Invest. Ophthalmol. Vis. Sci.* *52*, 3723–3729.

- Hobom, M., Dai, S., Marais, E., Lacinova, L., Hofmann, F., Klugbauer, N., and Str, B. (2000). Neuronal distribution and functional characterization of the calcium channel $\alpha_2\text{-2}$ subunit. *Eur. J. Neurosci.* *12*, 1217–1226.
- Hodgkin, A.L., and Huxley, A.F. (1952). A quantitative description of membrane current and its applications to conduction and excitation in nerve. *J. Physiol.* *117*, 500–544.
- Den Hollander, A.I., Koenekoop, R.K., Yzer, S., Lopez, I., Arends, M.L., Voesenek, K.E.J., Zonneveld, M.N., Strom, T.M., Meitinger, T., Brunner, H.G., et al. (2006). Mutations in the CEP290 (NPHP6) gene are a frequent cause of Leber congenital amaurosis. *Am. J. Hum. Genet.* *79*, 556–561.
- Den Hollander, A.I., Roepman, R., Koenekoop, R.K., and Cremers, F.P.M. (2008). Leber congenital amaurosis: genes, proteins and disease mechanisms. *Prog. Retin. Eye Res.* *27*, 391–419.
- Hong, D.-H. (2003). RPGR Isoforms in Photoreceptor Connecting Cilia and the Transitional Zone of Motile Cilia. *Invest. Ophthalmol. Vis. Sci.* *44*, 2413–2421.
- Hong, D.-H., and Li, T. (2002). Complex expression pattern of RPGR reveals a role for purine-rich exonic splicing enhancers. *Invest. Ophthalmol. Vis. Sci.* *43*, 3373–3382.
- Hoppa, M., Lana, B., Margas, W., Dolphin, A., and Ryan, T. (2012). Alpha 2 Delta Expression Sets Presynaptic Calcium Channel Abundance and Release Probability. *Nature* *486*, 122–125.
- Horn, R., and Korn, S.J. (1992). Prevention of rundown in electrophysiological recording. *Methods Enzymol.* *207*, 149–155.
- Hoskins, A. a, and Moore, M.J. (2012). The spliceosome: a flexible, reversible macromolecular machine. *Trends Biochem. Sci.* *37*, 179–188.
- Hu, J., Wu, Q., Li, T., Chen, Y., and Wang, S. (2013). Inhibition of high glucose-induced VEGF release in retinal ganglion cells by RNA interference targeting G protein-coupled receptor 91. *Exp. Eye Res.* *109*, 31–39.
- Huc, S., Monteil, A., Bidaud, I., Barbara, G., Chemin, J., and Lory, P. (2009). Regulation of T-type calcium channels: signalling pathways and functional implications. *Biochim. Biophys. Acta* *1793*, 947–952.
- Jacobson, S.G., Cideciyan, A. V., Ratnakaram, R., Heon, E., Schwartz, S.B., Roman, A.J., Peden, M.C., Aleman, T.S., Boye, S.L., Sumaroka, A., et al. (2012). Gene Therapy for Leber Congenital Amaurosis Caused by RPE65 Mutations: Safety and Efficacy in 15 Children and Adults Followed Up to 3 Years. *Arch. Ophthalmol.* *130*, 9–24.
- Järver, P., O’Donovan, L., and Gait, M.J. (2013). A Chemical View of Oligonucleotides for Exon Skipping and Related Drug Applications. *Nucleic Acid Ther.* *24*.
- Jean-Philippe, J., Paz, S., and Caputi, M. (2013). hnRNP A1: the Swiss army knife of gene expression. *Int. J. Mol. Sci.* *14*, 18999–19024.
- Jiang, L., Li, T.Z., Boye, S.E., Hauswirth, W.W., Frederick, J.M., and Baehr, W. (2013). RNAi-mediated gene suppression in a GCAP1(L151F) cone-rod dystrophy mouse model. *PLoS One* *8*, e57676.
- Jin, Y., Suzuki, H., Maegawa, S., Endo, H., Sugano, S., Hashimoto, K., Yasuda, K., and Inoue, K. (2003). A vertebrate RNA-binding protein Fox-1 regulates tissue-specific splicing via the pentanucleotide GCAUG. *EMBO J.* *22*, 905–912.

- Jones, L.P., Wei, S., and Yue, D.T. (1998). Mechanism of Auxiliary Subunit Modulation of Neuronal $\alpha 1E$ Calcium Channels. *J. Gen. Physiol.* *112*.
- Kadurin, I., Alvarez-Laviada, A., Ng, S.F.J., Walker-Gray, R., D'Arco, M., Fadel, M.G., Pratt, W.S., and Dolphin, A.C. (2012). Calcium currents are enhanced by $\alpha 2\delta$ -1 lacking its membrane anchor. *J. Biol. Chem.* *287*, 33554–33566.
- Kafasla, P., Mickleburgh, I., Llorian, M., Coelho, M., Gooding, C., Cherny, D., Joshi, A., Kotik-Kogan, O., Curry, S., Eperon, I.C., et al. (2012). Defining the roles and interactions of PTB. *Biochem. Soc. Trans.* *40*, 815–820.
- Kalbfuss, B., Mabon, S. a, and Misteli, T. (2001). Correction of alternative splicing of tau in frontotemporal dementia and parkinsonism linked to chromosome 17. *J. Biol. Chem.* *276*, 42986–42993.
- Kanasty, R., Dorkin, J.R., Vegas, A., and Anderson, D. (2013). Delivery materials for siRNA therapeutics. *Nat. Mater.* *12*, 967–977.
- Khanna, H., Hurd, T.W., Lillo, C., Shu, X., Parapuram, S.K., He, S., Akimoto, M., Wright, A.F., Margolis, B., Williams, D.S., et al. (2005). RPGR-ORF15, which is mutated in retinitis pigmentosa, associates with SMC1, SMC3, and microtubule transport proteins. *J. Biol. Chem.* *280*, 33580–33587.
- Kim, D., Perteza, G., Trapnell, C., Pimentel, H., Kelley, R., and Salzberg, S.L. (2013). TopHat2: accurate alignment of transcriptomes in the presence of insertions, deletions and gene fusions. *Genome Biol.* *14*, R36.
- Kinali, M., Arechavala-Gomez, V., Feng, L., Cirak, S., Hunt, D., Adkin, C., Guglieri, M., Ashton, E., Abbs, S., Nihoyannopoulos, P., et al. (2009). Local restoration of dystrophin expression with the morpholino oligomer AVI-4658 in Duchenne muscular dystrophy: a single-blind, placebo-controlled, dose-escalation, proof-of-concept study. *Lancet Neurol.* *8*, 918–928.
- Kirschner, R., Erturk, D., Zeitz, C., Sahin, S., Ramser, J., Cremers, F.P., Ropers, H.H., and Berger, W. (2001). DNA sequence comparison of human and mouse retinitis pigmentosa GTPase regulator (RPGR) identifies tissue-specific exons and putative regulatory elements. *Hum. Genet.* *109*, 271–278.
- Kleinman, M.E., Yamada, K., Takeda, A., Chandrasekaran, V., Nozaki, M., Baffi, J.Z., Albuquerque, R.J.C., Yamasaki, S., Itaya, M., Pan, Y., et al. (2008). Sequence- and target-independent angiogenesis suppression by siRNA via TLR3. *Nature* *452*, 591–597.
- Klugbauer, N., Lacinova, L., Hobom, M., and Hofmann, F. (2000). Molecular Diversity of the Calcium Channel $\alpha 2\delta$ Subunit. *J. Neurosci.* *19*, 684–691.
- Knoflach, D., Kerov, V., Sartori, S.B., Obermair, G.J., Schmuckermair, C., Liu, X., Sothilingam, V., Garrido, M.G., Baker, S.A., Glösmann, M., et al. (2013). Cav1.4 IT mouse as model for vision impairment in human congenital stationary night blindness type 2. *Channels* *7*.
- Kole, R., Krainer, A.R., and Altman, S. (2012). RNA therapeutics: beyond RNA interference and antisense oligonucleotides. *Nat. Rev. Drug Discov.* *11*, 125–140.
- Kornblihtt, A.R., Schor, I.E., Alló, M., Dujardin, G., Petrillo, E., and Muñoz, M.J. (2013). Alternative splicing: a pivotal step between eukaryotic transcription and translation. *Nat. Rev. Mol. Cell Biol.* *14*, 153–165.
- Koschak, A., Reimer, D., Walter, D., Hoda, J.-C., Heinzle, T., Grabner, M., and Striessnig, J. (2003). Cav1.4 α 1 subunits can form slowly inactivating dihydropyridine-sensitive L-type Ca²⁺ channels lacking Ca²⁺-dependent inactivation. *J. Neurosci.* *23*, 6041–6049.

- Koshkin, A.A., Singh, S.K., Nielsen, P., Rajwanshi, V.K., Kumar, R., Meldgaard, M., Olsen, C.E., and Wengel, J. (1998). LNA (Locked Nucleic Acids): Synthesis of the adenine, cytosine, guanine, 5-methylcytosine, thymine and uracil bicyclonucleoside monomers, oligomerisation, and unprecedented nucleic acid recognition. *Tetrahedron* *54*, 3607–3630.
- Krol, J., Loedige, I., and Filipowicz, W. (2010). The widespread regulation of microRNA biogenesis, function and decay. *Nat. Rev. Genet.* *11*, 597–610.
- Kuroyanagi, H. (2009). Fox-1 family of RNA-binding proteins. *Cell. Mol. Life Sci.* *66*, 3895–3907.
- Kurreck, J. (2003). Antisense technologies. Improvement through novel chemical modifications. *Eur. J. Biochem.* *270*, 1628–1644.
- Kurshan, P.T., Oztan, A., and Schwarz, T.L. (2009). Presynaptic $\alpha 2\delta$ -3 is required for synaptic morphogenesis independent of its Ca^{2+} -channel functions. *Nat. Neurosci.* *12*, 1415–1423.
- Lam, B.J., and Hertel, K.J. (2002). A general role for splicing enhancers in exon definition. *RNA* *8*, 1233–1241.
- Lana, B., Schlick, B., Martin, S., Pratt, W.S., Page, K.M., Goncalves, L., Rahman, W., Dickenson, A.H., Bauer, C.S., and Dolphin, A.C. (2014). Differential upregulation in DRG neurons of an $\alpha 2\delta$ -1 splice variant with a lower affinity for gabapentin after peripheral sensory nerve injury. *Pain* *155*, 522–533.
- Lareau, L.F., Brooks, A.N., Soergel, D.A.W., Meng, Q., and Brenner, S.E. (2007). The coupling of alternative splicing and nonsense-mediated mRNA decay. *Adv. Exp. Med. Biol.* *623*, 190–211.
- Lee, A., Wang, S., Williams, B., Hagen, J., Scheetz, T.E., and Haeseleer, F. (2014). Characterization of Cav1.4 Complexes ($\alpha 11.4$, $\beta 2$, $\alpha 2\delta 4$) in HEK293T cells and in the Retina. *J. Biol. Chem.*
- Lejeune, F., and Maquat, L.E. (2005). Mechanistic links between nonsense-mediated mRNA decay and pre-mRNA splicing in mammalian cells. *Curr. Opin. Cell Biol.* *17*, 309–315.
- Lewandowska, M.A. (2013). The missing puzzle piece: Splicing mutations. *Int. J. Clin. Exp. Pathol.* *6*, 2675–2682.
- Lim, K.H., Ferraris, L., Filloux, M.E., Raphael, B.J., and Fairbrother, W.G. (2011a). Using positional distribution to identify splicing elements and predict pre-mRNA processing defects in human genes. *Proc. Natl. Acad. Sci. U. S. A.* *108*, 11093–11098.
- Lim, K.H., Ferraris, L., Filloux, M.E., Raphael, B.J., and Fairbrother, W.G. (2011b). Using positional distribution to identify splicing elements and predict pre-mRNA processing defects in human genes. *Proc. Natl. Acad. Sci. U. S. A.* *108*, 11093–11098.
- Liu, X., Bulgakov, O. V., Darrow, K.N., Pawlyk, B., Adamian, M., Liberman, M.C., and Li, T. (2007). Usherin is required for maintenance of retinal photoreceptors and normal development of cochlear hair cells. *Proc. Natl. Acad. Sci. U. S. A.* *104*, 4413–4418.
- López-Bigas, N., Audit, B., Ouzounis, C., Parra, G., and Guigó, R. (2005). Are splicing mutations the most frequent cause of hereditary disease? *FEBS Lett.* *579*, 1900–1903.
- Maguire, A.M., Simonelli, F., Pierce, E.A., Pugh, E.N., Mingozzi, F., Bennicelli, J., Banfi, S., Marshall, K.A., Testa, F., Surace, E.M., et al. (2008). Safety and efficacy of gene transfer for Leber's congenital amaurosis.

- Maguire, A.M., High, K. a., Auricchio, A., Wright, J.F., Pierce, E. a., Testa, F., Mingozzi, F., Bennicelli, J.L., Ying, G.S., Rossi, S., et al. (2009). Age-dependent effects of RPE65 gene therapy for Leber's congenital amaurosis: a phase 1 dose-escalation trial. *Lancet* 374, 1597–1605.
- Malmivuo, J., and Plonsey, R. (1995). *Bioelectromagnetism: Principles and Applications of Bioelectric and Biomagnetic Fields*.
- Mansfield, S.G., Chao, H., and Walsh, C.E. (2004). RNA repair using spliceosome-mediated RNA trans-splicing. *Trends Mol. Med.* 10, 263–268.
- Marquis, J., Meyer, K., Angehrn, L., Kämpfer, S.S., Rothen-Rutishauser, B., and Schümperli, D. (2007). Spinal muscular atrophy: SMN2 pre-mRNA splicing corrected by a U7 snRNA derivative carrying a splicing enhancer sequence. *Mol. Ther.* 15, 1479–1486.
- Martin, K.R.G., Klein, R.L., and Quigley, H. a (2002). Gene delivery to the eye using adeno-associated viral vectors. *Methods* 28, 267–275.
- Martin P. (1995). New access to 2-O-alkylated ribonucleosides and properties of 2-O-alkylated oligoribonucleotides. *Helv. Chim. Acta* 486^504.
- Matsuo, M. (1996). Duchenne/Becker muscular dystrophy: from molecular diagnosis to gene therapy. *Brain Dev.* 7604, 167–172.
- Mavlyutov, T.A., Zhao, H., and Ferreira, P.A. (2002). Species-specific subcellular localization of RPGR and RPGRIP isoforms : implications for the phenotypic variability of congenital retinopathies among species. *II*, 1899–1907.
- McRory, J.E., Hamid, J., Doering, C.J., Garcia, E., Parker, R., Hamming, K., Chen, L., Hildebrand, M., Beedle, A.M., Feldcamp, L., et al. (2004). The CACNA1F gene encodes an L-type calcium channel with unique biophysical properties and tissue distribution. *J. Neurosci.* 24, 1707–1718.
- Meindl, A., Dry, K., Herrmann, K., Manson, F., Ciccodicola, A., Edgar, A., Carvalho, M.R., Achatz, H., Hellebrand, H., Lennon, A., et al. (1996). A gene (RPGR) with homology to the RCC1 guanine nucleotide exchange factor is mutated in X-linked retinitis pigmentosa (RP3). *Nat. Genet.* 13, 35–42.
- Mercer, A.J., Chen, M., and Thoreson, W.B. (2011). Lateral mobility of presynaptic L-type calcium channels at photoreceptor ribbon synapses. *J. Neurosci.* 31, 4397–4406.
- Mockel, a, Perdomo, Y., Stutzmann, F., Letsch, J., Marion, V., and Dollfus, H. (2011). Retinal dystrophy in Bardet-Biedl syndrome and related syndromic ciliopathies. *Prog. Retin. Eye Res.* 30, 258–274.
- Morgans, C.W., Bayley, P.R., Oesch, N.W., Ren, G., Akileswaran, L., and Taylor, W.R. (2005). Photoreceptor calcium channels: insight from night blindness. *Vis. Neurosci.* 22, 561–568.
- Murphy, W.J., Watkins, K.P., and Agabian, N. (1986). Identification of a novel Y branch structure as an intermediate in trypanosome mRNA processing: evidence for trans splicing. *Cell* 47, 517–525.
- Nachury, M. V, Seeley, E.S., and Jin, H. (2010). Trafficking to the ciliary membrane: how to get across the periciliary diffusion barrier? *Annu. Rev. Cell Dev. Biol.* 26, 59–87.
- Neidhardt, J., Glaus, A.E., Barthelmes, D., Zeitz, C., Fleischhauer, J., and Berger, W. (2007). Identification and Characterization of a Novel RPGR Isoform in Human Retina. *28*, 797–807.
- Niblock, M., and Gallo, J.-M. (2012). Tau alternative splicing in familial and sporadic tauopathies. *Biochem. Soc. Trans.* 40, 677–680.

- Nicholson, P., Yepiskoposyan, H., Metze, S., Zamudio Orozco, R., Kleinschmidt, N., and Mühlemann, O. (2010). Nonsense-mediated mRNA decay in human cells: mechanistic insights, functions beyond quality control and the double-life of NMD factors. *Cell. Mol. Life Sci.* 67, 677–700.
- Nielsen, P.E., Egholm, M., Berg, R.H., and Buchardt, O. (1991). Sequence-selective recognition of DNA by strand displacement with a thymine-substituted polyamide. *Science* 254, 1497–1500.
- Obika, S., Nanbu, D., Hari, Y., Andoh, J., Morio, K., Doi, T., and Imanishi, T. (1998). Stability and structural features of the duplexes containing nucleoside analogues with a fixed N-type conformation, 2'-O,4'-C-methyleneribonucleosides. *Tetrahedron Lett.* 39, 5401–5404.
- Osman, E.Y., Yen, P.-F., and Lorson, C.L. (2012). Bifunctional RNAs targeting the intronic splicing silencer N1 increase SMN levels and reduce disease severity in an animal model of spinal muscular atrophy. *Mol. Ther.* 20, 119–126.
- Owen, N., Zhou, H., Malygin, A. a, Sangha, J., Smith, L.D., Muntoni, F., and Eperon, I.C. (2011). Design principles for bifunctional targeted oligonucleotide enhancers of splicing. *Nucleic Acids Res.* 39, 7194–7208.
- Patel, S.B., and Bellini, M. (2008). The assembly of a spliceosomal small nuclear ribonucleoprotein particle. *Nucleic Acids Res.* 36, 6482–6493.
- Perrault, I., Delphin, N., Hanein, S., Gerber, S., Dufier, J.-L., Roche, O., Defoort-Dhellemmes, S., Dollfus, H., Fazzi, E., Munnich, A., et al. (2007). Spectrum of NPHP6/CEP290 mutations in Leber congenital amaurosis and delineation of the associated phenotype. *Hum. Mutat.* 28, 416.
- Petrs-Silva, H., and Linden, R. (2014). Advances in gene therapy technologies to treat retinitis pigmentosa. *Clin. Ophthalmol.* 8, 127–136.
- Pinotti, M., Rizzotto, L., Balestra, D., Lewandowska, M.A., Cavallari, N., Marchetti, G., Bernardi, F., and Pagani, F. (2008). U1-snRNA-mediated rescue of mRNA processing in severe factor VII deficiency. *Blood* 111, 2681–2684.
- Piva, F., Giulietti, M., Nocchi, L., and Principato, G. (2009). SpliceAid: A database of experimental RNA target motifs bound by splicing proteins in humans. *Bioinformatics* 25, 1211–1213.
- Pozzoli, U., and Sironi, M. (2005). Silencers regulate both constitutive and alternative splicing events in mammals. *Cell. Mol. Life Sci.* 62, 1579–1604.
- Qin, N., Yagel, S., Momplaisir, M., Codd, E.E., and Andrea, M.R.D. (2002). Molecular Cloning and Characterization of the Human Voltage-Gated Calcium Channel $\alpha 2\delta 4$ Subunit. *Mol. Pharmacol.* 62, 485–496.
- Reese, M.G., Eeckman, F.H., Kulp, D., and Haussler, D. (1997). Improved splice site detection in Genie. *J. Comput. Biol.* 4, 311–323.
- Reiners, J., Nagel-Wolfrum, K., Jürgens, K., Märker, T., and Wolfrum, U. (2006). Molecular basis of human Usher syndrome: Deciphering the meshes of the Usher protein network provides insights into the pathomechanisms of the Usher disease. *Exp. Eye Res.* 83, 97–119.
- Roepman, R., Van Duijnhoven, G., Rosenberg, T., Pinckers, A.J.L.G., Bleeker-Wagemakers, L.M., Bergen, A.A.B., Post, J., Beck, A., Reinhardt, R., Ropers, H.H., et al. (1996). Positional cloning of the gene for X-linked retinitis pigmentosa 3: Homology with the guanine-nucleotide-exchange factor RCC1. *Hum. Mol. Genet.* 5, 1035–1041.

- Roepman, R., Bernoud-hubac, N., Schick, D.E., Maugeri, A., Berger, W., Ropers, H., Cremers, F.P.M., and Ferreira, P.A. (2000). The retinitis pigmentosa GTPase regulator (RPGR) interacts with novel transport-like proteins in the outer segments of rod photoreceptors. *9*, 2095–2106.
- Saleh, A.F., Arzumanov, A.A., and Gait, M.J. (2012). Overview of alternative oligonucleotide chemistries for exon skipping. *Methods Mol. Biol.* *867*, 365–378.
- Sánchez-Alcudia, R., Pérez, B., Pérez-Cerdá, C., Ugarte, M., and Desviat, L.R. (2011). Overexpression of adapted U1snRNA in patients' cells to correct a 5' splice site mutation in propionic acidemia. *Mol. Genet. Metab.* *102*, 134–138.
- Sandoval, A., Oviedo, N., Andrade, A., and Felix, R. (2004). Glycosylation of asparagines 136 and 184 is necessary for the α_1 subunit-mediated regulation of voltage-gated Ca²⁺ channels. *FEBS Lett.* *576*, 21–26.
- Schlick, B., Flucher, B.E., and Obermair, G.J. (2012). VOLTAGE-ACTIVATED CALCIUM CHANNEL EXPRESSION PROFILES IN MOUSE BRAIN AND CULTURED HIPPOCAMPAL NEURONS. *Neuroscience* *167*, 786–798.
- Schmid, F., Glaus, E., Barthelmes, D., Fliegau, M., Gaspar, H., Nürnberg, G., Nürnberg, P., Omran, H., Berger, W., and Neidhardt, J. (2011). U1 snRNA-mediated gene therapeutic correction of splice defects caused by an exceptionally mild BBS mutation. *Hum. Mutat.* *32*, 815–824.
- Schmid, F., Hiller, T., Korner, G., Glaus, E., Berger, W., and Neidhardt, J. (2013). A gene therapeutic approach to correct splice defects with modified U1 and U6 snRNPs. *Hum. Gene Ther.* *24*, 97–104.
- De Sevilla Müller, L.P., Liu, J., Solomon, A., Rodriguez, A., and Brecha, N.C. (2013). Expression of voltage-gated calcium channel $\alpha_2\delta_4$ subunits in the mouse and rat retina. *J. Comp. Neurol.* *521*, 2486–2501.
- Seyhan, A. a (2011). RNAi: a potential new class of therapeutic for human genetic disease. *Hum. Genet.* *130*, 583–605.
- Shababi, M., Glascock, J., and Lorson, C.L. (2011). Combination of SMN trans-splicing and a neurotrophic factor increases the life span and body mass in a severe model of spinal muscular atrophy. *Hum. Gene Ther.* *22*, 135–144.
- Shen, W.Y., and Rakoczy, P.E. (2001). Uptake dynamics and retinal tolerance of phosphorothioate oligonucleotide and its direct delivery into the site of choroidal neovascularization through subretinal administration in the rat. *Antisense Nucleic Acid Drug Dev.* *11*, 257–264.
- Shen, W.Y., Garrett, K.L., da Cruz, L., Constable, I.J., and Rakoczy, P.E. (1999). Dynamics of phosphorothioate oligonucleotides in normal and laser photocoagulated retina. *Br. J. Ophthalmol.* *83*, 852–861.
- Shibata, H., Huynh, D.P., and Pulst, S.M. (2000). A novel protein with RNA-binding motifs interacts with ataxin-2. *Hum. Mol. Genet.* *9*, 1303–1313.
- Shirokov, R., Ferreira, G., Yi, J., and Ríos, E. (1998). Inactivation of Gating Currents of L-Type Calcium Channels Specific Role of the $\alpha_2\delta$ Subunit. *III*.
- Shu, X., Fry, a M., Tulloch, B., Manson, F.D.C., Crabb, J.W., Khanna, H., Faragher, a J., Lennon, a, He, S., Trojan, P., et al. (2005). RPGR ORF15 isoform co-localizes with RPGRIP1 at centrioles and basal bodies and interacts with nucleophosmin. *Hum. Mol. Genet.* *14*, 1183–1197.

- Sibley, C.R. (2014). Regulation of gene expression through production of unstable mRNA isoforms. *Biochem. Soc. Trans.* *42*, 1196–1205.
- Simonelli, F., Maguire, A.M., Testa, F., Pierce, E.A., Mingozzi, F., Bencicelli, J.L., Rossi, S., Marshall, K., Banfi, S., Surace, E.M., et al. (2010). Gene therapy for Leber's congenital amaurosis is safe and effective through 1.5 years after vector administration.
- Sinnetger-Brauns, M.J., Huber, I.G., Koschak, A., Wild, C., Obermair, G.J., Einzinger, U., Hoda, J.-C., Sartori, S.B., and Striessnig, J. (2009). Expression and 1,4-dihydropyridine-binding properties of brain L-type calcium channel isoforms. *Mol. Pharmacol.* *75*, 407–414.
- Sipos, I., Pika-Hartlaub, U., Hofmann, F., Flucher, B.E., and Melzer, W. (2000). Effects of the dihydropyridine receptor subunits gamma and alpha2delta on the kinetics of heterologously expressed L-type Ca²⁺ channels. *Pflugers Arch. Eur. J. Physiol.* *439*, 691–699.
- Skordis, L. a, Dunckley, M.G., Yue, B., Eperon, I.C., and Muntoni, F. (2003). Bifunctional antisense oligonucleotides provide a trans-acting splicing enhancer that stimulates SMN2 gene expression in patient fibroblasts. *Proc. Natl. Acad. Sci. U. S. A.* *100*, 4114–4119.
- Smith, a J., Bainbridge, J.W.B., and Ali, R.R. (2012). Gene supplementation therapy for recessive forms of inherited retinal dystrophies. *Gene Ther.* *19*, 154–161.
- Specht, D., Wu, S.-B., Turner, P., Dearden, P., Koentgen, F., Wolfrum, U., Maw, M., Brandstätter, J.H., and tom Dieck, S. (2009). Effects of presynaptic mutations on a postsynaptic Cacna1s calcium channel colocalized with mGluR6 at mouse photoreceptor ribbon synapses. *Invest. Ophthalmol. Vis. Sci.* *50*, 505–515.
- Springer, T.A. (2006). Complement and the Multifaceted Functions of VWA and Integrin I Domains. *Structure* *14*, 1611–1616.
- Sproat, B.S., Lamond, A.I., Beijer, B., Neuner, P., and Ryder, U. (1989). Highly efficient chemical synthesis of 2'-O-methyloligoribonucleotides and tetrabiotinylated derivatives; novel probes that are resistant to degradation by RNA or DNA specific nucleases. *Nucleic Acids Res.* *17*, 3373–3386.
- Stein-Streilein, J. (2008). Immune regulation and the eye. *Trends Immunol.* *29*, 548–554.
- Stenson, P.D., Ball, E. V, Mort, M., Phillips, A.D., Shiel, J. a, Thomas, N.S.T., Abeyasinghe, S., Krawczak, M., and Cooper, D.N. (2003). Human Gene Mutation Database (HGMD): 2003 update. *Hum. Mutat.* *21*, 577–581.
- Sterne-Weiler, T., Howard, J., Mort, M., Cooper, D.N., and Sanford, J.R. (2011). Loss of exon identity is a common mechanism of human inherited disease. *Genome Res.* *21*, 1563–1571.
- Striessnig, J., Bolz, H.J., and Koschak, A. (2010). Channelopathies in Cav1.1, Cav1.3, and Cav1.4 voltage-gated L-type Ca²⁺ channels. *Pflugers Arch.* *460*, 361–374.
- Summerton, J., and Weller, D. (1997). Morpholino antisense oligomers: design, preparation, and properties. *Antisense Nucleic Acid Drug Dev.* *7*, 187–195.
- Surace, E.M., and Auricchio, A. (2008). Versatility of AAV vectors for retinal gene transfer. *Vision Res.* *48*, 353–359.
- Susani, L., Pangrazio, A., Sobacchi, C., Taranta, A., Mortier, G., Savarirayan, R., Villa, A., Orchard, P., Vezzoni, P., Albertini, A., et al. (2004). TCIRG1-dependent recessive osteopetrosis: mutation analysis, functional identification of the splicing defects, and in vitro rescue by U1 snRNA. *Hum. Mutat.* *24*, 225–235.

- Sutton, R.E., and Boothroyd, J.C. (1986). Evidence for trans splicing in trypanosomes. *Cell* 47, 527–535.
- Tahara, M., Pergolizzi, R.G., Kobayashi, H., Krause, A., Luettich, K., Lesser, M.L., and Crystal, R.G. (2004). Trans-splicing repair of CD40 ligand deficiency results in naturally regulated correction of a mouse model of hyper-IgM X-linked immunodeficiency. *Nat. Med.* 10, 835–841.
- Tanner, G., Glaus, E., Barthelmes, D., Ader, M., Fleischhauer, J., Pagani, F., Berger, W., and Neidhardt, J. (2009). Therapeutic strategy to rescue mutation-induced exon skipping in rhodopsin by adaptation of U1 snRNA. *Hum. Mutat.* 30, 255–263.
- Tazi, J., Bakkour, N., and Stamm, S. (2009). Alternative splicing and disease. *Biochim. Biophys. Acta* 1792, 14–26.
- Thaler, S., Rejdak, R., Dietrich, K., Ladewig, T., Okuno, E., Kocki, T., Turski, W.A., Junemann, A., Zrenner, E., and Schuettauf, F. (2006). A selective method for transfection of retinal ganglion cells by retrograde transfer of antisense oligonucleotides against kynurenine aminotransferase II. *Mol. Vis.* 12, 100–107.
- Thorvaldsdóttir, H., Robinson, J.T., and Mesirov, J.P. (2013). Integrative Genomics Viewer (IGV): High-performance genomics data visualization and exploration. *Brief. Bioinform.* 14, 178–192.
- Uehara, H., Cho, Y., Simonis, J., Cahoon, J., Archer, B., Luo, L., Das, S.K., Singh, N., Ambati, J., and Ambati, B.K. (2013). Dual suppression of hemangiogenesis and lymphangiogenesis by splice-shifting morpholinos targeting vascular endothelial growth factor receptor 2 (KDR). *FASEB J.* 27, 76–85.
- Underwood, J.G., Boutz, P.L., Dougherty, J.D., Stoilov, P., and Black, D.L. (2005). Homologues of the *Caenorhabditis elegans* Fox-1 protein are neuronal splicing regulators in mammals. *Mol. Cell. Biol.* 25, 10005–10016.
- Vaishnav, A.K., Gollob, J., Gamba-vitalo, C., Hutabarat, R., Sah, D., Meyers, R., De, T., and Maraganore, J. (2010). A status report on RNAi therapeutics Review. *Silence* 1–13.
- Vandenberghe, L.H., and Auricchio, a (2012). Novel adeno-associated viral vectors for retinal gene therapy. *Gene Ther.* 19, 162–168.
- Vervoort, R., Lennon, A., Bird, A.C., Tulloch, B., Axton, R., Miano, M.G., Meindl, A., Meitinger, T., Ciccodicola, A., and Wright, A.F. (2000). Mutational hot spot within a new RPGR exon in X-linked retinitis pigmentosa. *Nat. Genet.* 25, 462–466.
- Villemare, J., Dion, I., Elela, S.A., and Chabot, B. (2003). Reprogramming alternative pre-messenger RNA splicing through the use of protein-binding antisense oligonucleotides. *J. Biol. Chem.* 278, 50031–50039.
- Vivek, A., and Aravind, L. (2000). Cache – a signaling domain common to channel subunits and a class of prokaryotic chemotaxis receptors. *Trends Biochem. Sci.* 0004, 535–537.
- Voigt, T., Meyer, K., Baum, O., and Schümperli, D. (2010). Ultrastructural changes in diaphragm neuromuscular junctions in a severe mouse model for Spinal Muscular Atrophy and their prevention by bifunctional U7 snRNA correcting SMN2 splicing. *Neuromuscul. Disord.* 20, 744–752.
- Wally, V., Murauer, E.M., and Bauer, J.W. (2012). Spliceosome-mediated trans-splicing: the therapeutic cut and paste. *J. Invest. Dermatol.* 132, 1959–1966.
- Wang, W., and El-Deiry, W. (2010). Large Insertions : Two Simple Steps Using QuikChange II Site-Directed Mutagenesis Kits. *Agil. Technol. Appl. Note* 4, 1–4.

- Weston, M.D., Eudy, J.D., Fujita, S., Yao, S., Usami, S., Cremers, C., Greenberg, J., Ramesar, R., Martini, a, Moller, C., et al. (2000). Genomic structure and identification of novel mutations in usherin, the gene responsible for Usher syndrome type IIa. *Am. J. Hum. Genet.* *66*, 1199–1210.
- Whittaker, C.A., and Hynes, R.O. (2002). Distribution and Evolution of von Willebrand / Integrin A Domains: Widely Dispersed Domains with Roles in Cell Adhesion and Elsewhere. *Mol. Biol. Cell* *13*, 3369–3387.
- Van Wijk, E., Pennings, R.J.E., te Brinke, H., Claassen, A., Yntema, H.G., Hoefsloot, L.H., Cremers, F.P.M., Cremers, C.W.R.J., and Kremer, H. (2004). Identification of 51 novel exons of the Usher syndrome type 2A (USH2A) gene that encode multiple conserved functional domains and that are mutated in patients with Usher syndrome type II. *Am. J. Hum. Genet.* *74*, 738–744.
- Wycisk, K.A., Budde, B., Feil, S., Skosyrski, S., Buzzi, F., Neidhardt, J., Glaus, E., Nürnberg, P., Ruether, K., and Berger, W. (2006a). Structural and functional abnormalities of retinal ribbon synapses due to Cacna2d4 mutation. *Invest. Ophthalmol. Vis. Sci.* *47*, 3523–3530.
- Wycisk, K.A., Zeitz, C., Feil, S., Wittmer, M., Forster, U., Neidhardt, J., Wissinger, B., Zrenner, E., Wilke, R., Kohl, S., et al. (2006b). Mutation in the auxiliary calcium-channel subunit CACNA2D4 causes autosomal recessive cone dystrophy. *Am. J. Hum. Genet.* *79*, 973–977.
- Yan, D., Swain, P.K., Breuer, D., Tucker, R.M., Wu, W., Fujita, R., Rehemtulla, A., Burke, D., and Swaroop, A. (1998). Biochemical characterization and subcellular localization of the mouse retinitis pigmentosa GTPase regulator (mRprgr). *J. Biol. Chem.* *273*, 19656–19663.
- Yuan, M.-K., Tao, Y., Yu, W.-Z., Kai, W., and Jiang, Y.-R. (2010). Lentivirus-mediated RNA interference of vascular endothelial growth factor in monkey eyes with iris neovascularization. *Mol. Vis.* *16*, 1743–1753.
- Zanetta, C., Nizzardo, M., Simone, C., Monguzzi, E., Bresolin, N., Comi, G.P., and Corti, S. (2014). Molecular therapeutic strategies for spinal muscular atrophies: current and future clinical trials. *Clin. Ther.* *36*, 128–140.
- Zeitz, C., Robson, A.G., and Audo, I. (2014). Congenital stationary night blindness: An analysis and update of genotype-phenotype correlations and pathogenic mechanisms. *Prog. Retin. Eye Res.*
- Zhao, Y., Hong, D., Pawlyk, B., Yue, G., Adamian, M., Grynberg, M., Godzik, A., and Li, T. (2003). The retinitis pigmentosa GTPase regulator (RPGR) - interacting protein : Subserving RPGR function and participating in disk morphogenesis. *100*.
- Zhou, Z., and Fu, X.-D. (2013). Regulation of splicing by SR proteins and SR protein-specific kinases. *Chromosoma* *122*, 191–207.
- Zhu, H., Qian, J., Wang, W., Yan, Q., Xu, Y., Jiang, Y., Zhang, L., Lu, F., Hu, W., Zhang, X., et al. (2013). RNA interference of GADD153 protects photoreceptors from endoplasmic reticulum stress-mediated apoptosis after retinal detachment. *PLoS One* *8*, e59339.

TABLES

TABLE 1. Splice-site sequences and scores for *Cacna2d4* exons 22 to 27.

	Score	Sequence 5' > 3'
E22 5'splice site	0.52	ctggagtgtgagttc
E23 3'splice site	0.92	ttctgtgactttaccctcaggtgacgaggaactggtgcgg
E23 5'splice site	0.85	tctctgagtacgtac
E24 3'splice site	0.93	tgttgttgctttgcctcgcagagagtcagagcctggcgtgg
E24 5'splice site	0.99	ctgacaggtgagccc
E25 3'splice site	0.43	acatcaatcctactctcacaggaagttcctgaccctgaag
E25 5'splice site	0.92	ggaccaggtaacgga
E25b 3'splice site	0.93	cctctctgtgcttccccagagtggaaaaaggagatgtg
E25b 5'splice site	0.99	tccaaggtgagatc
E26 3'splice site	0.98	caataattctcattttccagatagcccaggcaagccagtg
E26 5'splice site	1.00	gcagcaggtgagagc
E27 3'splice site	0.98	cctccttctgttctcagctgtgggcatccagatgcaa

A perfect match with the canonical 3' or 5' splice site sequence is indicated by 1. E25b scores are higher than those of E25, reflecting stronger splice sites.

TABLE 2. Biophysical parameters of different $\alpha_2\delta$ constructs coexpressed with Cav1.4 α_1 and β_3 .

	CD_{max}	$V_{0.5, act}$	K_{act}	$V_{0.5, inact}$	K_{inact}
$\alpha_2\delta_4$	$8.3 \pm 0.9^{***}$ N = 44	1.6 ± 0.6 N = 29	9.9 ± 0.3 N = 29	-20.2 ± 2.3 N = 15	-13.0 ± 1.0 N = 15
$\alpha_2\delta_4$ E25b	3.7 ± 0.5 N = 16	-1.0 ± 2.6 N = 9	11.4 ± 1.1 N = 9	ND	ND
$\alpha_2\delta_4$ mut	3.5 ± 0.6 N = 26	1.0 ± 1.8 N = 17	11.0 ± 0.6 N = 17	ND	ND
$\alpha_2\delta_1$	$13.1 \pm 1.6^{***}$ N = 22	-1.1 ± 0.5 N = 20	9.1 ± 0.2 N = 20	-17.8 ± 2.3 N = 29	-14.4 ± 1.3 N = 29
pIRES	2.5 ± 0.3 N = 30	0.5 ± 2.4 N = 18	10.8 ± 0.7 N = 18	ND	ND
A2 δ_4 Δ E16	1.6 ± 0.2 N = 18	ND	ND	ND	ND
A2 δ_4 Δ E23-26	1.6 ± 0.3 N = 6	ND	ND	ND	ND
A2 δ_4 Δ E23-25	1.0 ± 0.2 N = 7	ND	ND	ND	ND

Experiments were conducted in tsA-201 cells using 15mM Ca^{2+} as charge carrier. Data are given as mean \pm SEM. CD_{max} = maximum current density, $V_{0.5, act}$ = half-maximum activation voltage, K_{act} = slope parameter of the activation curve, $V_{0.5, inact}$ = half-maximum inactivation voltage, K_{inact} = slope parameter of the inactivation curve, N= sample size, ND= not determined. Statistically significant differences are indicated by asterisks ($P < 0.001 = ***$). For multiple comparisons (CD_{max} ; $V_{0.5, act}$; K_{act}), significance is given in relation to Cav1.4 $\alpha_1 + \beta_3 + pIRES$. For single comparison ($V_{0.5, inact}$; K_{inact}) significance is given in relation to Cav1.4 $\alpha_1 + \beta_3 + \alpha_2\delta_1$. Data for $\alpha_2\delta_1$ $V_{0.5, inact}$ and K_{inact} were taken from Burtscher et al.(Burtscher et al., 2014)

FIGURE LEGENDS

FIGURE 1. Scheme of *Cacna2d4* transcript and computational analysis of exon 25 splicing. **(A)** Schematic representation of *Cacna2d4* transcript (not in scale). The various exons are numbered. Positions of the von Willebrand factor A (VWF-A) domain (Springer, 2006; Whittaker and Hynes, 2002) and of the two Cache (Vivek and Aravind, 2000) domains of the protein are shown. The murine c.2451insC mutation site and of the resulting nonsense codon are indicated by black arrowheads. **(B)** IGV visualization of the RNA-seq eye sample GSM737548 aligned to *Cacna2d4* genomic sequence. Position of E25b has been included. Junctions represent reads spanning over two exons: alternative splicing of E25 and E25b can be observed. **(C)** SpliceAid prediction of E25 exonic splicing enhancers (ESE, positive scores) and silencers (ESS, negative scores). Predictions present only on the mutant E25 are boxed. The mutation mainly creates ESSs with high scores. The location of the insertion on E25 is underlined in black.

FIGURE 2. Qualitative and quantitative analysis of exon 25 alternative splicing in presence and absence of c.2451insC mutation. **(A)** Representative RT-PCR of WT and mutant mouse retinae. Plasmids containing *Cacna2d4* sequence with E25 (pE25) or with E25b (pE25b) were used as controls. Presence of both E25 and E25b can be observed. **(B)** Densitometric analysis of the RT-PCR on WT and mutant mouse retinae reveals a reduction of E25 containing plasmid ($P < 0.05$). **(C)** Quantification of *Cacna2d4* E25, E25b and 3' UTR using RT-qPCR of WT and mutant mouse retinae ($n=3$). A more pronounced reduction of E25 ($p < 0.001$) compared to E25b ($p < 0.05$) containing transcripts was observed. **(D)** Relative abundance of E25 over E25b containing transcripts in mouse retinae. The mutation favours E25b presence ($p < 0.001$). **(E)** Schematic representation of *Cacna2d4* splicing-reporter minigene. The length of the different exons (boxes) and introns (straight lines) is shown. Alternative splicing events leading to E25b inclusion are reported with dashed lines. The position of primers used in RT-PCR is shown with arrows. **(F)** Representative RT-PCR of HEK293T cells transfected with WT (WT MINI) and mutant (MUT MINI) minigenes. The first line

shows the occurrence of proper splicing between all exons included in the minigene. Two bands, close to 850 bp, are distinguishable. The lower is caused by E25 inclusion, the upper by E25b. The second line confirms the presence of E25b-containing transcripts alongside E25-containing ones. (G) Densitometric analysis of the RT-PCR on WT and mutant minigenes. The mutation acts on minigene splicing by favouring E25b inclusion. (H) Quantification of the two splicing isoforms (E25/E25b) in presence or absence of the mutation, by means of RT-qPCR in cells transfected with the minigenes (n=2). Data confirms that the mutation causes an increase in the levels of the splicing isoform including E25b (p<0.01). (I) Relative abundance of E25 over E25b containing transcripts in HEK293T cells transfected with minigene splicing reporter systems. The mutation favours E25b presence.

FIGURE 3. Analysis of $\alpha_2\delta_4$ Δ E16 splicing isoform presence in the CNS and neuroendocrine system. (A) RT-PCR with primers flanking E16 on mouse hippocampus (HC), pituitary gland (PG), hypothalamus (HPT), occipital cortex (OC), somatosensory cortex (SSC), cerebellum (CB), WT (RET WT) and mutant (RET MUT) retina. (B) Densitometric analysis of RT-PCR.

FIGURE 4. Effect of different $\alpha_2\delta_4$ variants on Cav1.4 mediated current density. (A) Scheme of the recording protocol and representative sample traces for some of the different tested conditions. (B) Representation of the changes in current density at the different voltages tested for $\alpha_2\delta_1$, $\alpha_2\delta_4$, $\alpha_2\delta_4$ E25b, $\alpha_2\delta_4$ MUT (c.2451insC), $\alpha_2\delta_4$ Δ E16, pIRES (empty vector). Mean values, SEM, and the best fits of the current voltage relation are shown. The total number of cells considered for each curve is reported in parentheses. (C) Voltage-dependent activation curve of $\alpha_2\delta_1$, $\alpha_2\delta_4$, $\alpha_2\delta_4$ E25b, $\alpha_2\delta_4$ MUT (c.2451insC), $\alpha_2\delta_4$ Δ E16, pIRES (empty vector). (D) Maximal current densities of cells measured in the presence of different $\alpha_2\delta_4$ subunits in comparison to $\alpha_2\delta_1$ and pIRES. For each condition mean and SEM are shown. Selected pairs of conditions were compared using Kruskal-Wallis test followed by Dunn's multiple comparison post-test (p < 0.001 = ***).

FIGURE 5. Effect of the coexpression of full length $\alpha_2\delta_4$ with other $\alpha_2\delta_4$ variants. The full length $\alpha_2\delta_4$ construct was cotransfected with equal amounts of other $\alpha_2\delta_4$ variants. No significant differences on maximal current density were observed in any of the tested conditions as compared with $\alpha_2\delta_4 + \alpha_2\delta_4$, or with $\alpha_2\delta_4 + \text{pIRES}$. As a result no dominant negative effect of the different variants on $\alpha_2\delta_4$ activity was observable in the employed experimental conditions.

Figure 2

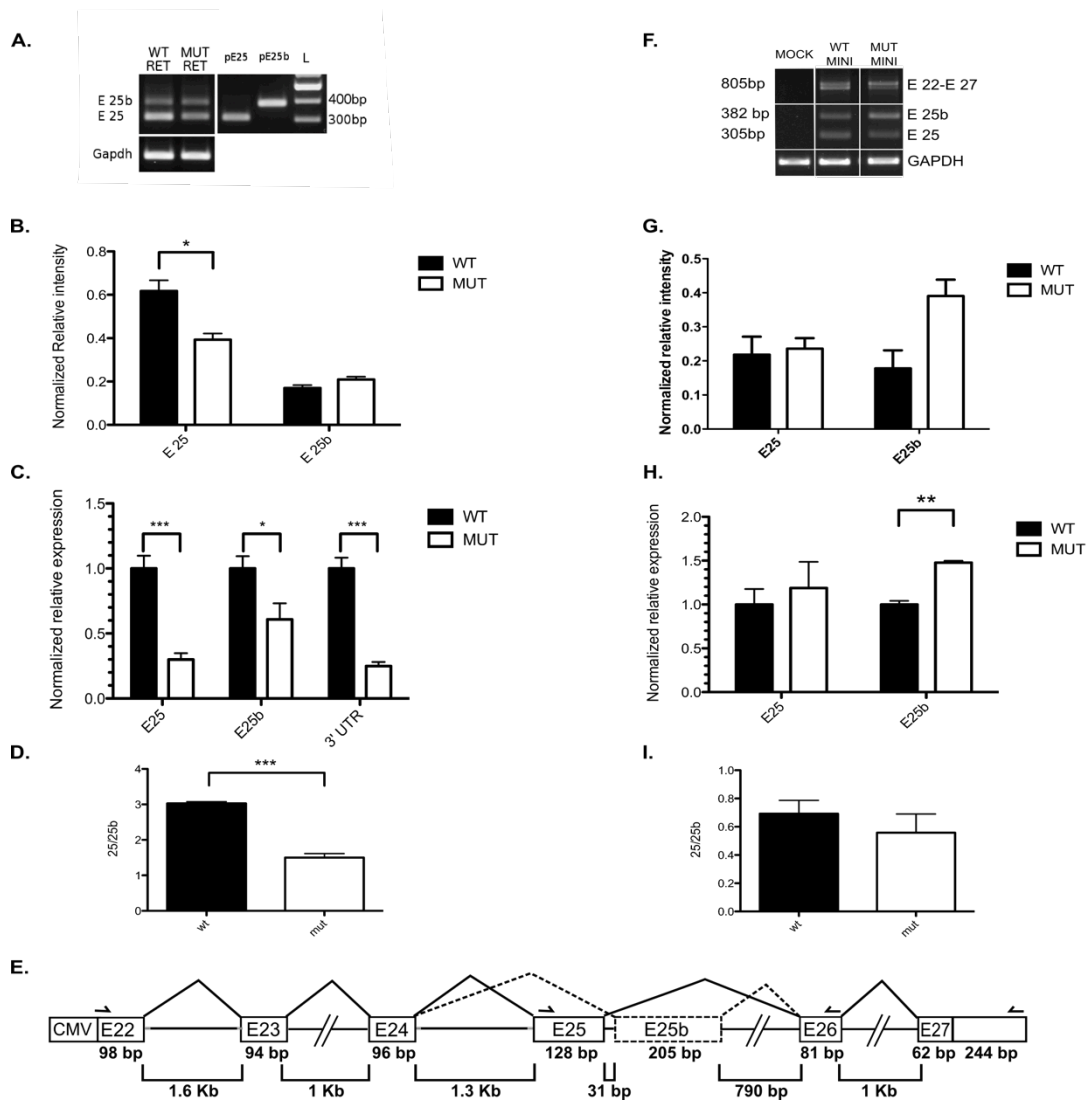


Figure 3

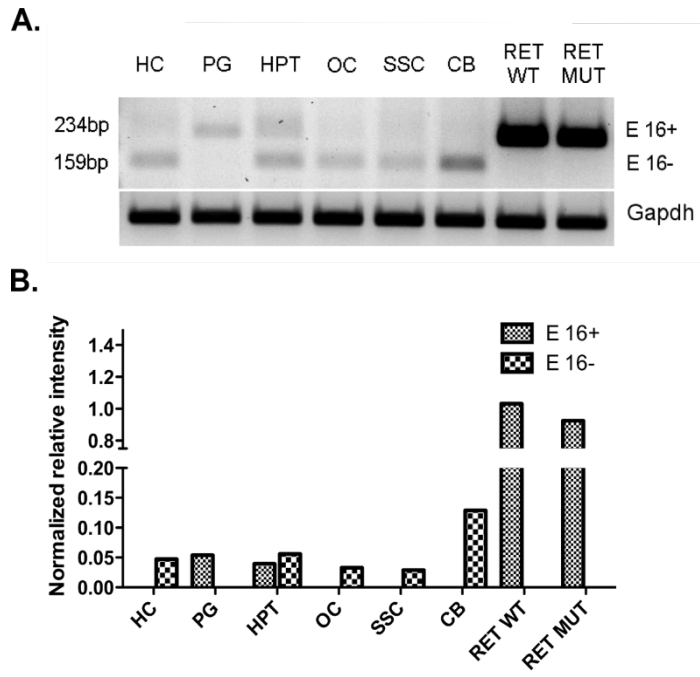


Figure 4

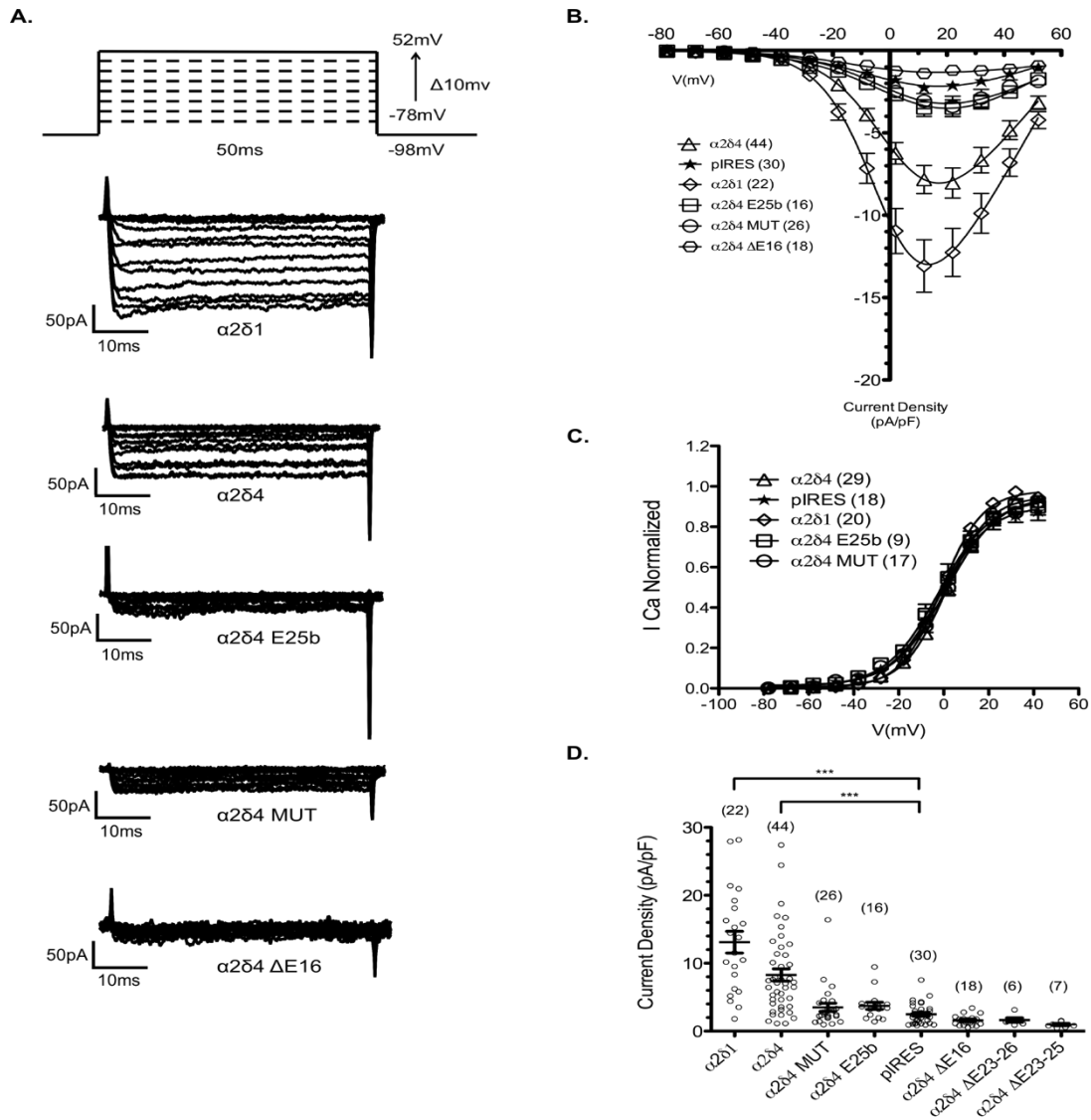
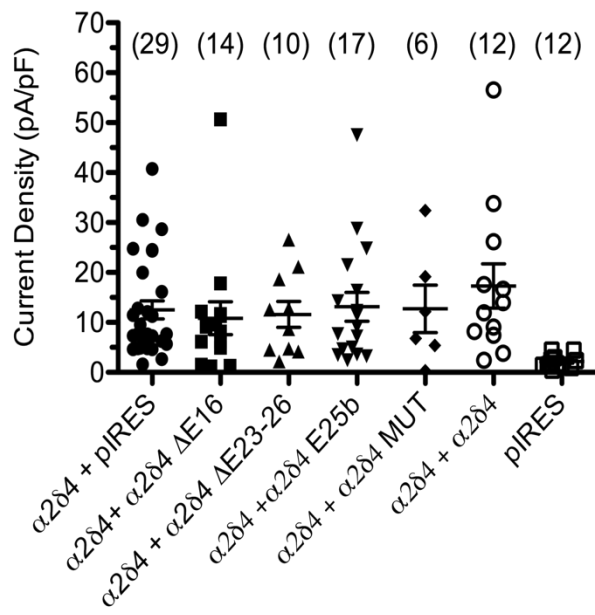
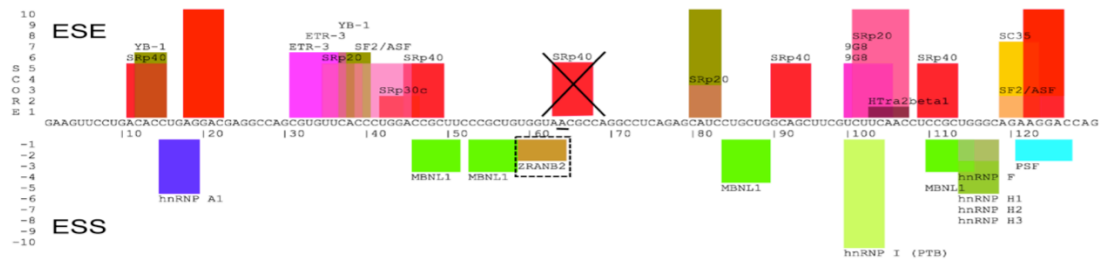


Figure 5



SUPPLEMENTARY MATERIAL

Figure S1.



LEGEND TO FIGURE S1. SpliceAid prediction of human mutation c.2406C→A effect on *CACNA2D4* E25. The position of the mutation is underlined with a black bar. Abolished ESE is crossed, while the new ESS is boxed.

TABLE S1. Primers and restriction enzymes used for minigene assembly.

Minigene Fragment	For/Rev	Sequence (5'-3')	Restriction enzymes
1	For	CTAAAGCTTATGATCTACTGTATCACAGA	HindIII
1	Rev	GTCGCTAGCAGTAATGCTCACTCGG	NheI
2	For	CGCACTAGTGTGGAAAGGAGTGATGGT	SpeI
2	Rev	TATGCGGCCGAGTCTGTTTTCTC	NotI
3	For	CTAGCGGCCGCACAGTCTTGATTGTTA	NotI
3	Rev	CAGACTAGTTCTTACATGAGACTTTGGAT	SpeI
4	For	GTAGCTAGCGGTGTAACATGGACTGG	NheI
4	Rev	CGTCTCGAGTCTGCTGCATGGCTGCC	Xho

TABLE S2. Primers used for RT-PCR and RT-qPCR

Target	For/Rev	Sequence (5'-3')	Application
Cacna2d4 E22	For	TATGATCTACTGTATCACAGATATCGAC	RT-PCR
pIRES2	Rev	CCACGATCCGATGGTTTGTATTTCAG	RT-PCR
Cacna2d4 E24	For	AGAGTCAGAGCCTGGCGTGG	RT-PCR
Cacna2d4 E26	Rev	CTGCTGCAATGGCCGTCTTCC	RT-PCR
GAPDH/Gapdh	For	GGCCAAGGTCATCCATGA	RT-PCR
GAPDH/Gapdh	Rev	TCAGTGTAGCCCAGGATG	RT-PCR
Cacna2d4 E15	For	GTGTAGTGGGCTCTGACGTG	RT-PCR
Cacna2d4 E17	Rev	TGGCGGTCCTCAGAATTTCA	RT-PCR
Cacna2d4 3'UTR	For	GTGGCGAGAAAAAGCAGAAC	RT-qPCR
Cacna2d4 3'UTR	Rev	CATTGTGAGCCACAGAAAGC	RT-qPCR
Cacna2d4 E25	For	CTGTGGTATCGCCAGGCCTCT	RT-qPCR
Cacna2d4 E25	Rev	GCAATGGCCGTCTTCCCATCC	RT-qPCR
Cacna2d4 E25b	For	TCCAGCATGGAGCAACGGGA	RT-qPCR
Cacna2d4 E25b	Rev	TGCTGCAATGGCCGTCTTCC	RT-qPCR
GAPDH/Gapdh	For	TGACCTCAACTACATGGTCTACA	RT-qPCR
GAPDH/Gapdh	Rev	CTTCCCATTCTCGGCCTTG	RT-qPCR

TABLE S3. SpliceAid complete prediction of splicing factor binding to the mutant murine E25 only.

Protein Name	Position in E25 mut	Recognized Sequence	Score	Function
hnRNP E1	83-89	CCCCCCC	-7	ESS
hnRNP E2	83-89	CCCCCCC	-7	ESS
hnRNP K	83-89	CCCCCCC	-7	ESS
HuR	83-89	CCCCCCC	-7	ESS
hnRNP I (PTB)	83-89	CCCCCCC	-7	ESS
hnRNP A1	83-89	CCCCCCC	-5	ESS
RBM5	83-89	CCCCCCC	-5	ESS
hnRNP U	83-89	CCCCCCC	-4	ESS
Nova-1	83-89	CCCCCCC	3	ESE

Exonic splicing silencer (ESS) or enhancer (ESE) are reported, together with their sequence and the computed prediction score. SpliceAid predicts target sequences of splicing enhancers and silencers: it gives positive scores for sequences bound by factors helping exon recognition and negative ones for sequences repressing exon recognition. The higher the score, the stronger is the ESE prediction; the lower the score, the stronger is the ESS prediction.

Splicing-Correcting Therapeutic Approaches for Retinal Dystrophies: Where Endogenous Gene Regulation and Specificity Matter

Niccolò Bacchi,¹ Simona Casarosa,^{1,2} and Michela A. Denti^{1,3}

¹Centre for Integrative Biology (CIBIO) - University of Trento, Trento, Italy

²Neuroscience Institute - National Research Council (CNR), Pisa, Italy

³Neuroscience Institute - National Research Council (CNR), Padova, Italy

Correspondence: Simona Casarosa, Centre for Integrative Biology (CIBIO) - University of Trento, Via Sommarive 9, 38123 Trento, Italy; casarosa@science.unitn.it; Michela A. Denti, Centre for Integrative Biology (CIBIO) - University of Trento, Via Sommarive 9, 38123 Trento, Italy; denti@science.unitn.it.

SC and MAD contributed equally to the work presented here and should therefore be regarded as equivalent authors.

Submitted: April 8, 2014

Accepted: April 11, 2014

Citation: Bacchi N, Casarosa S, Denti MA. Splicing-correcting therapeutic approaches for retinal dystrophies: where endogenous gene regulation and specificity matter. *Invest Ophthalmol Vis Sci.* 2014;55:3285-3294. DOI:10.1167/iovs.14-14544

Splicing is an important and highly regulated step in gene expression. The ability to modulate it can offer a therapeutic option for many genetic disorders. Antisense-mediated splicing-correction approaches have recently been successfully exploited for some genetic diseases, and are currently demonstrating safety and efficacy in different clinical trials. Their application for the treatment of retinal dystrophies could potentially solve a vast panel of cases, as illustrated by the abundance of mutations that could be targeted and the versatility of the technique. In this review, we will give an insight of the different therapeutic strategies, focusing on the current status of their application for retinal dystrophies.

Keywords: splicing correction, antisense oligonucleotides, retinal dystrophy, gene therapy

Retinal dystrophies are an extremely diversified group of genetic diseases all characterized by visual dysfunctions that can lead to blindness in the worst cases. Today there are more than 200 genes responsible for syndromic and non-syndromic retinal dystrophies,¹ each of them carrying several types of mutations leading to very different clinical phenotypes. The development of different gene therapy approaches has given a hope for the implementation of therapies for these otherwise incurable conditions. Messenger RNA splicing is an extremely complex and fundamental cellular process that has been so far barely considered as a therapeutic target,^{2,3} even if it can be seen as a highly appealing one for its importance in the cell context. The ability to modulate splicing can in fact offer several advantages over other conventional gene replacement approaches, especially in the context of retinal dystrophies. By definition, antisense-based therapeutic approaches act following base-pairing with their mRNA target, thus giving the possibility of obtaining a great specificity of action. Since they act at the mRNA level, the endogenous transcriptional regulation of the target gene is always maintained. This means that the therapeutic effect is obtained only where and when the target pre-mRNA is present. In a highly specialized and organized tissue like the retina, it is particularly important to maintain endogenous gene regulation. Therapeutic interven-

tions for delicate processes like the phototransduction cascade would require the preservation of this control for desirable outcomes.⁴ Splicing-correction approaches also allow a fine-tuning over the relative abundance of splicing isoforms because, by acting at a pre-mRNA level, it is relatively easy to modulate their ratio. The availability of several different molecular tools that can be used to manipulate splicing renders these approaches a versatile and promising strategy for the multitude of retinal dystrophies known today. Moreover, the retina has some characteristics that make it a perfect target tissue for those therapies. First of all, it is an easy tissue to access, and different drug delivery routes are in use today.^{5,6} Being that the eye is relatively small, enclosed, and separated from the rest of the body by the blood-brain barrier, it minimizes the required dose and systemic dissemination of the therapeutic agent, thus avoiding possible complications due to systemic side effects of the therapy.⁷ The eye is also an immune-privileged organ, limiting potential immune response to the delivered agent.⁸ The retina is composed by nondividing cells, thus it is easier to induce prolonged effects or transgene expression, without the need of using integrating vectors. Regarding gene delivery, the presence of different adeno-associated viral (AAV) vector serotypes able to efficiently and

TABLE. List of Genes Causing Retinal Diseases

Disease Category	Involved Genes
Cone or cone-rod dystrophy/dysfunctions	<i>ABCA4 ADAM9 AIPL1 BBS12 C2orf71 C8orf37 CA4 CABP4 CACNA1F CACNA2D4 CDHR1 CERKL CNGA3 CNGB3 CNNM4 CRB1 CRX GNAT2 GUCA1A GUCY2D KCVN2 MERK1 MKS1 NR2E3 NRL OPN1LW OPN1MW PDE6C PDE6H PTPN13 PROM1 PRPH2 RAB28 RAX2 RDH12 RIMS1 RLBP1 RPE65 RPGRIP1 TULP1 UNCL19</i>
Retinitis pigmentosa	<i>ABCA4 ARL2BP ARL6 BBS1 BEST1 C2orf71 C8orf37 CA4 CEP290 CERKL CLRN1 CNGA1 CNGB1 CRB1 CRX CYP4V2 DHDDS EMC1 EYS FAM161A FSCN2 GPR125 GRK1 GUCA1A GUCA1B GUCY2D IDH3B IMPDH1 IMPG2 KIAA1549 KLHL7 LCA5 LRAT MAK MERK1 MFRP MYO7A NR2E3 NRL OFD1 PDE6A PDE6B PDE6G PRCD PROM1 PRPF3 PRPF31 PRPF6 PRPF8 PRPH2 RBP3 RDH12 RGR RHO RLBP1 RP1 RP1L1 RP2 RP9 RPE65 RPGR RPGRIP1 SAG SEMA4A SNRNP200 SPATA7 TOPORS TULP1 USH2A VCAN ZNF513</i>
Leber congenital amaurosis	<i>AIPL1 BBS4 BEST1 CABP4 CEP290 CNGA3 CRB1 CRX DTHD1 GUCY2D IMPDH1 IQCB1 KCNJ13 LCA5 LRAT MERK1 MYO7A NMNAT1 NRL RD3 RDH12 RPE65 RPGRIP1 RPGRIP1L SPATA7 TULP1</i>
Macular dystrophy/degeneration	<i>ABCA4 ABCC6 BEST1 CNGB3 CRX EFEMP1 ELOVL4 GUCY2D PAX2 PROM1 PRPH2 RP1L1 TIMP3</i>
Stargardt disease	<i>ABCA4 ELOVL4 PRPH2 CFH HMCN1</i>
Age-related macular degeneration	<i>ABCA4 ARMS2 BEST1 C3 CFH ELOVL4 ERCC6 FBLN5 HMCN1 HTRA1 RAX2 SLC24A1</i>
Stationary night blindness	<i>CACNA1F CABP4 GNAT1 GPR179 GRK1 GRM6 LRIT3 NYX PDE6B RHO SAG SLC24A1 TRPM1</i>
Color blindness	<i>CNGA3 CNGB3 GNAT2 OPN1LW OPN1MW OPN1SW PDE6C PDE6H</i>
Usher syndrome	<i>ABHD12 CACNA1F CDH23 CIB2 CLRN1 DFNB31 GPR98 GUCY2D HARS LRAT MYO7A PCDH15 PDZD7 TRIM32 USH1C USH1G USH2A</i>
Chorioretinal atrophy/degeneration	<i>ABCA4 CRB1 TEAD1</i>
Retinal dystrophies/dysfunctions/degeneration	<i>ABCC6 ABCA4 ADAMTS18 AIPL1 BEST1 C1QTNF5 CAPN5 CDHR1 CERKL CHM CRB1 CYP4V2 FZD4 GUCA1B KCVN2 LRAT LRP5 MERK1 NDP NR2E3 NRL OTX2 PANK2 PLA2G5 PROM1 PRPH2 RD3 RDH12 RDH5 RGS9 RGS9BP RLBP1 RPE65 SLC24A1 TSPAN12</i>
Retinopathy of prematurity	<i>LRP5 NDP FZD4</i>
Optic atrophy/aplasia	<i>MFN2 OPA1 OPA3 OTX2 SLC24A1 TMEM126A WFS1</i>
Wagner syndrome	<i>VCAN COL2A1</i>
Bardet-Biedl syndrome	<i>ARL6 BBS1 BBS10 BBS12 BBS2 BBS4 BBS5 BBS7BBS9 CEP290 LZTFL1 MKKS MKS1 RPGRIP1L SDCCAG8 TRIM32 TTC8 WDPCP</i>
Other systemic/syndromic diseases involving the retina	<i>ABCC6 ABHD12 ADAMTS18 AH11 ALMS1 ATXN7 CC2D2A CDH3 CEP290 CISD2 CLN3 COL11A1 COL2A1 COL9A1 ERCC6 FLVCR1 GNPTG IFT140 INPP5E IQCB1 ITM2B JAG1 KIF11 LRP5 NPHP1 NPHP4 OFD1 OPA3 OTX2 PANK2 PAX2 PEX1 PEX2 PEX7 PHYH RBP4 RPGRIP1L SDCCAG8 TIMM8A TMEM237 TREX1 TTPA TTPA USH1C WFS1</i>

All RetNet identified genes have been searched and allocated to disease categories according to HGMD Professional entries from December 2013.

stably transduce all retina layers⁹ is a great advantage for splicing-modulating genetic tools.

THE MRNA SPLICING PROCESS

Once transcription of a gene begins in the nucleus, the transcript undergoes a complex series of cotranscriptional processes all devoted to the production of a mature mRNA, collectively dubbed "mRNA processing." One of these events, called mRNA splicing, consists in the removal of intervening sequences ("introns") and the joining of the coding portions of the transcript ("exons"). Messenger RNA splicing is a major way by which the cell can induce transcriptional diversity, mainly through alternative splicing, and apply a fine control on this diversity. The proper recognition of introns and exons is mediated by *cis*-acting sequences and *trans*-acting factors. The principal *cis*-acting elements that spatially organize the splicing reaction, consist in the splice donor (DS) site, the polypyrimidine tract (Py), the branch-site (BS), and the splice acceptor (AS) site. There are also other *cis*-acting sequences

that are fundamental for mRNA splicing¹⁰: exonic splicing enhancers (ESE) or silencers (ESS) that enhance or inhibit recognition of the exon in which they lay; intronic splicing enhancers (ISE) or silencers (ISS), intronic sequences that promote or suppress recognition of the nearby exons. *Trans*-acting factors are instead several proteins and ribonucleoproteins able to recognize the different *cis*-elements. Small nuclear RNA (snRNA) are constitutive components of the small nuclear ribonucleoproteins (snRNP) U1, U2, U4, U5, U6, and allow them to base-pair with different *cis*-acting sequences mediating the cascade of events leading to the splicing reaction. For example, the U1 snRNP recognizes the DS site, whereas U2 binds to the branch site. The other two groups of *trans*-acting splicing factors are represented by heterogeneous nuclear ribonucleoproteins (hnRNPs), that have mainly a repressive function, and by serine- and arginine-rich (SR) proteins, that play an important role in splicing regulations by mainly binding to ESE and ISE, thus promoting splicing.¹¹⁻¹⁵ All these factors assemble together in a precise temporal sequence in a complex called spliceosome, the cellular machinery devoted to the

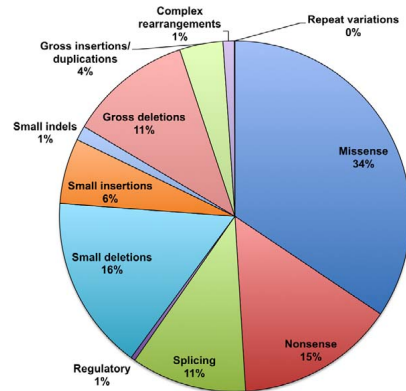


FIGURE 1. Mutation pattern of genes causing retinal diseases.

splicing process. For a more exhaustive description of the splicing process, we refer the reader to more detailed reviews.¹⁶⁻¹⁸

MUTATIONS LEADING TO RETINAL DISEASES

Retinal dystrophies are caused by mutations in many different genes, leading to a multitude of disease conditions¹⁻¹⁹ (Table). Today there are 219 genes identified as causative of retinal diseases, and the number is still growing.¹ The total number of known mutation for 208 of these genes, annotated in the Human Gene Mutation Database (provided in the public domain by HGMD Professional, <http://www.hgmd.cf.ac.uk/ac/index.php>), is 13,668.²⁰ The large majority of those are represented by missense mutations, accounting for 34% of the total (Fig. 1). Small deletions follow as the second most abundant type of genetic defect (16%). Bona fide splicing mutations represent an 11% of the total. Generally, mutations residing in introns are categorized as splicing mutations because the amino acid sequence of the protein is not altered, thus the problem most likely concerns proper splicing. These mutations can be located in any of the *cis*-acting elements present in introns. But splicing mutations can also be found in the exons, altering or not the coding sequence. In this case, their identification as a splicing mutation is much more difficult, as it requires analysis of the splicing pattern. Today it is believed that more than 25% of mutations, normally categorized as missense, nonsense, or silent, actually act by altering the splicing pattern.²¹⁻²⁵ Their effect can be the disruption of a *cis*-acting sequence, or the formation of a new one, resulting in exon skipping, intron retention, or use of alternative DS and AS sites. Correct identification of these mutations is of pivotal importance for the development of therapeutic approaches. Aside from splicing mutations, antisense-mediated splicing-correction approaches can potentially be utilized for the correction of missense and nonsense mutations, as well as for small insertions and deletions. In all cases where a mutation causes the introduction of a stop codon or frameshift leading to a premature termination of the transcript, the possibility to interfere with the proper recognition, by the splicing machinery, of the exon carrying the mutation (therapeutic exon skipping) can be the right strategy to follow. The result of this approach is a shorter mature mRNA, missing the portion

encoded by the skipped exon, but resulting in a restored ORF. It is then necessary to assess the functionality of the rescued smaller protein. This strategy is more easily applicable to genes where the mutated exon encodes for a repetitive structural element whose loss in the final protein product is less likely to cause structural and functional defects of the protein itself, whereas it is a riskier approach in other cases, where proper function of the skipped protein is less predictable.

ANTISENSE OLIGONUCLEOTIDES

A versatile tool to target splicing is represented by antisense oligonucleotides (AONs). These are chemically synthesized molecules, generally around 20 nucleotides long, able to mimic the RNA structure and bind, by reverse complementarity, to specific cellular RNA targets. Even if they are normally used to block mRNA translation or to degrade mRNA by RNase H-mediated cleavage, these effects are unwanted when the goal is to interfere with splicing. By the use of several different chemistries^{24,25} available today for their design, it is in fact possible to direct AONs toward splicing relevant sequences on the pre-mRNA, masking them, and to avoid RNase H activity after binding. The first splice-switch oligonucleotides used a phosphothioate linkage to join nucleosides (DNA-PS).²⁶ However, these AONs were retaining undesired RNase H activity.²⁴ A second generation of oligonucleotides was created from the DNA-PS structure. Inclusion at the 2' oxygen of a methyl (2'OMe) or a methoxyethyl (2'MOE) protecting group to increase oligonucleotides resistance to degradation and block RNase H activity originates 2'OMe-PS²⁷ and 2'MOE-PS²⁸ ribonucleosides, respectively. The third generation comprised locked nucleic acids (LNA), peptide nucleic acids (PNA), and phosphorodiamidate morpholino oligonucleotides (PMO). Locked nucleic acids derive from the addition of a methylene bridge between the 2' oxygen and the 5' carbon on a DNA-PS backbone.^{29,30} Locked nucleic acids have an increased affinity to target RNA and do not activate RNase H. In PNAs the DNA backbone is instead substituted by a peptide-like mimicry.³¹ Peptide nucleic acids do not cause RNase H degradation of their target and show strong affinity to it. Since they are neutrally charged, addition of a lysine residue is commonly used to increase their water solubility and cell-uptake. Phosphorodiamidate morpholino oligonucleotides derive from the substitution of the ribose rings with morpholine ones, and their joining by phosphorodiamidate groups.³² Phosphorodiamidate morpholino oligonucleotides are neutrally charged oligonucleotides that do not activate RNase H and are lowly susceptible to degradation. For a comprehensive understanding of these chemistries, we refer the reader to more specific reviews.^{24,25,33,34}

In order to be able to regulate splicing, AONs must gain access to the cell nucleus. There are different splicing regulatory sequences that have been so far targeted with AONs on pre-mRNA to achieve splicing modulation (Fig. 2). For example, by targeting splicing enhancers or silencers, it is possible to induce respectively exon skipping or exon retention by blocking access of splicing factors to their target sites. Another common target of AONs are splice sites that, when bound by an AON, are no longer free to take part in the splicing reaction, thus obliging the spliceosome to use alternative "downstream" sites, again inducing exon skipping. In few cases, AONs have been also engineered to carry an additional tail containing *cis*-acting sequences that can be bound by splicing factors able to enhance³⁵⁻³⁹ or silence⁴⁰⁻⁴³ splicing of specific exons. In this way, apart from their antisense activity toward a splicing-relevant sequence, these bifunctional AONs can induce additional effects depending on

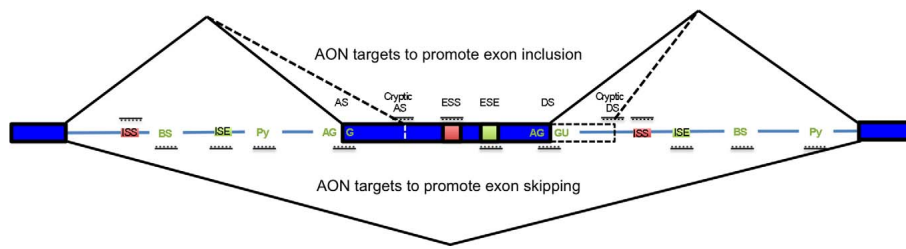


FIGURE 2. Possible AONs targets to induce splicing modulation. Schematic representation of *cis*-acting sequences that are possible target of AONs. *Cis*-acting sequences that promote exon recognition are reported in green, whereas sequences that suppress it are highlighted in red. Antisense oligonucleotides designed to induce exon skipping are shown in the bottom part. Antisense oligonucleotides designed to promote proper exon inclusion are shown in the upper part.

the sequence they carry on the tail. Since AONs act by base-pairing, they are generally believed to allow a high specificity of action for their desired target. No undesired misspliced products of the target gene or of chosen unrelated genes were in fact detected when investigated after therapeutic application of AONs.^{44,45} Even if these findings are not generalizable and proper design of the antisense molecule should always be considered, they underline the potentiality of AONs in the context of target selectivity. Splicing modulation finds its more advanced application in the cure of Duchenne muscular dystrophy (DMD). Duchenne muscular dystrophy is an X-linked recessive disease caused by mutations in the dystrophin gene. Dystrophin is an important cellular protein whose main role in muscle fibers is the connection of the cellular cytoskeleton with the extracellular matrix. Different mutations in the 79 exons of the gene cause protein truncation due to the loss of the open reading frame. The majority of these mutations can be addressed by exon skipping.⁴⁶ The commonly mutated exon 51 has been the first target for exon skipping. In the clinical trials completed so far for exon 51 skipping, the different chemistries applied (2'OMe-PS, PMOs) showed overall efficacy and absence of serious adverse effects.^{44,47-49}

A phase I clinical trial using a 2'MOE-PS oligonucleotide for splicing modulation has also been recently completed for spinal muscular atrophy (SMA), and a phase II trial has recently started.⁵⁰ Mutations in the survival motor neuron 1 (*SMN1*) gene are causative of the disease. In humans, *SMN1* has a paralogous, named *SMN2*. The two genes are identical, apart from a silent mutation in exon 7 of *SMN2*. This mutation, however, causes exon 7 of *SMN2* to be less recognized by the splicing machinery. If exon 7 is not included, the protein is truncated. So a therapeutic strategy is to mask exon 7 ESS using AONs, thus promoting exon 7 inclusion, which results in the

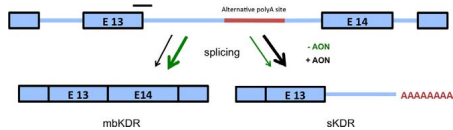


FIGURE 3. Antisense oligonucleotides approach for *KDR*. Scheme of action of AON against *KDR* exon 13 DS site: normally mbKDR, originating from intron 23 splicing, is more abundant than sKDR—that is, instead generated by the use of an alternative polyadenylation site in the retained intron 13. By interfering with the E13 DS site it was possible to increase the sKDR form, and decrease the mbKDR one.

production of a functional full length SMN protein from *SMN2* that can compensate for mutations on *SMN1*.

Antisense oligonucleotides are known to be able to target all retinal layers following intravitreal, subretinal, or topical administration.⁵¹⁻⁵⁶ They have long been used to elicit RNase H degradation or to block transcription in the eye for several different diseases, having been applied, for example, against cytomegalovirus (CMV), herpes simplex virus (HSV), vascular endothelial growth factor (VEGF), transforming growth factor- β (TGF- β), fibroblast growth factor (FGF).^{5,57}

An example of the use of splice-switch oligonucleotides in the eye is that of vascular endothelial growth factor receptor 2 (*KDR*). The *KDR* gene has two distinct products: membrane-bound KDR (mbKDR), that is prohemangiogenic, and soluble KDR (sKDR), antilymphangiogenic. Soluble KDR needs the recognition of an alternative polyadenylation site on *KDR* intron 13 to be translated. By intravitreal administration of PMO directed against murine *Kdr* exon 13 DS site, it was possible to increase the sKDR/mbKDR ratio at mRNA and protein level in the retina and vitreous, interfering with the spliceosome ability of mediating intron 13 splicing⁵⁸ (Fig. 3). This resulted in a block of hemangiogenesis and lymphangiogenesis in a model of choroidal neovascularization and corneal injury.⁵⁸ Another recent example of the use of AONs as splicing regulators to treat a retinal dystrophy is the one of the gene centrosomal protein 290kDa, (*CEP290*). Centrosomal protein

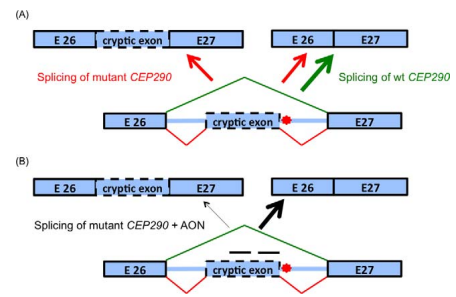


FIGURE 4. Antisense oligonucleotides approach for *CEP290*. (A) Proper joining of *CEP290* exon 26 and 27 (green lines and arrow) is impaired by a mutation in intron 26 (red star). The mutation causes the aberrant inclusion of a cryptic exon in a portion of the mature mRNA (red arrows). (B) Using different AONs (black lines) it was possible to increase the fraction of correctly spliced mRNA (black arrows).

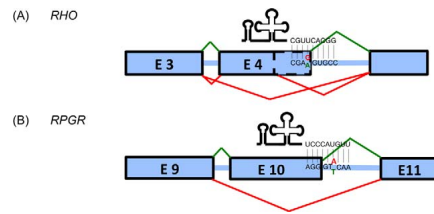


FIGURE 5. Mutation-adapted U1 snRNA for *RHO* and *RPGR* DS site mutations. The altered splicing pattern caused by the different mutations is reported in red. The correct splicing pattern is reported in green. The antisense sequence of the best U1 snRNA used to correct the effect of each mutation is reported. (A) Mutation at the last base of exon 4 of *RHO* causes skipping of the exon or missplicing due to the use of an alternative DS site. (B) An intronic mutation affecting the DS site of exon 10 of *RPGR* leads to exon 10 skipping.

290kDa mutations are responsible for ~15%^{59,60} of Leber congenital amaurosis cases, as well as for other genetic diseases such as Joubert syndrome, Senior-Løken syndrome, Meckel-Gruber syndrome, and Bardet-Biedl syndrome. A transition on intron 26 (c.2991+1655A>G) is among the most common mutations of *CEP290*.⁶¹ The mutation introduces a new DS site on intron 26, causing an aberrant exon to be included in the mature messenger RNA between exon 26 and 27. This aberrant exon carries a stop codon, resulting in a premature truncation of the protein. By the design of 2'OMe-PS directed toward predicted ESE sequences at the 3' of the aberrant exon it was possible to demonstrate, on patient fibroblast, its skipping from the mature mRNA, so to efficiently restore proper splicing between exon 26 and 27⁶² (Fig. 4). Another study by Gerard X and colleagues,⁶³ by using 2'OMe-PS targeting a different predicted ESE sequence, came to a similar result. Moreover, they were able to show an increase of full length protein levels in patient fibroblast following AON administration, as well as a faster ciliation.

CHIMERIC AND ADAPTED SNRNAs

The use of AONs as a therapeutic approach for genetic diseases poses one major problem. Their effect is time-limited, so to have a durable effect, repeated administration is required. In this view, the use of engineered snRNAs offer a major advantage, as they can be delivered in expression cassettes in the same way as it is done in conventional gene replacement therapies. By using viral or nonviral delivery systems, it is in fact possible to transduce or transfect target cells, and then produce the snRNA exploiting endogenous transcription. Like for AONs, one of the advantages of this class of RNA molecules is their specificity of action, as undesired activity of snRNAs has not been reported so far.^{64,65} Today there are two classes of snRNAs that have been successfully modified to be able to modulate splicing: U1 and U7. The first step of spliceosome assembly is mediated by U1 recognition of the DS site.⁶⁶ U7 snRNA is instead not involved in splicing, but in the processing of the 3' end of histone mRNA.⁶⁷ They both can be used to manipulate splicing exactly as AONs. Antisense U1 and U7 snRNA have been applied for masking *cis*-acting sequences, thus inducing therapeutic exon skipping, for Duchenne muscular dystrophy.^{68–70} Bifunctional U7 snRNA, acting in a similar way as bifunctional AONs, have also been designed for DMD⁷¹ and SMA.^{72,73}

Small nuclear RNAs can also be applied to a specific set of mutations not targetable by AONs. When a mutation disrupts a DS site, it leads to complete or partial loss of the splicing machinery's ability to recognize it. The design of mutation-adapted U1 snRNA able to interact by base-pairing with the mutated splice site can reestablish spliceosome recognition.^{64,74} This is possible by exploiting U1 natural function in splicing. Unfortunately, the same strategy is so far not applicable in a similar way to mutations of the AS site. It is also possible to engineer any viral vector with even a combination of different snRNAs, by taking advantage of their limited size.⁷⁰ Tanner and colleagues⁷⁵ applied mutation-adapted U1 snRNAs to rhodopsin (*RHO*), one of the genes responsible for autosomal dominant retinitis pigmentosa. An exonic point mutation interfering with the DS site was found responsible for exon 4 missplicing. By using minigenes as reporter systems in COS 7 cells, they were able to show rescue of exon 4 proper recognition with an efficiency of around 90% after treatment with mutation-adapted U1 snRNAs⁷⁵ (Fig. 5). The same strategy was used for a splice donor mutation of *RPGR* inducing exon 10 skipping. Proper inclusion of exon 10 was achieved in patient fibroblast using mutation-adapted U1snRNAs⁷⁶ (Fig. 5). Mutations in Bardet-Biedl syndrome (BBS) 1 result in more than 20% of cases of BBS, a ciliopathy characterized by retinal dystrophy, cognitive impairment, obesity, polydactyly, hypogonadism, and renal disease.⁷⁷ Bardet-Biedl syndrome 1 is a member of a protein complex called BBSome, involved in trafficking of vesicles to the cilia.⁷⁸ Schmidt and collaborators⁷⁹ identified in a family affected by BBS a splice donor mutation on exon 5 of BBS1 causing missplicing. They were able to show, after administration of mutation-adapted U1 snRNAs, restoration of proper splicing in COS-7 cells, using minigenes as splicing reporter. Similar results were obtained in patient-derived fibroblast transduced with lentiviral vectors encoding for the modified U1-snRNAs (Fig. 6). A recent innovative approach has been developed for the treatment of mutations occurring at position +5 of DS sites.⁶⁵ The synergic use of both mutation-adapted U1 and U6 snRNAs was sufficient to achieve efficient correction of aberrant splicing caused by BBS1 mutations, whereas the only use of mutation-adapted U1 snRNAs resulted in low levels of splicing correction.

TRANS-SPLICING

Another correction approach that acts at the splicing level is spliceosome-mediated RNA *trans*-splicing (SMaRT). This technology is based on a cellular process, called *trans*-splicing. First discovered in trypanosome,^{80,81} *trans*-splicing has been also described in mammals.^{82,83} It consists in the ability of two different pre-mRNAs to originate a chimeric mature mRNA following a recombination event during splicing. *Trans*-splicing can be exploited to correct aberrant mRNA by using an artificial RNA sequence, called pre-*trans*-splicing molecule (PTM). The PTM consists of a correct portion of the cDNA of the gene of interest, flanked by a region containing all important element for splicing and the binding domain (BD), important for specific binding of the PTM to the target endogenous pre mRNA, mainly on an intronic sequence. There are three types of PTMs that can be exploited to achieve 5' *trans*-splicing, 3' *trans*-splicing or internal exon replacement, correcting respectively the 5', the 3', or a central region of a transcript (Fig. 7). Pre-*trans*-splicing molecules are delivered in expressing vectors as in a normal gene transfer approach. They have been administered *in vivo* using different viral vectors,^{84–86} or nonviral delivery systems.^{87–89} The peculiarity of this technique, compared with other splicing-correction approaches, is the fact that it is mutation-independent, thus the

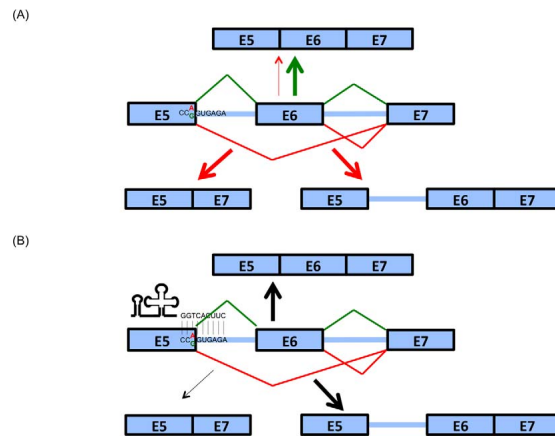


FIGURE 6. Mutation-adapted U1 snRNA for *BBS1* DS site mutations. (A) Normal splicing of *BBS1* (green) is altered (red) by a mutation at the end of exon 5. The mutation causes exon 6 skipping (bottom left) or intron 5 retention (bottom right). (B) Black arrows represent the correcting effect of the best mutation-adapted U1 snRNA, able to partially restore proper splicing. Arrows dimension represent the amount of the different splicing products.

same PTM can be used to treat different mutations located in the same region of the transcript.

Even if SMaRT has never been applied so far for the correction of a genetic disease of the retina, it has been successfully tested in several *in vivo* models for spinal muscular atrophy,⁸⁸ hemophilia A,⁹⁰ hyper-IgM X-linked immunodeficiency,⁸⁶ and tauopathy.⁸⁴ As there are already exhaustive reviews^{91,92} about the first three *in vivo* approaches, to give an example of possible application of SMaRT, we spend a few words on the last and more novel one regarding tauopathy caused by mutations in *MAPT*, the gene encoding tau protein. Tau, a protein important for microtubule stabilization in the CNS, is subject to active alternative splicing as it is present in

humans with six different isoforms.⁹³ Tau exon 10 encodes for a tandem repeat and by alternative splicing originates two sets of different tau isoforms: with 4 (4R; +E10) or 3 (3R; -E10) tandem repeats. Splicing mutations that lead to a change in the levels of E10 containing transcripts cause an imbalance in the 4R/3R isoform ratio, and lead to frontotemporal dementia with parkinsonism linked to chromosome 17 (FTDP-17). Avale and colleagues⁸⁴ designed a PTM for 3' *trans*-splicing with the BD binding to intron 9, and carrying the cDNA of the last three exons of tau (E10-E11-E12). They applied the PTMs to Htau mice that express only human *MAPT*, resulting in equal amounts of 4R and 3R.⁹⁴ Since normal adult mice express only the 4R isoform, the model recapitulates the effect of a

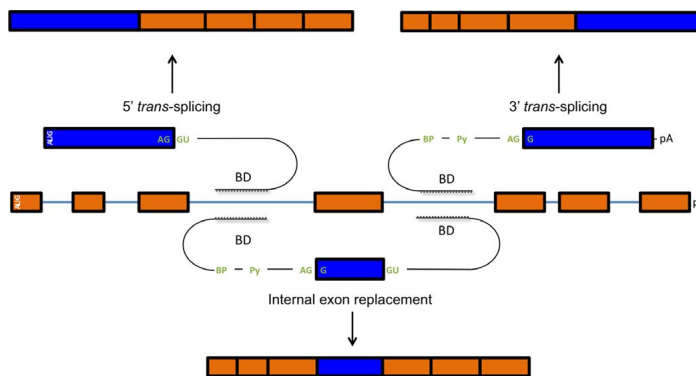


FIGURE 7. Schematic representation of the three possible *trans*-splicing approaches. The different PTMs are constituted by a region harboring: splicing *cis*-acting sequences, shown in green; the coding sequence in blue; and the BD. The mature mRNA resulting from the three *trans*-splicing approaches is shown with the endogenous sequence in orange, and in blue the sequence introduced by the PTMs.

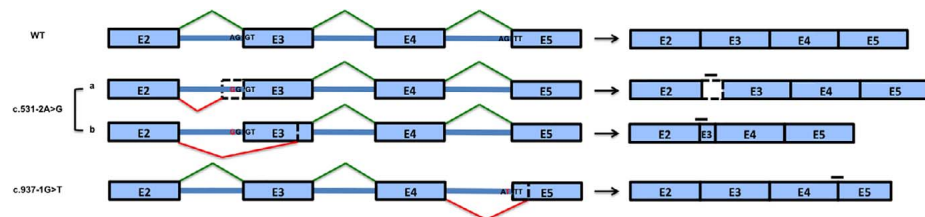


FIGURE 8. RNA interference for adRP splicing mutations. *Left*: the effect on splicing of the two *RHO* mutations c.531-2A>G and c.937-1G>T is shown. Mutation c.531-2A>G originates two misspliced products (A, B). *Right*: The different misspliced products can be selectively recognized by siRNA (black lines) targeting sequences or exon-exon junctions absent in the WT transcript. Small interfering RNA directed toward misspliced product b of c.531-2A>G mutation was not able to discriminate between the WT mature mRNA and the aberrant one. Adapted from Hernan et al.¹⁰⁸

splicing mutation abolishing E10 inclusion. Following delivery of the PTM in the prefrontal cortex of Htau mice by stereotaxic injection using lentiviral vectors, they were able to show effective *trans*-splicing at RNA and protein level.

RNA INTERFERENCE

RNA interference (RNAi) is a regulatory mechanism used by the cell to silence specific transcripts at the posttranscriptional level. The endogenous effectors of this mechanism are micro RNAs (miRNAs). They are transcribed into primary precursors (pri-miRNA) that are then cleaved first by Drosha into a ~70-bp precursor hairpin (pre-miRNA), and then by Dicer into a ~22-bp RNA/RNA duplex.⁹⁵ One of the two strands (the guide strand) is then loaded into the RNA-induced silencing complex (RISC) as a mature miRNA, where it can recognize complementary mRNAs. Silencing by RISC is caused by translational repression if the complementarity between the miRNA and its target mRNA is not perfect. When the miRNA perfectly matches its target, silencing is instead mediated by cleavage and subsequent degradation of the mRNA. Small interfering RNAs (siRNAs) are double-stranded RNA molecules that result from processing by Dicer of exogenous double-stranded RNAs. Alternatively, they can be chemically synthesized and delivered as such for therapeutic purposes. Small interfering RNAs are directly loaded into RISC. Another class of interfering RNA is composed by short hairpin RNA (shRNAs), stem-loop structures that enter the miRNA processing pathway as substrates for Dicer. Short hairpin RNAs are often obtained from the transcription of a delivered DNA transgene hereby guaranteeing stable expression. On the contrary, the effect of siRNA is transient, even if different chemistries are today available to improve their stability. Small interfering RNAs have already been used to treat retinal diseases for a few years. The first RNAi therapeutic applications to enter the clinical phase have in fact been two naked siRNAs developed for the treatment of AMD: Bevasiranib, directed against VEGF; and AGN211745, targeting VEGF receptor (VEGFR1). Clinical development of these two drugs has been discontinued during the last years, mainly because of their failure in meeting efficacy endpoints.⁹⁶ Even if other clinical trials are in progress for other naked siRNA,⁹⁷ the lessons that we can learn from the two described trials is that it is a challenge to deliver naked siRNA into cells, even in an easy system such as the eye, and that their efficacy is not mediated by RNAi, but via an off-target sequence independent effect on cell surface Toll-like receptor-3 (TLR3).^{98,99} New chemistries seem to overcome these limitations,¹⁰⁰ and the availability of different types of formulations (polymer- or lipid-coated nanoparticles, oligonucleotide nano-

particles, and conjugates delivery systems⁹⁷) can potentially help in improving cellular uptake in the retina. However, the current trend for in vivo applications is to utilize viral vectors to deliver shRNAs to different retinal layers.^{101–106}

By exploiting the mechanism of RNAi-mediated gene silencing, it is possible to solve different situations in which correct splicing is compromised. Mutations that cause impairment in the splicing process can lead to misspliced products that in some cases can show a dominant negative or a gain of function effect. If this is the case, the simple decrease of the misspliced mRNA, without affecting the correctly spliced counterpart, can revert the pathological condition. This is possible using RNAi.¹⁰⁷ A recent example of the application of this strategy in the retina has been shown for retinitis pigmentosa.¹⁰⁸ Mutations in rhodopsin (*RHO*) are the most prevalent cause of autosomal dominant retinitis pigmentosa (adRP), accounting for 25% of the cases.¹⁰⁹ Two mutations causing adRP (c.531-2A>G and c.937-1G>T) generate missplicing products. They abolish the proper recognition of the DS site of exon 3 and 5, respectively. Mutation c.531-2A>G originates two misspliced mRNAs with a partial intron 2 retention or a partial deletion of exon 3. Mutation c.937-1G>T results in a partial deletion of exon 5. Using RNAi against the misspliced mRNA, it was possible to successfully decrease their level without affecting the properly spliced isoform, with the exception of the second product of c.531-2A>G mutation, where the RNAi was not able to distinguish between the wild type (WT) and the aberrant mRNA (Fig. 8).

CONCLUSIONS AND FUTURE PERSPECTIVES

Antisense-mediated, splicing-correction approaches, after their first and successful application for DMD, acquired a momentum that prompted the efforts for their application to several disease conditions. Citing only some of the main applications in the CNS, splicing modulation therapies have been implemented for ataxia telangiectasia (AT), frontotemporal dementia, and parkinsonism linked to chromosome 17 (FTDP-17), Alzheimer disease (AD), spinocerebellar ataxia (SCA), neurofibromatosis type 1 (NF1), and many others.¹¹⁰

So far their application in the eye has just begun, showing great promise. However, there are some limitations that need to be faced for a successful implementation of such therapies. The first drawback is that, apart from *trans*-splicing, all other approaches are patient-specific. Even if the shift toward personalized medicine offers great advantages in a long-term frame, its development poses many challenges in the immediate future. The limited number of patients treatable with each antisense molecule raises questions on the feasibility

of normal clinical trials. Moreover, the current need to consider antisense therapies, even of the same class and for the same disease, as different drugs if they are targeting different mutations, creates a great economic obstacle to their development. Luckily a debate between researchers and regulatory agencies has already started on these issues.¹¹¹ Another problem regarding the retina is the difficulties of having relevant animal models that would allow splicing manipulation of the gene of interest. The implementation of such models will definitely foster clinical application of splicing-correction approaches for retinal dystrophies.

Acknowledgments

The authors thank Erik Dassi for his helpful assistance in retrieving and analyzing data from HGMD.

Supported by the Italian Ministry of Health, Young Italian Researchers Grant 2008, Project GR-2008-1136933.

Disclosure: N. Bacchi, None; S. Casarosa, None; M.A. Denti, None

References

- Daiger SP, Rossiter BJF, Greenberg J, Christoffels AHW. Data services and software for identifying genes and mutations causing retinal degeneration. *Invest Ophthalmol Vis Sci*. 1998;39:S295.
- Havens MA, Duelli DM, Hastings ML. Targeting RNA splicing for disease therapy. *Wiley Interdiscip Rev RNA*. 2013;4:247-266.
- Bonnal S, Vigevani L, Valcárcel J. The spliceosome as a target of novel antitumour drugs. *Nat Rev Drug Discov*. 2012;11:847-859.
- Smith AJ, Bainbridge JWB, Ali RR. Gene supplementation therapy for recessive forms of inherited retinal dystrophies. *Gene Ther*. 2012;19:154-161.
- Gomes Dos Santos AL, Bochot A, Fattal E. Intraocular delivery of oligonucleotides. *Curr Pharm Biotechnol*. 2005;6:7-15.
- Martin KR, Klein RL, Quigley HA. Gene delivery to the eye using adeno-associated viral vectors. *Methods*. 2002;28:267-275.
- Surace EM, Auricchio A. Versatility of AAV vectors for retinal gene transfer. *Vision Res*. 2008;48:353-359.
- Stein-Streilein J. Immune regulation and the eye. *Trends Immunol*. 2008;29:548-554.
- Vandenberghe LH, Auricchio A. Novel adeno-associated viral vectors for retinal gene therapy. *Gene Ther*. 2012;19:162-168.
- Lam BJ, Hertel KJ. A general role for splicing enhancers in exon definition. *RNA*. 2002;8:1233-1241.
- Zhou Z, Fu X-D. Regulation of splicing by SR proteins and SR protein-specific kinases. *Chromosoma*. 2013;122:191-207.
- Pozzoli U, Sironi M. Silencers regulate both constitutive and alternative splicing events in mammals. *Cell Mol Life Sci*. 2005;62:1579-1604.
- Kafasla P, Mickleburgh I, Llorian M, et al. Defining the roles and interactions of PTB. *Biochem Soc Trans*. 2012;40:815-820.
- Jean-Philippe J, Paz S, Caputi M. hnRNP A1: the Swiss army knife of gene expression. *Int J Mol Sci*. 2013;14:18999-19024.
- Busch A, Hertel KJ. Evolution of SR protein and hnRNP splicing regulatory factors. *Wiley Interdiscip Rev RNA*. 2012;3:1-12.
- De Conti L, Baralle M, Buratti E. Exon and intron definition in pre-mRNA splicing. *Wiley Interdiscip Rev RNA*. 2013;4:49-60.
- Kornblihtt AR, Schor IE, Alló M, Dujardin G, Petrillo E, Muñoz MJ. Alternative splicing: a pivotal step between eukaryotic transcription and translation. *Nat Rev Mol Cell Biol*. 2013;14:153-165.
- Hoskins AA, Moore MJ. The spliceosome: a flexible, reversible macromolecular machine. *Trends Biochem Sci*. 2012;37:179-188.
- Berger W, Kloeckener-Gruissem B, Neidhardt J. The molecular basis of human retinal and vitreoretinal diseases. *Prog Retin Eye Res*. 2010;29:335-375.
- Stenson PD, Ball EV, Mort M, et al. Human Gene Mutation Database (HGMD): 2003 update. *Hum Mutat*. 2003;21:577-581.
- López-Bigas N, Audit B, Ouzounis C, Parra G, Guigó R. Are splicing mutations the most frequent cause of hereditary disease? *FEBS Lett*. 2005;579:1900-1903.
- Sterne-Weiler T, Howard J, Mort M, Cooper DN, Sanford JR. Loss of exon identity is a common mechanism of human inherited disease. *Genome Res*. 2011;21:1563-1571.
- Lim KH, Ferraris L, Filloux ME, Raphael BJ, Fairbrother WG. Using positional distribution to identify splicing elements and predict pre-mRNA processing defects in human genes. *Proc Natl Acad Sci U S A*. 2011;108:11093-11108.
- Saleh AF, Arzumanov AA, Gait MJ. Overview of alternative oligonucleotide chemistries for exon skipping. *Methods Mol Biol*. 2012;867:365-378.
- Järver P, O'Donovan L, Gait MJ. A chemical view of oligonucleotides for exon skipping and related drug applications. *Nucleic Acid Ther*. 2013;24:37-47.
- De Clercq E, Eckstein E, Merigan TC. Interferon induction increased through chemical modification of a synthetic polyribonucleotide. *Science*. 1969;165:1137-1139.
- Sproat BS, Lamond AL, Beijer B, Neuner P, Ryder U. Highly efficient chemical synthesis of 2'-O-methyloligoribonucleotides and tetrabiotinylated derivatives; novel probes that are resistant to degradation by RNA or DNA specific nucleases. *Nucleic Acids Res*. 1989;17:3373-3386.
- Martin P. New access to 2-O-alkylated ribonucleosides and properties of 2-O-alkylated oligoribonucleotides. *Helv Chim Acta*. 1995;78:486-504.
- Koshkin AA, Singh SK, Nielsen P, et al. LNA (locked nucleic acids): synthesis of the adenine, cytosine, guanine, 5-methylcytosine, thymine and uracil bicyclonucleoside monomers, oligomerisation, and unprecedented nucleic acid recognition. *Tetrahedron*. 1998;54:3607-3630.
- Obika S, Nanbu D, Hari Y, et al. Stability and structural features of the duplexes containing nucleoside analogues with a fixed N-type conformation, 2'-O,4'-C-methylenetribo-nucleosides. *Tetrahedron Lett*. 1998;39:5401-5404.
- Nielsen PE, Egholm M, Berg RH, Buchardt O. Sequence-selective recognition of DNA by strand displacement with a thymine-substituted polyamide. *Science*. 1991;254:1497-1500.
- Summerton J, Weller D. Morpholino antisense oligomers: design, preparation, and properties. *Antisense Nucleic Acid Drug Dev*. 1997;7:187-195.
- Kole R, Kraimer AR, Altman S. RNA therapeutics: beyond RNA interference and antisense oligonucleotides. *Nat Rev Drug Discov*. 2012;11:125-140.
- Kurreck J. Antisense technologies. Improvement through novel chemical modifications. *Eur J Biochem*. 2003;270:1628-1644.
- Baughan T, Shababi M, Coady TH, Dickson AM, Tullis GE, Lorson CL. Stimulating full-length SMN2 expression by delivering bifunctional RNAs via a viral vector. *Mol Ther*. 2006;14:54-62.
- Baughan TD, Dickson A, Osman EY, Lorson CL. Delivery of bifunctional RNAs that target an intronic repressor and increase SMN levels in an animal model of spinal muscular atrophy. *Hum Mol Genet*. 2009;18:1600-1611.
- Owen N, Zhou H, Malygin AA, et al. Design principles for bifunctional targeted oligonucleotide enhancers of splicing. *Nucleic Acids Res*. 2011;39:7194-7208.

38. Skordis LA, Dunckley MG, Yue B, Eperon IC, Muntoni F. Bifunctional antisense oligonucleotides provide a trans-acting splicing enhancer that stimulates SMN2 gene expression in patient fibroblasts. *Proc Natl Acad Sci U S A*. 2003;100:4114-4119.
39. Osman EY, Yen PF, Lorson CL. Bifunctional RNAs targeting the intronic splicing silencer N1 increase SMN levels and reduce disease severity in an animal model of spinal muscular atrophy. *Mol Ther*. 2012;20:119-126.
40. Dickson A, Osman E, Lorson CL. A negatively acting bifunctional RNA increases survival motor neuron both in vitro and in vivo. *Hum Gene Ther*. 2008;19:1307-1315.
41. Villemain J, Dion I, Elela SA, Chabot B. Reprogramming alternative pre-messenger RNA splicing through the use of protein-binding antisense oligonucleotides. *J Biol Chem*. 2003;278:50031-50039.
42. Gendron D, Carriero S, Garneau D, et al. Modulation of 5' splice site selection using tailed oligonucleotides carrying splicing signals. *BMC Biotechnol*. 2006;6:5.
43. Brosseau JP, Lucier JF, Lamarche AA, et al. Redirecting splicing with bifunctional oligonucleotides. *Nucleic Acids Res*. 2013;42:e40.
44. Van Deutekom JC, Janson AA, Ginjaar IB, et al. Local dystrophin restoration with antisense oligonucleotide PRO051. *N Engl J Med*. 2007;357:2677-2686.
45. Kalbfuss B, Mabon SA, Misteli T. Correction of alternative splicing of tau in frontotemporal dementia and parkinsonism linked to chromosome 17. *J Biol Chem*. 2001;276:42986-42993.
46. Aartsma-Rus A, Fokkema I, Verschuuren J, et al. Theoretic applicability of antisense-mediated exon skipping for Duchenne muscular dystrophy mutations. *Hum Mutat*. 2009;30:293-299.
47. Kinali M, Arechavala-Gomez V, Feng L, et al. Local restoration of dystrophin expression with the morpholino oligomer AVI-4658 in Duchenne muscular dystrophy: a single-blind, placebo-controlled, dose-escalation, proof-of-concept study. *Lancet Neurol*. 2009;8:918-928.
48. Cirak S, Arechavala-Gomez V, Guglieri M, et al. Exon skipping and dystrophin restoration in patients with Duchenne muscular dystrophy after systemic phosphorodiamidate morpholino oligomer treatment: an open-label, phase 2, dose-escalation study. *Lancet*. 2011;378:595-605.
49. Goemans NM, Tulinus M, van den Akker JT, et al. Systemic administration of PRO051 in Duchenne's muscular dystrophy. *N Engl J Med*. 2011;364:1513-1522.
50. Zanetta C, Nizzardo M, Simone C, et al. Molecular therapeutic strategies for spinal muscular atrophies: current and future clinical trials. *Clin Ther*. 2014;36:128-140.
51. Bhisitkul RB, Robinson GS, Moulton RS, Claffey KP, Gragoudas ES, Miller JW. An antisense oligodeoxynucleotide against vascular endothelial growth factor in a nonhuman primate model of iris neovascularization. *Arch Ophthalmol*. 2005;123:214-219.
52. Shen WY, Garrett KL, da Cruz L, Constable JJ, Rakoczy PE. Dynamics of phosphorothioate oligonucleotides in normal and laser photocoagulated retina. *Br J Ophthalmol*. 1999;83:852-861.
53. Dvorchik BH, Marquis JK. Disposition and toxicity of a mixed backbone antisense oligonucleotide, targeted against human cytomegalovirus, after intravitreal injection of escalating single doses in the rabbit. *Drug Metab Dispos*. 2000;28:1255-1261.
54. Shen WY, Rakoczy PE. Uptake dynamics and retinal tolerance of phosphorothioate oligonucleotide and its direct delivery into the site of choroidal neovascularization through subretinal administration in the rat. *Antisense Nucleic Acid Drug Dev*. 2001;11:257-264.
55. Cloutier F, Lawrence M, Goody R, et al. Antiangiogenic activity of aganirsen in nonhuman primate and rodent models of retinal neovascular disease after topical administration. *Invest Ophthalmol Vis Sci*. 2012;53:1195-1203.
56. Thaler S, Rejdak R, Dietrich K, et al. A selective method for transfection of retinal ganglion cells by retrograde transfer of antisense oligonucleotides against kynurenine aminotransferase II. *Mol Vis*. 2006;12:100-107.
57. Fattal E, Bochot A. Ocular delivery of nucleic acids: antisense oligonucleotides, aptamers and siRNA. *Adv Drug Deliv Rev*. 2006;58:1203-1223.
58. Uehara H, Cho Y, Simonis J, et al. Dual suppression of hemangiogenesis and lymphangiogenesis by splice-shifting morpholinos targeting vascular endothelial growth factor receptor 2 (KDR). *FASEB J*. 2013;27:76-85.
59. Den Hollander AI, Roepman R, Koenekoop RK, Cremers FP. Leber congenital amaurosis: genes, proteins and disease mechanisms. *Prog Retin Eye Res*. 2008;27:391-419.
60. Perrault I, Delphin N, Hanein S, et al. Spectrum of NPHP6/CEP290 mutations in Leber congenital amaurosis and delineation of the associated phenotype. *Hum Mutat*. 2007;28:416.
61. Den Hollander AI, Koenekoop RK, Yzer S, et al. Mutations in the CEP290 (NPHP6) gene are a frequent cause of Leber congenital amaurosis. *Am J Hum Genet*. 2006;79:556-561.
62. Collin RW, den Hollander AI, van der Velde-Visser SD, Bencicelli J, Bennett J, Cremers FP. Antisense oligonucleotide (AON)-based therapy for Leber congenital amaurosis caused by a frequent mutation in CEP290. *Mol Ther Nucleic Acids*. 2012;27:1:e14.
63. Gerard X, Perrault I, Hanein S, et al. AON-mediated exon skipping restores ciliation in fibroblasts harboring the common Leber congenital amaurosis CEP290 mutation. *Mol Ther Nucleic Acids*. 2012;26:e29.
64. Pinotti M, Rizzotto L, Balestra D, et al. U1-siRNA-mediated rescue of mRNA processing in severe factor VII deficiency. *Blood*. 2008;111:2681-2684.
65. Schmid F, Hiller T, Korner G, Glaus E, Berger W, Neidhardt J. A gene therapeutic approach to correct splice defects with modified U1 and U6 snRNPs. *Hum Gene Ther*. 2013;24:97-104.
66. Patel SB, Bellini M. The assembly of a spliceosomal small nuclear ribonucleoprotein particle. *Nucleic Acids Res*. 2008;36:6482-6493.
67. Dominski Z, Marzluff WF. Formation of the 3' end of histone mRNA: getting closer to the end. *Gene*. 2007;396:373-390.
68. Denti MA, Rosa A, D'Antona G, et al. Body-wide gene therapy of Duchenne muscular dystrophy in the mdx mouse model. *Proc Natl Acad Sci U S A*. 2006;103:3758-3763.
69. Denti MA, Incitti T, Sthandier O, et al. Long-term benefit of adeno-associated virus/antisense-mediated exon skipping in dystrophic mice. *Hum Gene Ther*. 2008;19:601-608.
70. Goyenvalle A, Wright J, Babbs A, Wilkins V, Garcia L, Davies KE. Engineering multiple U7snRNA constructs to induce single and multiexon-skipping for Duchenne muscular dystrophy. *Mol Ther*. 2012;20:1212-1221.
71. Goyenvalle A, Babbs A, van Ommen G-JB, Garcia L, Davies KE. Enhanced exon-skipping induced by U7 snRNA carrying a splicing silencer sequence: promising tool for DMD therapy. *Mol Ther*. 2009;17:1234-1240.
72. Marquis J, Meyer K, Angehrn L, Kämpfer SS, Rothen-Rutishauser B, Schümperli D. Spinal muscular atrophy: SMN2 pre-mRNA splicing corrected by a U7 snRNA derivative carrying a splicing enhancer sequence. *Mol Ther*. 2007;15:1479-1486.
73. Voigt T, Meyer K, Baum O, Schümperli D. Ultrastructural changes in diaphragm neuromuscular junctions in a severe mouse model for Spinal Muscular Atrophy and their prevention by bifunctional U7 snRNA correcting SMN2 splicing. *Neuromuscul Disord*. 2010;20:744-752.
74. Susani L, Pangrazio A, Sobacchi C, et al. TCIRG1-dependent recessive osteopetrosis: mutation analysis, functional identi-

- fication of the splicing defects, and in vitro rescue by U1 snRNA. *Hum Mutat.* 2004;24:225-235.
75. Tanner G, Glaus E, Barthelmes D, et al. Therapeutic strategy to rescue mutation-induced exon skipping in rhodopsin by adaptation of U1 snRNA. *Hum Mutat.* 2009;30:255-263.
 76. Glaus E, Schmid F, Da Costa R, Berger W, Neidhardt J. Gene therapeutic approach using mutation-adapted U1 snRNA to correct a RPGR splice defect in patient-derived cells. *Mol Ther.* 2011;19:936-941.
 77. Mockel A, Perdomo Y, Stutzmann F, Letsch J, Marion V, Dollfus H. Retinal dystrophy in Bardet-Biedl syndrome and related syndromic ciliopathies. *Prog Retin Eye Res.* 2011;30:258-274.
 78. Nachury MV, Seeley ES, Jin H. Trafficking to the ciliary membrane: how to get across the periciliary diffusion barrier? *Annu Rev Cell Dev Biol.* 2010;26:59-87.
 79. Schmid F, Glaus E, Barthelmes D, et al. U1 snRNA-mediated gene therapeutic correction of splice defects caused by an exceptionally mild BBS mutation. *Hum Mutat.* 2011;32:815-824.
 80. Sutton RE, Boothroyd JC. Evidence for trans splicing in trypanosomes. *Cell.* 1986;47:527-535.
 81. Murphy WJ, Watkins KP, Agabian N. Identification of a novel Y branch structure as an intermediate in trypanosome mRNA processing: evidence for trans splicing. *Cell.* 1986;47:517-525.
 82. Flouriot G, Brand H, Seraphin B, Gannon E. Natural trans-spliced mRNAs are generated from the human estrogen receptor-alpha (hER alpha) gene. *J Biol Chem.* 2002;277:26244-26251.
 83. Caudevilla C, Serra D, Miliar A, et al. Natural trans-splicing in carnitine octanoyltransferase pre-mRNAs in rat liver. *Proc Natl Acad Sci U S A.* 1998;95:12185-12190.
 84. Avale ME, Rodriguez-Martín T, Gallo JM. Trans-splicing correction of tau isoform imbalance in a mouse model of tau mis-splicing. *Hum Mol Genet.* 2013;22:2603-2611.
 85. Chao H, Mansfield SG, Bartel RC, et al. Phenotype correction of hemophilia A mice by spliceosome-mediated RNA trans-splicing. *Nat Med.* 2003;9:1015-1019.
 86. Tahara H, Pergolizzi RG, Kobayashi H, et al. Trans-splicing repair of CD40 ligand deficiency results in naturally regulated correction of a mouse model of hyper-IgM X-linked immunodeficiency. *Nat Med.* 2004;10:835-841.
 87. Shababi M, Glascock J, Lorson CL. Combination of SMN trans-splicing and a neurotrophic factor increases the life span and body mass in a severe model of spinal muscular atrophy. *Hum Gene Ther.* 2011;22:135-144.
 88. Coady TH, Lorson CL. Trans-splicing-mediated improvement in a severe mouse model of spinal muscular atrophy. *J Neurosci.* 2010;30:126-130.
 89. Coady TH, Baughan TD, Shababi M, Passini MA, Lorson CL. Development of a single vector system that enhances trans-splicing of SMN2 transcripts. *PLoS One.* 2008;3:e3468.
 90. Chao H, Mansfield SG, Bartel RC, et al. Phenotype correction of hemophilia A mice by spliceosome-mediated RNA trans-splicing. *Nat Med.* 2003;9:1015-1019.
 91. Wally V, Muraier EM, Bauer JW. Spliceosome-mediated trans-splicing: the therapeutic cut and paste. *J Invest Dermatol.* 2012;132:1959-1966.
 92. Mansfield SG, Chao H, Walsh CE. RNA repair using spliceosome-mediated RNA trans-splicing. *Trends Mol Med.* 2004;10:263-268.
 93. Niblock M, Gallo JM. Tau alternative splicing in familial and sporadic tauopathies. *Biochem Soc Trans.* 2012;40:677-680.
 94. Andorfer C, Kress Y, Espinoza M, et al. Hyperphosphorylation and aggregation of tau in mice expressing normal human tau isoforms. *J Neurochem.* 2003;86:582-590.
 95. Krol J, Loedige I, Filipowicz W. The widespread regulation of microRNA biogenesis, function and decay. *Nat Rev Genet.* 2010;11:597-610.
 96. Vaishnav AK, Gollob J, Gamba-Vitalo C, et al. A status report on RNAi therapeutics. *Silence.* 2010:14.
 97. Kanasty R, Dorkin JR, Vegas A, Anderson D. Delivery materials for siRNA therapeutics. *Nat Mater.* 2013;12:967-977.
 98. Kleinman ME, Yamada K, Takeda A, et al. Sequence- and target-independent angiogenesis suppression by siRNA via TLR3. *Nature.* 2008;452:591-597.
 99. Cho WG, Albuquerque RJ, Kleinman ME, et al. Small interfering RNA-induced TLR3 activation inhibits blood and lymphatic vessel growth. *Proc Natl Acad Sci U S A.* 2009;106:7137-7142.
 100. Byrne M, Tzekov R, Wang Y, et al. Novel hydrophobically modified asymmetric RNAi compounds (sd-rxRNA) demonstrate robust efficacy in the eye. *J Ocul Pharmacol Ther.* 2013;29:855-864.
 101. Askou AL, Pournaras JC, Pihlmann M, et al. Reduction of choroidal neovascularization in mice endothelial growth factor short hairpin RNA. *J Gene Med.* 2012;14:632-641.
 102. Hu J, Wu Q, Li T, Chen Y, Wang S. Inhibition of high glucose-induced VEGF release in retinal ganglion cells by RNA interference targeting G protein-coupled receptor 91. *Exp Eye Res.* 2013;109:31-39.
 103. Zhu H, Qian J, Wang W, et al. RNA interference of GADD153 protects photoreceptors from endoplasmic reticulum stress-mediated apoptosis after retinal detachment. *PLoS One.* 2013;8:e59339.
 104. Chadderton N, Millington-Ward S, Palfi A, et al. Improved retinal function in a mouse model of dominant retinitis pigmentosa following AAV-delivered gene therapy. *Mol Ther.* 2009;17:593-599.
 105. Yuan MK, Tao Y, Yu W-Z, Kai W, Jiang Y-R. Lentivirus-mediated RNA interference of vascular endothelial growth factor in monkey eyes with iris neovascularization. *Mol Vis.* 2010;16:1743-1753.
 106. Jiang L, Li TZ, Boye SE, Hauswirth WW, Frederick JM, Baehr W. RNAi-mediated gene suppression in a GCAP1(L151F) cone-rod dystrophy mouse model. *PLoS One.* 2013;8:e57676.
 107. Seyhan AA. RNAi: a potential new class of therapeutic for human genetic disease. *Hum Genet.* 2011;130:583-605.
 108. Hernan I, Gamundi MJ, Planas E, Borrás E, Maseras M, Carballo M. Cellular expression and siRNA-mediated interference of rhodopsin cis-acting splicing mutants associated with autosomal dominant retinitis pigmentosa. *Invest Ophthalmol Vis Sci.* 2011;52:3723-3729.
 109. Fingert JH, Oh K, Chung M, et al. Association of a novel mutation in the retinol dehydrogenase 12 (RDH12) gene with autosomal dominant retinitis pigmentosa. *Arch Ophthalmol.* 2008;126:1301-1307.
 110. Siva K, Covello G, Denti MA. Exon-skipping antisense oligonucleotides to correct missplicing in neurogenetic diseases. *Nucleic Acid Ther.* 2014;24:69-86.
 111. Muntoni F. The development of antisense oligonucleotide therapies for Duchenne muscular dystrophy: report on a TREAT-NMD workshop hosted by the European Medicines Agency (EMA), on September 25th 2009. *Neuromuscul Disord.* 2010;20:355-362.

11.2 List of supplementary tables and figures attached to the work

- Figure S1: Alignment of human and mouse CACNA2D4 exons 23-24-25-26.
- Figure S2: Alignment of human and mouse CACNA2D4 proteins.
- Figure S3: Equivalence of the standard curve for pE25 and pE25b plasmid RT-qPCR.
- Table S1: List of all identified genes causing retinal dystrophies and potentially targetable with splicing-correction approaches.
- Table S2: List of all mutations found in RetNet genes on HGMD.
- Table S3: List of all USH2A mutations present in HGMD. Highlighted mutations refers to those present in exons 29, 30, 32, 38, 43, 45, 50, 53, 56, 59 and 62.
- Table S4: List of all primers utilized in RT-PCR and RT-qPCR



FIGURE S1. Alignment of human and mouse CACNA2D4 exons 23-24-25-26. ClustalW2 alignment is visualized with Jalview. The sequence corresponding to the different exons is highlighted.

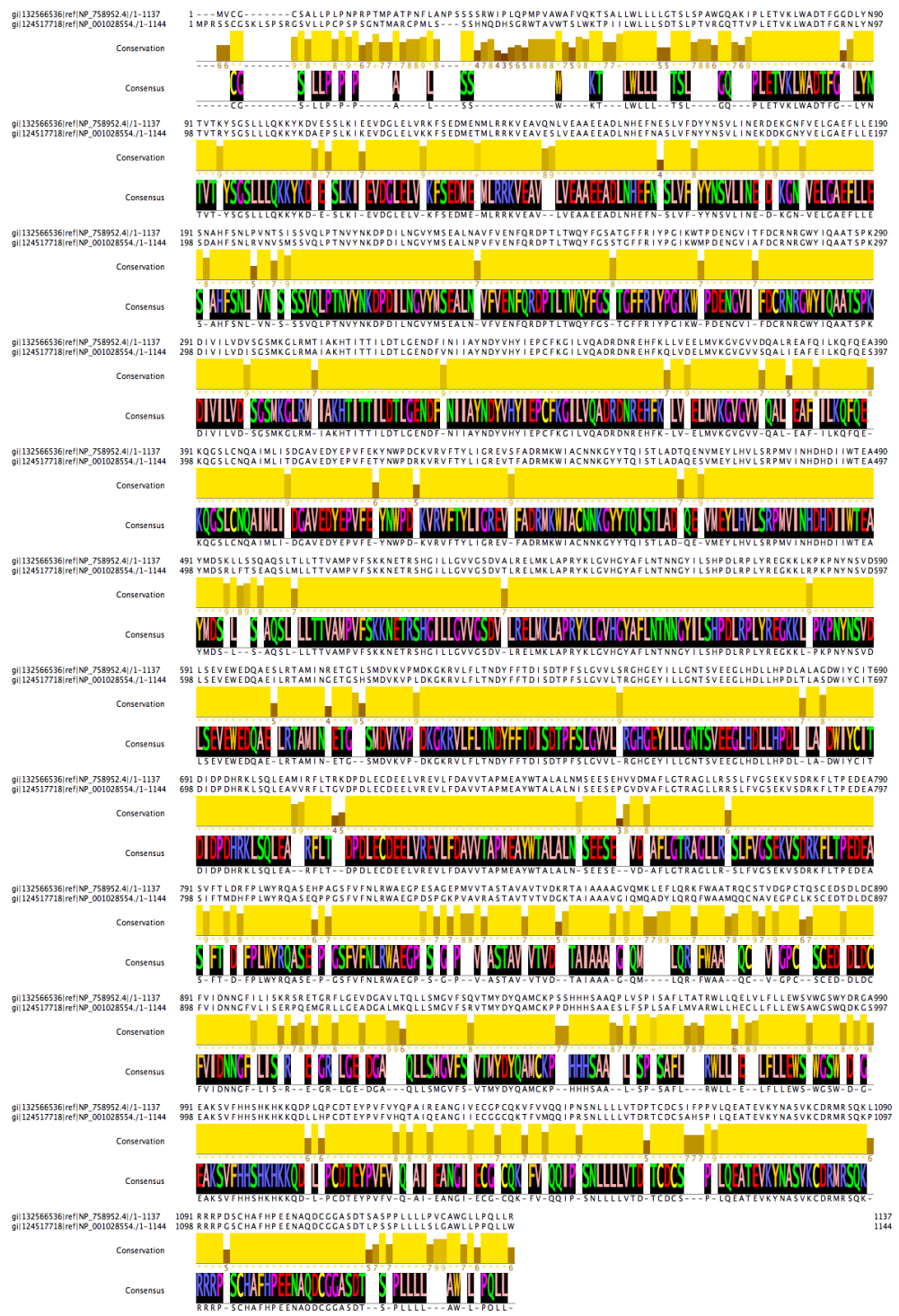


FIGURE S2. Alignment of human and mouse CACNA2D4 proteins. ClustalW2 alignment is visualized with Jalview. Conservation score and consensus are reported. The homology is of 85%.

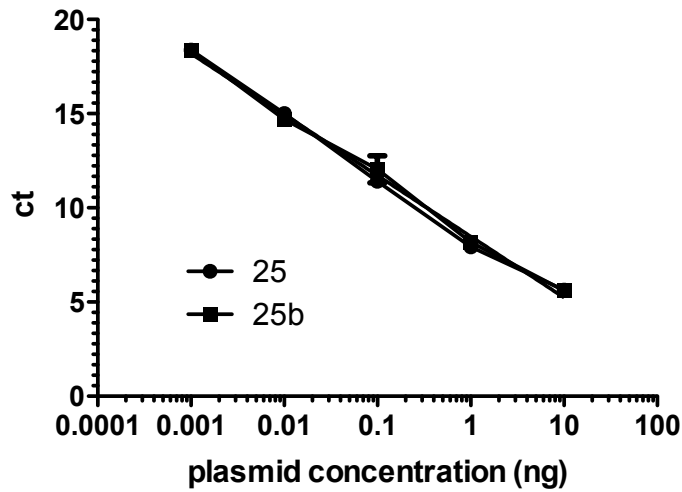


FIGURE S3. Equivalence of the standard curve for pE25 and pE25b plasmids RT-qPCR. Each point of the two fitted curve is represented as mean \pm SD (N=5). The two curves for pE25 and pE25b can be represented by a single straight line with y-intercept = 8.48 and slope = -3.23 (Extra sum-of-square F test).

Target	For/Rev	Sequence (5'-3')	Application
Cacna2d4 E22	For	TATGATCTACTGTATCACAGATATCGAC	RT-PCR
pIRES2	Rev	CCACGATCCGATGGTTTGTATTACAG	RT-PCR
Cacna2d4 E24	For	AGAGTCAGAGCCTGGCGTG	RT-PCR
Cacna2d4 E26	Rev	CTGCTGCAATGGCCGTCTTCC	RT-PCR
GAPDH/Gapdh	For	GGCCAAGGTCATCCATGA	RT-PCR
GAPDH/Gapdh	Rev	TCAGTGTAGCCCAGGATG	RT-PCR
Cacna2d4 E15	For	GTGTAGTGGGCTCTGACGTG	RT-PCR
Cacna2d4 E17	Rev	TGGCGGTCCTCAGAATTCA	RT-PCR
Cacna2d4 3'UTR	For	GTGGCGAGAAAAGCAGAAAC	RT-qPCR
Cacna2d4 3'UTR	Rev	CATTGTGAGCCACAGAAAGC	RT-qPCR
Cacna2d4 E25	For	CTGTGGTATCGCCAGGCCTCT	RT-qPCR
Cacna2d4 E25	Rev	GCAATGGCCGTCTTCCATCC	RT-qPCR
Cacna2d4 E25b	For	TCCAGCATGGAGCAACGGGA	RT-qPCR
Cacna2d4 E25b	Rev	TGCTGCAATGGCCGTCTTCC	RT-qPCR
GAPDH/Gapdh	For	TGACCTCAACTACATGGTCTACA	RT-qPCR
GAPDH/Gapdh	Rev	CTTCCCATTCTCGGCCTTG	RT-qPCR
RPGR E9	For	CGGCCTTATGTATACTTTTGG	RT-PCR
BGH	Rev	TAGAAGGCACAGTCGAGG	RT-PCR

TABLE S4. List of primers utilized for RT-PCR and RT-qPCR.

12 Acknowledgments

This thesis is the end of a long and challenging journey full of incredible people who have contributed to it in one way or another, consciously or unconsciously. As any fascinating journey, it is sad when it ends. Nevertheless I will always remember all of it, and especially all I gained from everyone I met in these fantastic four years in Trento.

First of all I am grateful to my tutor, Prof. Michela Denti, and to my advisor, Dr. Simona Casarosa, for having chosen me for developing such a fascinating project. I would have hardly found a more interesting one on which to embark. I really appreciated your extraordinary care in me and in all the problems I faced. Your punctual suggestions and feedback have been extremely important at every step of this adventure. I hope you will continue to supervise future students together, since I really enjoyed your collaboration.

I would then like to thank Prof. Paolo Macchi for having wisely organized such a great PhD school, and for all the energy he is constantly spending in it for the benefit of all the PhD students. Together with Paolo, I would like to thank the secretary of the PhD school, Betty Balduin, for her constant assistance in almost any matter.

I would like to acknowledge the precious contribution of my external referees, Prof. Mirko Pinotti, Prof. Andrew Webster, and Prof. Willeke van Roon. I would like to thank them for all their suggestions on how to meliorate the work, and for all the time they have spent reading my thesis. I really appreciated their effort and interesting comments.

I extend my gratitude to Prof. Alexandra Koschak, who has hosted me in her lab to learn and perform electrophysiology, and has provided a crucial contribution to this work. I also would like to mention the precious assistance of her lab members, and especially that of Verena, Klaus, and Dagmar. I miss you guys!

I need also to mention our director, Prof. Alessandro Quattrone, for having been able to build such a fascinating and dynamic research institute.

This has been a great journey especially thanks to the presence of my PhD colleagues Francesca and Kavita, with whom I started four years ago and with whom I am

finishing today. I hope all the best for your future, wherever it will take you. And thanks for standing me for such a long time!

I express my gratitude to all members of my two labs, and especially to all the postdocs: Margherita, Valerio, Andrea, Giusy (and Giovanni, even if he is from another lab).

A big thank you to my flatmates, Francesca, Nicola, Marco and Ilaria, to my friends and (present or past) colleagues Erik, Sara, Chiara, Antonio, Albertomaria, Francis, Mattia, Micaela, Sabrina, Giulia, Roberta, Laura.

Thank you Elena for all your visits to Trento and Vienna, for your constant support and for your fantastic spirit.

I finally address a special thank to my parents, Ulisse and Cinzia, and to my brother Umberto, for having always been a constant reference point in my life.